Electronic Supplementary Material (ESI) for Organic & Biomolecular Chemistry.

Identification of Crucial Bottlenecks in Engineered Polyketide Biosynthesis Using the Monensin Gene Cluster as a Model System

*Marius Grote, Susanna Kushnir, Niclas Pryk, David Möller, Julian Erver, Ahmed Ismail-Ali, Frank Schulz**

1 General Remarks

Chapter 2 contains additional information on the LC-HRMS method used in this manuscript. All released intermediates that were detected via LC-HRMS are listed in **chapter 3.**
Additional figures in **chapter 4** illustrate the extracted ion chromatograms of those intermediates, released in fermentations of additional null mutants and from precursor directed biosynthesis discussed in the manuscript.
Chapter 5 comprises all mass spectrometric characterization of the derivatives of final products (premonensin A and B) by null mutations in the reductive loops or precursor directed biosynthesis. All mass spectrometric data for the detectable intermediates released from the respective assembly lines are stated. mSigma values represent the match of the measured and calculated isotope pattern for the sum formula calculated from the exact mass. [1-3] <10: excellent agreement. <80 acceptable agreement. Especially for low intensities values are not representative or not determined (n.d.).
MS^2 data for the fragmentation of premonensin derivatives and intermediates released in the mutants starting from module 10. MS^2 data of earlier intermediates are omitted from the SI as they do not fragment under the given conditions. mSigma values for MS^2 data are not stated as low intensities in general resulted in not representative or not available (n.d.) values.
Chapter 6 lists the NMR data collected for the premonensin derivatives purified from a fermentation of *Streptomyces cinnamonensis* A495 $ER2^0DH8^0$.
Chapter 7 gives an overview of amino acid sequences of ketosynthases from the monensin gene cluster and four additional polyether antibiotic PKS searching for a motif correlating with their substrate acceptance.
Chapter 8 contains details on cloning, expression and enrichment of the three hydrolases MonAIX, MonAX and Orf31 discussed in the manuscript. Also, the in vitro methods for the colorimetric assay are given. Oligonucleotides used in the study are listed.
Chapter 9 contains all data for the synthesis and characterization of compounds used in the *in vitro* assay.

2 LC-HRMS Method

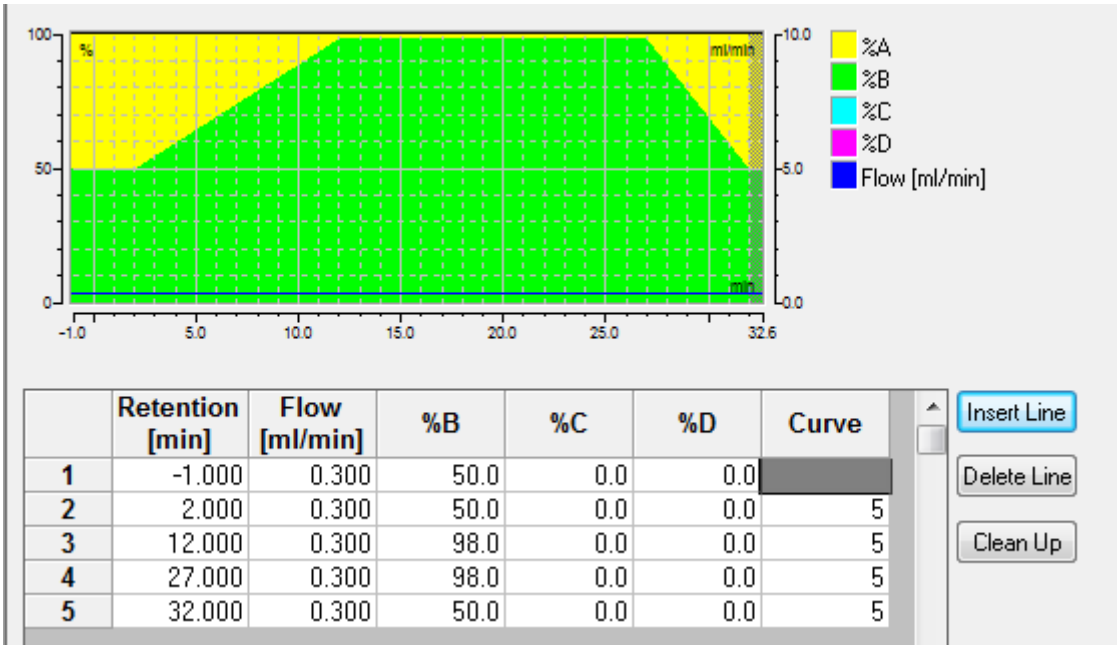

	Retention [min]	Flow [ml/min]	%B	%C	%D	Curve
1	-1.000	0.300	50.0	0.0	0.0	
2	2.000	0.300	50.0	0.0	0.0	5
3	12.000	0.300	98.0	0.0	0.0	5
4	27.000	0.300	98.0	0.0	0.0	5
5	32.000	0.300	50.0	0.0	0.0	5

Insert Line
Delete Line
Clean Up

Figure S 1: HPLC profile used throughout the analysis. The MS method is listed on the following pages. HPLC-HRMS analysis was run on an Ultimate 3000 HPLC System (consisting of a pump, autosampler, column oven and UV detector) coupled to a compact mass spectrometer (BRUKER DALTONIK GmbH, Life Sciences, Bremen, Germany) using the standard electrospray ionization source. All solvents were LC-MS grade (Chromasolv). A NUCLEODUR C18 Isis column (Macherey&Nagel, 150/2, 1.8 µm), was used for chromatographic separation. For internal calibration a lock mass of 622.028960 (Hexakis(1H,1H,2H-perfluoroethoxy)phosphazene) and sodium formiate clusters were used.

otofControl

General Information

Method Name:	110-1300 autoMSMS pos_.m	**Saved:**	2018/09/05 09:38:08+02:00
Application Name:	Bruker otofControl	**Application Version:**	4.1.3.5
Device Type:	compact	**Device Serial Number:**	8255754.20147
Operator:	Demo User	**Host:**	COMPACT-20147
Operating System:	Windows 7 Professional	**Organisation:**	Bruker Daltonik GmbH

Chromatogram

Chromatogram Traces

Enabled	Color	Type	Masses	Width	Polarity	Filter
On	Red	BPC			±	MS
On	Blue	TIC			±	MS
On	Black	TIC			±	All MS/MS

SPL

Scheduled Precursor List:	Off

Segment 1

0 .... 0.02 min

Main

Polarity:	Positive	**Scan Mode:**	MS
Mass Range from:	110 m/z	**Mass Range to:**	1300 m/z
Rolling Average:	Off	**Rolling Average No.:**	2
Spectra rate:	8.00 Hz	**View:**	Expert

Mode

Save Spectra:	Line and Profile Spectra	**Line Spectra Calculation:**	Use Maximum Intensity
Absolute Threshold (per 1000 sum.):	25 cts.	**Peak Summation Width:**	3 pts.
		Focus Active:	Off
Mark as Calibration Segment:	Off		

Source

Source:	ESI		
End Plate Offset:	500 V	**Capillary:**	4500 V
Nebulizer:	2.2 Bar	**Dry Gas:**	10.0 l/min
Dry Temp:	220 °C	**Divert Valve:**	Waste 1-6

Tune

Funnel 1 RF:	150.0 Vpp	**Funnel 2 RF:**	200.0 Vpp
isCID Energy:	0.0 eV	**Hexapole RF:**	50.0 Vpp
Ion Energy:	4.0 eV	**Low Mass:**	90.0 m/z
Collision Energy:	7.0 eV	**Pre Pulse Storage:**	5.0 µs
Stepping:	On	**Mode:**	Basic
Collision RF from:	550.0 Vpp	**Collision RF to:**	550.0 Vpp
Transfer Time from:	80.0 µs	**Transfer Time to:**	80.0 µs
Timing from:	50 %	**Timing to:**	50 %
Collision Energy from:	100 %	**Collision Energy to:**	250 %
Timing from:	50 %	**Timing to:**	50 %

MS/MS

Auto MS/MS:	Off

MRM

MRM:	Off

isCID

isCID (MS-MS/MS):	Off

bbCID

bbCID (MS-MS/MS):	Off

Segment 2

0.02 .... 0.3 min

Main

Polarity:	Positive	**Scan Mode:**	MS
Mass Range from:	110 m/z	**Mass Range to:**	1300 m/z
Rolling Average:	Off	**Rolling Average No.:**	2
Spectra rate:	8.00 Hz	**View:**	Expert

Mode

Save Spectra:	Line and Profile Spectra	**Line Spectra Calculation:**	Use Maximum Intensity
Absolute Threshold (per 1000 sum.):	25 cts.	**Peak Summation Width:**	3 pts.
		Focus Active:	Off
Mark as Calibration Segment:	On		

Source

Source:	ESI		
End Plate Offset:	500 V	**Capillary:**	4500 V
Nebulizer:	2.2 Bar	**Dry Gas:**	10.0 l/min
Dry Temp:	220 °C	**Divert Valve:**	Source 1-2

Tune

Funnel 1 RF:	150.0 Vpp	**Funnel 2 RF:**	200.0 Vpp
isCID Energy:	0.0 eV	**Hexapole RF:**	50.0 Vpp
Ion Energy:	4.0 eV	**Low Mass:**	90.0 m/z
Collision Energy:	7.0 eV	**Pre Pulse Storage:**	5.0 µs
Stepping:	On	**Mode:**	Basic
Collision RF from:	550.0 Vpp	**Collision RF to:**	550.0 Vpp
Transfer Time from:	80.0 µs	**Transfer Time to:**	80.0 µs
Timing from:	50 %	**Timing to:**	50 %
Collision Energy from:	100 %	**Collision Energy to:**	250 %
Timing from:	50 %	**Timing to:**	50 %

MS/MS

Auto MS/MS:	Off

MRM

MRM:	Off

isCID

isCID (MS-MS/MS):	Off

bbCID

bbCID (MS-MS/MS):	Off

Segment 3

0.3 .... unlimited min

Main

Polarity:	Positive	**Scan Mode:**	Auto MS/MS
Mass Range from:	110 m/z	**Mass Range to:**	1300 m/z
Rolling Average:	Off	**Rolling Average No.:**	2
Spectra rate:	8.00 Hz	**View:**	Expert

Mode

Save Spectra:	Line and Profile Spectra	**Line Spectra Calculation:**	Use Maximum Intensity
Absolute Threshold (per 1000 sum.):	25 cts.	**Peak Summation Width:**	3 pts.
		Focus Active:	Off
Mark as Calibration Segment:	Off		

Source

Source:	ESI		
End Plate Offset:	500 V	**Capillary:**	4500 V
Nebulizer:	2.2 Bar	**Dry Gas:**	10.0 l/min
Dry Temp:	220 °C	**Divert Valve:**	Waste 1-6

Tune

Funnel 1 RF:	150.0 Vpp	**Funnel 2 RF:**	200.0 Vpp
isCID Energy:	0.0 eV	**Hexapole RF:**	50.0 Vpp
Ion Energy:	4.0 eV	**Low Mass:**	90.0 m/z
Collision Energy:	7.0 eV	**Pre Pulse Storage:**	5.0 µs
Stepping:	On	**Mode:**	Basic
Collision RF from:	550.0 Vpp	**Collision RF to:**	550.0 Vpp
Transfer Time from:	80.0 µs	**Transfer Time to:**	80.0 µs
Timing from:	50 %	**Timing to:**	50 %
Collision Energy from:	100 %	**Collision Energy to:**	250 %
Timing from:	50 %	**Timing to:**	50 %

MS/MS

Auto MS/MS:	On		
Precursor Ion List:	Exclude	**Cycle Time:**	0.5 sec
Threshold (per 1000 sum.) Absolute:	400 cts	**Active Exclusion:**	On
		Exclude after:	3 Spectra
		Reconsider Precursor:	On
Release after:	0.20 min.	**Smart Exclusion:**	Off
if Curent Intens./Prev. Intens.:	1.8		
Smart Exclusion:	2 x		

Exclude Mass List

Mass Range Start	Mass Range End	
102.08	102.18	1
621.98	622.08	2
643.96	644.06	3
659.94	660.04	4

Auto MS/MS Preference

Preferred Range:	Off		
Preferred Range Low:	2	**Preferred Range High:**	5
Exclude Singly:	Off	**Exclude unknown:**	Off
Group Length:	3	**Strict Active Exclusion:**	Off
Sort Precursors by:	Intensity	**Preferred mass list:**	Empty list

Auto MS/MS Multi CE

Auto MS/MS Multi CE: Off

SILE

SILE: Off

CID

Fallback Charge State: 1 z

Isolation + Fragmentation List

Type	Mass [m/z]	Width [m/z]	Collision Energy [eV]	Charge State	
Base	100.00	4.00	20.0	1	1
Base	500.00	5.00	20.0	1	2
Base	1000.00	6.00	20.0	1	3
Base	1300.00	8.00	30.0	1	4

CID Acquisition

Acquisition:	On	**Spectra Rate MS:**	8.00 Hz
MS/MS low (per 1000 sum.):	10000.0 cts.	**MS/MS low:**	1600 x
MS/MS high:	100000.0 cts.	**MS/MS high:**	800 x
Total Cycle Time Range:	n/a sec	**Absolute Threshold :**	n/a cts.

MRM

MRM: Off

isCID

isCID (MS-MS/MS): Off

bbCID

bbCID (MS-MS/MS): Off

3 Overview of Hop-Off Intermediates

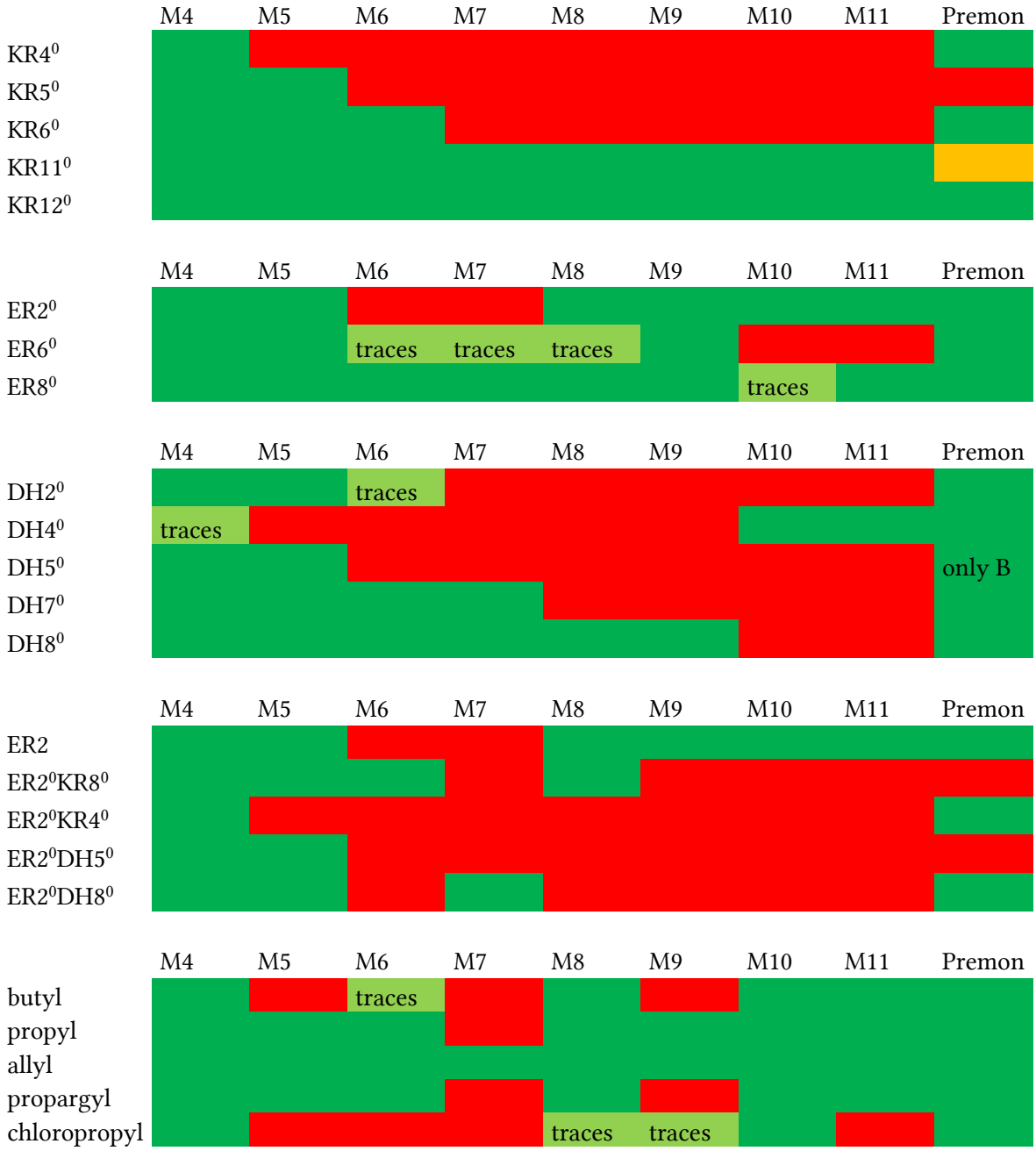

Figure S 2: Overview of the detected intermediates released from the assembly line of different mutants of *S. cinnamonensis* A495. DH: Dehydratase. KR: Ketoreductase. ER: Enoylreductase. M: Modules. Green denotes for detected intermediates released from the listed modules while red ones were not detectable. Earlier intermediates were not detected due to sample preparation and the hydrophilicity of corresponding intermediates. The last column represents the final product (a derivative of premonensin). For mutant KR11^0 a cyclisation typical for the release of premonensin is not possible and the linear product was detected. In addition to null mutants, precursor directed biosynthesis was applied and released intermediates with a new-to-nature side chain introduced in module 5 were monitored.

4 Extracted Ion Chromatograms

This chapter illustrate the extracted ion chromatograms of intermediates released in fermentations of additional null mutants and in precursor directed biosynthesis not shown in the manuscript. All traces show extracted ion chromatograms ($[M+Na]^+ \pm 0.005$ m/z). The intermediate released from module 4 is shown in green. In module 5 either a methyl or ethyl side is incorporated and hence intermediates A (blue, ethyl side chain) and B (red, methyl side chain) are detectable. Structures of detected intermediates are shown in chapter 5.

4.1 Further ER^0 Mutants

In addition to the mutant *S. cinnamonensis* A495 ER2^0 extensively discussed in the manuscript the variants ER6^0 and ER8^0 have been analyzed.

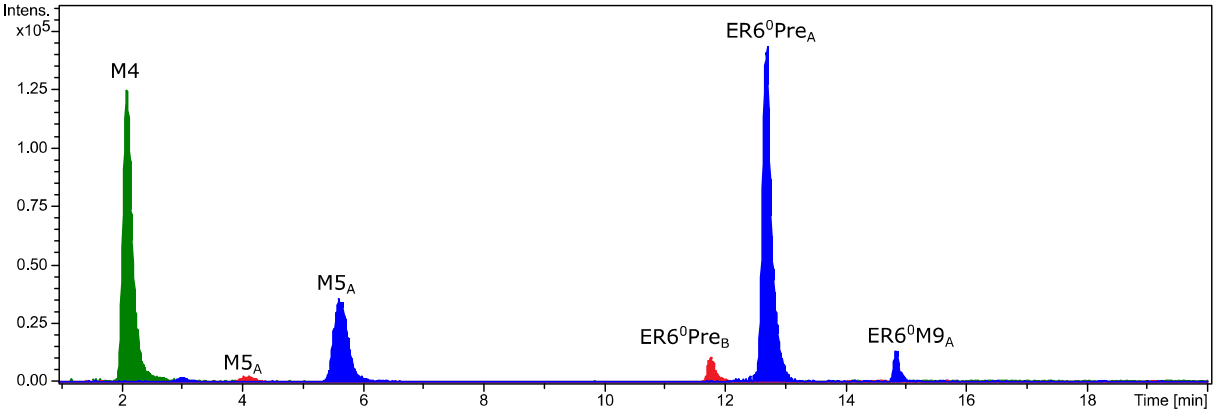

Figure S 3: Extracted ion chromatograms indicating the hop-off products (ER6^{0}MX and MX) and the final products (ER6^{0}Pre$_{A/B)}$ in a fermentation extract of *S. cinnamonensis* A495 ER6^0.

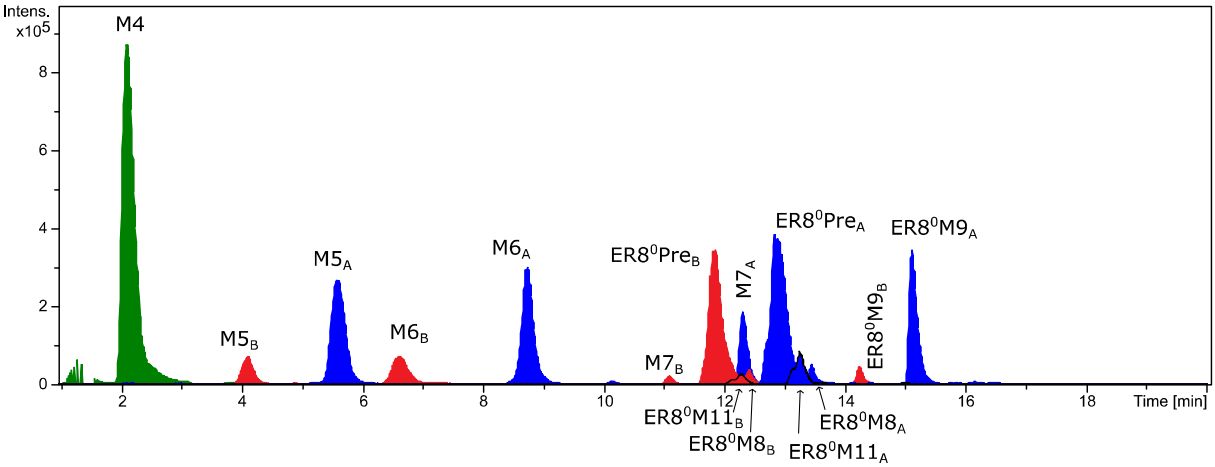

Figure S 4: Extracted ion chromatograms indicating the hop-off products (ER8^{0}MX and MX) and the final products (ER8^{0}Pre$_{A/B)}$ in a fermentation extract of *S. cinnamonensis* A495 ER8^0.

4.2 Further KR^0 Mutants

In addition to the mutants *S. cinnamonensis* A495 KR4/5/6^0 discussed in the manuscript the variants KR11^0 and KR12^0 have been analyzed.

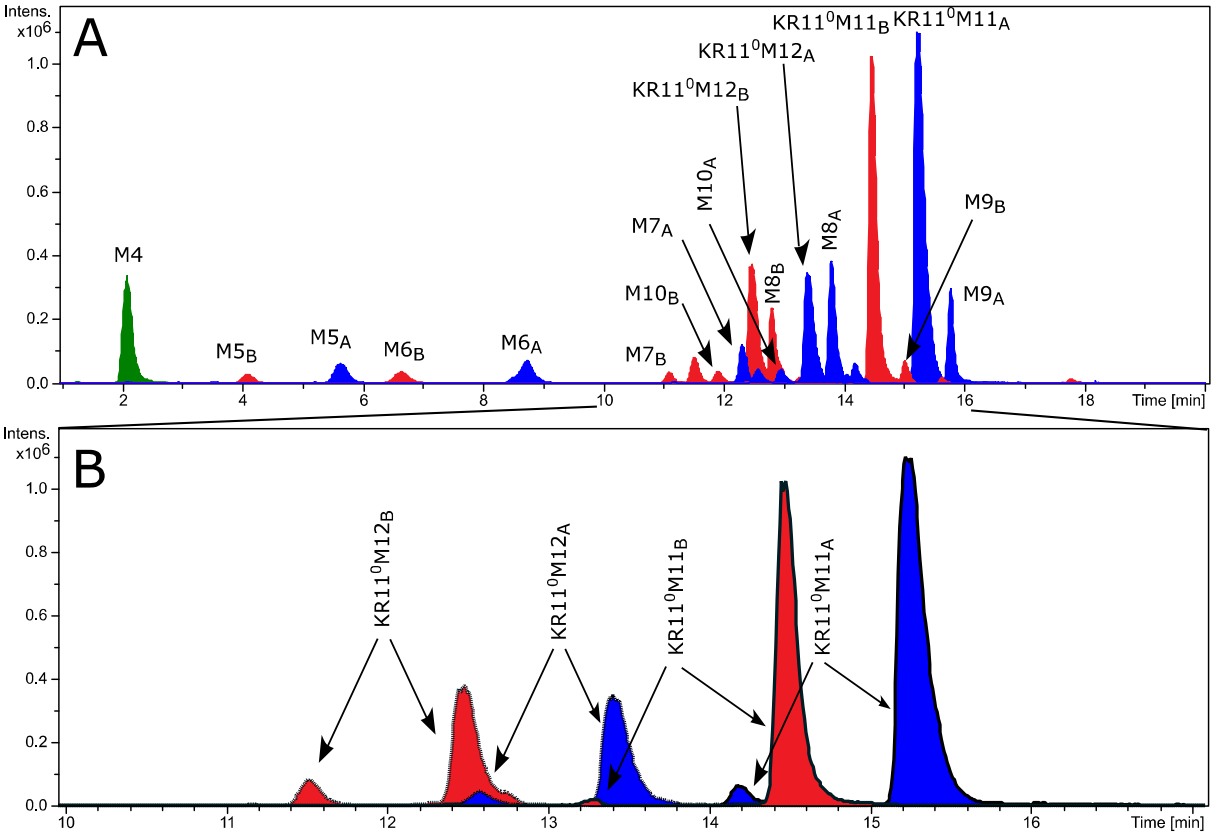

Figure S 5: A. Extracted ion chromatograms indicating the hop-off products (KR11^{0}MX and MX) and the final products (KR11^{0}M12$_{A/B}$) in a fermentation extract of *S. cinnamonensis* A495 KR11^0. A cyclization of the final products is not possible. **B.** For KR11^{0}M11$_{A/B}$ (decarboxylated) and KR11^{0}M12$_{A/B}$ two peaks each were observed with equal mass and MS^2 spectra.

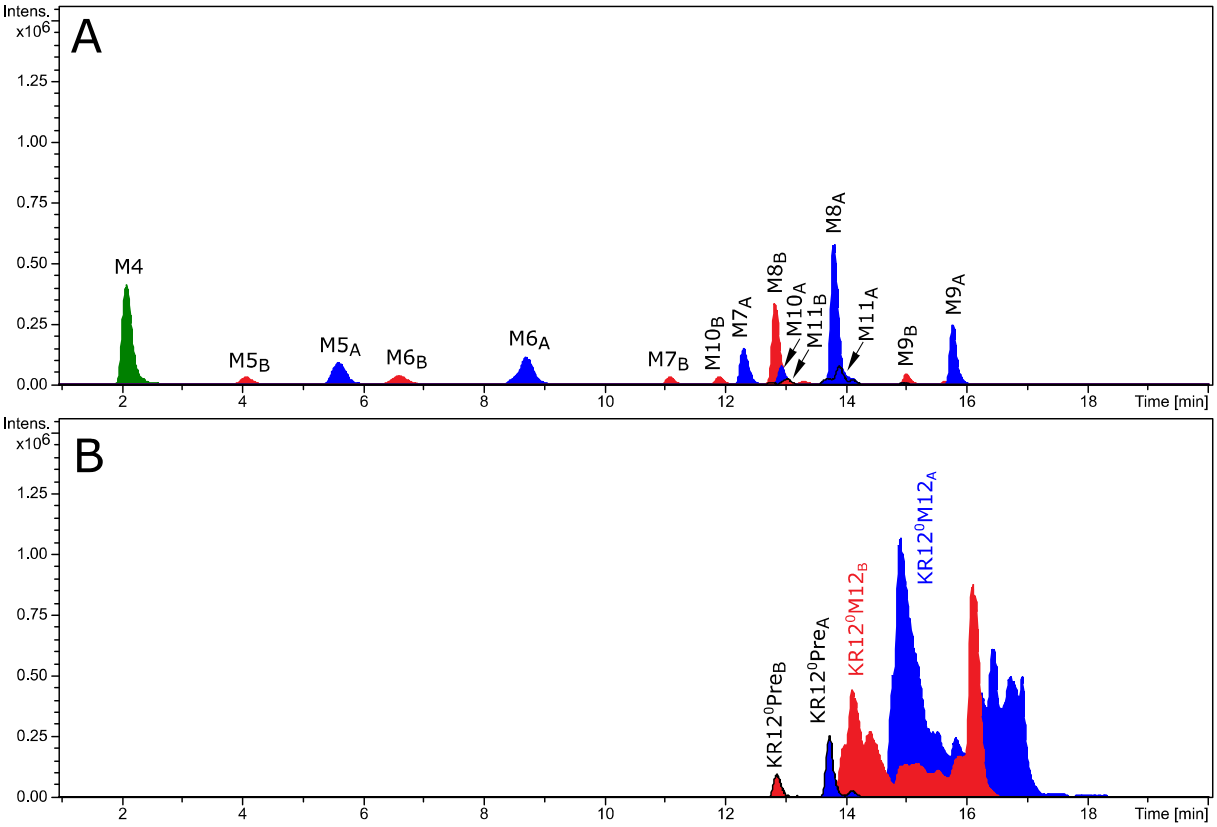

Figure S 6: A. Extracted ion chromatograms indicating the native hop-off products (M4-M11) in a fermentation extract from *S. cinnamonensis* A495 KR12^0. **B.** Extracted ion chromatograms indicating the final products (KR12^{0}Pre$_{A/B)}$ in a fermentation extract of *S. cinnamonensis* A495 KR12^0. The decarboxylated M12 hop-off products (KR12^{0}M12$_{A/B}$) elute over 2.5 minutes in the LC with identical HRMS and MS^2 spectra (see chapter 5).

4.3 DH^0 Mutants

For null mutants targeting the dehydratase domain modules 2, 4, 5, 7 and 8 were chosen for analysis.

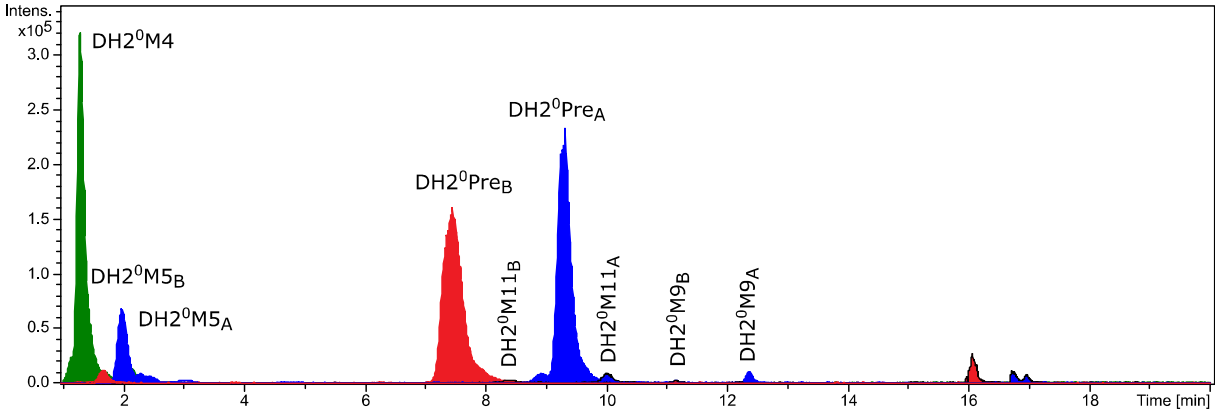

Figure S 7: Extracted ion chromatograms indicating the hop-off products (DH2^{0}MX) and the final products (DH2^{0}Pre$_{A/B)}$ in a fermentation extract of *S. cinnamonensis* A495 DH2^0.

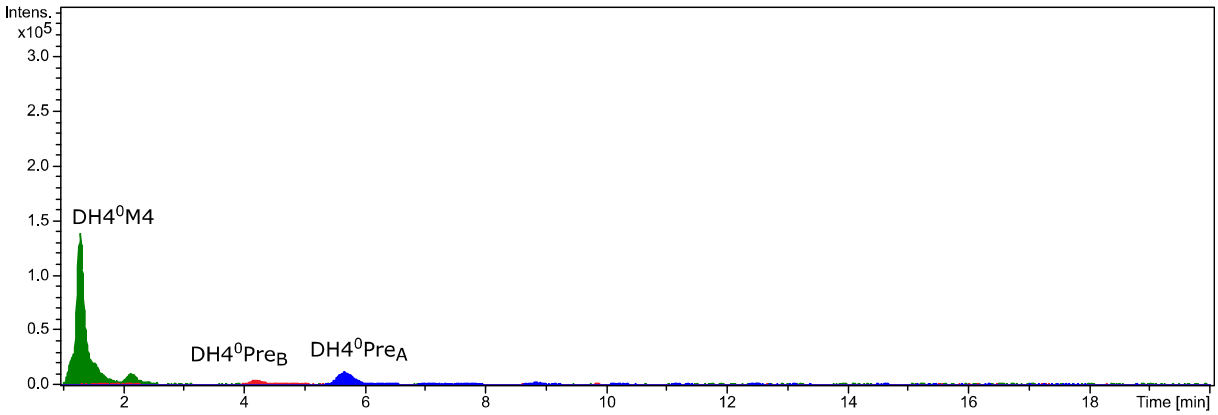

Figure S 8: Extracted ion chromatograms indicating the hop-off product (DH4^{0}M4) and the final products (DH4^{0}Pre$_{A/B)}$ in a fermentation extract of *S. cinnamonensis* A495 DH4^0.

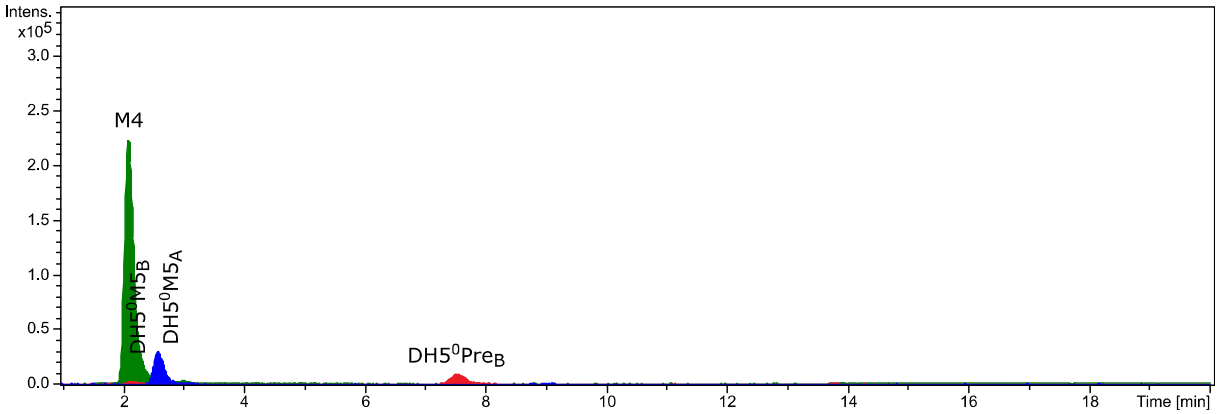

Figure S 9: Extracted ion chromatograms indicating the hop-off products (DH5^{0}M5$_{A/B}$ and the natural intermediate M4) and the final product (DH5^{0}Pre$_{B)}$ in a fermentation extract of *S. cinnamonensis* A495 DH5^0. For DH5^{0}Pre$_A$ only trace amounts have been detected.

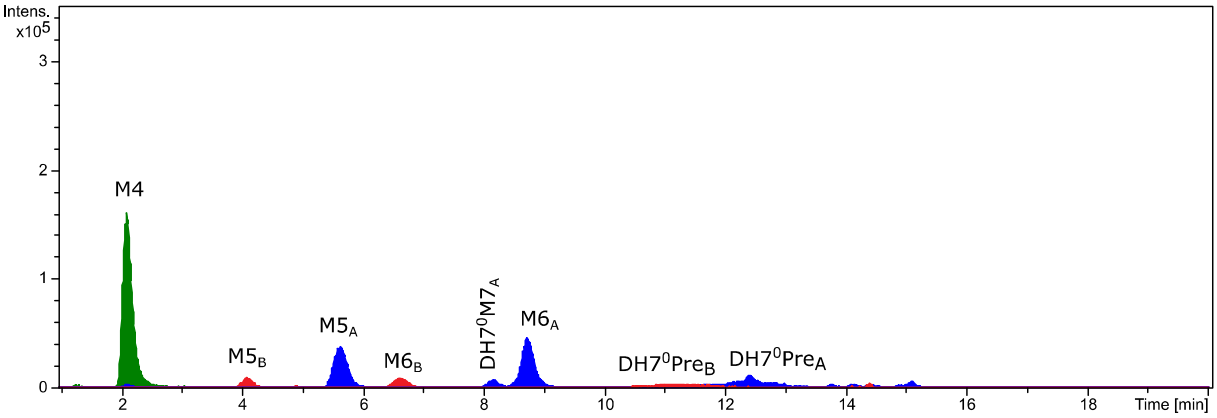

Figure S 10: Extracted ion chromatograms indicating the hop-off products ($DH7^0M7_A$ and the natural intermediates M4, $M5_{A/B}$ and $M6_{A/B}$) and the final products ($DH7^0Pre_{A/B}$) in a fermentation extract of *S. cinnamonensis* A495 $DH7^0$. The intermediate $DH7^0M7_B$ was not detectable.

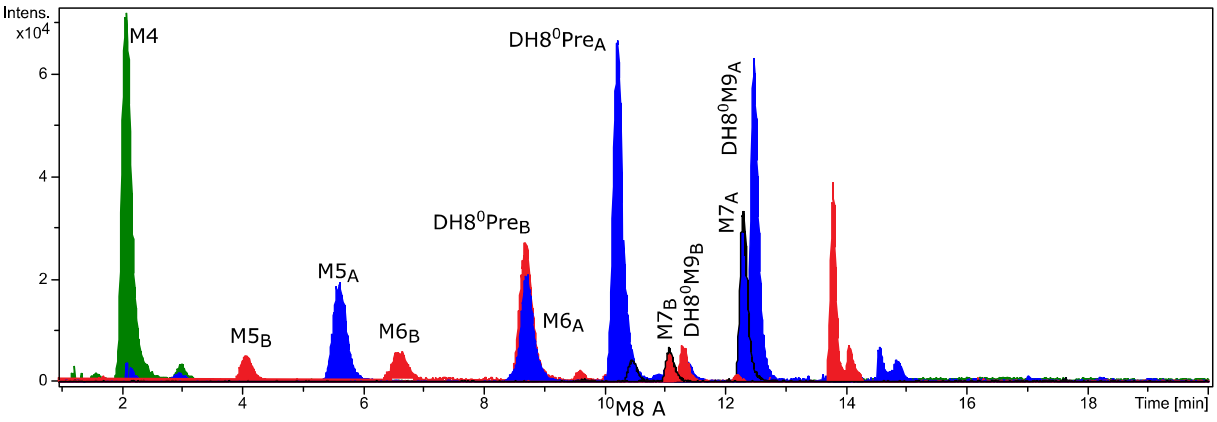

Figure S 11: Extracted ion chromatograms indicating the hop-off products ($DH5^0MX_{A/B}$ and the natural intermediate M4-7) and the final products ($DH8^0Pre_{A/B}$) in a fermentation extract of *S. cinnamonensis* A495 $DH8^0$.

4.4 Double Null Mutants

We investigated the combination of redox variations in engineered premonensin biosynthesis. Mutation $ER2^0$ was individually combined with mutations $KR4^0$, $DH5^0$, $KR8^0$ and $DH8^0$. This miniature library combined the productive $ER2^0$ mutation with one productive and one unproductive DH^0 and KR^0 variant, respectively. The assembly line regarding variants $ER2^0KR8^0$ and $ER2^0DH5^0$ ended in the targeted modules 8 and 5, respectively. By contrast, variants $ER2^0KR4^0$ and $ER2^0DH8^0$ gave rise to the corresponding doubly-modified premonensin derivatives.

Figure S 12: Extracted ion chromatograms indicating the hop-off products in a fermentation of *S. cinnamonensis* A495 ER2^{0}DH8^0. After the second targeted module (5) no further intermediates or the final products were detected.

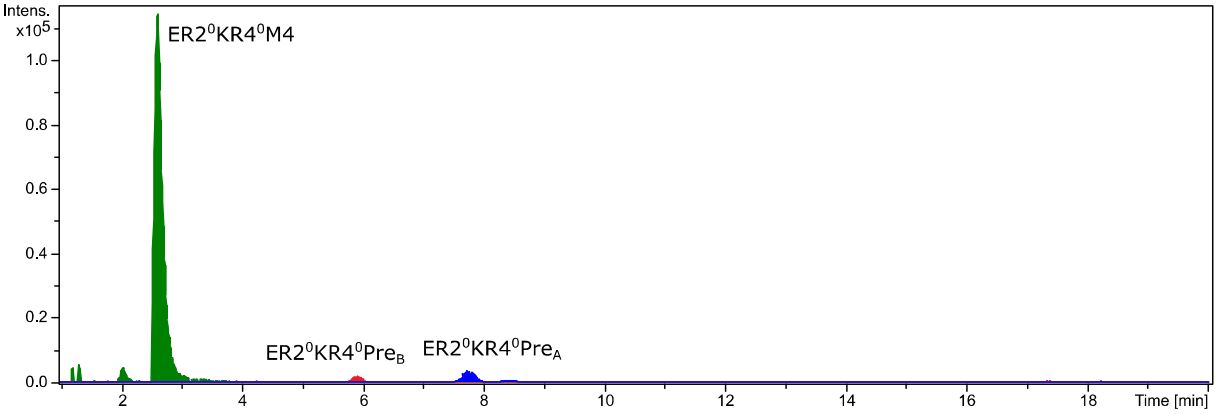

Figure S 13: Extracted ion chromatograms indicating the hop-off products and the final products in a fermentation of *S. cinnamonensis* A495 ER2^{0}KR4^0. After the second targeted module (4) no further intermediates were detected.

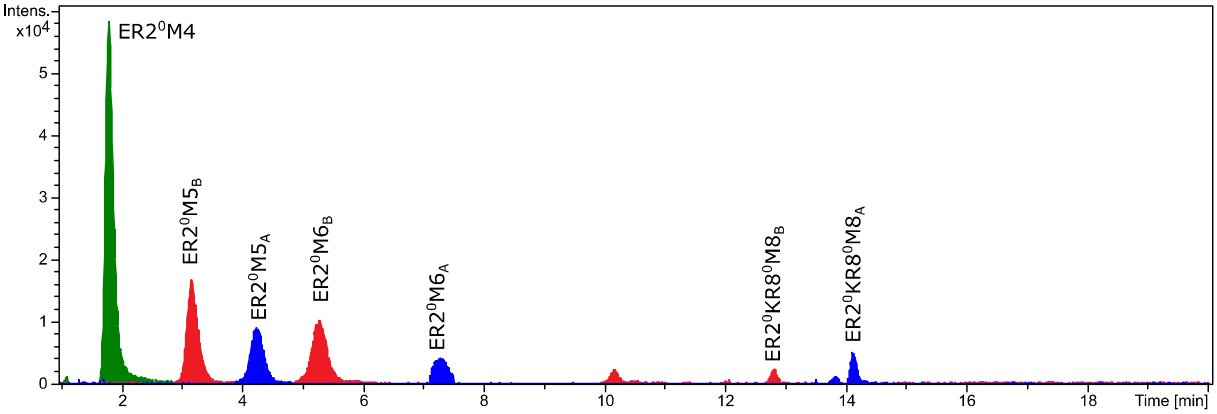

Figure S 14: Extracted ion chromatograms indicating the hop-off products in a fermentation of *S. cinnamonensis* A495 ER2^{0}KR8^0. After the second targeted module (8) no further intermediates or the final products were detected.

4.5 Precursor Directed Biosynthesis

In addition to mutagenesis-induced redox derivatizations, structural alterations in premonensin and monensin were described to be amendable by precursor-directed biosynthesis. **S**ynthetic extender unit analogues were accepted by monAT5 and incorporated into the polyketide backbone.
S. cinnamonensis A495 was fermented in the presence of allyl(All)-, propargyl(Pg)-, propyl(Pr)-, butyl(Bu)-, and chloropropyl(Cl)-substituted malonic acid diethyl ester, as described previously. As expected, all previously reported corresponding premonensin derivatives (allyl-, propargyl-, propyl- and butylpremonensin) were detected by LC-HRMS, furthermore, very small quantities of the previously undescribed chloropropylpremonensin. The following extracted ion chromatograms indicate the detected intermediates with a non-natural side chain.

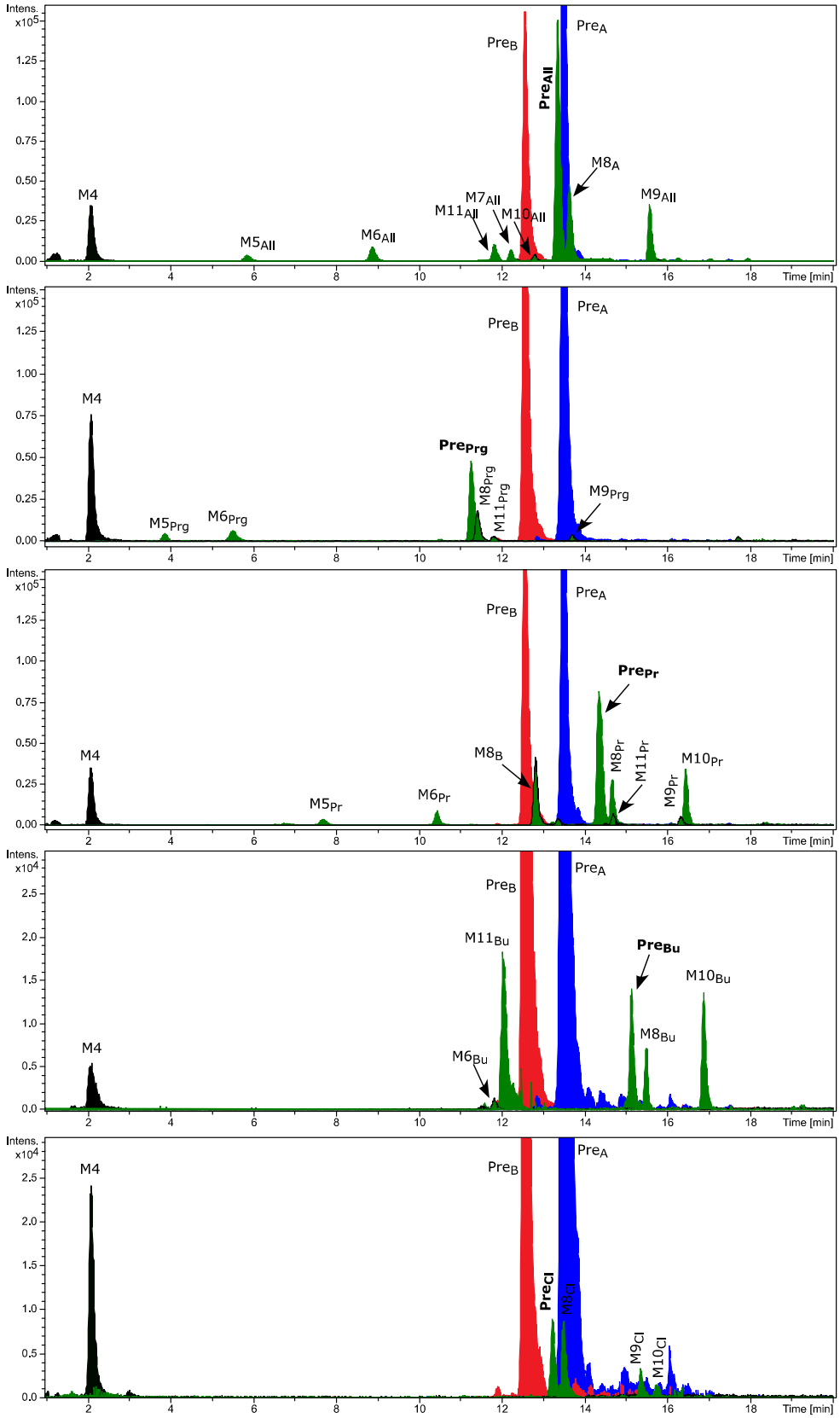

Figure S 15: Extracted ion chromatograms indicating the hop-off products in a fermentation of *S. cinnamonensis* A495 supplied with different new-to-nature building blocks. Chromatograms in green represent the released intermediates with a non-natural side chain. The usual final products $Pre_{A/B}$ are shown in the background in blue and red respectively.

5 Mass Spectrometric Data for Premonensin Derivatives and their Intermediates from the Biosynthetic Pathways

This chapter comprises all mass spectrometric data for the derivatized final products ($Pre_{A/B}$) altered trough null mutations or precursor directed biosynthesis. All mass spectrometric data of the detectable intermediates released from the respective assembly lines are shown. mSigma values represent the match of the measured and calculated isotope pattern for the sum formula calculated from the exact mass. <10: excellent agreement. <80 acceptable agreement. Especially for low intensities values are not representative or not determined (n.d.).

MS^2 data for the fragmentation of intermediates are given for the derivatized premonensin derivatives and intermediates released from modules 10 and 11. MS^2 data of earlier intermediates are omitted from the SI as they don't fragment under the given conditions. mSigma values for MS^2 data are not stated as low intensities in general resulted in not representative or not determined (n.d.) values.

In cases of very low intensities for fragment ions no high-resolution masses were obtained and are labeled with an asterisks.

5.1 Premonensin A and B ($Pre_{A/B}$) as Final Products of the Biosynthetic Assembly Line

Table S 1: Characteristic adducts of $Pre_{A/B}$.

	meas. *m/z*	ion formula	calc. *m/z*	err [ppm]	mSigma
		Pre_B			
	525.3933	$C_{34}H_{53}O_4$	525.3938	1.0	9
	543.4039	$C_{34}H_{55}O_5$	543.4044	1.0	1
	561.4146	$C_{34}H_{57}O_6$	561.4150	0.7	1
	578.4410	$C_{34}H_{60}NO_6$	578.4415	1.0	42
	583.3966	$C_{34}H_{56}NaO_6$	583.3969	0.6	3
	599.3707	$C_{34}H_{56}KO_6$	599.3708	0.2	71
		Pre_A			
	539.4087	$C_{35}H_{55}O_4$	539.4095	1.5	42
	557.4196	$C_{35}H_{57}O_5$	557.4201	0.8	3
	575.4302	$C_{35}H_{59}O_6$	575.4306	0.7	2
	592.4567	$C_{35}H_{62}NO_6$	592.4572	0.8	13
	597.4123	$C_{35}H_{58}NaO_6$	597.4126	0.4	1
	613.3862	$C_{35}H_{58}KO_6$	613.3865	0.4	74

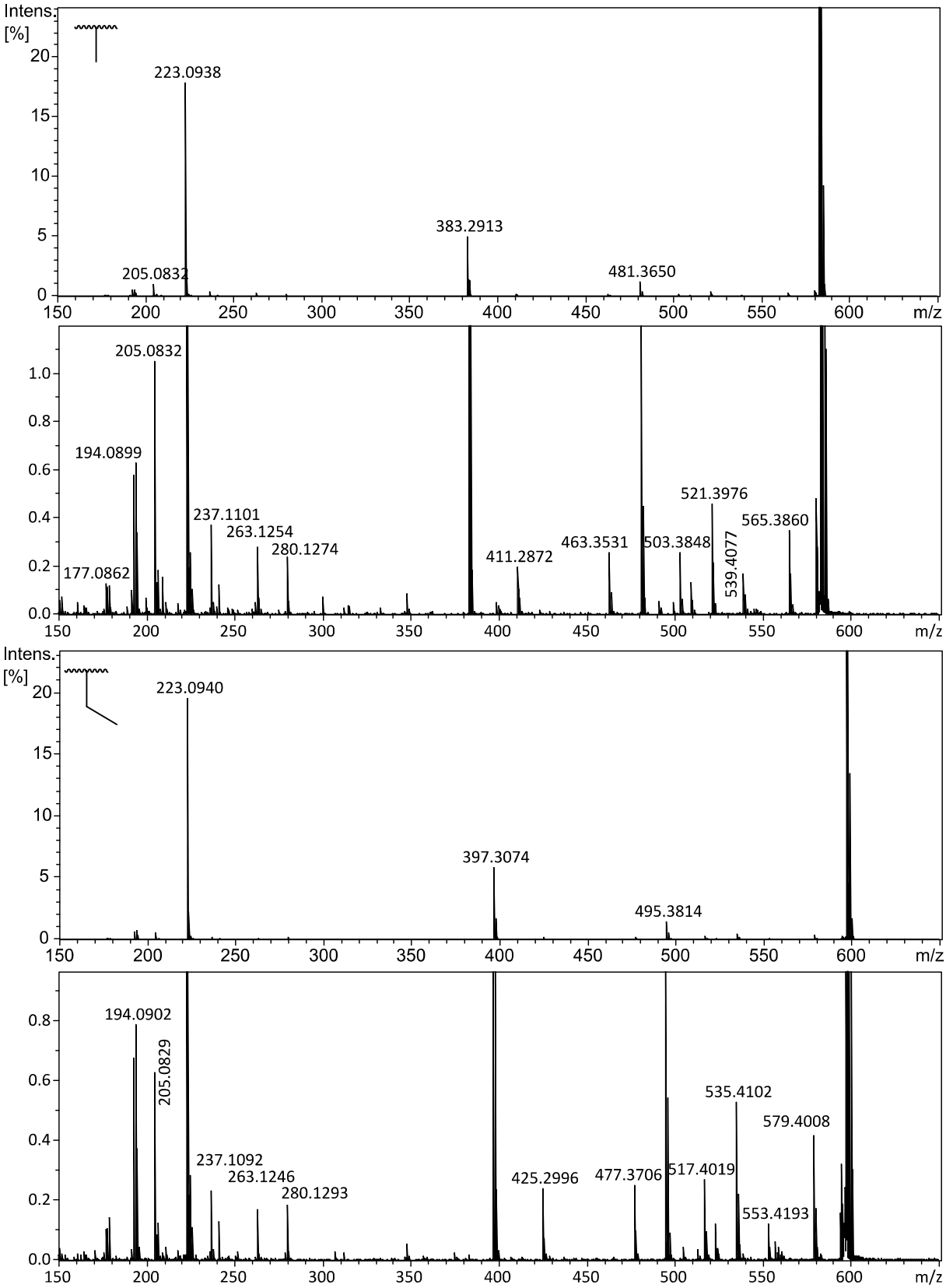

Figure S 16: MS^2 spectra of $Pre_{A/B}$.

Table S 2: Mass spectrometric data of the fragment ions of $Pre_{A/B}$.

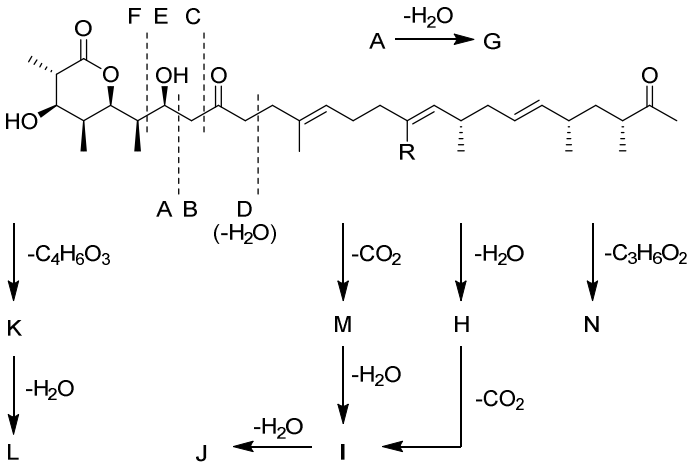

	meas. *m/z*	ion formula	*m/z*	err [ppm]
		Pre_B		
F	193.0832	$C_9H_{14}NaO_3$	193.0835	**1.8**
G	205.0832	$C_{10}H_{14}NaO_3$	205.0835	**1.4**
A	223.0938	$C_{10}H_{16}NaO_4$	223.0941	**1.4**
C	237.1101	$C_{11}H_{18}NaO_4$	237.1097	**-1.4**
D	263.1254	$C_{13}H_{20}NaO_4$	263.1254	**-0.1**
B	383.2913	$C_{24}H_{40}NaO_2$	383.2921	**1.9**
E	411.2872	$C_{25}H_{40}NaO_3$	411.2870	**-0.5**
L	463.3531	$C_{30}H_{48}NaO_2$	463.3547	**3.3**
K	481.3650	$C_{30}H_{50}NaO_3$	481.3652	**0.5**
J	503.3848	$C_{33}H_{52}NaO_2$	503.3860	**2.2**
N	509.3588	$C_{31}H_{50}NaO_4$	509.3601	**2.5**
I	521.3976	$C_{33}H_{54}NaO_3$	521.3965	**-2.2**
M	539.4077	$C_{33}H_{56}NaO_4$	539.4071	**-1.1**
H	565.3860	$C_{34}H_{54}NaO_5$	565.3863	**0.6**
		Pre_A		
F	193.0832	$C_9H_{14}NaO_3$	193.0835	**1.7**
G	205.0829	$C_{10}H_{14}NaO_3$	205.0835	**3.1**
A	223.0940	$C_{10}H_{16}NaO_4$	223.0941	**0.2**
C	237.1092	$C_{11}H_{18}NaO_4$	237.1097	**2.0**
D	263.1246	$C_{13}H_{20}NaO_4$	263.1254	**3.0**
B	397.3074	$C_{25}H_{42}NaO_2$	397.3077	**0.7**
E	425.2996	$C_{26}H_{42}NaO_3$	425.3026	**7.0**
L	477.3706	$C_{31}H_{50}NaO_2$	477.3703	**-0.6**
K	495.3814	$C_{31}H_{52}NaO_3$	495.3809	**-1.0**
J	517.4019	$C_{34}H_{54}NaO_2$	517.4016	**-0.5**
N	523.3744	$C_{32}H_{52}NaO_4$	523.3758	**2.7**
I	535.4102	$C_{34}H_{56}NaO_3$	535.4122	**3.7**
M	553.4193	$C_{34}H_{58}NaO_4$	553.4227	**6.2**
H	579.4008	$C_{35}H_{56}NaO_5$	579.4020	**2.0**

5.2 Hop-Off Products in Fermentations of *S. cinnamonensis* A495

Intermediates M4 and M5-11$_{A/B}$ released from the biosynthetic pathway were detected in extracts of fermentations using LC-HRMS. Exemplary MS spectra are shown for the most abundant intermediates M8$_B$ and M8$_A$. Mass spectrometric data for all intermediates are listed on the following page. Afterwards MS^2 analysis is given for intermediates M10$_{A/B}$, M11$_{A/B}$ and M12$_{A/B}$. M12$_{A/B}$ are non-cyclized final products detected in very low abundancies. MS^2 data of earlier intermediates are omitted from the SI as they do not fragment under the given conditions.

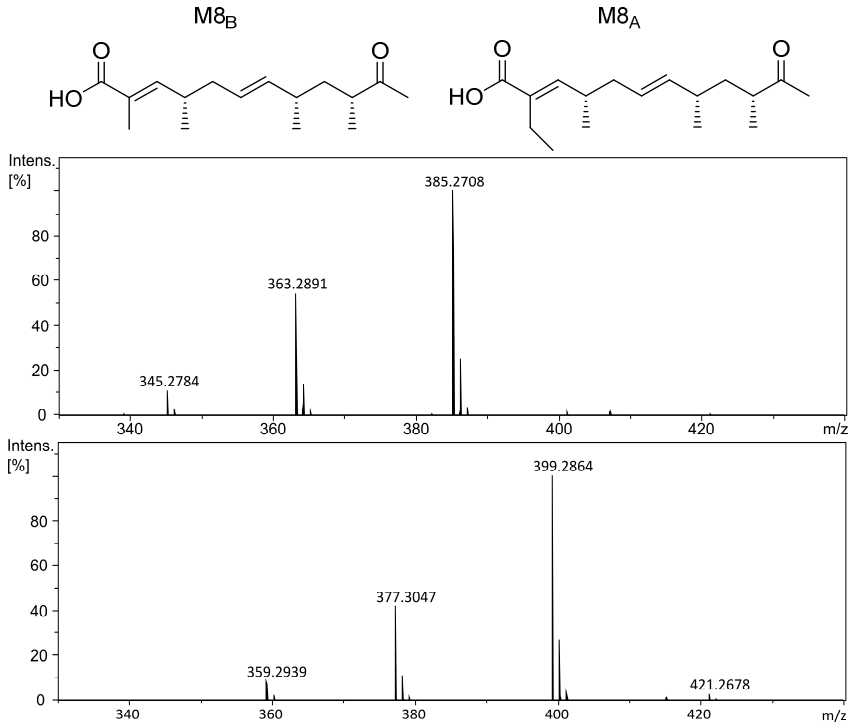

Figure S 17: Exemplary MS spectra of intermediates M8$_B$ and M8$_A$ from the premonensin biosynthetic pathway with characteristic adducts.

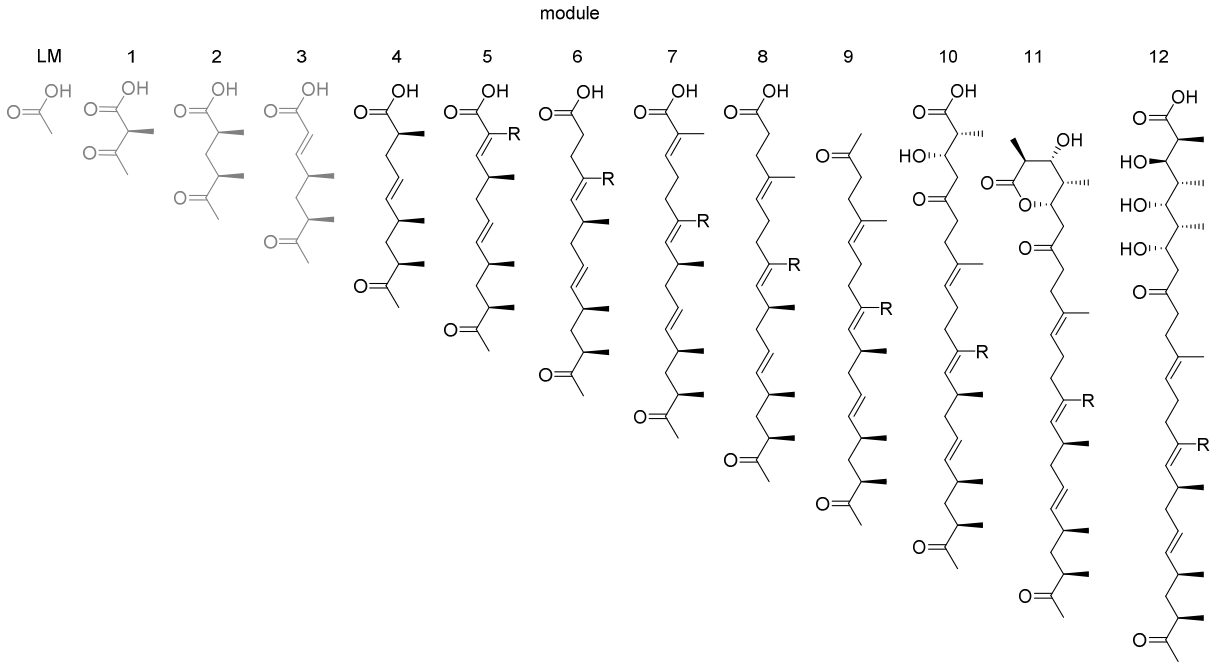

Figure S 18: Overview of the intermediates released from the assembly line of premonensin. Intermediates in grey were not detected due to sample preparation. LM = loading module.

Table S 3: Overview of the mass spectrometric data of different adducts of the hop-off intermediates released from the premonensin biosynthetic pathway in *S. cinnamonensis* A495.

	Meas. m/z	ion formula	Sum Formula	m/z	err [ppm]	mSigma
M4	209.1537	$C_{13}H_{21}O_2$	$C_{13}H_{22}O_3$	209.1536	**-0.6**	3
	227.1642	$C_{13}H_{23}O_3$		227.1642	**0.1**	2
	249.1462	$C_{13}H_{22}NaO_3$		249.1461	**-0.3**	1
M5$_B$	249.1851	$C_{16}H_{25}O_2$	$C_{16}H_{26}O_3$	249.1849	**-0.9**	17
	267.1953	$C_{16}H_{27}O_3$		267.1955	**0.5**	16
	289.1771	$C_{16}H_{26}NaO_3$		289.1774	**1.0**	12
M5$_A$	263.2004	$C_{17}H_{27}O_2$	$C_{17}H_{28}O_3$	263.2006	**0.6**	53
	281.2114	$C_{17}H_{29}O_3$		281.2111	**-1.0**	28
	303.1929	$C_{17}H_{28}NaO_3$		303.1931	**0.7**	26
M6$_B$	277.2159	$C_{18}H_{29}O_2$	$C_{18}H_{30}O_3$	277.2162	**1.1**	13
	295.2266	$C_{18}H_{31}O_3$		295.2268	**0.6**	5
	317.2084	$C_{18}H_{30}NaO_3$		317.2087	**1.1**	6
M6$_A$	291.2315	$C_{19}H_{31}O_2$	$C_{19}H_{32}O_3$	291.2319	**1.4**	33
	309.2422	$C_{19}H_{33}O_3$		309.2424	**0.6**	10
	331.2242	$C_{19}H_{32}NaO_3$		331.2244	**0.6**	9
M7$_B$	317.2472	$C_{21}H_{33}O_2$	$C_{21}H_{34}O_3$	317.2475	**1.1**	28
	335.2576	$C_{21}H_{35}O_3$		335.2581	**1.3**	19
	357.2400	$C_{21}H_{34}NaO_3$		357.2400	**0.1**	5
M7$_A$	331.2631	$C_{22}H_{35}O_2$	$C_{22}H_{36}O_3$	331.2632	**0.3**	8
	349.2735	$C_{22}H_{37}O_3$		349.2737	**0.7**	26
	371.2555	$C_{22}H_{36}NaO_3$		371.2557	**0.5**	6
M8$_B$	345.2784	$C_{23}H_{37}O_2$	$C_{23}H_{38}O_3$	345.2788	**1.3**	5
	363.2891	$C_{23}H_{39}O_3$		363.2894	**0.9**	6
	385.2708	$C_{23}H_{38}NaO_3$		385.2713	**1.3**	2
M8$_A$	359.2939	$C_{24}H_{39}O_2$	$C_{24}H_{40}O_3$	359.2945	**1.4**	5
	377.3047	$C_{24}H_{41}O_3$		377.3050	**1.0**	3
	399.2864	$C_{24}H_{40}NaO_3$		399.2870	**1.4**	3
M9$_B$	343.2990	$C_{24}H_{39}O$	$C_{24}H_{40}O_2$	343.2995	**1.5**	452
	361.3095	$C_{24}H_{41}O_2$		361.3101	**1.7**	26
	383.2913	$C_{24}H_{40}NaO_2$		383.2921	**1.9**	6
M9$_A$	357.3130	$C_{25}H_{41}O$	$C_{25}H_{42}O_2$	357.3152	**6.1**	51
	375.3251	$C_{25}H_{43}O_2$		375.3258	**1.7**	3
	397.3070	$C_{25}H_{42}NaO_2$		397.3077	**1.8**	1
M10$_B$	445.3308	$C_{28}H_{45}O_4$	$C_{28}H_{46}O_5$	445.3312	**1.0**	2
	463.3411	$C_{28}H_{47}O_5$		463.3418	**1.6**	5
	485.3234	$C_{28}H_{46}NaO_5$		485.3237	**0.8**	3
M10$_A$	459.3458	$C_{29}H_{47}O_4$	$C_{29}H_{48}O_5$	459.3469	**2.3**	6
	477.3565	$C_{29}H_{49}O_5$		477.3575	**2.0**	4
	499.3389	$C_{29}H_{48}NaO_5$		499.3394	**1.0**	4
M11$_B$	485.3623	$C_{31}H_{49}O_4$	$C_{31}H_{50}O_5$	485.3625	**0.6**	46
	503.3723	$C_{31}H_{51}O_5$		503.3731	**1.5**	8
	525.3544	$C_{31}H_{50}NaO_5$		525.3550	**1.1**	2
M11$_A$	499.3771	$C_{32}H_{51}O_4$	$C_{32}H_{52}O_5$	499.3782	**2.1**	34
	517.3881	$C_{32}H_{53}O_5$		517.3888	**1.3**	6
	539.3700	$C_{32}H_{52}NaO_5$		539.3707	**1.3**	10
M12$_B$	601.4068	$C_{34}H_{58}NaO_7$	$C_{34}H_{58}O_7$	601.4075	**1.1**	11
M12$_A$	615.4224	$C_{35}H_{60}NaO_7$	$C_{35}H_{60}O_7$	615.4231	**1.2**	11

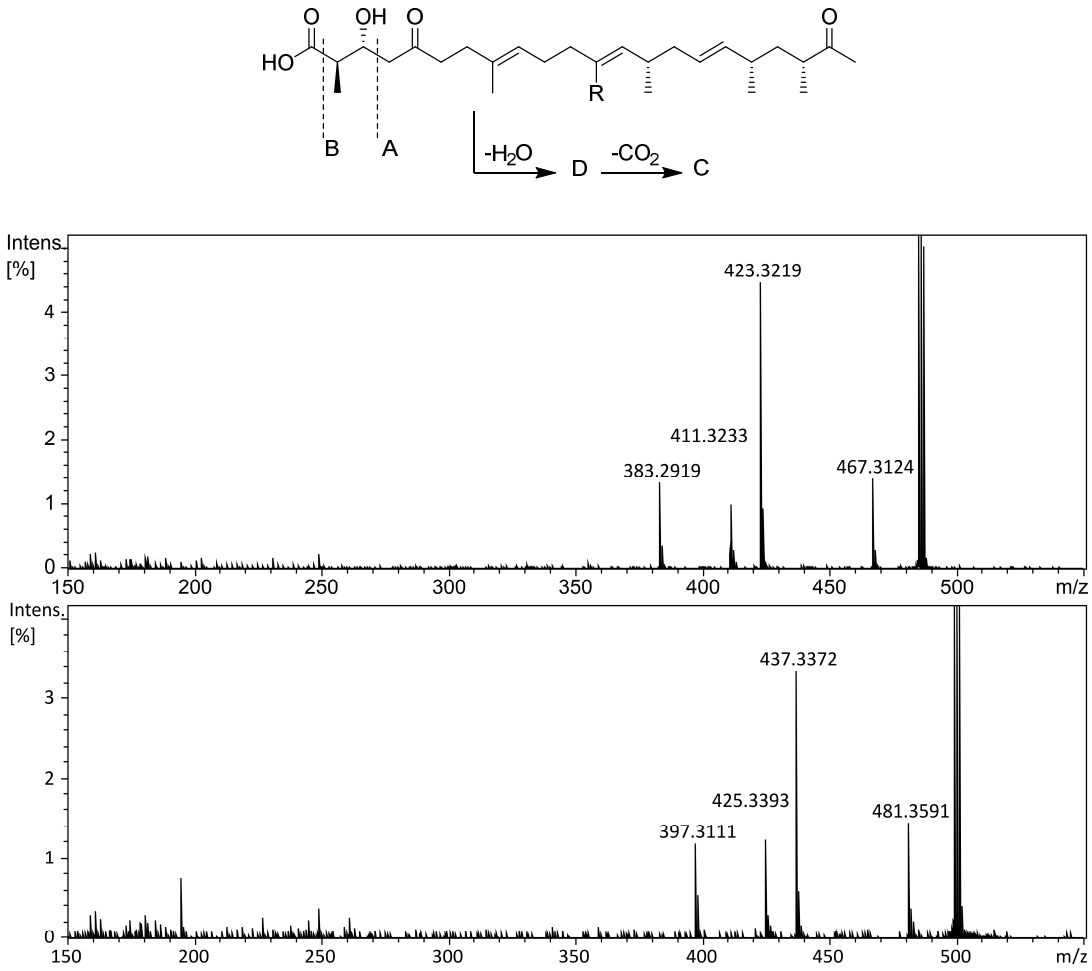

Figure S 19: MS^2 spectra of the hop-off product $M10_{A/B}$

Table S 4: Mass spectrometric data of the fragment ions of $M10_{A/B}$.

	Meas. m/z	ion formula	m/z	err [ppm]
		$M10_B$		
A	383.2919	$C_{24}H_{40}NaO_2$	383.2921	**0.5**
B	411.3233	$C_{26}H_{44}NaO_2$	411.3234	**0.2**
C	423.3219	$C_{27}H_{44}NaO_2$	423.3234	**3.5**
D	467.3124	$C_{28}H_{44}NaO_4$	467.3132	**1.6**
		$M10_A$		
A	397.3111	$C_{25}H_{42}NaO_2$	397.3077	**-8.7**
B	425.3393	$C_{27}H_{46}NaO_2$	425.3390	**-0.8**
C	437.3372	$C_{28}H_{46}NaO_2$	437.3390	**4.2**
D	481.3591	$C_{29}H_{46}NaO_4$	481.3294	**61.7**

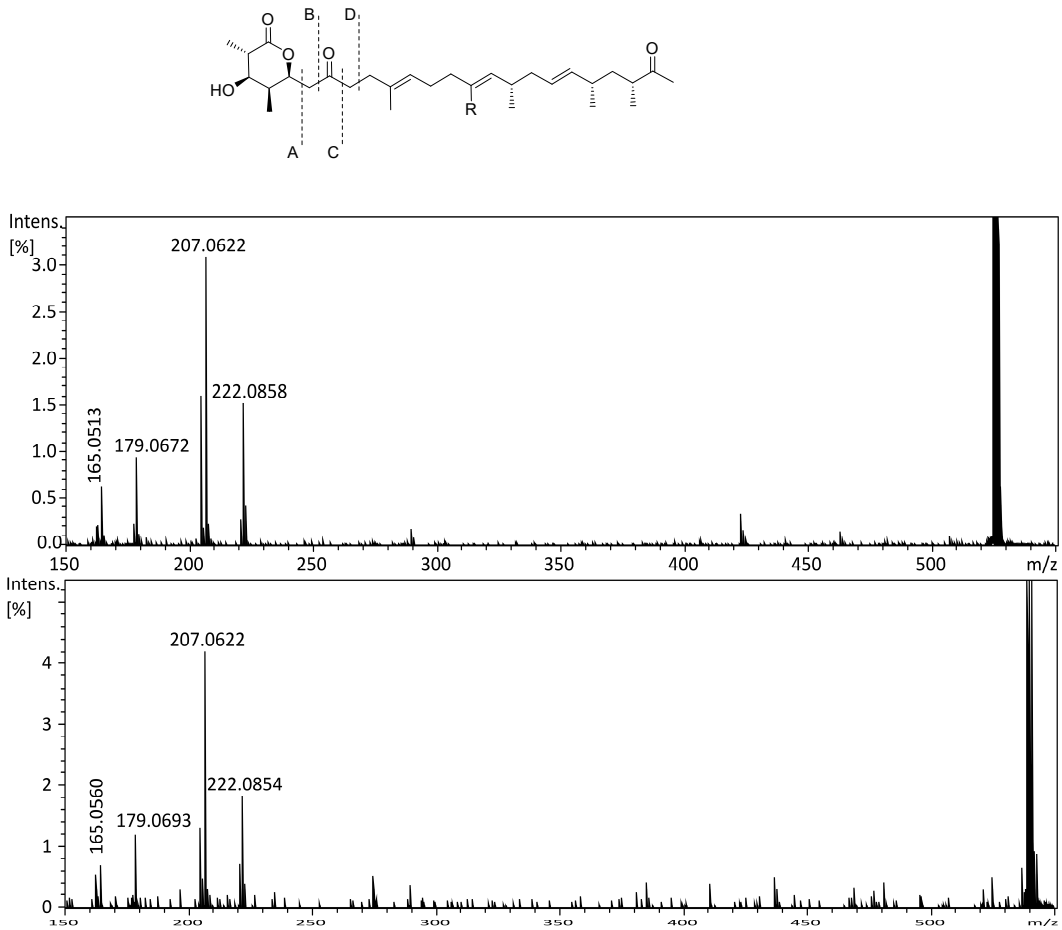

Figure S 20: MS^2 spectra of the hop-off product $M11_{A/B}$

Table S 5: Mass spectrometric data of the fragment ions of $M11_{A/B}$

Fragment	Meas. m/z	ion formula	m/z	err [ppm]
		$M11_B$		
A	165.0513	$C_7H_{10}NaO_3$	165.0522	**5.5**
B	179.0672	$C_8H_{12}NaO_3$	179.0679	**3.8**
C	207.0622	$C_9H_{12}NaO_4$	207.0628	**2.8**
D	222.0858	$C_{10}H_{15}NaO_4$	222.0863	**2.3**
		$M11_A$		
A	165.0560	$C_7H_{10}NaO_3$	165.0522	**-23.2**
B	179.0693	$C_8H_{12}NaO_3$	179.0679	**-8.2**
C	207.0622	$C_9H_{12}NaO_4$	207.0628	**2.6**
D	222.0854	$C_{10}H_{15}NaO_4$	222.0863	**4.1**

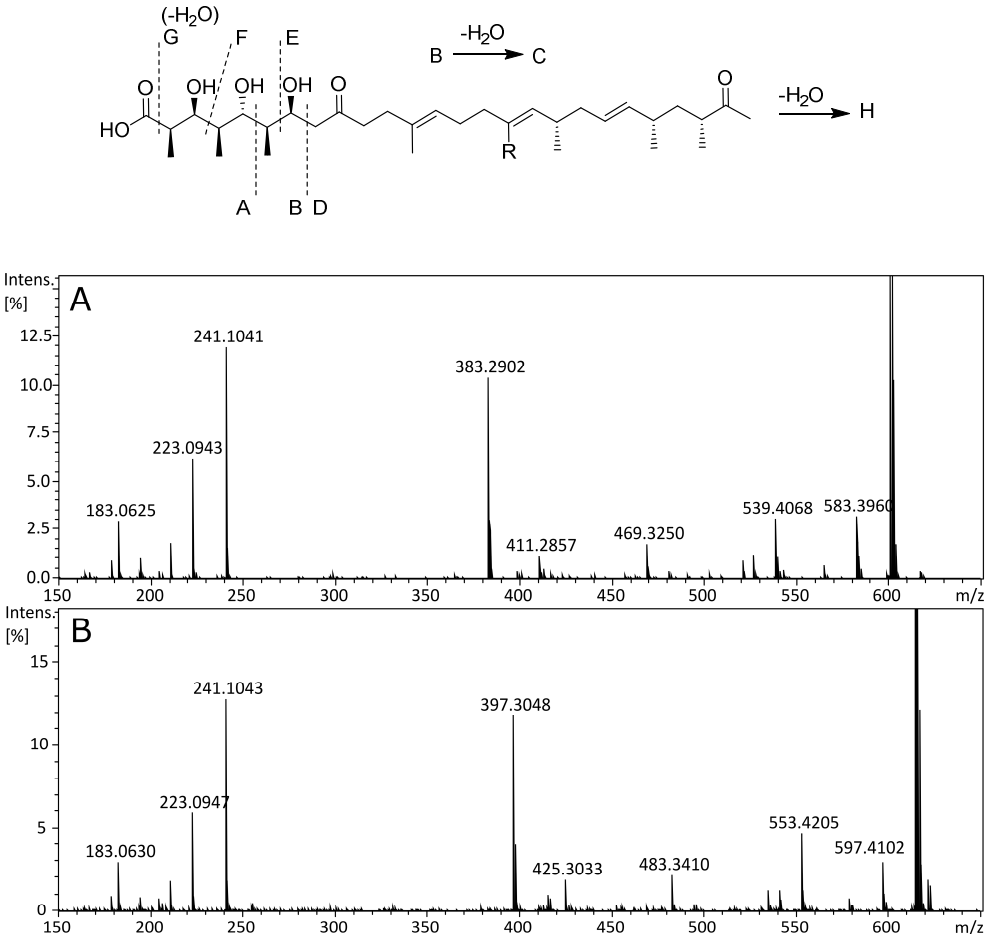

Figure S 21: MS^2 spectra of the hop-off product $M12_{A/B}$ without lactonization (only trace amounts compared to $Pre_{A/B}$)

Table S 6: Mass spectrometric data of the fragment ions of $M12_{A/B}$ without typical lactonization.

Fragment	Meas. m/z	ion formula	m/z	err [ppm]
		$M12_B$		
A	183.0625	$C_7H_{12}NaO_4$	183.0628	**1.7**
B	223.0943	$C_{10}H_{16}NaO_4$	223.0941	**-0.9**
C	241.1041	$C_{10}H_{18}NaO_5$	241.1046	**2.2**
D	383.2902	$C_{24}H_{40}NaO_2$	383.2921	**4.8**
E	411.2857	$C_{25}H_{40}NaO_3$	411.2870	**3.1**
F	469.3250	$C_{28}H_{46}NaO_4$	469.3288	**8.1**
G	539.4068	$C_{33}H_{56}NaO_4$	539.4071	**0.4**
H	583.3960	$C_{34}H_{56}NaO_6$	583.3969	**1.6**
		$M12_A$		
A	183.0630	$C_7H_{12}NaO_4$	183.0628	**-1.2**
B	223.0947	$C_{10}H_{16}NaO_4$	223.0941	**-2.8**
C	241.1043	$C_{10}H_{18}NaO_5$	241.1046	**1.5**
D	397.3048	$C_{25}H_{42}NaO_2$	397.3077	**7.3**
E	425.3033	$C_{26}H_{42}NaO_3$	425.3026	**-1.6**
F	483.3410	$C_{29}H_{48}NaO_4$	483.3445	**7.2**
G	553.4205	$C_{34}H_{58}NaO_4$	553.4227	**4.0**
H	597.4102	$C_{35}H_{58}NaO_6$	597.4126	**3.9**

5.3 ER2^0 Mutant – Premonensin Derivatives and Hop-Off Products

5.3.1 ER2^0 Premonensin A and B (ER2^{0}Pre$_{A/B}$)

Tab. 1: Characteristic adducts of ER2^{0}Pre$_{A/B}$.

	meas. m/z	ion formula	calc. m/z	err [ppm]	mSigma
		ER2^{0}Pre$_B$			
	523.3776	$C_{34}H_{51}O_4$	523.3782	**1.1**	39
	541.3881	$C_{34}H_{53}O_5$	541.3888	**1.1**	8
	559.3988	$C_{34}H_{55}O_6$	559.3993	**0.9**	1
	576.4253	$C_{34}H_{58}NO_6$	576.4259	**0.9**	42
	581.3808	$C_{34}H_{54}NaO_6$	581.3813	**0.9**	3
	597.3557	$C_{34}H_{54}KO_6$	597.3552	**-0.8**	71
		ER2^{0}Pre$_A$			
	537.3932	$C_{35}H_{53}O_4$	537.3938	**1.2**	41
	555.4034	$C_{35}H_{55}O_5$	555.4044	**1.7**	12
	573.4149	$C_{35}H_{57}O_6$	573.4150	**0.2**	4
	590.4409	$C_{35}H_{60}NO_6$	590.4415	**1.0**	45
	595.3963	$C_{35}H_{56}NaO_6$	595.3969	**1.0**	3
	611.3714	$C_{35}H_{56}KO_6$	611.3708	**-0.9**	75

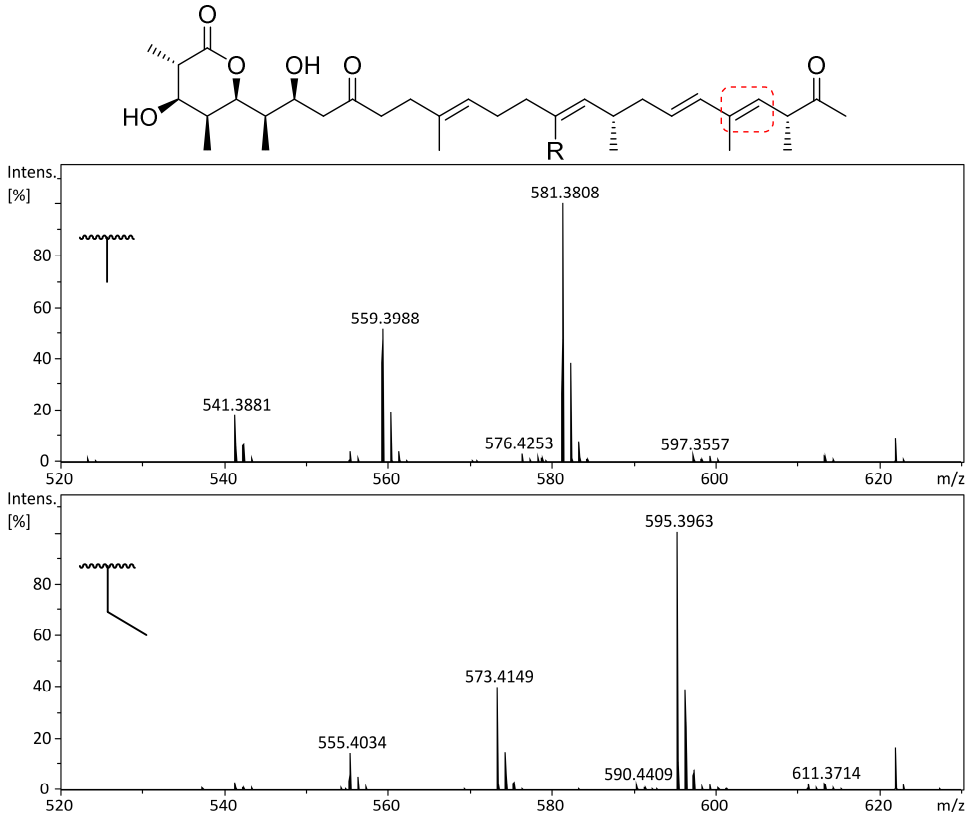

Figure S 22: MS spectra of ER2^{0}Pre$_{A/B}$ with characteristic adducts.

Table S 7: Mass spectrometric data of the fragment ions of ER2^{0}Pre$_{A/B}$.

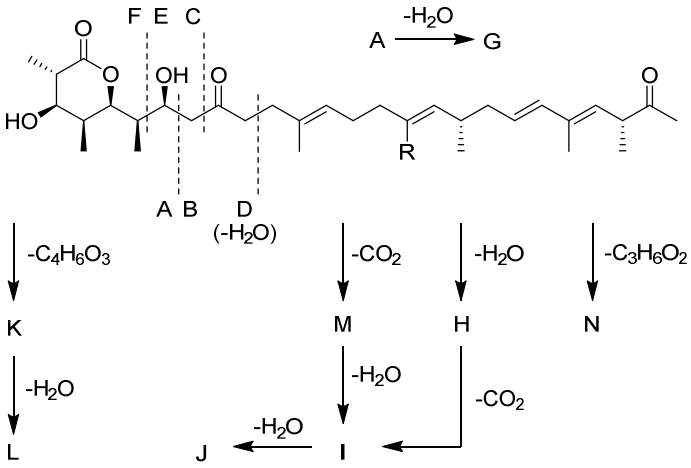

Fragment	meas. m/z	ion formula	m/z	err [ppm]
		ER2^{0}Pre$_B$		
F	193.0828	$C_9H_{14}NaO_3$	193.0835	**3.9**
G	205.0832	$C_{10}H_{14}NaO_3$	205.0835	**1.5**
A	223.0938	$C_{10}H_{16}NaO_4$	223.0941	**1.5**
C	237.1093	$C_{11}H_{18}NaO_4$	237.1097	**1.6**
D	263.1248	$C_{13}H_{20}NaO_4$	263.1254	**2.2**
B	381.2755	$C_{24}H_{38}NaO_2$	381.2764	**2.4**
E	409.2693	$C_{25}H_{38}NaO_3$	409.2713	**4.8**
L	461.3419	$C_{30}H_{46}NaO_2$	461.3390	**-6.2**
K	479.3481	$C_{30}H_{48}NaO_3$	479.3496	**3.0**
J	501.3716	$C_{33}H_{50}NaO_2$	501.3703	**-2.5**
N	507*			
I	519.3810	$C_{33}H_{52}NaO_3$	519.3809	**-0.2**
M	537*			
H	563.3679	$C_{34}H_{52}NaO_5$	563.3707	**5.1**
		ER2^{0}Pre$_A$		
F	193.0839	$C_9H_{14}NaO_3$	193.0835	**-2.0**
G	205.0836	$C_{10}H_{14}NaO_3$	205.0835	**-0.4**
A	223.0933	$C_{10}H_{16}NaO_4$	223.0941	**3.4**
C	237.1090	$C_{11}H_{18}NaO_4$	237.1097	**3.2**
D	263.1232	$C_{13}H_{20}NaO_4$	263.1254	**8.3**
B	395.291	$C_{25}H_{40}NaO_2$	395.2921	**2.8**
E	423*			
L	475*			
K	493.3682	$C_{31}H_{50}NaO_3$	493.3652	**-6.1**
J	515*			
N	-			
I	533*			
M	-			
H	577.3807	$C_{31}H_{54}NaO_8$	577.3711	**-16.7**

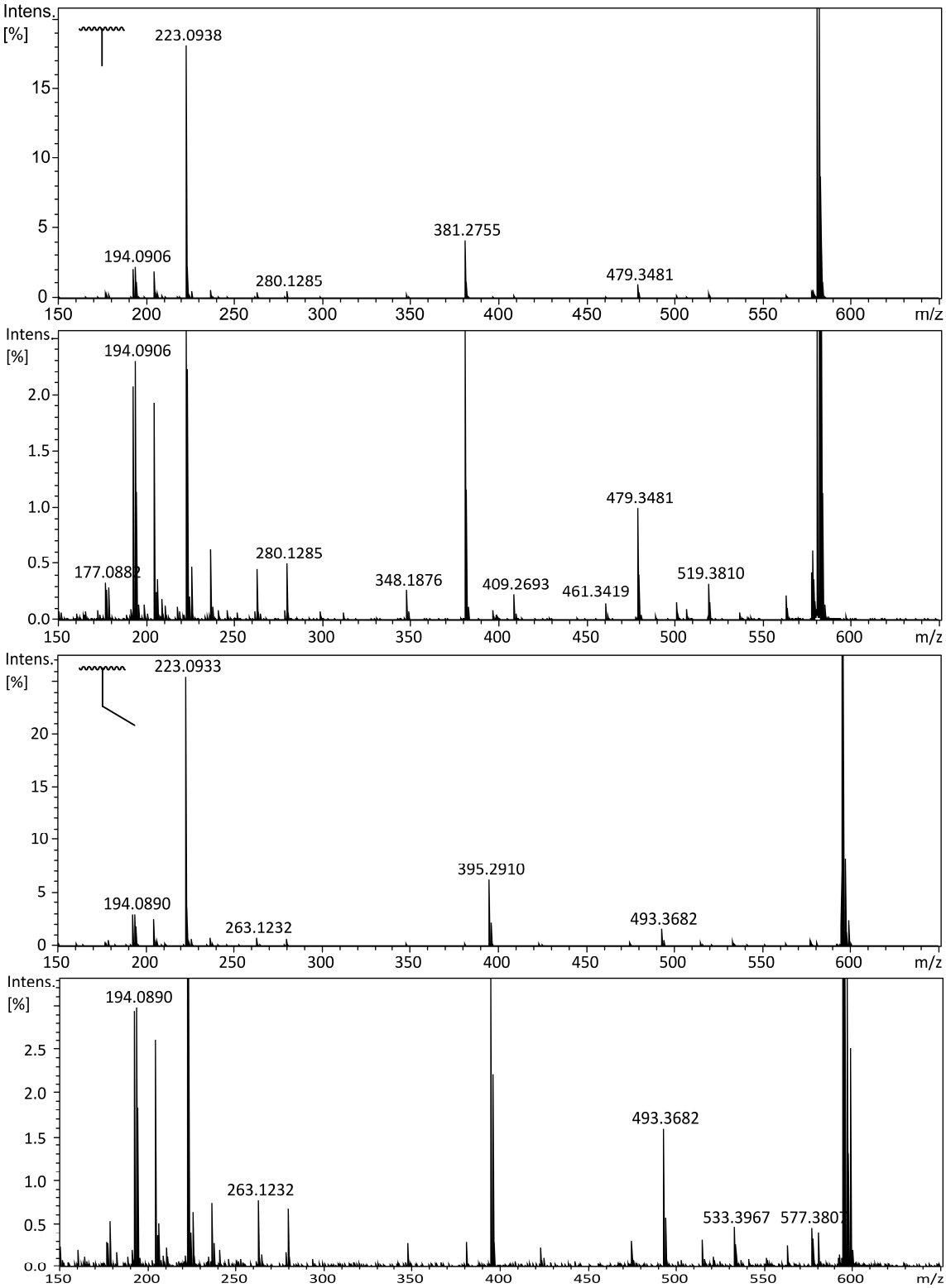

Figure S 23: MS^2 spectra of $ER2^0Pre_{A/B}$.

5.3.2 Hop-Off Products ER2^0

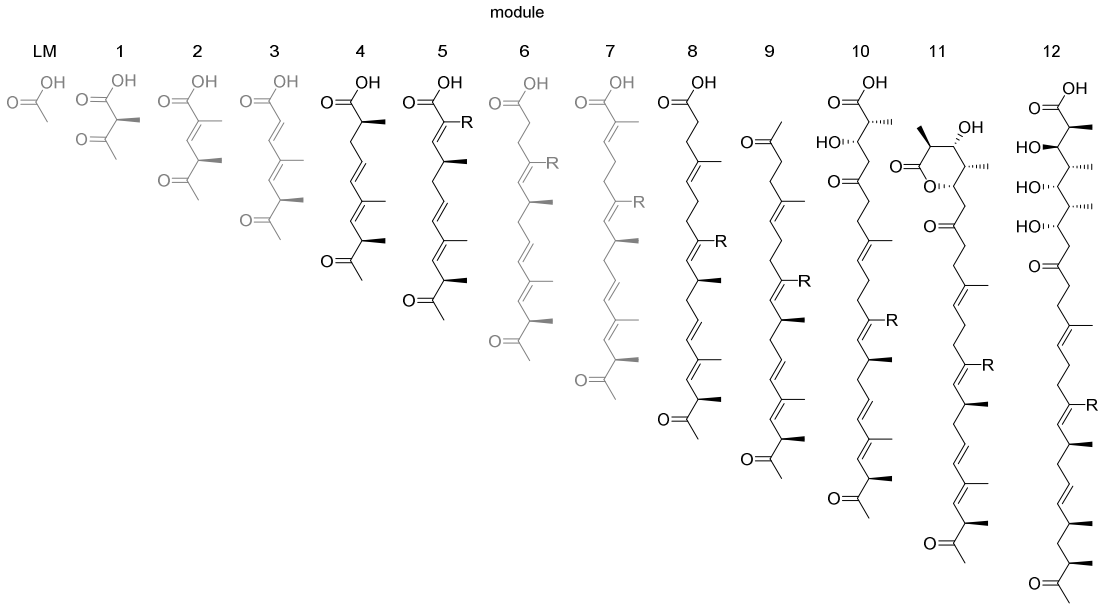

Figure S 24: Overview of the intermediates released from the assembly line of premonensin. Intermediates released from module 6 and 7 were not detectable. LM = loading module.

Table S 8: Overview of the mass spectrometric data of different adducts of the hop-off intermediates from the premonensin biosynthetic pathway in *S. cinnamonensis* A495 ER2^0.

	Meas. m/z	ion formula	Sum Formula	m/z	err [ppm]	mSigma
ER2^{0}M4	207.1362	$C_{13}H_{19}O_2$	$C_{13}H_{20}O_3$	207.1356	**-3.3**	173
	225.1483	$C_{13}H_{21}O_3$		225.1485	**0.8**	20
	247.1312	$C_{13}H_{20}NaO_3$		247.1305	**-2.8**	83
ER2^{0}M5$_B$	247.1675	$C_{16}H_{23}O_2$	$C_{16}H_{24}O_3$	247.1693	**7.2**	20
	265.1800	$C_{16}H_{25}O_3$		265.1798	**-0.6**	143
	287.1619	$C_{16}H_{24}NaO_3$		287.1618	**-0.5**	15
ER2^{0}M5$_A$	261.1842	$C_{17}H_{25}O_2$	$C_{17}H_{26}O_3$	261.1849	**2.8**	35
	279.1965	$C_{17}H_{27}O_3$		279.1955	**-3.9**	50
	301.1771	$C_{17}H_{26}NaO_3$		301.1774	**1.0**	23
ER2^{0}M8$_B$	361.2731	$C_{23}H_{37}O_3$	$C_{23}H_{36}O_3$	361.2737	**1.7**	23
	383.2550	$C_{23}H_{36}NaO_3$		383.2557	**1.6**	10
ER2^{0}M8$_A$	375.2887	$C_{24}H_{39}O_3$	$C_{24}H_{38}O_3$	375.2894	**1.7**	25
	397.2709	$C_{24}H_{38}NaO_3$		397.2713	**1.1**	23
ER2^{0}M9$_B$	381.2760	$C_{24}H_{38}NaO_2$	$C_{24}H_{38}O_2$	381.2764	**1.1**	4
ER2^{0}M9$_A$	395.2917	$C_{25}H_{40}NaO_2$	$C_{25}H_{40}O_2$	395.2921	**0.9**	7
ER2^{0}M10$_B$	443.3159	$C_{28}H_{43}O_4$	$C_{28}H_{44}O_5$	443.3156	**-0.7**	35
	461.3251	$C_{28}H_{45}O_5$		461.3262	**2.3**	29
	483.3091	$C_{28}H_{44}NaO_5$		483.3081	**-2.0**	29
ER2^{0}M10$_A$	467.3125	$C_{29}H_{45}NaO_4$	$C_{29}H_{46}O_5$	467.3132	**1.4**	43
	475.3403	$C_{29}H_{47}O_5$		475.3418	**3.1**	n.a.
	497.3240	$C_{29}H_{46}NaO_5$		497.3237	**-0.6**	33
ER2^{0}M11$_B$	501.3578	$C_{31}H_{49}O_5$	$C_{31}H_{48}O_5$	501.3575	**-0.6**	211
	523.3394	$C_{31}H_{48}NaO_5$		523.3394	**0.0**	44
ER2^{0}M11$_A$	515.3691	$C_{32}H_{51}O_5$	$C_{32}H_{50}O_5$	515.3731	**7.8**	111
	537.3517	$C_{32}H_{50}NaO_5$		537.3550	**6.1**	51
ER2^{0}M12$_B$	599.3913	$C_{34}H_{56}NaO_7$	$C_{34}H_{56}O_7$	599.3918	**0.9**	4
ER2^{0}M12$_A$	613.4067	$C_{35}H_{58}NaO_7$	$C_{35}H_{58}O_7$	613.4075	**1.3**	3

Table S 9: Mass spectrometric data of the fragment ions of ER2^{0}M12$_{A/B}$ without the typical lactonization. For the fragmentation pattern see Figure S 21. For further hop-off products no MS^2 spectra were recorded due to very low intensity in MS1 (ER2^{0}M12$_{A/B}$).

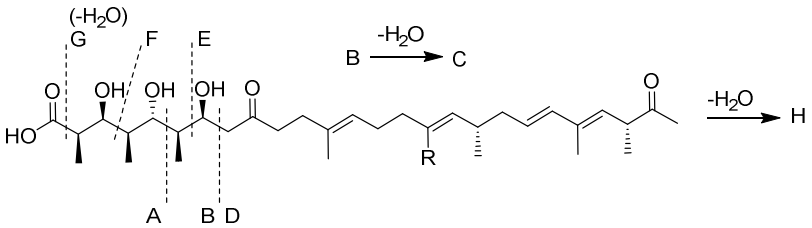

Fragment	Meas. m/z	ion formula	m/z	err [ppm]
		ER2^{0}M12$_B$		
A	183.0624	$C_7H_{12}NaO_4$	183.0628	**2.0**
B	223.0935	$C_{10}H_{16}NaO_4$	223.0941	**2.8**
C	241.1041	$C_{10}H_{18}NaO_5$	241.1046	**2.4**
D	381.2749	$C_{24}H_{38}NaO_2$	381.2764	**4.0**
E	409.2697	$C_{25}H_{38}NaO_3$	409.2713	**3.9**
F	467.3136	$C_{28}H_{44}NaO_4$	467.3132	**-1.0**
G	537.3895	$C_{33}H_{54}NaO_4$	537.3914	**3.5**
H	581.3789	$C_{34}H_{54}NaO_6$	581.3813	**4.1**
		ER2^{0}M12$_A$		
A	183.0638	$C_7H_{12}NaO_4$	183.0628	**-5.7**
B	223.0939	$C_{10}H_{16}NaO_4$	223.0941	**1.0**
C	241.1035	$C_{10}H_{18}NaO_5$	241.1046	**4.5**
D	395.2904	$C_{25}H_{40}NaO_2$	395.2921	**4.3**
E	423.2855	$C_{26}H_{40}NaO_3$	423.2870	**3.5**
F	481.3265	$C_{29}H_{46}NaO_4$	481.3288	**4.9**
G	551.4059	$C_{34}H_{56}NaO_4$	551.4071	**2.2**
H	595.3979	$C_{35}H_{56}NaO_6$	595.3969	**-1.7**

5.4 Further ER^0 Mutants – Premonensin Derivatives and Hop-Off Products

5.4.1 ER6^0 Premonensin A and B

Tab. 2: Mass spectrometric data of characteristic adducts of ER6^{0}Pre$_{A/B}$.

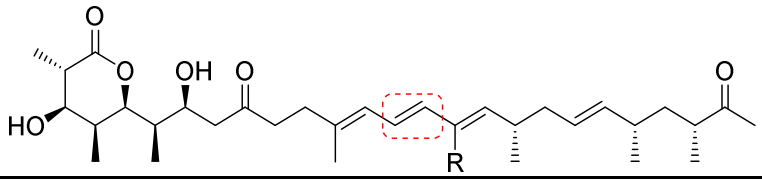

	meas. m/z	ion formula	calc. m/z	err [ppm]	mSigma
		ER6^{0}Pre$_B$			
	559.3991	$C_{34}H_{55}O_6$	559.3993	**0.4**	16
	576.4238	$C_{34}H_{58}NO_6$	576.4259	**3.6**	44
	581.3807	$C_{34}H_{54}NaO_6$	581.3813	**0.9**	16
	597.3546	$C_{34}H_{54}KO_6$	597.3552	**1.0**	19
		ER6^{0}Pre$_A$			
	573.4143	$C_{35}H_{57}O_6$	573.4150	**1.1**	5
	590.4407	$C_{35}H_{60}NO_6$	590.4415	**1.5**	49
	595.3963	$C_{35}H_{56}NaO_6$	595.3969	**0.9**	3
	611.3706	$C_{35}H_{56}KO_6$	611.3708	**0.4**	34

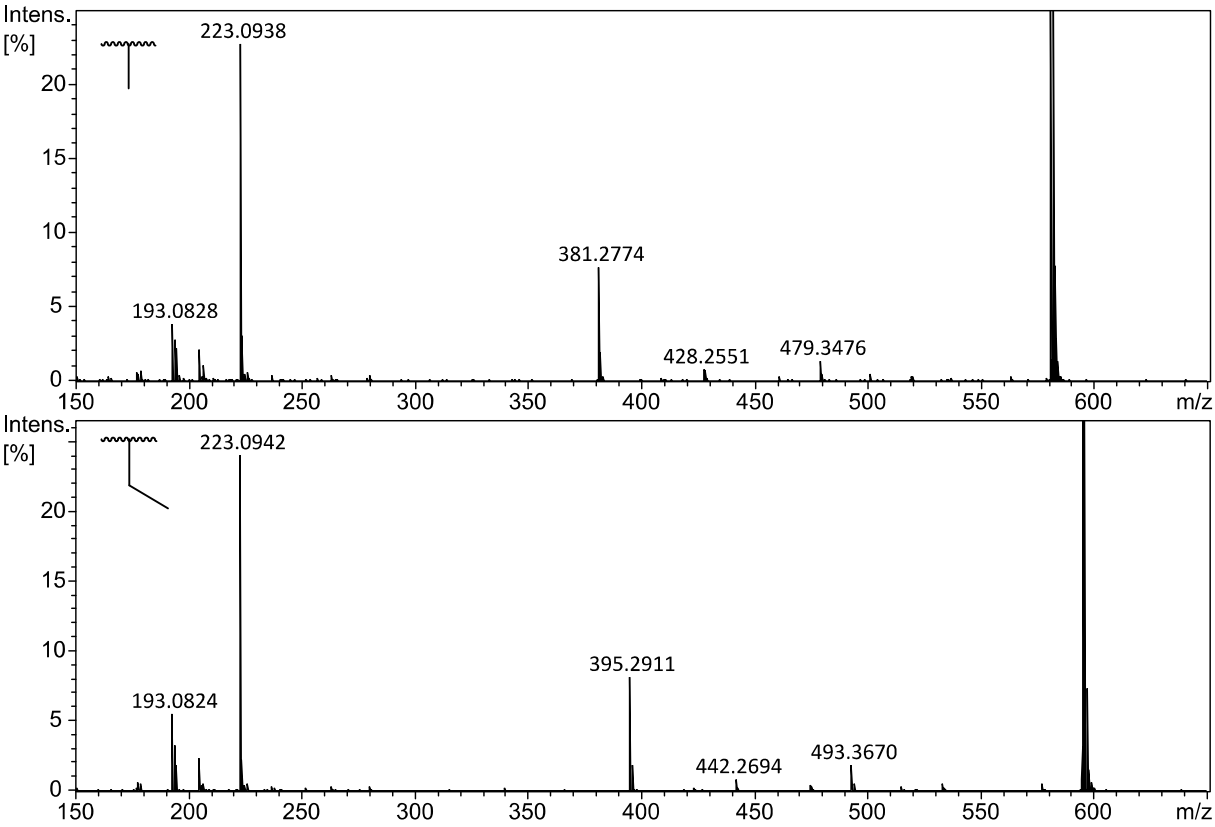

Figure S 25: MS^2 spectra of ER6^{0}Pre$_{A/B}$.

Table S 10: Mass spectrometric data of the fragment ions of ER6^{0}Pre$_{A/B}$.

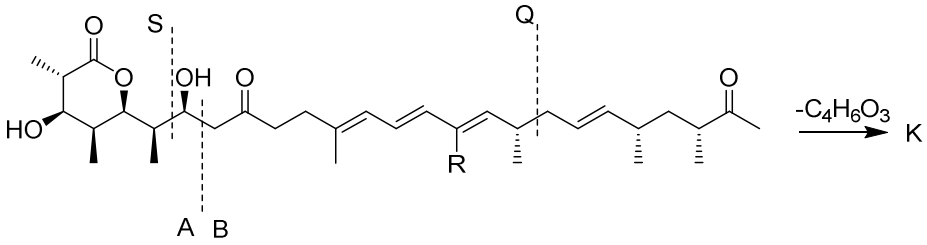

Fragment	Meas. m/z	ion formula	m/z	err [ppm]
		ER6^{0}Pre$_B$		
S	193.0828	$C_9H_{14}NaO_3$	193.0835	**3.5**
A	223.0938	$C_{10}H_{16}NaO_4$	223.0941	**1.2**
Q	428.2551	$C_{24}H_{37}NaO_5$	428.2533	**-4.1**
B	381.2774	$C_{24}H_{38}NaO_2$	381.2764	**-2.6**
K	479.3476	$C_{30}H_{48}NaO_3$	479.3496	**4.2**
		ER6^{0}Pre$_A$		
S	193.0824	$C_9H_{14}NaO_3$	193.0835	**5.7**
A	223.0942	$C_{10}H_{16}NaO_4$	223.0941	**-0.3**
Q	442.2694	$C_{25}H_{39}NaO_5$	442.2690	**-1.0**
B	395.2911	$C_{25}H_{40}NaO_2$	395.2921	**2.4**
K	493.3670	$C_{31}H_{50}NaO_3$	493.3652	**-3.6**

5.4.2 ER8^0 Premonensin A and B

Table S 11: Mass spectrometric data of characteristic adducts of ER8^{0}Pre$_{A/B}$.

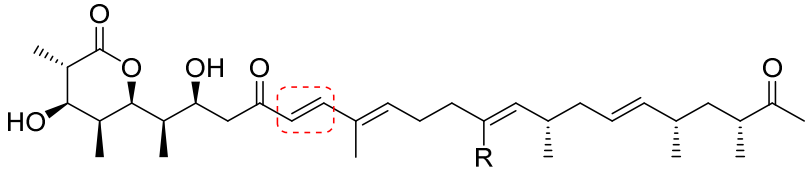

	meas. m/z	ion formula	calc. m/z	err [ppm]	mSigma
		ER8^{0}Pre$_B$			
	559.3990	$C_{34}H_{55}O_6$	559.3993	**0.6**	1
	576.4256	$C_{34}H_{58}NO_6$	576.4259	**0.4**	74
	581.3808	$C_{34}H_{54}NaO_6$	581.3813	**0.8**	2
	597.3551	$C_{34}H_{54}KO_6$	597.3552	**0.1**	19
		ER8^{0}Pre$_A$			
	573.4147	$C_{35}H_{57}O_6$	573.4150	**0.5**	3
	590.4409	$C_{35}H_{60}NO_6$	590.4415	**1.1**	44
	595.3965	$C_{35}H_{56}NaO_6$	595.3969	**0.6**	4
	611.3720	$C_{35}H_{56}KO_6$	611.3708	**-1.9**	22

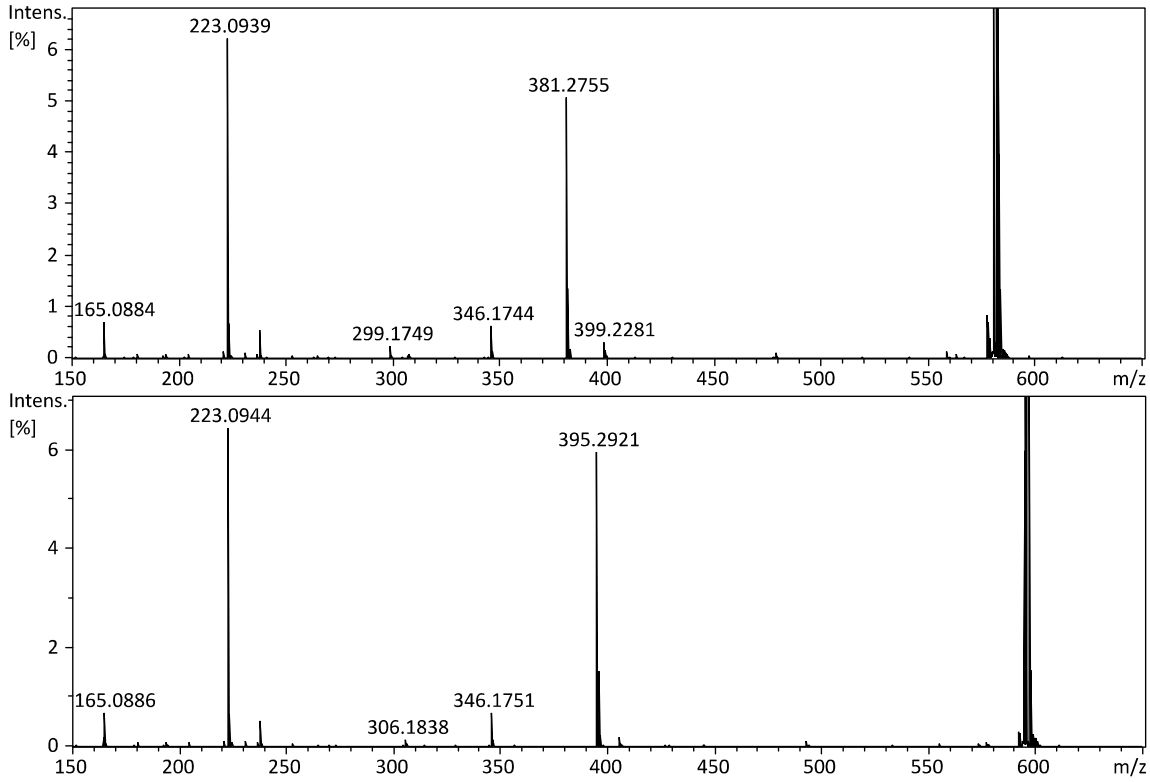

Figure S 26: MS^2 spectra of ER8^{0}Pre$_{A/B}$.

Table S 12: Mass spectrometric data of the fragment ions of ER8^{0}Pre$_{A/B}$.

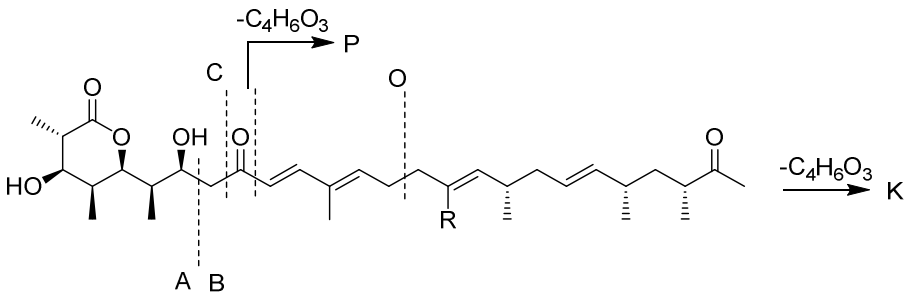

Fragment	Meas. m/z	ion formula	m/z	err [ppm]
		ER8^{0}Pre$_B$		
P	165.0884	$C_8H_{14}NaO_2$	165.0886	**1.2**
A	223.0939	$C_{10}H_{16}NaO_4$	223.0941	**1.0**
C	238.1174	$C_{11}H_{19}NaO_4$	238.1176	**0.8**
O	346.1744	$C_{18}H_{27}NaO_5$	346.1751	**1.9**
B	381.2755	$C_{24}H_{38}NaO_2$	381.2764	**2.4**
K	479.3480	$C_{30}H_{48}NaO_3$	479.3496	**3.2**
		ER8^{0}Pre$_A$		
P	165.0886	$C_8H_{14}NaO_2$	165.0886	**0.0**
A	223.0944	$C_{10}H_{16}NaO_4$	223.0941	**-1.4**
C	238.1177	$C_{11}H_{19}NaO_4$	238.1176	**-0.6**
O	346.1751	$C_{18}H_{27}NaO_5$	346.1751	**0.0**
B	395.2921	$C_{25}H_{40}NaO_2$	395.2921	**-0.2**
K	493.3659	$C_{31}H_{50}NaO_3$	493.3652	**-1.4**

5.4.3 Hop-Off Products from the Biosynthesis of ER6^0 and ER8^0 Premonensin A and B

Table S 13: Overview of the mass spectrometric data of different adducts of the hop-off intermediates from the premonensin biosynthetic pathway in *S. cinnamonensis* A495 ER6^0.

	Meas. m/z	ion formula	Sum Formula	m/z	err [ppm]	mSigma
ER6^{0}M6$_B$	295.2253	$C_{18}H_{31}O_3$	$C_{18}H_{30}O_3$	295.2268	**5.1**	n.a.
	317.2085	$C_{18}H_{30}NaO_3$		317.2087	**0.6**	n.a.
ER6^{0}M6$_A$	309.2413	$C_{19}H_{33}O_3$	$C_{19}H_{32}O_3$	309.2424	**3.6**	23
	331.2239	$C_{19}H_{32}NaO_3$		331.2244	**1.5**	16
ER6^{0}M7$_B$	355.2242	$C_{21}H_{32}NaO_3$	$C_{21}H_{32}O_3$	355.2244	**0.6**	22
ER6^{0}M7$_A$	347.2584	$C_{22}H_{35}O_3$	$C_{22}H_{34}O_3$	347.2581	**-1.1**	n.a.
	369.2396	$C_{22}H_{34}NaO_3$		369.2400	**1.1**	19
ER6^{0}M8$_B$	383.2557	$C_{23}H_{36}NaO_3$	$C_{23}H_{36}O_3$	383.2557	**-0.1**	222
ER6^{0}M8$_A$	375.2887	$C_{24}H_{39}O_3$	$C_{24}H_{38}O_3$	375.2894	**1.7**	28
	397.2708	$C_{24}H_{38}NaO_3$		397.2713	**1.3**	23
ER6^{0}M9$_B$	381.2757	$C_{24}H_{38}NaO_2$	$C_{24}H_{38}O_2$	381.2764	**1.7**	17
ER6^{0}M9$_A$	373.3082	$C_{25}H_{41}O_2$	$C_{25}H_{40}O_2$	373.3101	**5.1**	n.a.
	395.2914	$C_{25}H_{40}NaO_2$		395.2921	**1.6**	24

Table S 14: Overview of the mass spectrometric data of different adducts of the hop-off intermediates from the premonensin biosynthetic pathway in *S. cinnamonensis* A495 ER6^0.

	Meas. m/z	ion formula	Sum Formula	m/z	err [ppm]	mSigma
ER8^{0}M8$_B$	383.2553	$C_{23}H_{36}NaO_3$	$C_{23}H_{36}O_3$	383.2557	**1.0**	6
ER8^{0}M8$_A$	397.2708	$C_{24}H_{38}NaO_3$	$C_{24}H_{38}O_3$	397.2713	**1.4**	14
ER8^{0}M9$_B$	359.2939	$C_{24}H_{39}O_2$	$C_{24}H_{38}O_2$	359.2945	**1.5**	22
	381.2760	$C_{24}H_{38}NaO_2$		381.2764	**1.1**	4
ER8^{0}M9$_A$	373.3096	$C_{25}H_{41}O_2$	$C_{25}H_{40}O_2$	373.3101	**1.4**	3
	395.2915	$C_{25}H_{40}NaO_2$		395.2921	**1.3**	3
ER8^{0}M10$_B$	461.3255	$C_{28}H_{45}O_5$	$C_{28}H_{44}O_5$	461.3262	**1.5**	29
	483.3074	$C_{28}H_{44}NaO_5$		483.3081	**1.4**	29
ER8^{0}M10$_A$	475.3413	$C_{29}H_{47}O_5$	$C_{29}H_{46}O_5$	475.3418	**1.0**	8
	497.3232	$C_{29}H_{46}NaO_5$		497.3237	**1.2**	7
ER2^{0}M11$_B$	501.3570	$C_{31}H_{49}O_5$	$C_{31}H_{48}O_5$	501.3575	**0.9**	35
	523.3387	$C_{31}H_{48}NaO_5$		523.3394	**1.4**	19
ER2^{0}M11$_A$	515.3728	$C_{32}H_{51}O_5$	$C_{32}H_{50}O_5$	515.3731	**0.7**	6
	537.3546	$C_{32}H_{50}NaO_5$		537.3550	**0.8**	4

5.5 KR^0 Mutants – Premonensin Derivatives and Hop-Off Products

5.5.1 KR4^{0}Pre$_{A/B}$

Table S 15: Mass spectrometric data of characteristic adducts of KR4^{0}Pre$_{A/B}$.

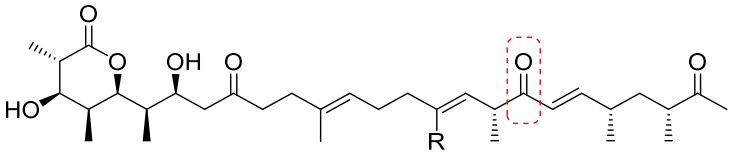

	meas. m/z	ion formula	calc. m/z	err [ppm]	mSigma
		KR4^{0}Pre$_B$			
	575.3938	$C_{34}H_{55}O_7$	575.3942	**0.7**	48
	597.3761	$C_{34}H_{54}NaO_7$	597.3762	**0.1**	11
	613.3495	$C_{34}H_{54}KO_7$	613.3501	**1.1**	22
		KR4^{0}Pre$_A$			
	589.4090	$C_{35}H_{57}O_7$	589.4099	**1.4**	8
	611.3911	$C_{35}H_{56}NaO_7$	611.3918	**1.1**	1
	627.3649	$C_{35}H_{56}KO_7$	627.3658	**1.4**	21

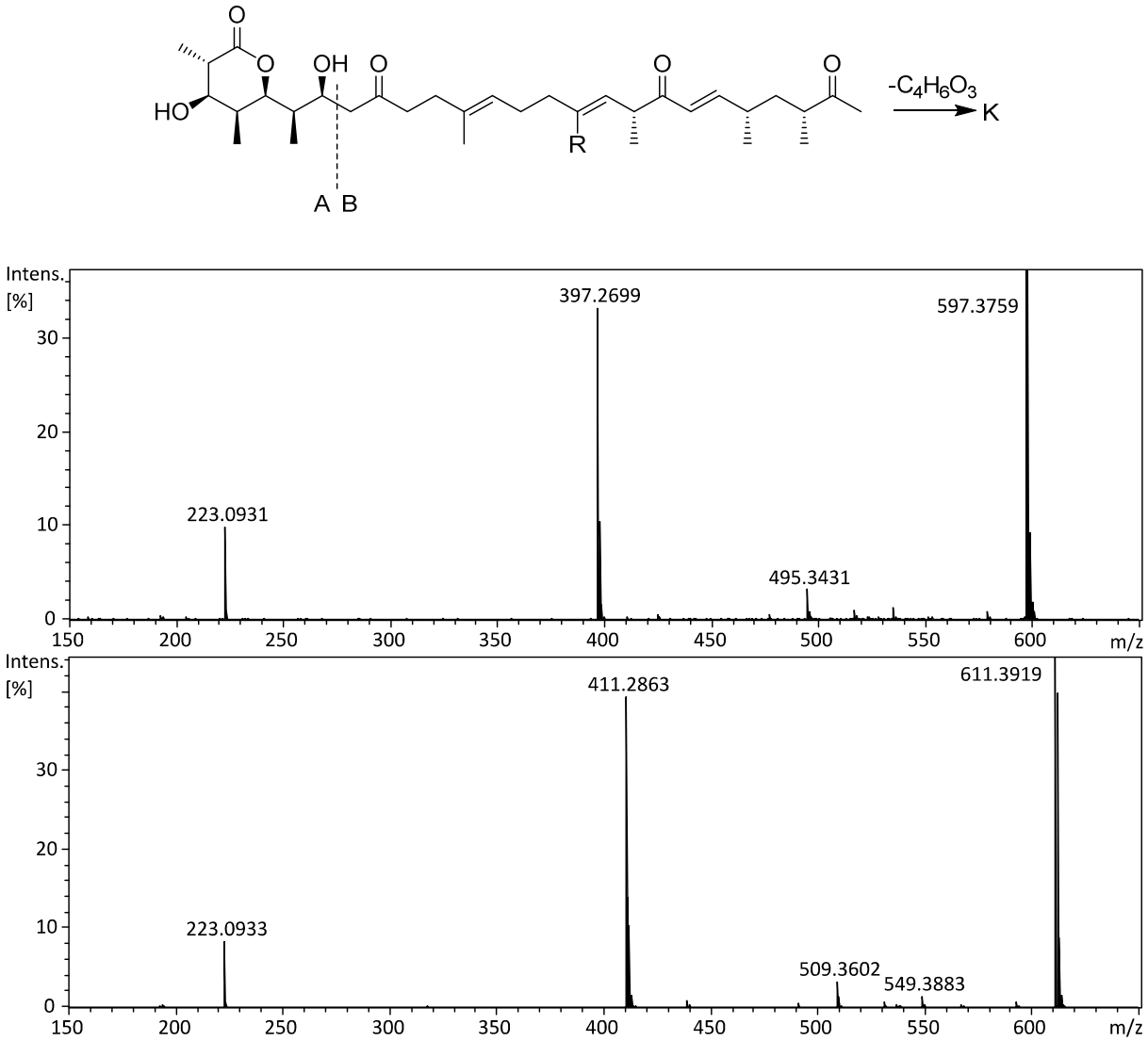

Figure S 27: MS^2 spectra of KR4^{0}Pre$_{A/B}$.

Table S 16: Mass spectrometric data of the fragment ions of KR4^{0}Pre$_{A/B}$.

Fragment	Meas. m/z	ion formula	m/z	err [ppm]
KR4^{0}Pre$_B$				
A	223.0931	$C_{10}H_{16}NaO_4$	223.0941	**4.2**
B	397.2699	$C_{24}H_{38}NaO_3$	397.2713	**3.5**
K	495.3431	$C_{30}H_{48}NaO_4$	495.3445	**2.8**
KR4^{0}Pre$_A$				
A	223.0933	$C_{10}H_{16}NaO_4$	223.0941	**3.7**
B	411.2863	$C_{25}H_{40}NaO_3$	411.2870	**1.7**
K	509.3602	$C_{31}H_{50}NaO_4$	509.3601	**-0.2**

5.5.2 KR6^{0}Pre$_{A/B}$

Table S 17: Mass spectrometric data of characteristic adducts of KR6^{0}Pre$_{A/B}$.

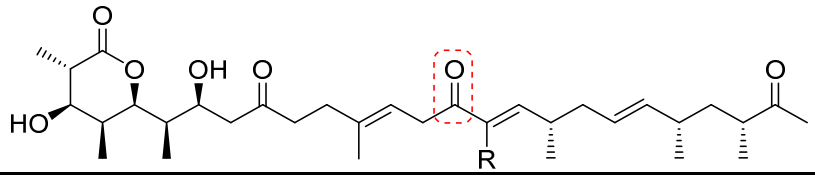

	meas. m/z	ion formula	calc. m/z	err [ppm]	mSigma
		KR6^{0}Pre$_B$			
	575.393	$C_{34}H_{55}O_7$	575.3942	**2.2**	48
	597.3761	$C_{34}H_{54}NaO_7$	597.3762	**0.2**	8
	613.3508	$C_{34}H_{54}KO_7$	613.3501	**-1.0**	n.a.
		KR6^{0}Pre$_A$			
	589.4096	$C_{35}H_{57}O_7$	589.4099	**0.5**	9
	611.3915	$C_{35}H_{56}NaO_7$	611.3918	**0.5**	6
	627.3658	$C_{35}H_{56}KO_7$	627.3658	**0.0**	n.a.

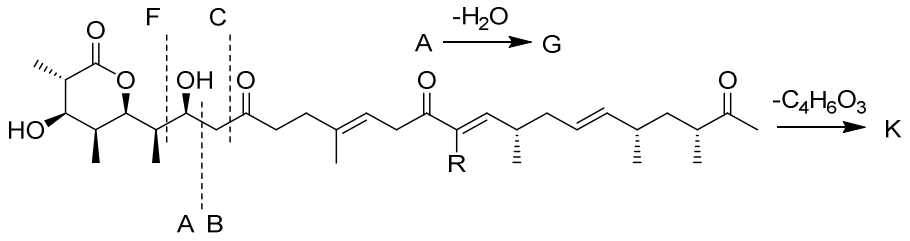

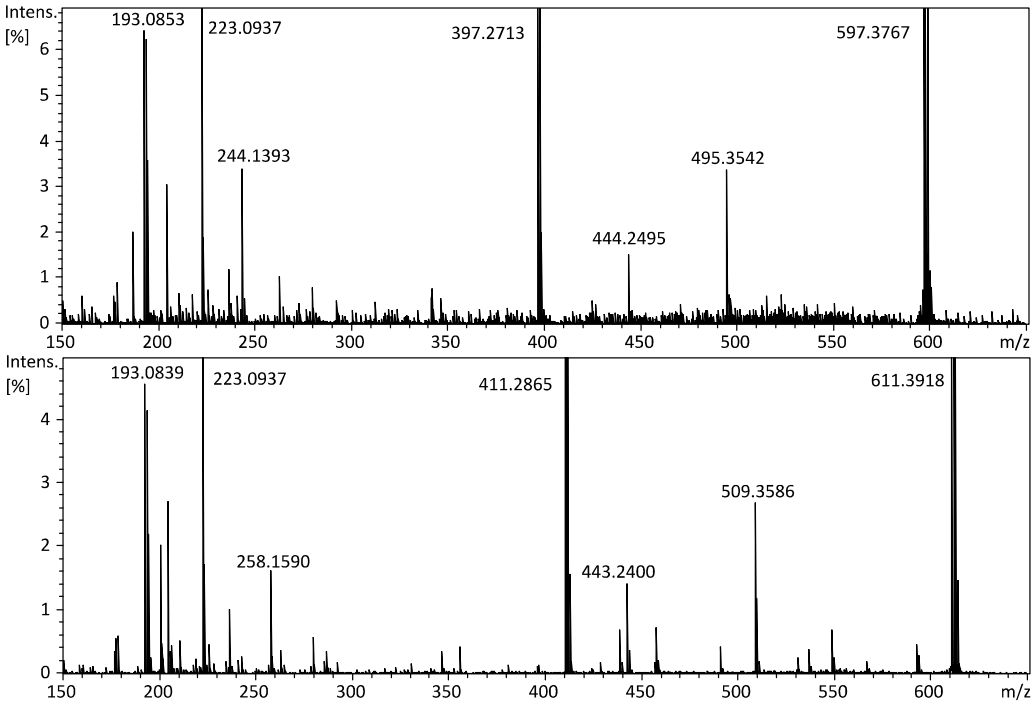

Figure S 28: MS^2 spectra of KR6^{0}Pre$_{A/B}$.

Tab. 3: Mass spectrometric data of the fragment ions of KR6^{0}Pre$_{A/B}$. *Only very low intensities detected.

Fragment	meas. m/z	ion formula	m/z	err [ppm]
		KR6^{0}Pre$_B$		
F	193.0853	$C_9H_{14}NaO_3$	193.0835	**-9.3**
G	205.09*			
A	223.0937	$C_{10}H_{16}NaO_4$	223.0941	**1.8**
C	237.11*			
B	383.2913	$C_{24}H_{40}NaO_2$	383.2921	**1.9**
K	495.35*			
		KR6^{0}Pre$_A$		
F	193.0839	$C_9H_{14}NaO_3$	193.0835	**-2.1**
G	205.0830	$C_{10}H_{14}NaO_3$	205.0835	**2.7**
A	223.0937	$C_{10}H_{16}NaO_4$	223.0941	**1.9**
C	237.1096	$C_{11}H_{18}NaO_4$	237.1097	**-0.4**
B	397.3074	$C_{25}H_{42}NaO_2$	397.3077	**0.7**
K	509.3586	$C_{31}H_{50}NaO_4$	509.3601	**3.0**

5.5.3 KR11^{0}Pre$_{A/B}$

Table S 18: Mass spectrometric data of characteristic adducts of KR11^{0}Pre$_{A/B}$. The typical lactonization of premonensin is not possible due to the missing hydroxy group.

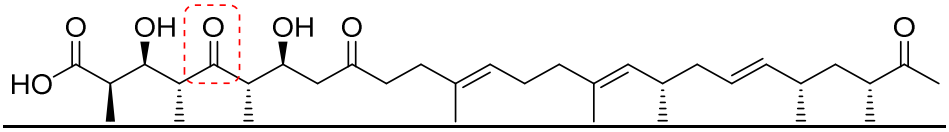

	meas. m/z	ion formula	calc. m/z	err [ppm]	mSigma
		KR11^{0}Pre$_B$			
	575.393	$C_{34}H_{55}O_7$	575.3942	**2.2**	48
	597.3761	$C_{34}H_{54}NaO_7$	597.3762	**0.2**	8
	613.3508	$C_{34}H_{54}KO_7$	613.3501	**-1.0**	n.a.
		KR11^{0}Pre$_A$			
	589.4096	$C_{35}H_{57}O_7$	589.4099	**0.5**	9
	611.3915	$C_{35}H_{56}NaO_7$	611.3918	**0.5**	6
	627.3658	$C_{35}H_{56}KO_7$	627.3658	**0.0**	n.a.

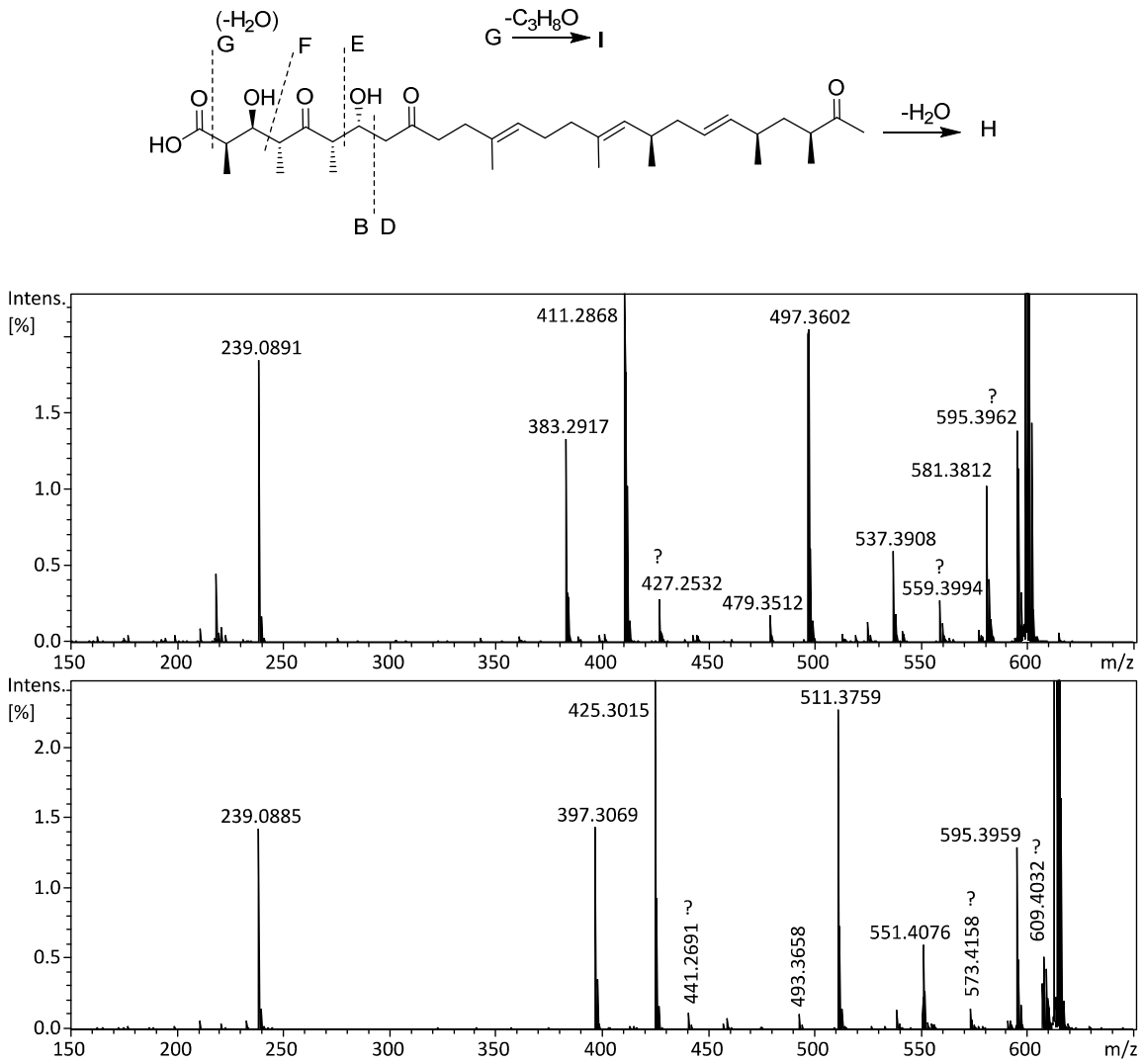

Figure S 29: MS^2 spectra of $KR11^0Pre_{A/B}$.

Table S 19: Mass spectrometric data of the fragment ions of $KR11^0Pre_{A/B}$.

Fragment	meas. m/z	ion formula	m/z	err [ppm]
Modul $KR11^0$ B				
B	239.0891	$C_{10}H_{16}NaO_5$	239.0890	**-0.5**
D	383.2917	$C_{24}H_{40}NaO_2$	383.2921	**0.8**
E	411.2868	$C_{25}H_{40}NaO_3$	411.2870	**0.5**
F	497.3602	$C_{30}H_{50}NaO_4$	497.3601	**-0.1**
G	537.3908	$C_{33}H_{54}NaO_4$	537.3914	**1.2**
H	581.3812	$C_{34}H_{54}NaO_6$	581.3813	**0.1**
I	479.3512	$C_{30}H_{48}NaO_3$	479.3496	**-3.5**
Modul $KR11^0$ A				
B	239.0885	$C_{10}H_{16}NaO_5$	239.0890	**1.9**
D	397.3069	$C_{25}H_{42}NaO_2$	397.3077	**1.9**
E	425.3015	$C_{26}H_{42}NaO_3$	425.3026	**2.6**
F	511.3759	$C_{31}H_{52}NaO_4$	511.3758	**-0.3**
G	551.4076	$C_{34}H_{56}NaO_4$	551.4071	**-0.9**
H	595.3959	$C_{35}H_{56}NaO_6$	595.3969	**1.7**
I	493.3658	$C_{31}H_{50}NaO_3$	493.3652	**-1.1**

5.5.4 KR12^{0}Pre$_{A/B}$

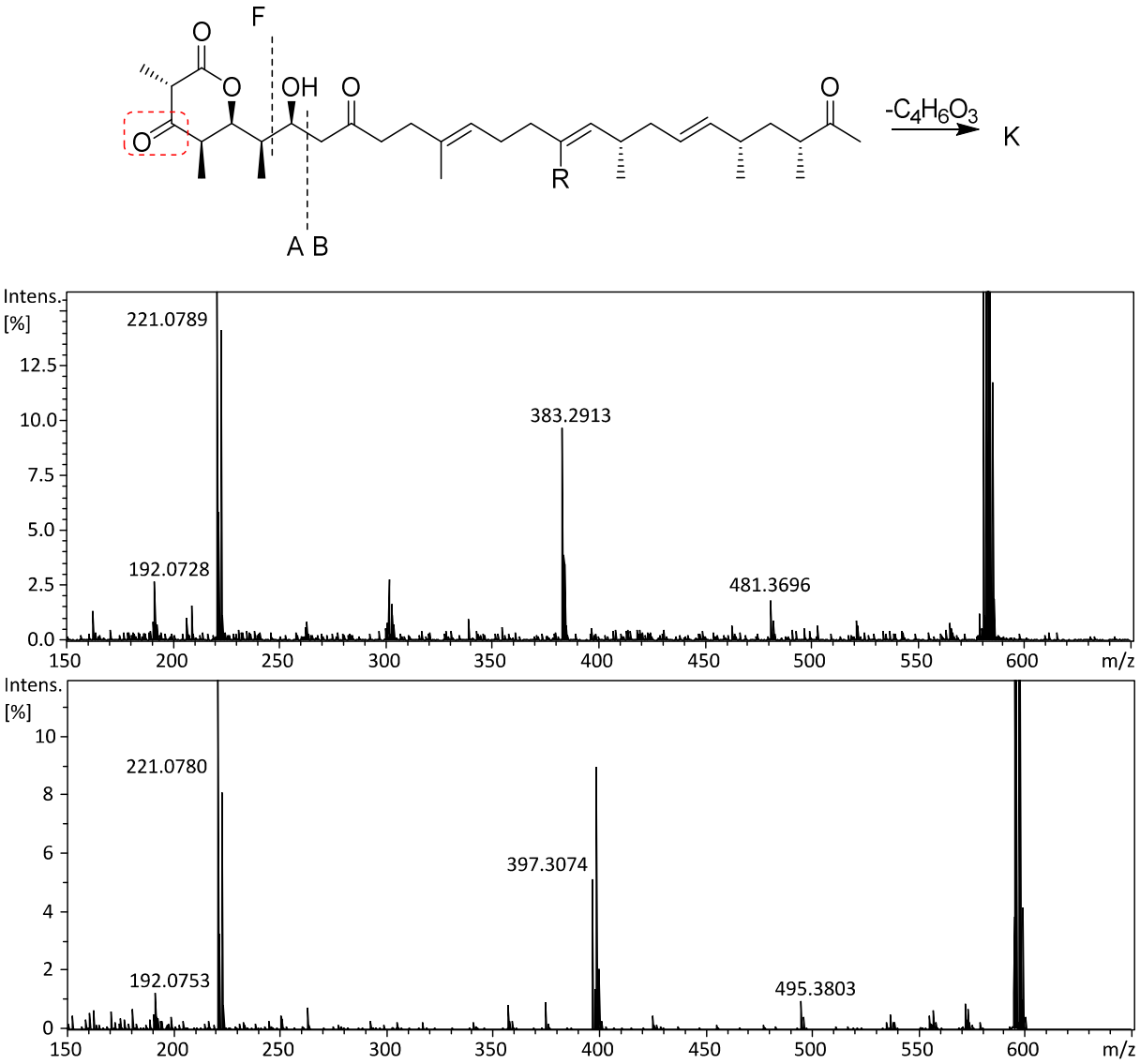

Figure S 30: MS^2 spectra of KR12^{0}Pre$_{A/B}$.

Table S 20: Mass spectrometric data of the fragment ions of KR12^{0}Pre$_{A/B}$

Fragment	Meas. m/z	ion formula	m/z	err [ppm]
		KR12^{0}Pre$_B$		
F	192.1*	$C_9H_{13}NaO_3$		
A	221.0789	$C_{10}H_{14}NaO_4$	221.0784	**-2.0**
B	383.2913	$C_{24}H_{40}NaO_2$	383.2921	**2.0**
K	481.4*	$C_{30}H_{50}NaO_3$		
		KR12^{0}Pre$_A$		
F	192.0753	$C_9H_{13}NaO_3$	192.0757	**2.1**
A	221.0780	$C_{10}H_{14}NaO_4$	221.0784	**1.9**
B	397.3074	$C_{25}H_{42}NaO_2$	397.3077	**0.7**
K	495.3803	$C_{31}H_{52}NaO_3$	495.3809	**1.2**

5.5.5 Hop-Off intermediates from KR^0 Mutants

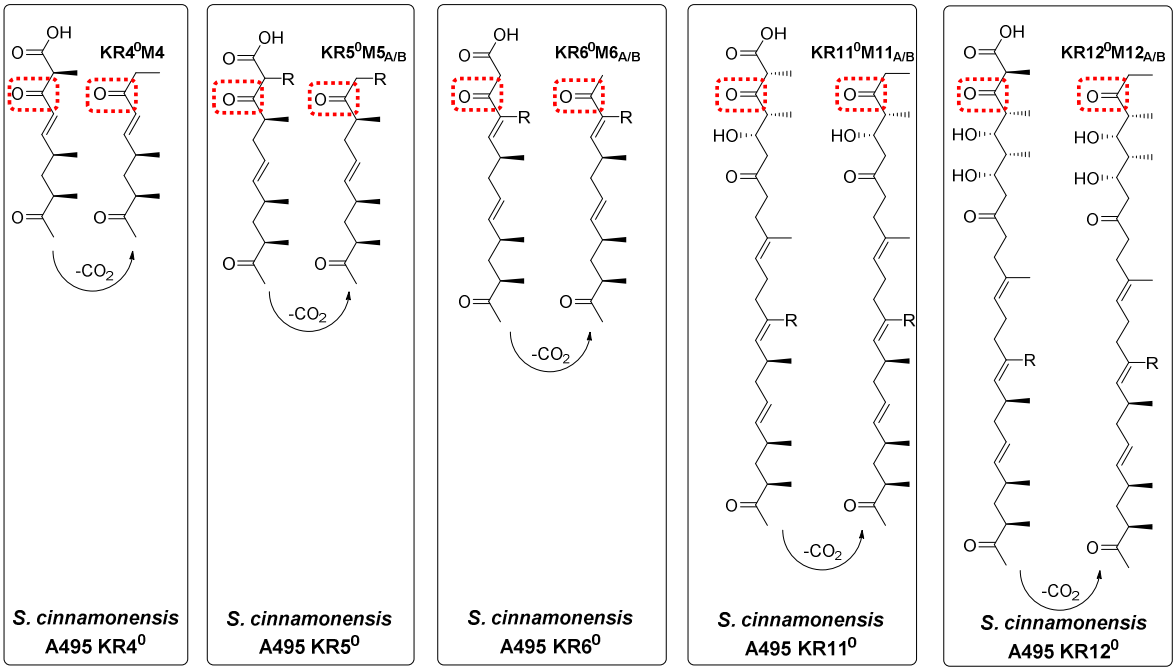

Figure S 31: Hop-off intermediates from the premonensin assembly line of different KR^0 mutants. All intermediates were detected in the decarboxylated form.

Table S 21: Mass spectrometric data of hop-of products from a fermentation of *S. cinnamonensis* A495 KR4^0. After the targeted module no, released intermediate could be detected.

	Meas. m/z	ion formula	Sum Formula	m/z	err [ppm]	mSigma
KR4^{0}M4	179.1428	$C_{12}H_{19}O$	$C_{12}H_{20}O_2$	179.1430	**1.5**	19
	197.1533	$C_{12}H_{21}O_2$		197.1536	**1.7**	3
	219.1352	$C_{12}H_{20}NaO_2$		219.1356	**1.5**	7

Table S 22: Mass spectrometric data of hop-of products from a fermentation of *S. cinnamonensis* A495 KR5^0. After the targeted module no, released intermediate could be detected.

	Meas. m/z	ion formula	Sum Formula	m/z	err [ppm]	mSigma
KR5^{0}M5$_B$	221.1896	$C_{15}H_{25}O$	$C_{15}H_{26}O_2$	221.1900	**1.7**	9
	239.2004	$C_{15}H_{27}O_2$		239.2006	**0.9**	15
	261.1822	$C_{15}H_{26}NaO_2$		261.1825	**1.1**	2
KR5^{0}M5$_A$	235.2057	$C_{16}H_{27}O$	$C_{16}H_{28}O_2$	235.2056	**-0.4**	12
	253.2165	$C_{16}H_{29}O_2$		253.2162	**-1.2**	7
	275.1983	$C_{16}H_{28}NaO_2$		275.1982	**-0.5**	3

Table S 23: Mass spectrometric data of hop-of products from a fermentation of *S. cinnamonensis* A495 KR6^0. After the targeted module no, released intermediate could be detected.

	Meas. m/z	ion formula	Sum Formula	m/z	err [ppm]	mSigma
KR6^{0}M6$_B$	265.2161	$C_{17}H_{29}O_2$	$C_{17}H_{28}O_2$	265.2162	**0.4**	1
	287.1980	$C_{17}H_{28}NaO_2$		287.1982	**0.5**	1
KR6^{0}M6$_A$	261.2210	$C_{18}H_{29}O$	$C_{18}H_{30}O_2$	261.2213	**1.2**	12
	279.2317	$C_{18}H_{31}O_2$		279.2319	**0.6**	2
	301.2136	$C_{18}H_{30}NaO_2$		301.2138	**0.7**	2

Table S 24: Mass spectrometric data of hop-of products from a fermentation of *S. cinnamonensis* A495 KR11^0.

	Meas. m/z	ion formula	Sum Formula	m/z	err [ppm]	mSigma
KR11^{0}M11$_B$	457.3663	$C_{30}H_{49}O_3$	$C_{30}H_{50}O_4$	457.3676	**2.9**	6
	475.3771	$C_{30}H_{51}O_4$		475.3782	**2.3**	14
	497.3592	$C_{30}H_{50}NaO_4$		497.3601	**1.8**	14
KR11^{0}M11$_A$	471.3826	$C_{31}H_{51}O_3$	$C_{31}H_{52}O_4$	471.3833	**1.5**	9
	489.3930	$C_{31}H_{53}O_4$		489.3938	**1.7**	17
	511.3752	$C_{31}H_{52}NaO_4$		511.3758	**1.2**	29

Table S 25: Mass spectrometric data of hop-of products from a fermentation of *S. cinnamonensis* A495 KR12^0.

	Meas. m/z	ion formula	Sum Formula	m/z	err [ppm]	mSigma
KR12^{0}M12$_B$	555.4014	$C_{33}H_{56}NaO_5$	$C_{33}H_{56}O_5$	555.4020	**1.0**	48
KR12^{0}M12$_A$	569.4174	$C_{34}H_{58}NaO_5$	$C_{34}H_{58}O_5$	569.4176	**0.0**	16

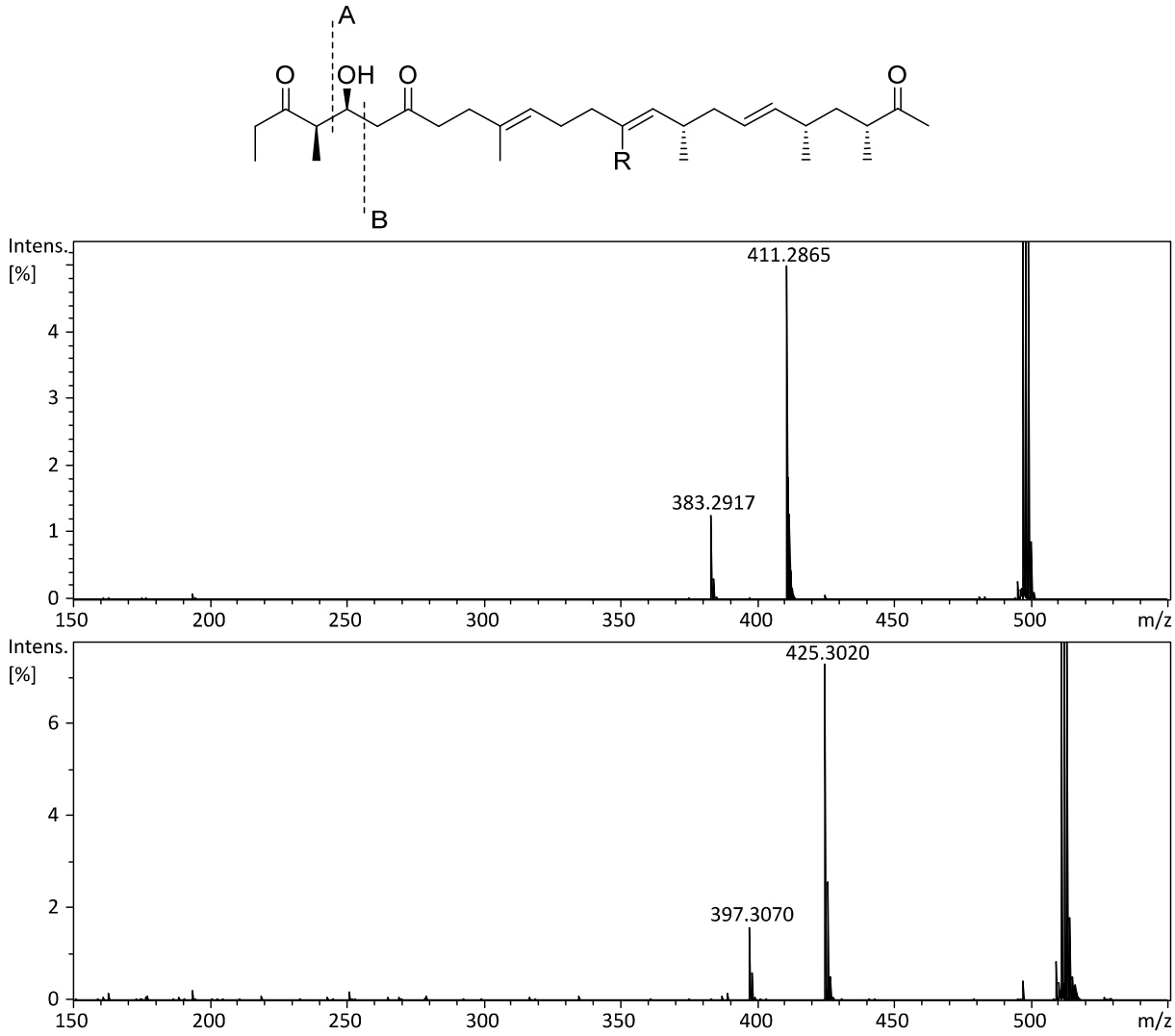

Figure S 32: MS^2 spectra of the hop-off intermediates $KR11^0M11_{A/B}$ in their typical decarboxylated form.

Table S 26: Mass spectrometric data of the fragment ions $KR11^0M11_{A/B}$.

Fragment	meas. m/z	ion formula	m/z	err [ppm]
		$KR11^0M11_B$		
B	383.2918	$C_{24}H_{40}NaO_2$	383.2921	**0.6**
A	411.2866	$C_{25}H_{40}NaO_3$	411.2870	**0.8**
		$KR11^0M11_A$		
B	397.3073	$C_{25}H_{42}NaO_2$	397.3077	**1.0**
A	425.3023	$C_{26}H_{42}NaO_3$	425.3026	**0.7**

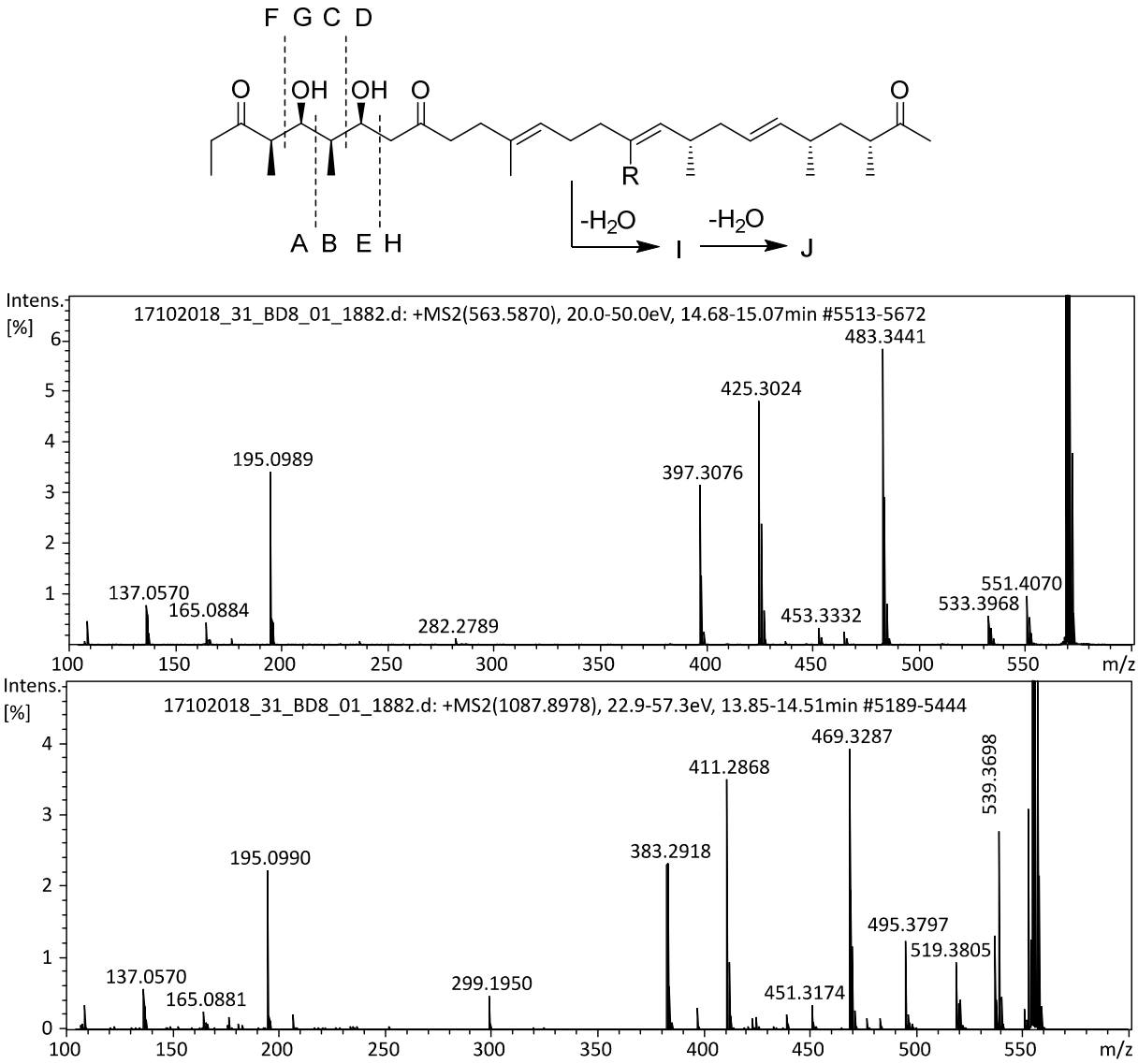

Figure S 33: MS^2 spectra of the hop-off intermediates $KR12^0M12_{A/B}$ in their typical decarboxylated form.

Table S 27: Mass spectrometric data of the fragment ions $KR12^{0}M12_{A/B.}$

Fragment	meas. m/z	ion formula	m/z	err [ppm]
		$KR12^{0}M12_{B}$		
F	109.0258	$C_4H_6NaO_2$	109.0260	**2.2**
A	137.0570	$C_6H_{10}NaO_2$	137.0573	**2.0**
C	165.0881	$C_8H_{14}NaO_2$	165.0886	**3.0**
E	195.0990	$C_9H_{16}NaO_3$	195.0992	**1.0**
H	383.2918	$C_{24}H_{40}NaO_2$	383.2921	**0.8**
D	411.2868	$C_{25}H_{40}NaO_3$	411.2870	**0.4**
B	439.3206	$C_{27}H_{44}NaO_3$	439.3183	**-5.4**
G-H20	451.3174	$C_{28}H_{44}NaO_3$	451.3183	**1.9**
G	469.3287	$C_{28}H_{46}NaO_4$	469.3288	**0.3**
J	519.3805	$C_{33}H_{52}NaO_3$	519.3809	**0.6**
I	537.3915	$C_{33}H_{54}NaO_4$	537.3914	**-0.1**
		$KR12^{0}M12_{A}$		
F	109.0259	$C_4H_6NaO_2$	109.0260	**1.0**
A	137.0570	$C_6H_{10}NaO_2$	137.0573	**2.4**
C	165.0884	$C_8H_{14}NaO_2$	165.0886	**1.2**
E	195.0989	$C_9H_{16}NaO_3$	195.0992	**1.2**
H	397.3076	$C_{25}H_{42}NaO_2$	397.3077	**0.3**
D	425.3024	$C_{26}H_{42}NaO_3$	425.3026	**0.4**
B	453.3332	$C_{28}H_{46}NaO_3$	453.3339	**1.7**
G-H20	465.3345	$C_{29}H_{46}NaO_3$	465.3339	**-1.3**
G	483.3441	$C_{29}H_{48}NaO_4$	483.3445	**0.8**
J	533.3968	$C_{34}H_{54}NaO_3$	533.3965	**-0.6**
I	551.4070	$C_{34}H_{56}NaO_4$	551.4071	**0.2**

5.6 DH^0 Mutants – Premonensin Derivatives and Hop-Off Products

5.6.1 DH2^0 Premonensin

Table S 28: Mass spectrometric data of characteristic adducts of DH2^{0}Pre$_{A/B}$.

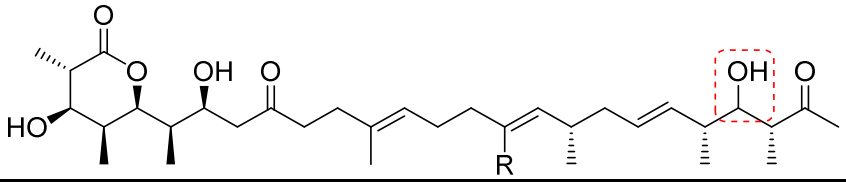

	meas. m/z	ion formula	calc. m/z	err [ppm]	mSigma
		DH2^{0}Pre$_B$			
	559.3987	$C_{32}H_{56}NaO_6$	559.3969	**-3.3**	25
	577.4092	$C_{32}H_{58}NaO_7$	577.4075	**-2.9**	131
	599.3913	$C_{34}H_{56}NaO_7$	599.3918	**0.9**	44
		DH2^{0}Pre$_A$			
	573.4143	$C_{33}H_{58}NaO_6$	573.4126	**-3.0**	32
	591.4250	$C_{33}H_{60}NaO_7$	591.4231	**-3.2**	189
	613.4070	$C_{35}H_{58}NaO_7$	613.4075	**0.8**	58

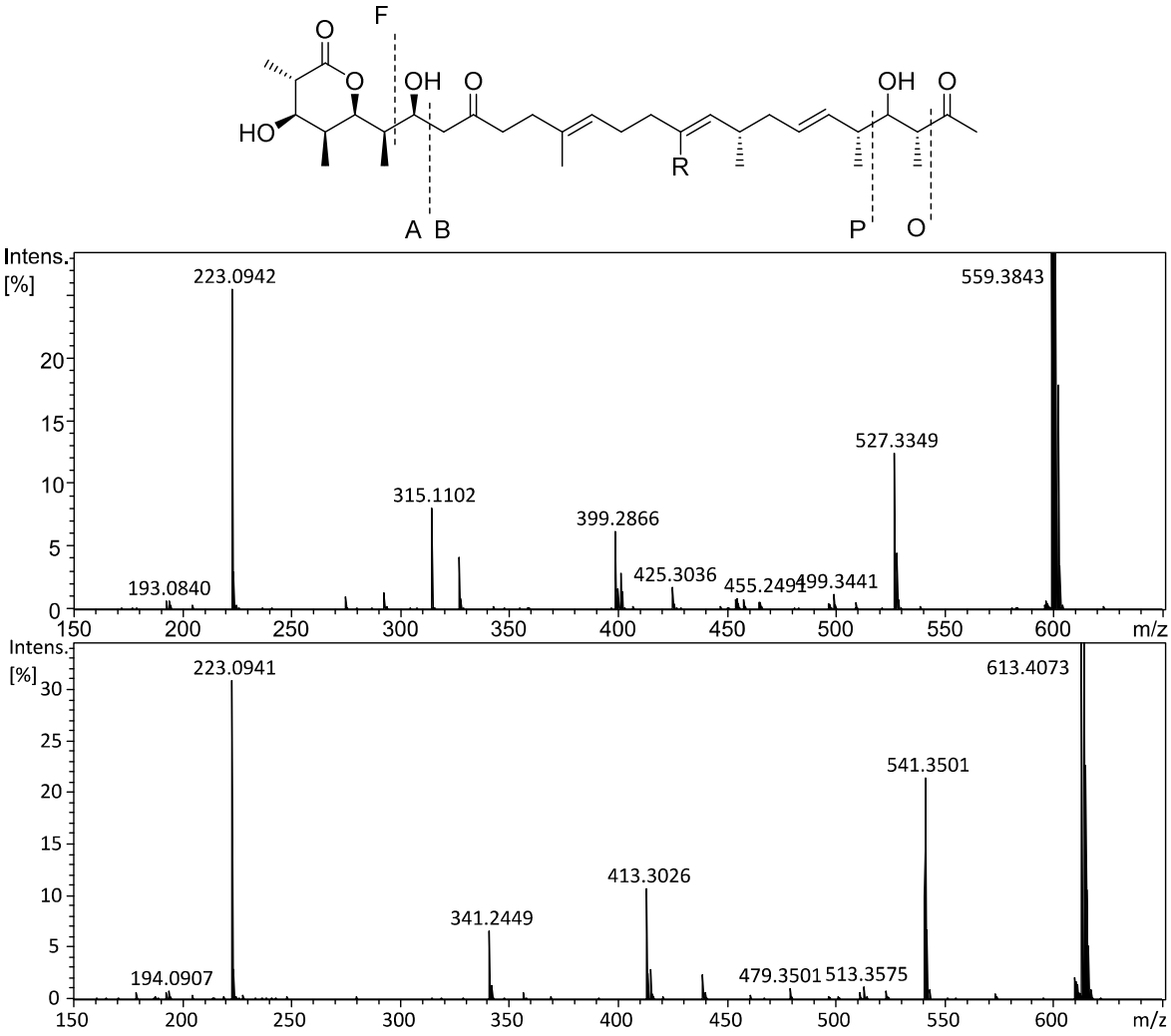

Figure S 34: MS^2 spectra of DH2^{0}Pre$_{A/B}$.

Table S 29: Mass spectrometric data of the fragment ions of DH2^{0}Pre$_{A/B}$.

Fragment	meas. m/z	ion formula	m/z	err [ppm]
		DH2^{0}Pre$_{A/B}$		
F	193.0840	$C_9H_{14}NaO_3$	193.0835	**-2.7**
A	223.0942	$C_{10}H_{16}NaO_4$	223.0941	**-0.3**
B	399.2866	$C_{24}H_{40}NaO_3$	399.2870	**0.9**
P	499.3441	$C_{29}H_{48}NaO_5$	499.3394	**-9.5**
O	527.3349	$C_{30}H_{48}NaO_6$	527.3343	**-1.1**
		DH2^{0}Pre$_{A/B}$		
F	193.0841	$C_9H_{14}NaO_3$	193.0835	**-2.7**
A	223.0941	$C_{10}H_{16}NaO_4$	223.0941	**0.0**
B	413.3026	$C_{25}H_{42}NaO_3$	413.3026	**0.1**
P	513.3575	$C_{30}H_{50}NaO_5$	513.3550	**-4.8**
O	541.3501	$C_{31}H_{50}NaO_6$	541.3500	**-0.2**

5.6.2 DH4^0 Premonensin

Table S 30: Mass spectrometric data of characteristic adducts of DH4^{0}Pre$_{A/B}$.

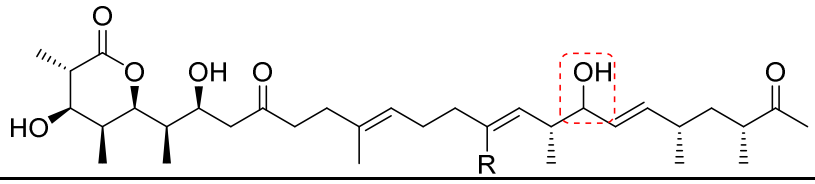

	meas. m/z	ion formula	calc. m/z	err [ppm]	mSigma
		DH4^{0}Pre$_B$			
	541.3884	$C_{34}H_{53}O_5$	541.3888	**0.6**	n.a.
	559.3993	$C_{34}H_{55}O_6$	559.3993	**0.0**	48
	599.3916	$C_{34}H_{56}NaO_7$	599.3918	**0.4**	11
		DH4^{0}Pre$_A$			
	555.4038	$C_{35}H_{55}O_5$	555.4044	**1.1**	43
	573.4134	$C_{35}H_{57}O_6$	573.415	**2.7**	42
	613.4067	$C_{35}H_{58}NaO_7$	613.4075	**1.2**	11

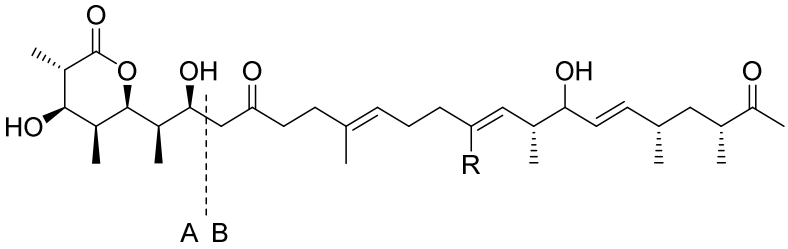

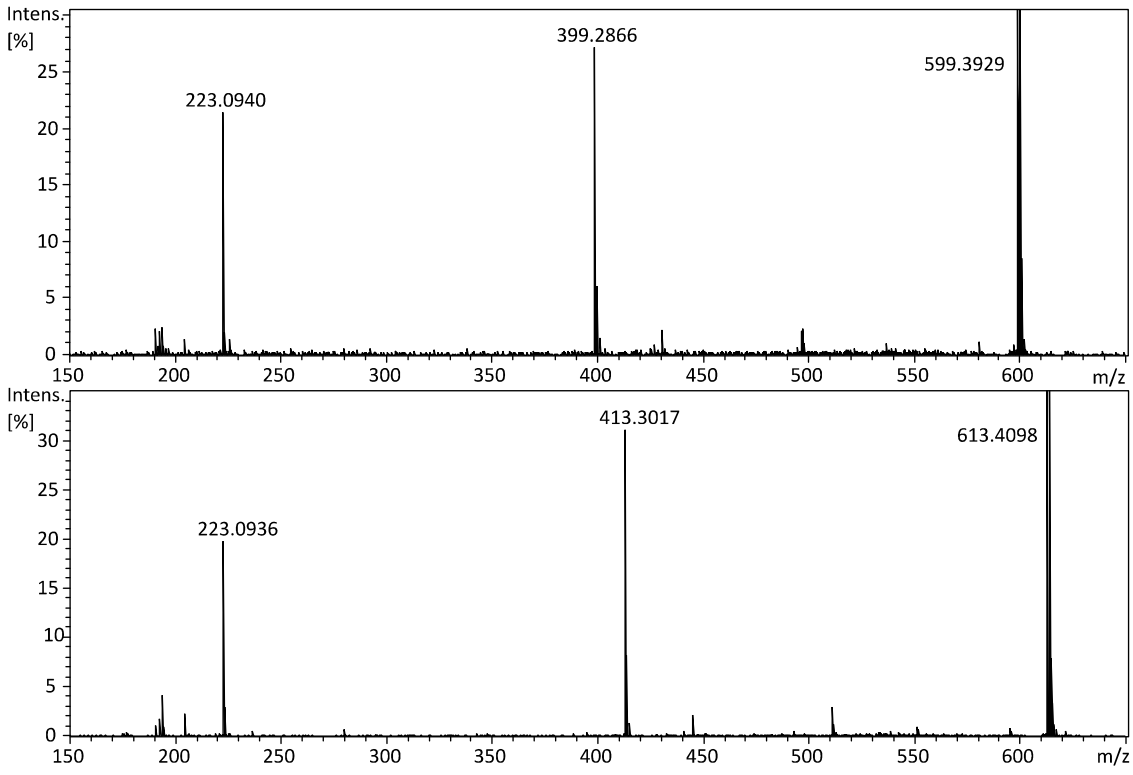

Figure S 35: MS^2 spectra of DH4^{0}Pre$_{A/B}$.

Table S 31: Mass spectrometric data of the fragment ions of DH4^{0}Pre$_{A/B}$.

Fragment	meas. m/z	ion formula	m/z	err [ppm]
		DH4^{0}Pre$_{A/B}$		
A	223.0940	$C_{10}H_{16}NaO_4$	223.0941	**0.2**
B	399.2866	$C_{24}H_{40}NaO_3$	399.2870	**0.9**
		DH4^{0}Pre$_{A/B}$		
A	223.0936	$C_{10}H_{16}NaO_4$	223.0941	**2.3**
B	413.3017	$C_{25}H_{42}NaO_3$	413.3026	**2.1**

5.6.3 DH5^0 Premonensin

Table S 32: Mass spectrometric data of characteristic adducts of DH5^{0}Pre$_{A/B}$.

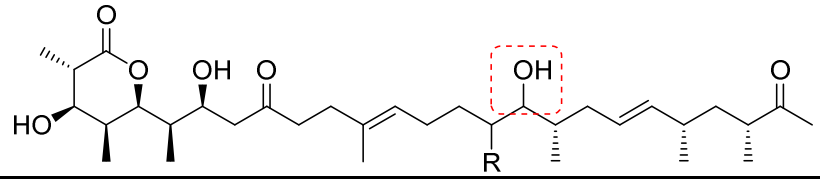

	meas. m/z	ion formula	calc. m/z	err [ppm]	mSigma
		DH5^{0}Pre$_B$			
	561.4180	$C_{34}H_{57}O_6$	561.4150	**-5.4**	54
	579.4241	$C_{34}H_{59}O_7$	579.4255	**2.5**	21
	601.4062	$C_{34}H_{58}NaO_7$	601.4075	**2.1**	11
		DH5^{0}Pre$_A$			
	615.4232	$C_{35}H_{60}NaO_7$	615.4231	**-0.2**	51

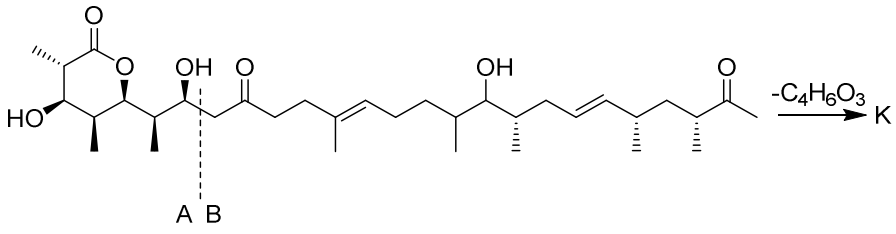

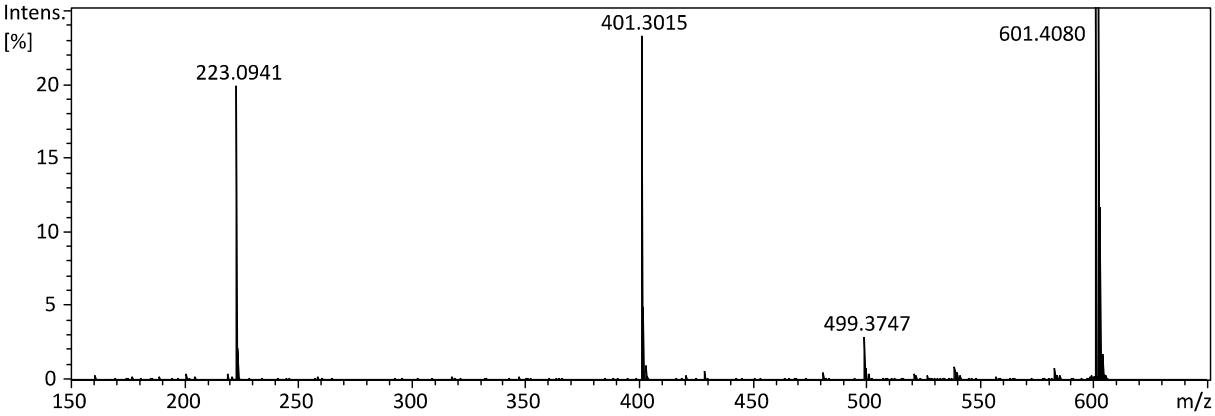

Figure S 36: MS^2 spectrum of DH4^{0}Pre$_B$. For the A form with an ethyl group only traces of the final product (DH5^{0}Pre$_A$) were detected.

Table S 33: Mass spectrometric data of the fragment ions of DH5^{0}Pre$_B$.

Fragment	meas. m/z	ion formula	m/z	err [ppm]
		DH5^{0}Pre$_{A/B}$		
A	223.0941	$C_{10}H_{16}NaO_4$	223.0941	**0.1**
B	401.3015	$C_{24}H_{42}NaO_3$	401.3026	**2.8**
K	499.3747	$C_{30}H_{52}NaO_4$	499.3758	**2.2**

5.6.4 DH7^0 Premonensin

Table S 34: Mass spectrometric data of characteristic adducts of DH7^{0}Pre$_{A/B}$.

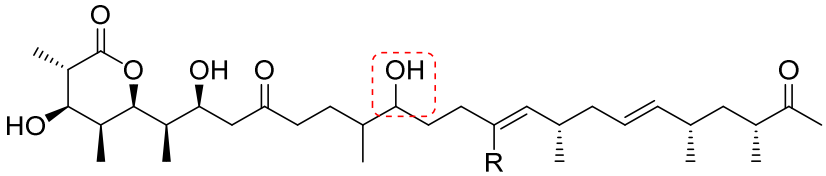

	meas. m/z	ion formula	calc. m/z	err [ppm]	mSigma
		DH7^{0}Pre$_B$			
	561.4149	$C_{34}H_{57}O_6$	561.4150	0.1	18
	601.4072	$C_{34}H_{58}NaO_7$	601.4075	0.4	29
		DH7^{0}Pre$_A$			
	575.4302	$C_{35}H_{59}O_6$	575.4306	0.7	9
	615.4225	$C_{35}H_{60}NaO_7$	615.4231	1.0	35

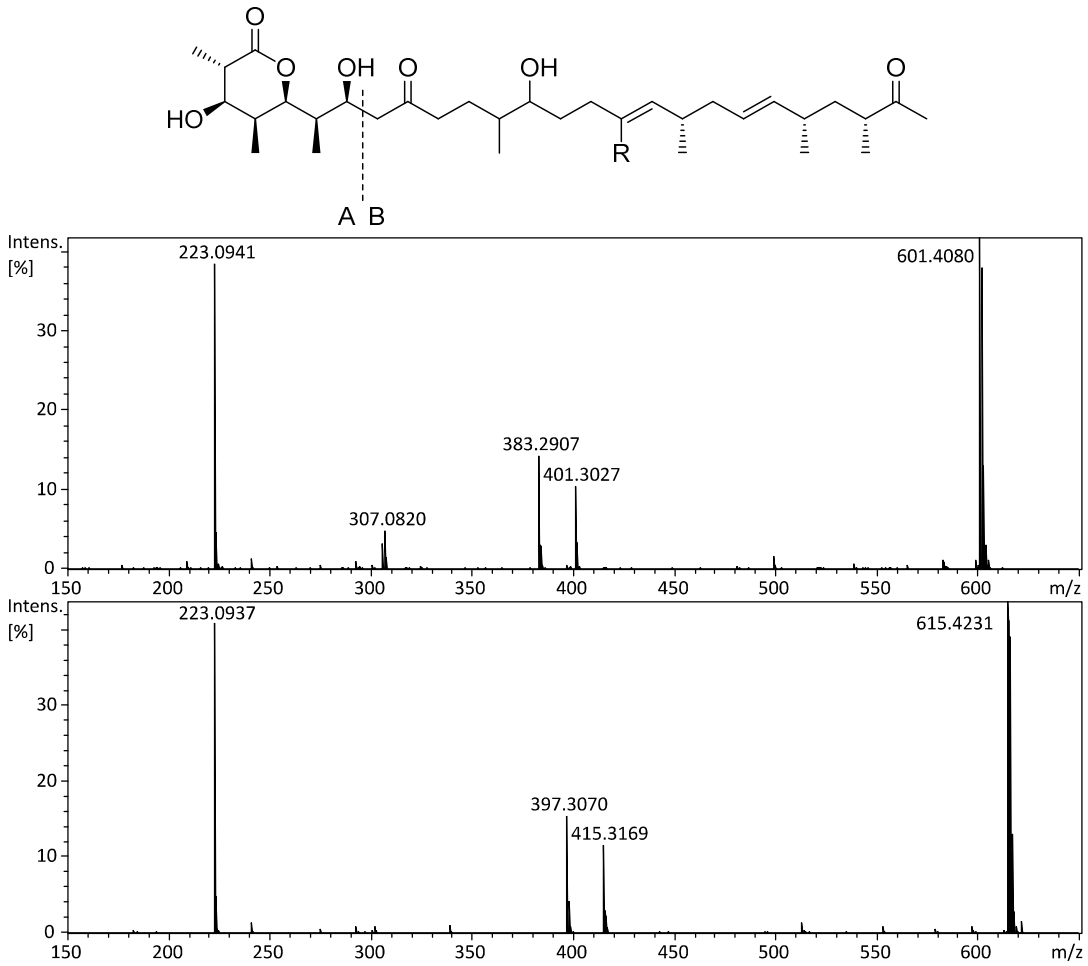

Figure S 37: MS^2 spectra of DH7^{0}Pre$_{A/B}$.

Table S 35: Mass spectrometric data of the fragment ions of DH7^{0}Pre$_{A/B}$.

Fragment	meas. m/z	ion formula	m/z	err [ppm]
		DH7^{0}Pre$_{A/B}$		
A	223.0941	$C_{10}H_{16}NaO_4$	223.0941	**-0.1**
B-H$_2$0	383.2907	$C_{24}H_{40}NaO_2$	383.2921	**3.4**
B	401.3027	$C_{24}H_{42}NaO_3$	401.3026	**-0.2**
		DH7^{0}Pre$_{A/B}$		
A	223.0937	$C_{10}H_{16}NaO_4$	223.0941	**1.6**
B-H$_2$0	397.3070	$C_{25}H_{42}NaO_2$	397.3077	**1.8**
B	415.3169	$C_{25}H_{44}NaO_3$	415.3183	**3.3**

5.6.5 DH8^0 Premonensin

Table S 36: Mass spectrometric data of characteristic adducts of DH8^{0}Pre$_{A/B}$.

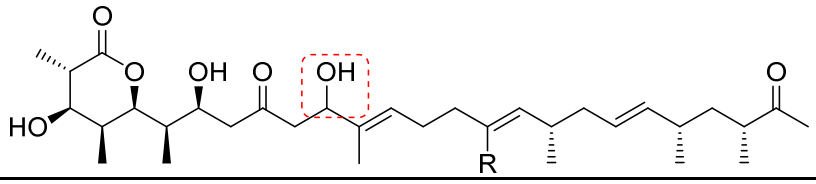

	meas. m/z	ion formula	calc. m/z	err [ppm]	mSigma
		DH8^{0}Pre$_B$			
	541.3881	$C_{34}H_{53}O_5$	541.3888	**1.2**	11
	559.3985	$C_{34}H_{55}O_6$	559.3993	**1.5**	3
	599.3911	$C_{34}H_{56}NaO_7$	599.3918	**1.1**	4
		DH8^{0}Pre$_A$			
	555.4037	$C_{35}H_{55}O_5$	555.4044	**1.3**	6
	573.4142	$C_{35}H_{57}O_6$	573.4150	**1.3**	2
	613.4065	$C_{35}H_{58}NaO_7$	613.4075	**1.6**	5

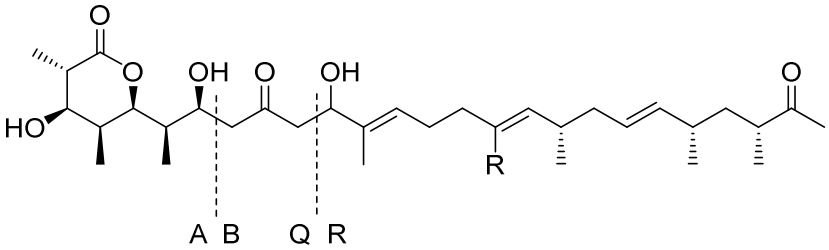

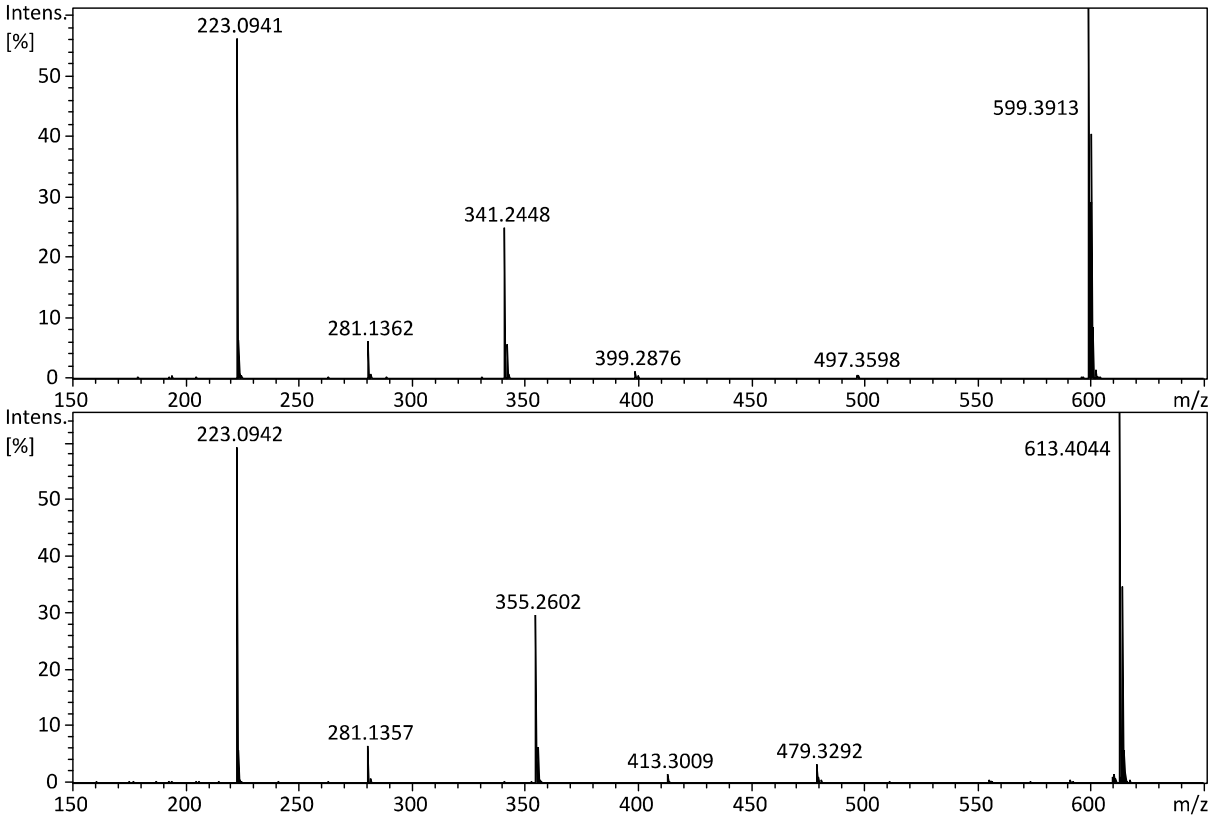

Figure S 38: MS^2 spectra of DH8^{0}Pre$_{A/B}$.

Table S 37: Mass spectrometric data of the fragment ions of DH8^{0}Pre$_{A/B}$.

Fragment	meas. m/z	ion formula	m/z	err [ppm]
		DH8^{0}Pre$_{A/B}$		
A	223.0941	$C_{10}H_{16}NaO_4$	223.0941	**0.1**
Q	281.1362	$C_{13}H_{22}NaO_5$	281.1359	**-1.0**
R	341.2448	$C_{21}H_{34}NaO_2$	341.2451	**1.0**
B	399.2876	$C_{24}H_{40}NaO_3$	399.287	**-1.5**
		DH8^{0}Pre$_{A/B}$		
A	223.0942	$C_{10}H_{16}NaO_4$	223.0941	**-0.5**
Q	281.1357	$C_{13}H_{22}NaO_5$	281.1359	**0.9**
R	355.2602	$C_{22}H_{36}NaO_2$	355.2608	**1.5**
B	413.3009	$C_{25}H_{42}NaO_3$	413.3026	**4.2**

5.6.6 Hop-Off Intermediates from DH^0 Mutants

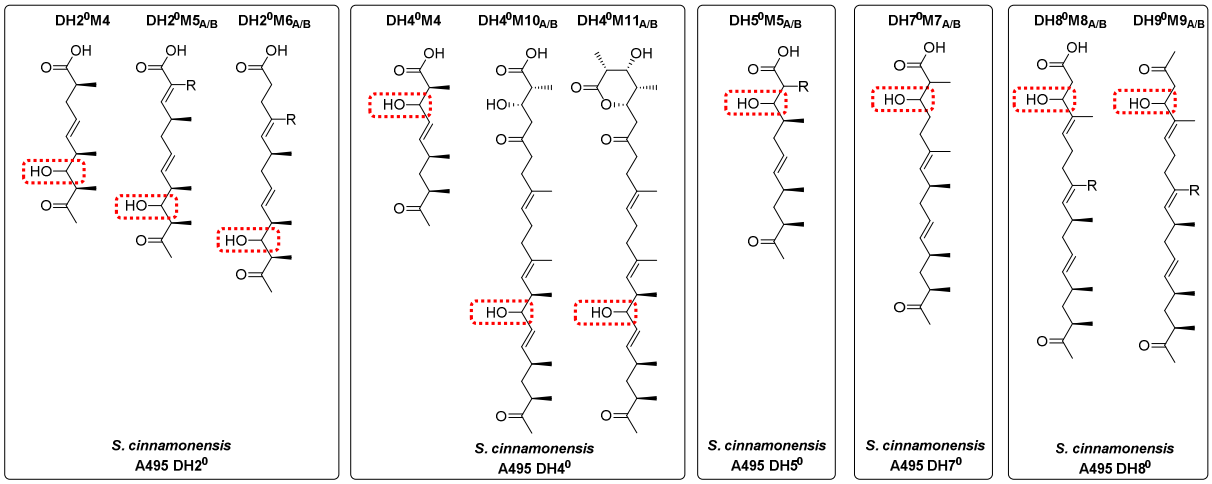

Table S 38: Overview of the mass spectrometric data of different adducts of the hop-off intermediates from the premonensin biosynthetic pathway in *S. cinnamonensis* A495 DH2^0.

	Meas. m/z	ion formula	Sum Formula	m/z	err [ppm]	mSigma
DH2^{0}M4	225.1483	$C_{13}H_{21}O_3$	$C_{13}H_{22}O_4$	225.1485	**0.8**	10
	243.1589	$C_{13}H_{23}O_4$		243.1591	**0.8**	11
	265.1409	$C_{13}H_{22}NaO_4$		265.1410	**0.4**	24
DH2^{0}M5$_B$	305.1721	$C_{16}H_{26}NaO_4$	$C_{16}H_{26}O_4$	305.1723	**0.7**	13
DH2^{0}M5$_A$	319.1877	$C_{17}H_{28}NaO_4$	$C_{17}H_{28}O_4$	319.1880	**0.8**	20

Table S 39: Overview of the mass spectrometric data of different adducts of the hop-off intermediates from the premonensin biosynthetic pathway in *S. cinnamonensis* A495 DH4^0.

	Meas. m/z	ion formula	Sum Formula	m/z	err [ppm]	mSigma
DH4^{0}M4	265.1413	$C_{13}H_{22}NaO_4$	$C_{13}H_{22}O_4$	265.1410	**-1.1**	21

Table S 40: Overview of the mass spectrometric data of different adducts of the hop-off intermediates from the premonensin biosynthetic pathway in *S. cinnamonensis* A495 $DH5^0$.

	Meas. m/z	ion formula	Sum Formula	m/z	err [ppm]	mSigma
$DH5^0M5_B$	307.1878	$C_{18}H_{27}O_4$	$C_{18}H_{26}O_4$	307.1904	**8.3**	69
$DH5^0M5_A$	281.2109	$C_{17}H_{29}O_3$	$C_{17}H_{30}O_4$	281.2111	**0.6**	14
	299.2214	$C_{17}H_{31}O_4$		299.2217	**1.1**	27
	321.2033	$C_{17}H_{30}NaO_4$		321.2036	**1.0**	15

Table S 41: Overview of the mass spectrometric data of different adducts of the hop-off intermediates from the premonensin biosynthetic pathway in *S. cinnamonensis* A495 $DH7^0$.

	Meas. m/z	ion formula	Sum Formula	m/z	err [ppm]	mSigma
$DH7^0M7_B$	not detected					
$DH7^0M7_A$	223.0941	$C_{10}H_{16}NaO_4$	$C_{10}H_{16}NaO_4$	223.0941	-0.1	9.8
	383.2907	$C_{24}H_{40}NaO_2$	$C_{24}H_{40}NaO_2$	383.2921	3.4	n.a.
	401.3027	$C_{24}H_{42}NaO_3$	$C_{24}H_{42}NaO_3$	401.3026	-0.2	n.a.

Table S 42: Overview of the mass spectrometric data of different adducts of the hop-off intermediates from the premonensin biosynthetic pathway in *S. cinnamonensis* A495 $DH8^0$.

	Meas. m/z	ion formula	Sum Formula	m/z	err [ppm]	mSigma
$DH8^0M8_B$	361.2730	$C_{23}H_{37}O_3$	$C_{23}H_{38}O_4$	361.2737	**2.0**	n.a.
	401.2655	$C_{23}H_{38}NaO_4$		401.2662	**1.9**	23
$DH8^0M8_A$	375.2886	$C_{24}H_{39}O_3$	$C_{24}H_{40}O_4$	375.2894	**2.1**	18
	415.2816	$C_{24}H_{40}NaO_4$		415.2819	**0.8**	6

5.7 Double Mutants Nulling Two Reductive Domains

5.7.1 ER2^{0}DH8^0

Table S 43: Mass spectrometric data of characteristic adducts of ER2^{0}DH8^{0}Pre$_{A/B}$.

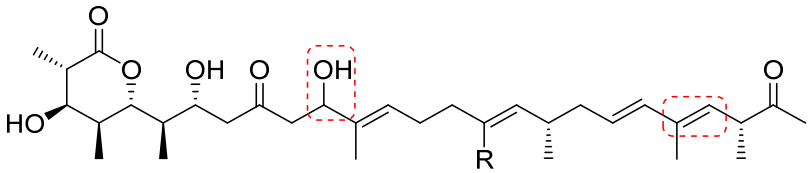

	meas. m/z	ion formula	calc. m/z	err [ppm]	mSigma
	ER2^{0}DH8^{0}Pre$_B$				
	557.3834	$C_{34}H_{53}O_6$	557.3837	0.5	4
	575.3949	$C_{34}H_{55}O_7$	575.3942	-1.2	n.a.
	597.3763	$C_{34}H_{54}NaO_7$	597.3762	-0.2	3
	613.3502	$C_{34}H_{54}KO_7$	613.3501	-0.1	72
	ER2^{0}DH8^{0}Pre$_B$				
	571.3989	$C_{35}H_{55}O_6$	571.3993	0.7	4
	589.4099	$C_{35}H_{57}O_7$	589.4099	0.0	n.a.
	611.3919	$C_{35}H_{56}NaO_7$	611.3918	-0.1	8
	627.3665	$C_{35}H_{56}KO_7$	627.3658	-1.2	74

Table S 44: Mass spectrometric data of characteristic adducts of ER2^{0}DH8^{0}Pre$_{A/B}$ (dehydrated).

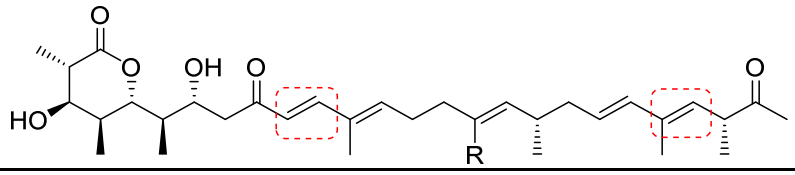

	meas. m/z	ion formula	calc. m/z	err [ppm]	mSigma
	ER2^{0}DH8^{0}Pre$_B$ (-H$_2$O)				
	557.3831	$C_{34}H_{53}O_6$	557.3837	1.0	10
	579.3653	$C_{34}H_{52}NaO_6$	579.3656	0.5	14
	595.3417	$C_{34}H_{52}KO_6$	595.3395	-3.6	72
	ER2^{0}DH8^{0}Pre$_B$ (-H$_2$O)				
	571.3978	$C_{35}H_{55}O_6$	571.3993	2.6	40
	593.3806	$C_{35}H_{54}NaO_6$	593.3813	1.1	19

5.7.2 ER2^{0}KR4^0

Table S 45: Mass spectrometric data of characteristic adducts of ER2^{0}KR4^{0}Pre$_{A/B}$.

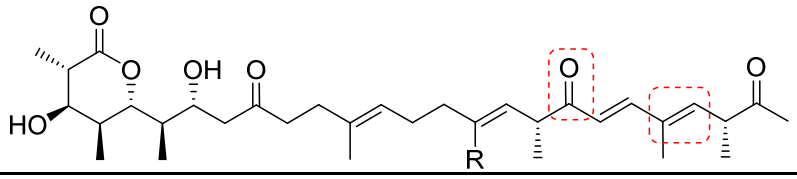

	meas. m/z	ion formula	calc. m/z	err [ppm]	mSigma
		ER2^{0}KR4^{0}Pre$_B$			
	555.3691	$C_{34}H_{51}O_6$	555.3680	-1.9	45
	573.3778	$C_{34}H_{53}O_7$	573.3786	1.4	13
	595.3596	$C_{34}H_{52}NaO_7$	595.3605	1.5	11
		ER2^{0}KR4^{0}Pre$_B$			
	569.3839	$C_{35}H_{53}O_6$	569.3837	-0.5	34
	587.3941	$C_{35}H_{55}O_7$	587.3942	0.2	18
	609.3764	$C_{35}H_{54}NaO_7$	609.3762	-0.4	9

5.7.3 Hop-Off Intermediates from Double Null Mutants

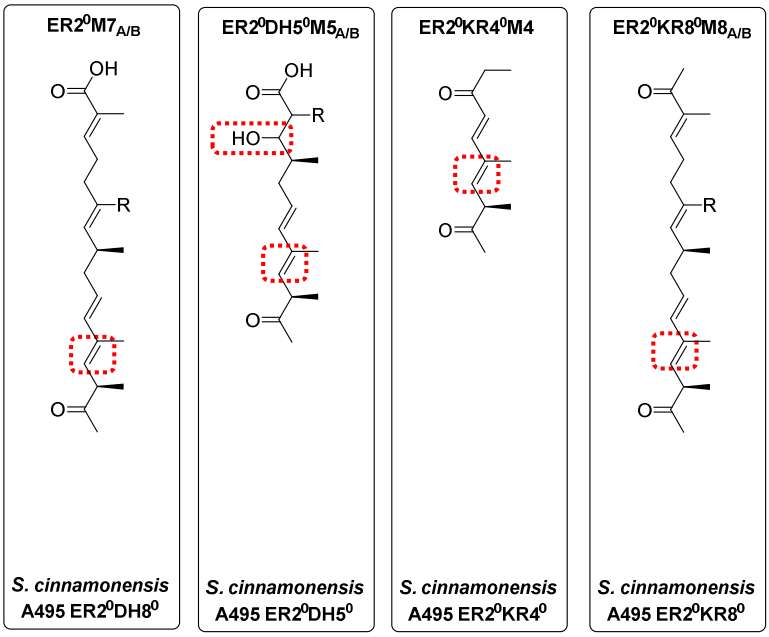

Figure S 39: New hop-off intermediates from the premonensin assembly line of different double null mutants. The intermediates from KR^0 mutants decarboxylated as shown. ER2^{0}M7$_{A/B}$ were not detectable in the single mutant ER2^0.

Table S 46: Overview of the mass spectrometric data of different adducts of the hop-off intermediates from the premonensin biosynthetic pathway in *S. cinnamonensis* A495 ER2^{0}DH8^0.

	Meas. m/z	ion formula	Sum Formula	m/z	err [ppm]	mSigma
ER2^{0}M7$_B$	333.2421	$C_{21}H_{33}O_3$	$C_{21}H_{32}O_3$	333.2424	**0.9**	19
	355.2238	$C_{21}H_{32}NaO_3$		355.2244	**1.6**	2
ER2^{0}M7$_A$	347.2587	$C_{22}H_{35}O_3$	$C_{22}H_{34}O_3$	347.2581	**-1.9**	21
	369.2395	$C_{22}H_{34}NaO_3$		369.24	**1.4**	6

Table S 47: Overview of the mass spectrometric data of different adducts of the hop-off intermediates from the premonensin biosynthetic pathway in *S. cinnamonensis* A495 ER2^{0}DH5^0.

	Meas. m/z	ion formula	Sum Formula	m/z	err [ppm]	mSigma
ER2^{0}DH5^{0}M5$_B$	283.1896	$C_{16}H_{27}O_4$	$C_{16}H_{26}O_4$	283.1904	**2.8**	70
	305.1717	$C_{16}H_{26}NaO_4$		305.1723	**2.0**	53
ER2^{0}DH5^{0}M5$_A$	297.2052	$C_{17}H_{29}O_4$	$C_{17}H_{28}O_4$	297.2060	**2.7**	64
	319.1877	$C_{17}H_{28}NaO_4$		319.1880	**0.8**	46

Table S 48: Overview of the mass spectrometric data of different adducts of the hop-off intermediates from the premonensin biosynthetic pathway in *S. cinnamonensis* A495 ER2^{0}KR4^0.

	Meas. m/z	ion formula	Sum Formula	m/z	err [ppm]	mSigma
ER2^{0}KR4^{0}M4	177.1273	$C_{12}H_{17}O$	$C_{12}H_{18}O_2$	177.1274	**0.5**	6
	195.1379	$C_{12}H_{19}O_2$		195.1380	**0.2**	5
	217.1198	$C_{12}H_{18}NaO_2$		217.1199	**0.4**	56

Table S 49: Overview of the mass spectrometric data of different adducts of the hop-off intermediates from the premonensin biosynthetic pathway in *S. cinnamonensis* A495 ER2^{0}KR8^0.

	Meas. m/z	ion formula	Sum Formula	m/z	err [ppm]	mSigma
ER2^{0}KR8^{0}M8$_B$	331.2645	$C_{22}H_{35}O_2$	$C_{22}H_{34}O_2$	331.2632	**-4.2**	188
	353.2448	$C_{22}H_{34}NaO_2$		353.2451	**0.9**	23
ER2^{0}KR8^{0}M8$_A$	345.2809	$C_{23}H_{37}O_2$	$C_{23}H_{36}O_2$	345.2788	**-6.2**	n.a.
	367.2628	$C_{23}H_{36}NaO_2$		367.2608	**0.5**	23

5.8 Precursor Directed Biosynthesis – Premonensin Derivatives and Hop-Off Intermediates

5.8.1 Premonensin Derivatives (Pre$_X$) Resulting from a Precursor Directed Biosynthesis

Table S 50: Overview of the mass spectrometric data of different premonensin derivatives resulting from a precursor directed biosynthesis in fermentations of *S. cinnamonensis* A495. Bu: Butyl. Prg: Propargyl. All: Allyl. Pr: Propyl. Cl: 3-chloropropyl.

	meas. m/z	ion formula	calc. m/z	err [ppm]	mSigma
		Pre$_{Bu}$			
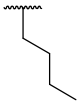	585.4499	$C_{37}H_{61}O_5$	585.4514	**2.4**	16
	603.4612	$C_{37}H_{63}O_6$	603.4619	**1.1**	10
	625.4439	$C_{37}H_{62}NaO_6$	625.4439	**-0.1**	3
	641.4242	$C_{37}H_{62}KO_6$	641.4178	**-10.0**	31
		Pre$_{Prg}$			
	567.4044	$C_{36}H_{55}O_5$	567.4044	**0.1**	10
	585.4145	$C_{36}H_{57}O_6$	585.4150	**0.7**	6
	607.3970	$C_{36}H_{56}NaO_6$	607.3969	**-0.2**	5
	623.3713	$C_{36}H_{56}KO_6$	623.3708	**-0.8**	7
		Pre$_{All}$			
	569.4188	$C_{36}H_{57}O_5$	569.4201	**2.1**	9
	587.4298	$C_{36}H_{59}O_6$	587.4306	**1.4**	3
	609.4120	$C_{36}H_{58}NaO_6$	609.4126	**0.9**	6
	625.3857	$C_{36}H_{58}KO_6$	625.3865	**1.2**	4
		Pre$_{Pr}$			
	571.4341	$C_{36}H_{59}O_5$	571.4357	**2.8**	7
	589.4453	$C_{36}H_{61}O_6$	589.4463	**1.6**	4
	611.4273	$C_{36}H_{60}NaO_6$	611.4282	**1.6**	5
	627.4018	$C_{36}H_{60}KO_6$	627.4021	**0.6**	75
		Pre$_{Cl}$			
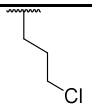	605.3965	$C_{36}H_{58}ClO_5$	605.3967	**0.5**	67
	623.4063	$C_{36}H_{60}ClO_6$	623.4073	**1.6**	21
	645.3898	$C_{36}H_{59}ClNaO_6$	645.3892	**-0.8**	14
	661.3627	$C_{36}H_{59}ClKO_6$	661.3632	**0.7**	78

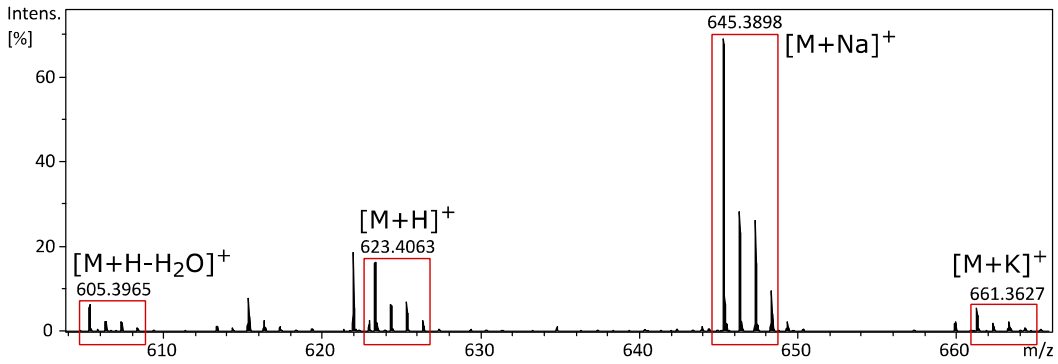

Figure S 40: Detection of typical adducts of premonensin derivatives from a precursor directed biosynthesis with the example of Pre$_{Cl}$. The adducts show a characteristic isotope pattern for the chloride containing derivative.

Table S 51: Mass spectrometric data of the fragment ions premonensin derivatives resulting from a precursor directed biosynthesis. Bu: Butyl. Prg: Propargyl. All: Allyl. Pr: Propyl. Cl: 3-chloropropyl. *Only very low intensities were detected.

Fragment	meas. m/z	ion formula	m/z	err [ppm]
		Pre$_{Pr}$		
F	193.0833	$C_9H_{14}NaO_3$	193.0835	**1.0**
G	205.08*			
A	223.0935	$C_{10}H_{16}NaO_4$	223.0941	**2.5**
C	237.1092	$C_{11}H_{18}NaO_4$	237.1097	**2.4**
D	261.13*			
B	411.3222	$C_{26}H_{44}NaO_2$	411.3234	**2.8**
E	439.3219	$C_{27}H_{44}NaO_3$	439.3183	**-8.3**
L	491.3845	$C_{32}H_{52}NaO_2$	491.3860	**2.9**
K	509.3947	$C_{32}H_{54}NaO_3$	509.3965	**3.5**
J	531.4138	$C_{35}H_{56}NaO_2$	531.4173	**6.5**
N	537.39*			
I	549.4273	$C_{35}H_{58}NaO_3$	549.4278	**1.0**
M	567.43*			
H	593.4207	$C_{36}H_{58}NaO_5$	593.4176	**-5.2**
		Pre$_{All}$		
F	193.0837	$C_9H_{14}NaO_3$	193.0835	**-1.2**
G	205.10*			
A	223.0939	$C_{10}H_{16}NaO_4$	223.0941	**0.7**
C	437.3005	$C_{27}H_{42}NaO_3$	437.3026	**4.9**
D	263.12*			
B	409.3069	$C_{26}H_{42}NaO_2$	409.3077	**1.8**
E	437.30*			
L	489.3687	$C_{32}H_{50}NaO_2$	489.3703	**3.2**
K	507.3787	$C_{32}H_{52}NaO_3$	507.3809	**4.3**
J	529.3998	$C_{35}H_{54}NaO_2$	529.4016	**3.5**
N	535.3760	$C_{33}H_{52}NaO_4$	535.3758	**-0.4**
I	547.4127	$C_{35}H_{56}NaO_3$	547.4122	**-1.0**
M	565.4180	$C_{35}H_{58}NaO_4$	565.4227	**8.3**
H	591.4037	$C_{36}H_{56}NaO_5$	591.4020	**-2.9**
		Pre$_{Prg}$		
F	193.0843	$C_9H_{14}NaO_3$	193.0835	**-4.3**
G	-			
A	223.0942	$C_{10}H_{16}NaO_4$	223.0941	**-0.3**
C	-			
D	263.14*			
B	407.2905	$C_{26}H_{40}NaO_2$	407.2921	**3.8**
E	435.2869	$C_{27}H_{40}NaO_3$	435.2870	**0.1**
L	487.36*			
K	505.3666	$C_{32}H_{50}NaO_3$	505.3652	**-2.7**
J	527.37*			
N	533.36*			
I	545.3935	$C_{35}H_{54}NaO_3$	545.3965	**5.6**
M	563.41*			
H	589.3865	$C_{36}H_{54}NaO_5$	589.3863	**-0.3**

Fragment	meas. m/z	ion formula	m/z	err [ppm]
		Pre_{Bu}		
F	193.0855	$C_9H_{14}NaO_3$	193.0835	**-10.1**
G	205.0833	$C_{10}H_{14}NaO_3$	205.0835	**0.8**
A	223.0941	$C_{10}H_{16}NaO_4$	223.0941	**0.0**
C	237.11*			
D	263.12*			
B	425.3372	$C_{27}H_{46}NaO_2$	425.3390	**4.2**
E	453.3357	$C_{28}H_{46}NaO_3$	453.3339	**-3.9**
L	505.4003	$C_{33}H_{54}NaO_2$	505.4016	**2.6**
K	523.4108	$C_{33}H_{56}NaO_3$	523.4122	**2.6**
J	545.4363	$C_{36}H_{58}NaO_2$	545.4329	**-6.2**
N	551.39*			
I	563.4435	$C_{36}H_{60}NaO_3$	563.4435	**-0.1**
M	581.46*			
H	607.4390	$C_{37}H_{60}NaO_5$	607.4333	**-9.3**
		Pre_{Cl}		
F	193.08*			
G	205.08*			
A	223.0947	$C_{10}H_{16}NaO_4$	223.0941	**-2.7**
C	-			
D	-			
B	445.2873	$C_{26}H_{43}ClNaO_2$	445.2844	**-6.6**
E	-			
L	-			
K	543.38*			
J	-			
N	-			
I	-			
M	601.40*			
H	-			
B-HCl	409.3077	$C_{26}H_{42}NaO_2$	409.3077	**-0.1**
K-HCl	507.39*			
I-HCl	547.41*			
-HCl	609.4138	$C_{36}H_{58}NaO_6$	609.4126	**-2.0**

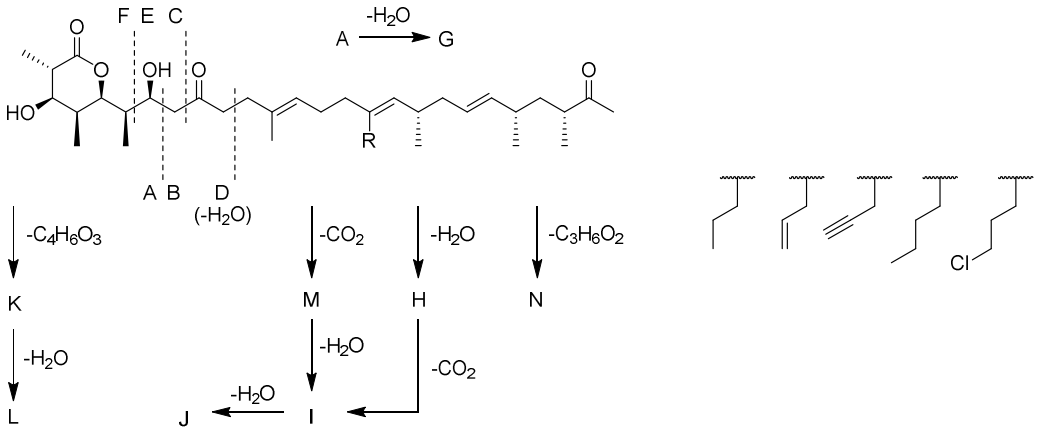

Figure S 41: Fragmentation pattern of premonensin and its derivatives from the precursor directed biosynthesis. For Pre_{Cl} additional loss of HCl was observed.

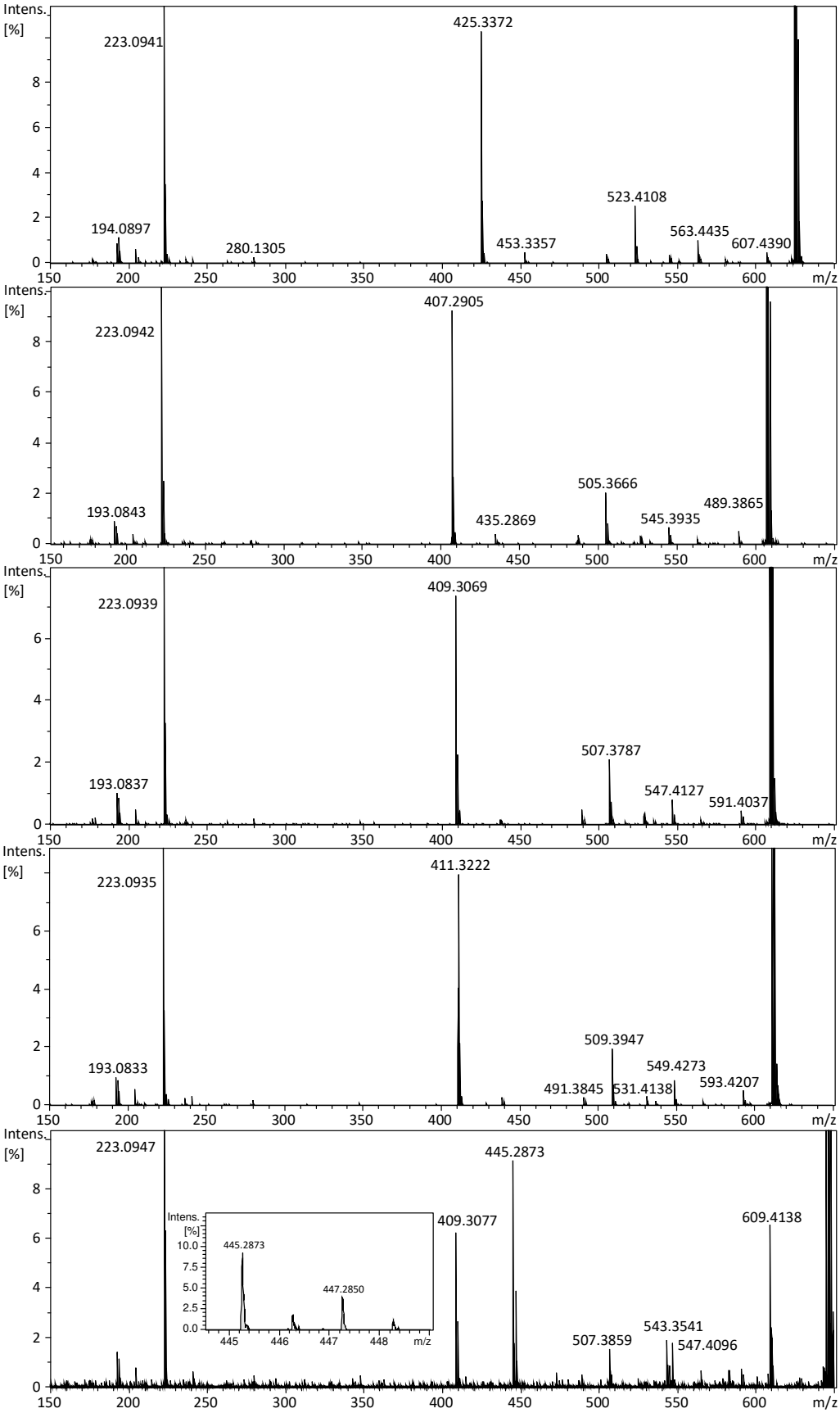

Figure S 42: MS^2 spectra of premonensin derivatives from a precursor directed biosynthesis in *S. cinnamonensis* A495. From top to bottom: Pre_{Bu}, Pre_{Prg}, Pre_{All}, Pre_{Pr} and Pre_{Cl}. For Pre_{Cl} the isotope pattern of fragments is in accord to the presence or absence of chlorine in the respective fragment.

5.8.2 Hop-Off Intermediates from the Premonensin Biosynthesis with New-to-Nature Side Chains

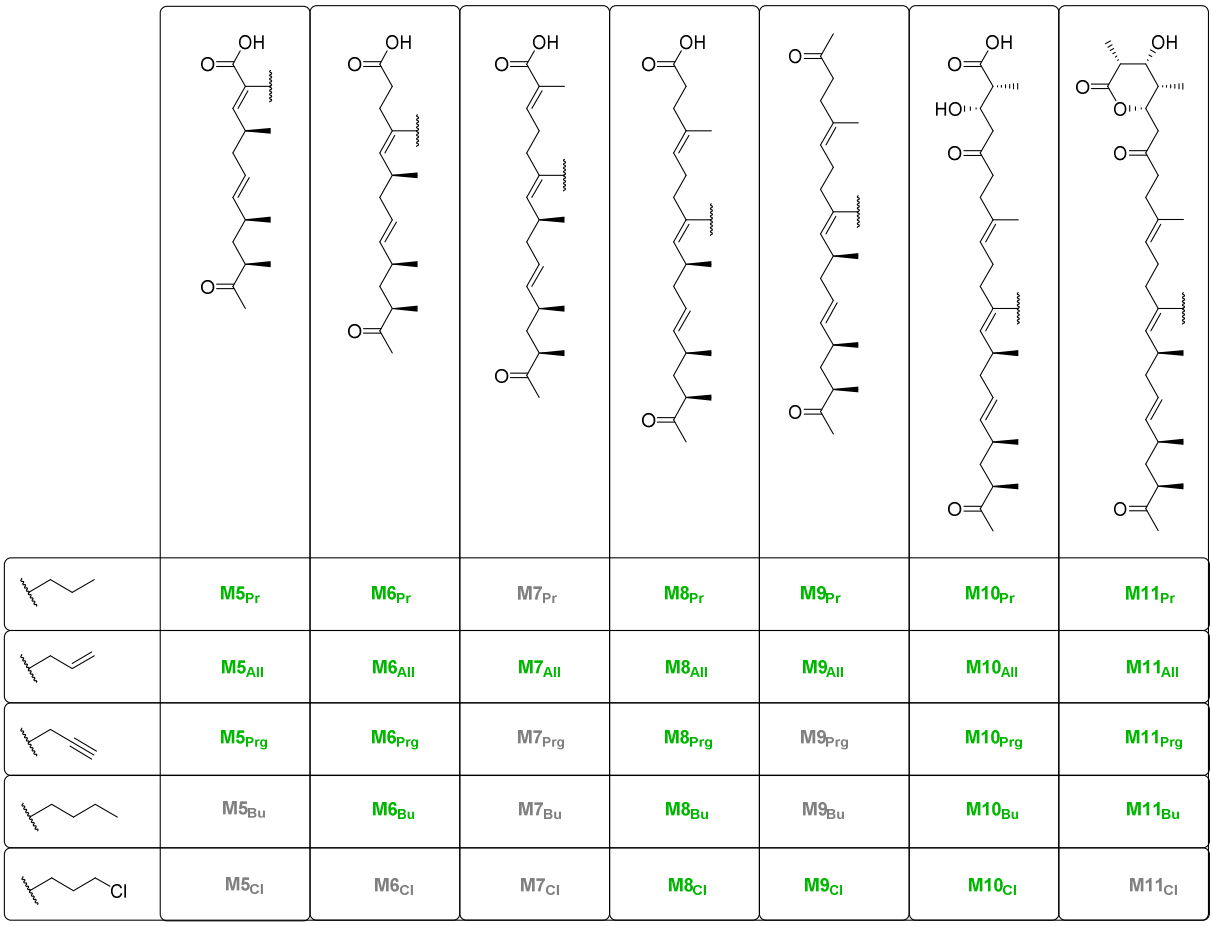

Figure S 43: Hop-off intermediates from the premonensin assembly line after incorporation of new-to-nature side chains (in module 5) by precursor directed biosynthesis. All fragments in green have been detected by LC-HRMS.

Table S 52: Overview of the mass spectrometric data of different adducts of the hop-off intermediates from the premonensin biosynthetic pathway in *S. cinnamonensis* A495 supplying allyl (All) malonic acid as a building block.

	Meas. m/z	ion formula	Sum Formula	m/z	err [ppm]	mSigma
M5$_{All}$	293.2110	$C_{18}H_{29}O_3$	$C_{18}H_{28}O_3$	293.2111	**0.5**	344
	315.1915	$C_{18}H_{28}NaO_3$		315.1931	**5.0**	17
M6$_{All}$	303.2331	$C_{20}H_{31}O_2$	$C_{20}H_{32}O_3$	303.2319	**-4.1**	63
	321.2419	$C_{20}H_{33}O_3$		321.2424	**1.5**	25
	343.2227	$C_{20}H_{32}NaO_3$		343.2244	**4.8**	7
M7$_{All}$	343.2629	$C_{23}H_{35}O_2$	$C_{23}H_{36}O_3$	343.2632	**0.8**	32
	361.2729	$C_{23}H_{37}O_3$		361.2737	**2.3**	22
	383.2552	$C_{23}H_{36}NaO_3$		383.2557	**1.3**	13
M8$_{All}$	371.2944	$C_{25}H_{39}O_2$	$C_{25}H_{40}O_3$	371.2945	**0.1**	3
	389.3047	$C_{25}H_{41}O_3$		389.3050	**0.8**	3
	411.2865	$C_{25}H_{40}NaO_3$		411.2870	**1.2**	6
M9$_{All}$	387.3250	$C_{26}H_{43}O_2$	$C_{26}H_{42}O_2$	387.3258	**2.0**	32
	409.3074	$C_{26}H_{42}NaO_2$		409.3077	**0.8**	1
M10$_{All}$	511.3391	$C_{30}H_{48}NaO_5$	$C_{30}H_{48}O_5$	511.3394	**0.7**	42
M11$_{All}$	511.3781	$C_{33}H_{51}O_4$	$C_{33}H_{52}O_5$	511.3782	**0.2**	26
	539.3706	$C_{32}H_{52}NaO_5$		539.3707	**0.2**	28
	551.3702	$C_{33}H_{52}NaO_5$		551.3707	**0.9**	4

Table S 53: Overview of the mass spectrometric data of different adducts of the hop-off intermediates from the premonensin biosynthetic pathway in *S. cinnamonensis* A495 supplying butyl (Bu) malonic acid as a building block. *M11$_{Bu}$ was atypically mainly detected in the linear form.

	Meas. m/z	ion formula	Sum Formula	m/z	err [ppm]	mSigma
M6$_{Bu}$	337.2726	$C_{21}H_{37}O_3$	$C_{21}H_{36}O_3$	337.2737	**3.2**	25
	359.2562	$C_{21}H_{36}NaO_3$		359.2557	**-1.5**	19
M8$_{Bu}$	405.3352	$C_{26}H_{45}O_3$	$C_{26}H_{44}O_3$	405.3363	**2.7**	n.a.
	427.3175	$C_{26}H_{44}NaO_3$		427.3183	**1.9**	19
M10$_{Bu}$	527.3707	$C_{31}H_{52}NaO_5$	$C_{31}H_{52}O_5$	527.3707	**0.0**	11
M11$_{Bu}$	563.4309	$C_{34}H_{59}O_6$	$C_{34}H_{58}O_6$	563.4306	**-0.6**	10
*	585.4114	$C_{34}H_{58}NaO_6$		585.4126	**2.0**	18

Table S 54: Overview of the mass spectrometric data of different adducts of the hop-off intermediates from the premonensin biosynthetic pathway in *S. cinnamonensis* A495 supplying propyl (Pr) malonic acid as a building block.

	Meas. m/z	ion formula	Sum Formula	m/z	err [ppm]	mSigma
M5$_{Pr}$	295.2256	$C_{16}H_{32}NaO_3$	$C_{18}H_{30}O_3$	295.2244	**-4.0**	n.a.
	317.2083	$C_{18}H_{30}NaO_3$		317.2087	**1.2**	17
M6$_{Pr}$	305.2474	$C_{20}H_{33}O_2$	$C_{20}H_{34}O_3$	305.2475	**0.4**	25
	323.2583	$C_{20}H_{35}O_3$		323.2581	**-0.7**	4
	345.2392	$C_{20}H_{34}NaO_3$		345.2400	**2.4**	7
M8$_{Pr}$	373.3104	$C_{25}H_{41}O_2$	$C_{25}H_{42}O_3$	373.3101	**-0.9**	14
	391.3203	$C_{25}H_{43}O_3$		391.3207	**1.0**	1
	413.3023	$C_{25}H_{42}NaO_3$		413.3026	**0.8**	8
M9$_{Pr}$	389.3405	$C_{26}H_{45}O_2$	$C_{26}H_{44}O_2$	389.3414	**2.2**	n.a.
	411.3215	$C_{26}H_{44}NaO_2$		411.3234	**4.5**	29
M10$_{Pr}$	513.3544	$C_{30}H_{50}NaO_5$	$C_{30}H_{50}O_5$	513.3550	**1.3**	9
M11$_{Pr}$	513.3940	$C_{33}H_{53}O_4$	$C_{33}H_{54}O_5$	513.3938	**-0.3**	n.a.
	531.4033	$C_{33}H_{55}O_5$		531.4044	**2.1**	39
	553.3862	$C_{33}H_{54}NaO_5$		553.3863	**0.3**	20

Table S 55: Overview of the mass spectrometric data of different adducts of the hop-off intermediates from the premonensin biosynthetic pathway in *S. cinnamonensis* A495 supplying propargyl (Prg) malonic acid as a building block.

	Meas. m/z	ion formula	Sum Formula	m/z	err [ppm]	mSigma
M5$_{Prg}$ (traces)	273.1884	$C_{18}H_{25}O_2$	$C_{18}H_{26}O_3$	273.1849	**-12.8**	18
	291.1973	$C_{18}H_{27}O_3$		291.1955	**-6.3**	15
	313.1776	$C_{18}H_{26}NaO_3$		313.1774	**-0.6**	24
M6$_{Prg}$ (traces)	341.2084	$C_{20}H_{30}NaO_3$	$C_{20}H_{30}O_3$	341.2087	**0.8**	23
M8$_{Prg}$	369.2779	$C_{25}H_{37}O_2$	$C_{25}H_{38}O_3$	369.2788	**2.6**	24
	387.2892	$C_{25}H_{39}O_3$		387.2894	**0.4**	11
	409.2704	$C_{25}H_{38}NaO_3$		409.2713	**2.3**	7
M10$_{Prg}$	509.3230	$C_{30}H_{46}NaO_5$	$C_{30}H_{46}O_5$	509.3237	**1.5**	45
M11$_{Prg}$	527.3716	$C_{33}H_{51}O_5$	$C_{33}H_{50}O_5$	527.3731	**2.9**	688
	549.3535	$C_{33}H_{50}NaO_5$		549.3550	**2.7**	23

Table S 56: Overview of the mass spectrometric data of different adducts of the hop-off intermediates from the premonensin biosynthetic pathway in *S. cinnamonensis* A495 supplying 3-chloropropyl (Cl) malonic acid as a building block.

	Meas. m/z	ion formula	Sum Formula	m/z	err [ppm]	mSigma
M8$_{Cl}$	425.2813	$C_{25}H_{42}ClO_3$	$C_{25}H_{41}ClO_3$	425.2817	**0.9**	10
	447.2631	$C_{25}H_{41}ClNaO_3$		447.2636	**1.2**	10
M9$_{Cl}$	445.2841	$C_{26}H_{43}ClNaO_2$	$C_{26}H_{43}ClO_2$	445.2844	**0.6**	44
M10$_{Cl}$	547.3157	$C_{30}H_{49}ClNaO_5$	$C_{30}H_{49}ClO_5$	547.3161	**0.7**	14

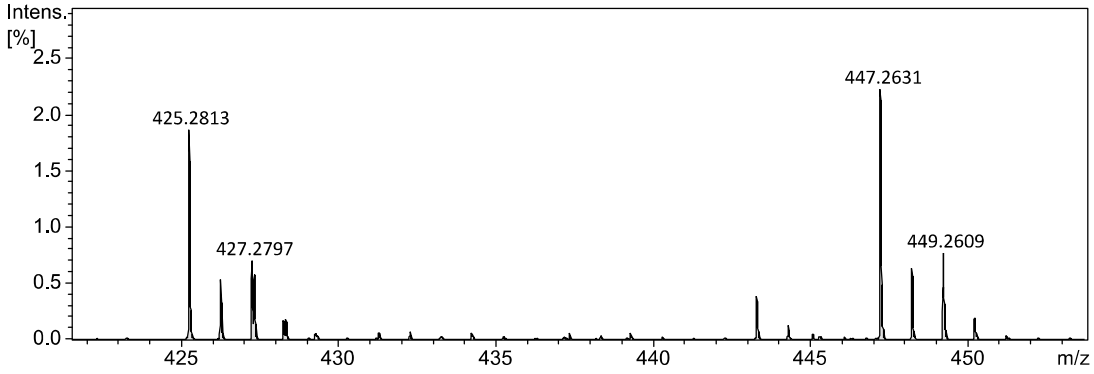

Figure S 44: Exemplary MS spectrum showing two adducts of the hop-off intermediate M8$_{Cl}$ with the characteristic isotope patterns.

6 NMR Data of Premonensin Derivatives

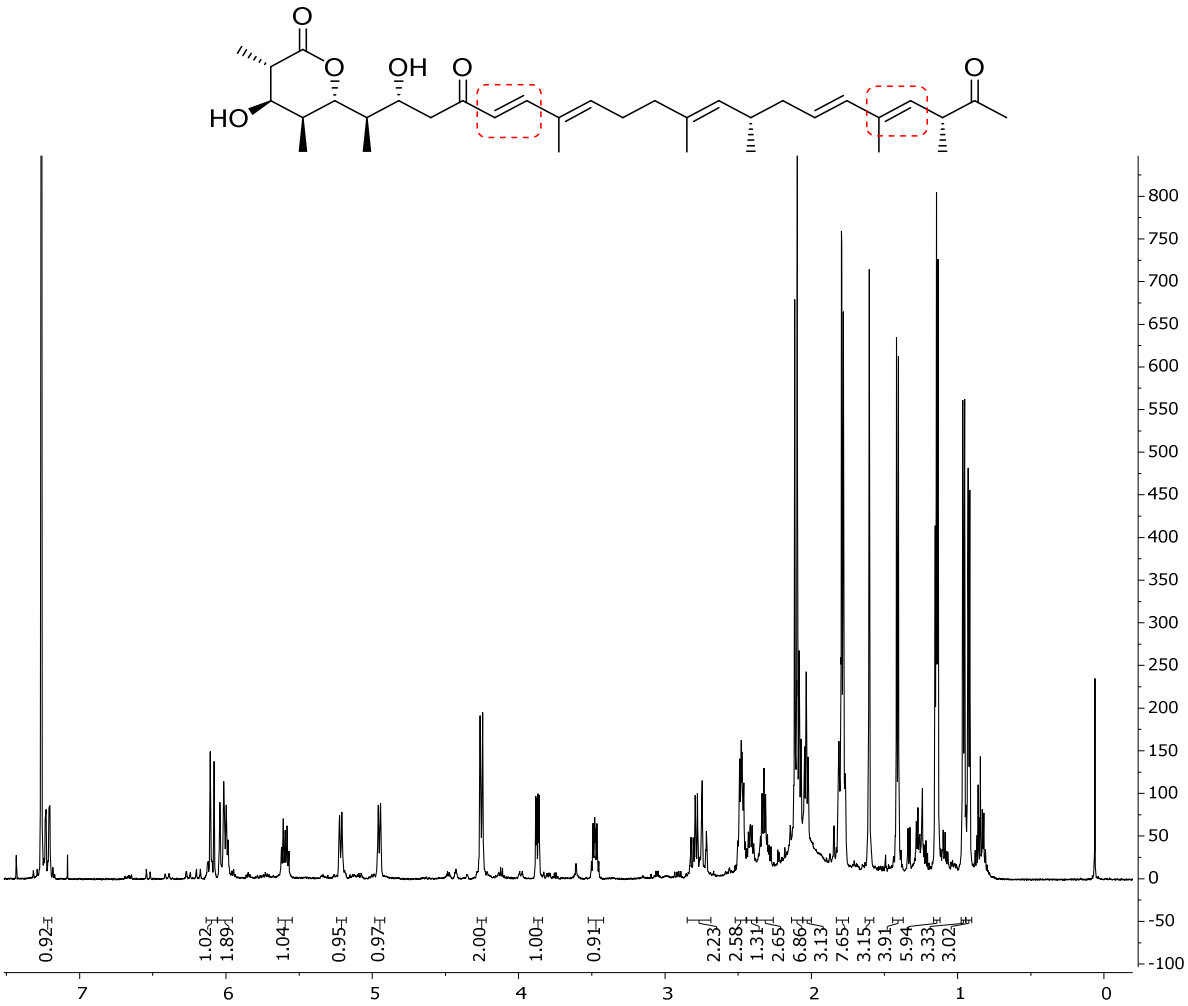

Figure S 45: ^{1}H-NMR of isolated ER2^{0}DH8^{0}Pre$_{B}$ dehydrated during the purification.

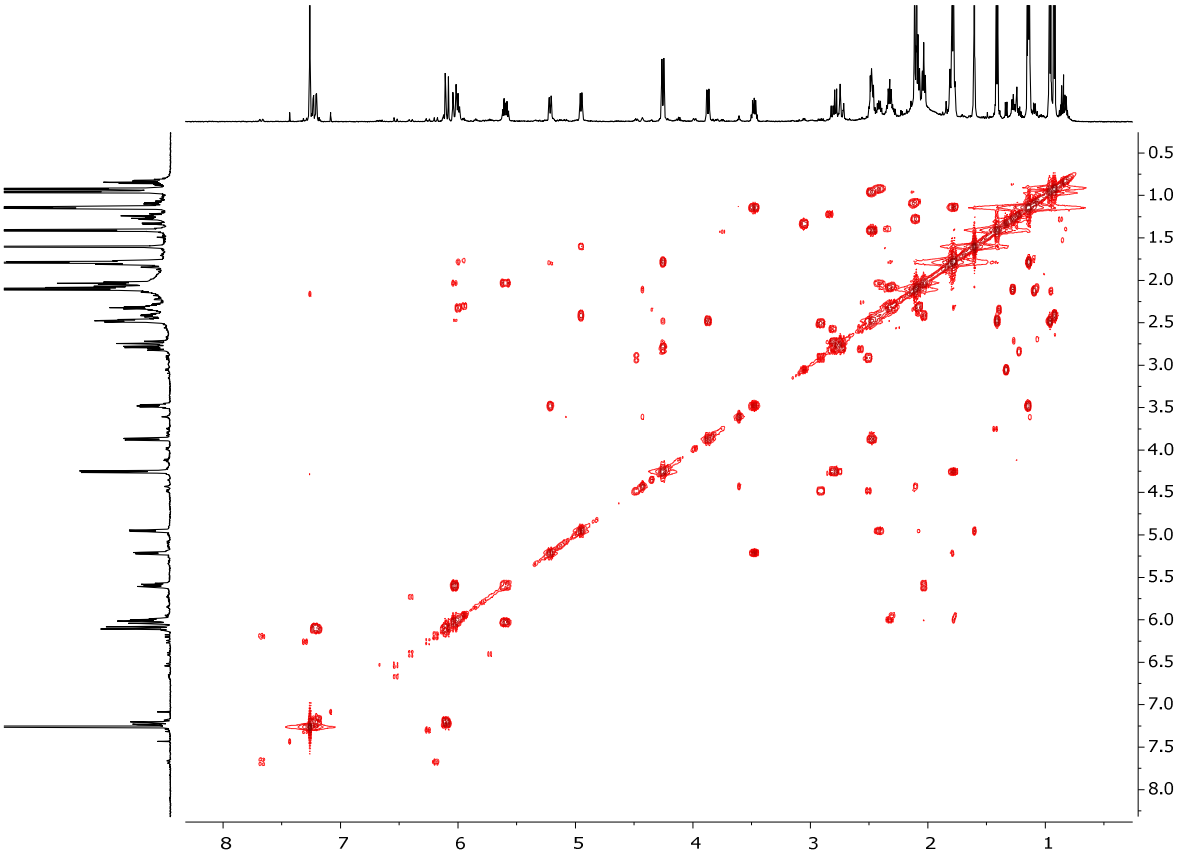

Figure S 46: COSY spectrum of isolated ER2^{0}DH8^{0}Pre$_{B}$ dehydrated during the purification.

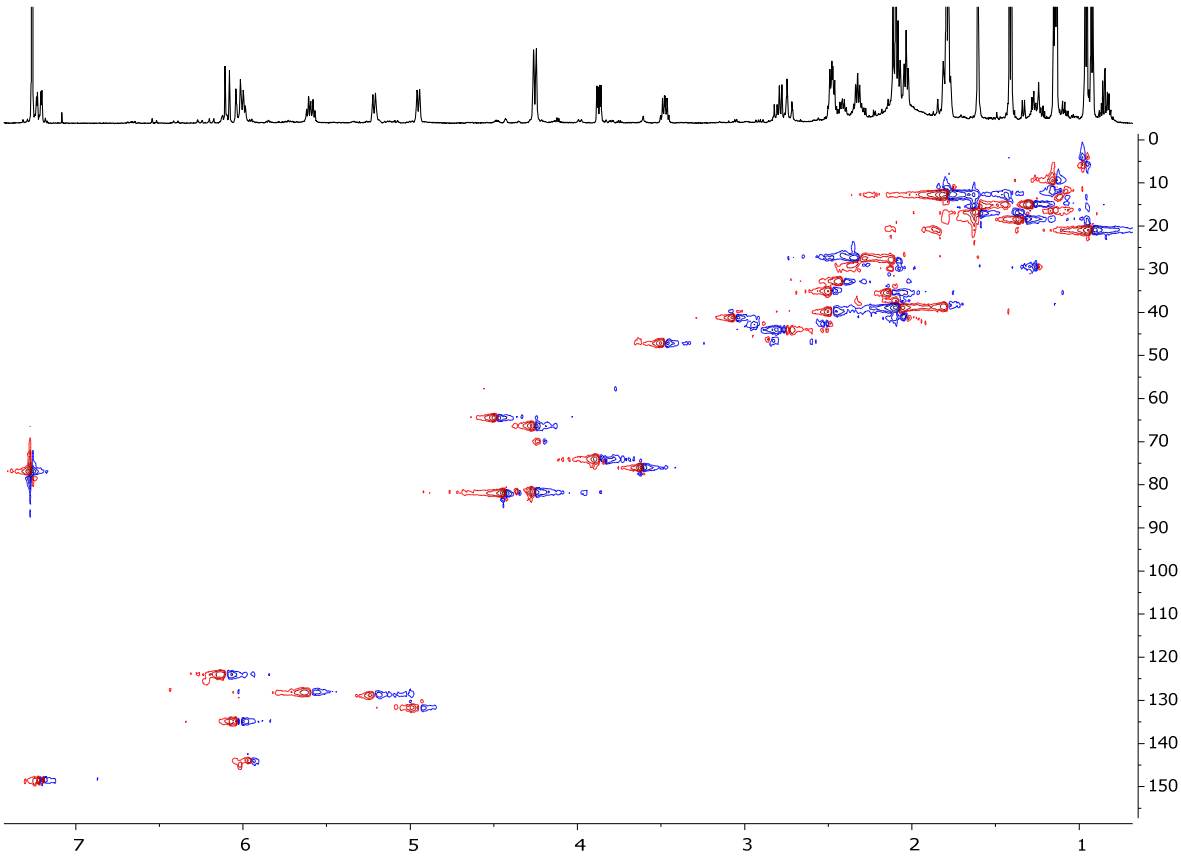

Figure S 47: HSQC spectrum of isolated ER2^{0}DH8^{0}Pre$_{B}$ dehydrated during the purification.

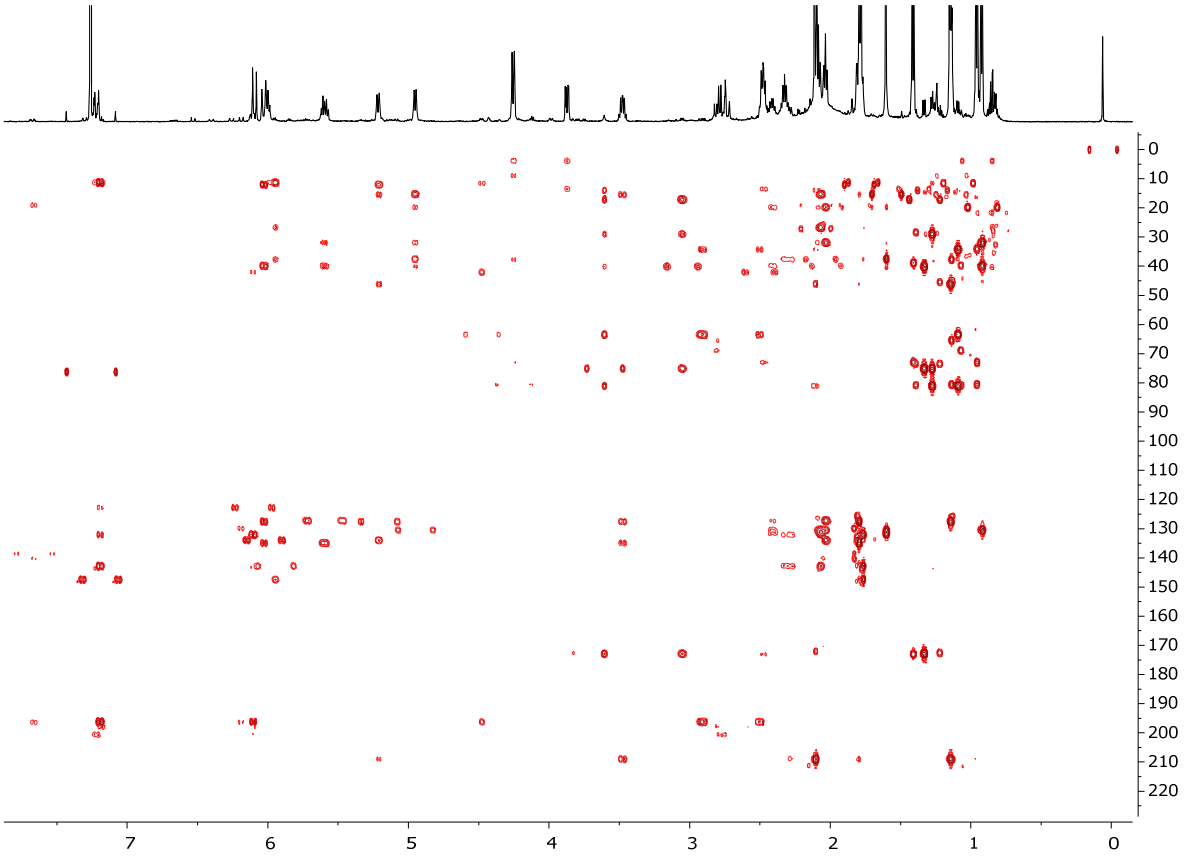

Figure S 48: HMBC spectrum of isolated ER2^{0}DH8^{0}Pre$_B$ dehydrated during the purification.

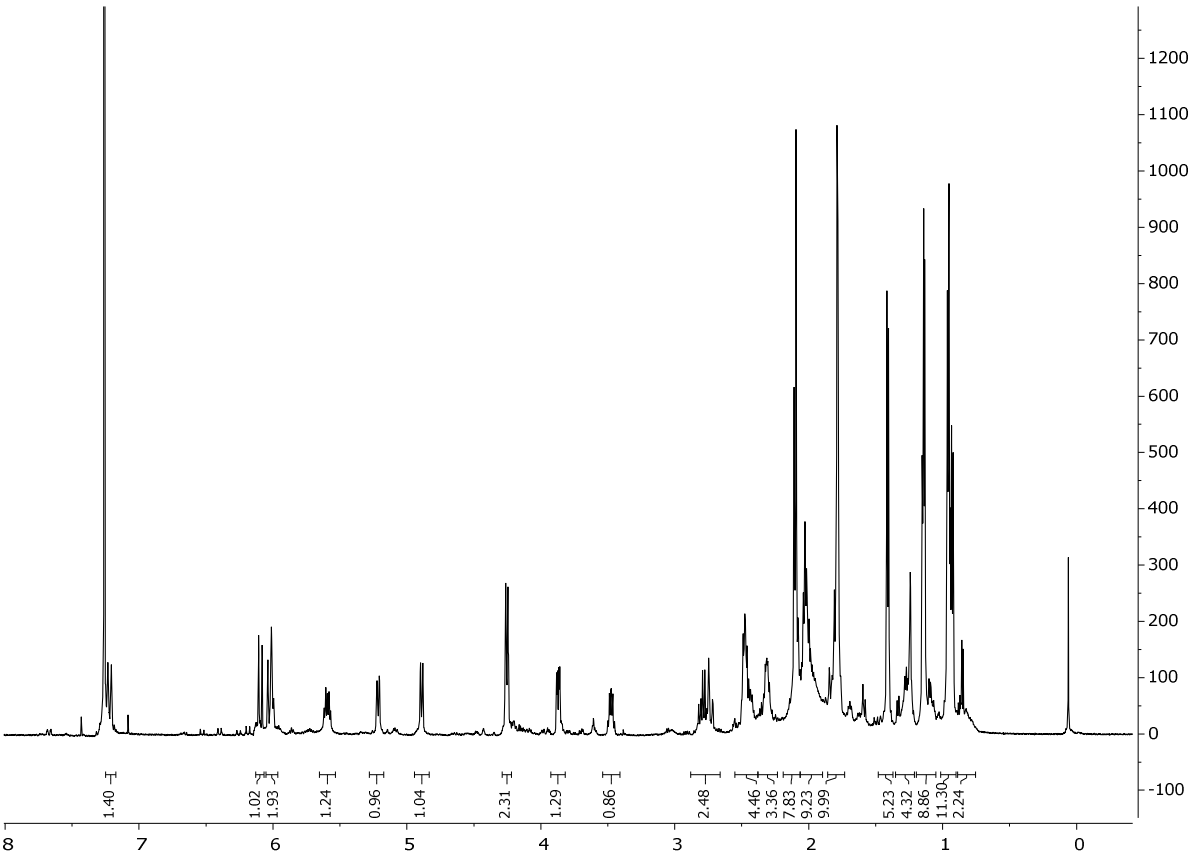

Figure S 49: ^{1}H-NMR of isolated ER2^{0}DH8^{0}Pre$_A$ dehydrated during the purification.

Table S 57: Signal assignment for the NMR of ER2^{0}DH8^{0}Pre$_B$ (dehydrated). ^{13}C data were assigned using the HSQC-spectrum if possible.

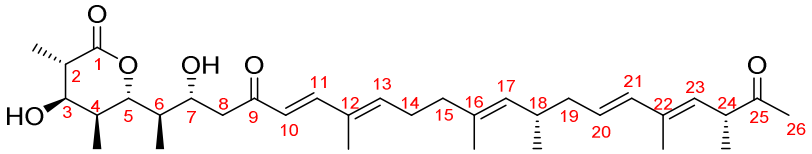

Position	^{1}H [ppm]		*J* [Hz]	^{13}C [ppm]
1	-	-	-	174.0
2	2.47	m	-	
2´	1.41	d	7.1	
3	3.87	dd	4.2/10.3	74.0
4	2.79	m	-	
4´	0.96	d	7.0	4.8
5	4.26	m	-	66.4 or 81.5
6	1.79	m	-	
6´	1.14	m	-	
7	4.26	m	-	66.4 or 81.5
8	2.74/2.47	m/m	-	
9	-	-	-	197.4 or 201.8
10	6.10	d	15.3	123.9
11	7.21	dd	3.0/15.4	148.6
12	-	-	-	
12´	1.79	m	-	
13	6.00	t	7.5	144.9
14	2.33	m	-	
15	2.09	m	-	
16	-	-	-	
16´	1.61	s	-	16.2
17	4.96	d	9.3	131.8
18	2.42	m	-	
18´	0.93	d	6.8	20.2
19	2.04	m	-	
20	5.60	dt	7.2/15.2	128.1
21	6.03	d	7.5	134.8
22	-	-	-	
22´	1.80	m	-	
23	5.21	d	9.9	128.8
24	3.48	dq	6.8/9.6	47.0
24´	1.15	m	-	
25	-	-	-	210.2
26	2.10	m	-	

7 Ketosynthase Alignments and Phylogenetic Tree

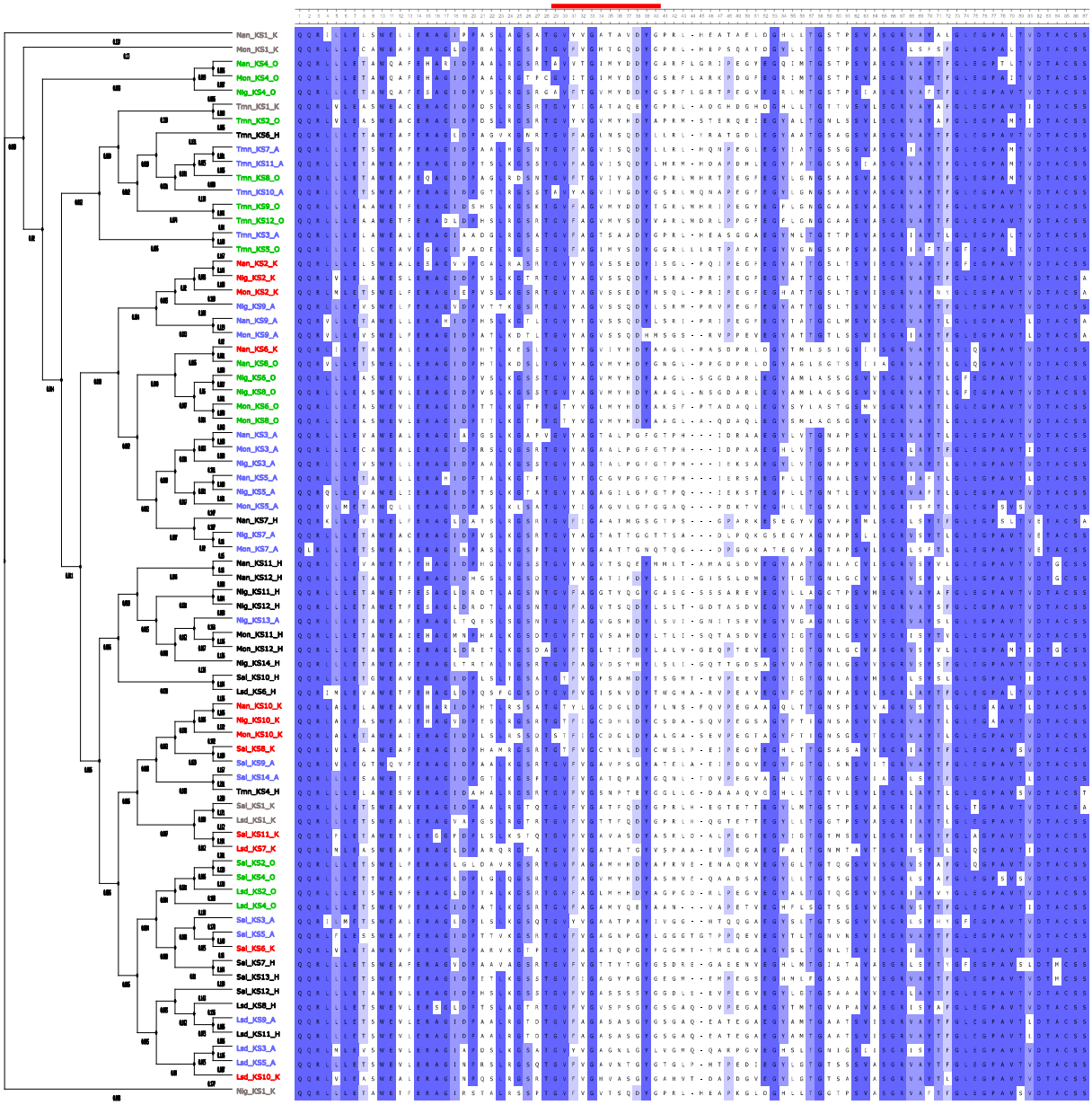

Figure S 50: Phylogenetic tree of ketosynthase sequences from 5 different gene clusters of polyether antibiotics.[4] Mon: Monensin.[5, 6] Lsd: Lasalocid.[7, 8] Sal: Salinomycin.[9] Nan: Nanchangmycin.[10] Tmn: Tetronomycin.[11] Numbers indicate the module number of elongation modules in the respective gene cluster. The color used for ketosynthase names represent the redox state of the incoming intermediate from upstream modules. K: Ketone. H: Hydroxyl. O: Olefin. A: Alkane. Modules in grey represent KS from the first elongation module always accepting a β-ketone as incoming intermediate. The sequence alignment represents a part of the whole domain with a highly variable region. The region labeled in red was used by Zhang et. al[12] establishing fingerprint regions for the type of incoming polyketide intermediate.

8 MonAIX, MonAX and Orf31, Streptomyces Manipulation

8.1 Cloning

The gene of interest was amplified by PCR using the primer pair 1711 and 1712 and genomic DNA of *Streptomyces cinnamonensis* (1 ng of gen. DNA, 1 M Betain, 1 µM of each Primer, Phusion High-Fidelity PCR Master Mix). PCR was performed using 2xPhusion Flash Master Mix in an Pico thermal Cycler (Finnzym). MonAIX, MonAX and Orf31 were amplified from the genomic DNA *S. cinnamonensis* A495 using oligos 1464/1465, 1431/1432 and 1711/1712 respectively. All PCR products were DpnI digested and gel purified (PeqGold gel extraction kit, Peqlab). MonAIX and MonAX were cloned into expression vector pET28(+) (Novagen) with N-terminalHis-tag into the NdeI/XhoI restriction sites. Orf31 was cloned into pETM60 as a fusion protein with NusA using NcoI and HindIII restriction sites. Screening of the positive clones was done by colony PCR and confirmed by the sequencing. Oligonucleotides are listed in table S58.

8.2 Expression and Purification

For Expressions BL21-CodonPlus (DE3)-RP was used. While soluble expression of Orf31 and fusion proteins in pETM30 and pETM40 failed under varying conditions, Orf31_NusA (pETM60) could be express as a soluble fusion protein. 1 L of medium was inoculated with 10 mL of an overnight culture and was supplemented with kanamycin and cultivated with 180 rpm at 30 °C. Expression was induced with 0.1 mM IPTG at OD_{600} of 0.7 and the culture was shaken with 180 rpm at 18 °C for 14-18 h.
Expression of MonAIX and MonAX (pET-28a(+)) was done as described for Orf31_NusA. Cells where harvested by centrifugation (3900 xg, 4 °C, 20 min) and cell pellets stored at -20 °C until further usage. Cell pellets of 1 L culture were resuspended in 15 mL of lysis buffer (50 mM Na_2HPO_4, 300 mM NaCl, 10 % Glycerol, 0.5 % Triton X-100, pH=7.8) and lysed by sonication on ice (4x 20 sec, 50% duty cycle). Cell debris was removed by centrifugation (3900 xg, 4 °C, 20 min), the supernatant was supplied with 10 mM of imidazole and transferred to Ni-NTA columns for enrichment and purification.
Five column volumes of lysis buffer with 20 mM of imidazole were used for washing and elution was done with 120 mM imidazole. Fractions containing the desired proteins were pooled, concentrated by centrifugation and a MWCO of 10 kDa. Desalting and buffer exchange were done on PD10 columns. Protein concentration was determined using Bradford reagents with a BSA standard for calibration. Due to the impurity of Orf31_NusA densitometry was used to determine percentage of 40 % target protein. Proteins were frozen in liquid nitrogen and stored in assay buffer (50 mM Tris, 1 mM EDTA, 10 % glycerol, pH=7.5) at -20 °C.

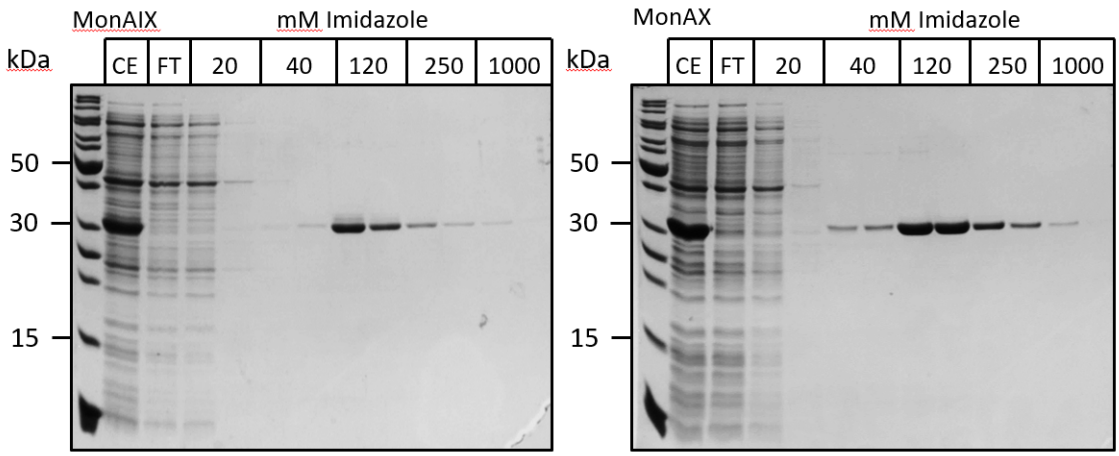

Figure S 51: SDS-PAGE of samples from the purification of MonAIX (left, 30.3 kDa) and MonAX (right, 32.1 kDa) with the crude extract (CE), flow through (FT) and fractions from washing with different imidazole concentrations to determine purification conditions.

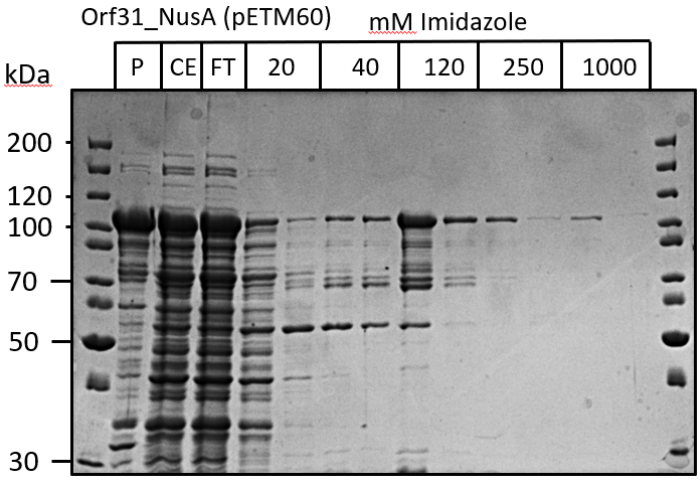

Figure S 52: SDS-PAGE of samples from the purification of the fusion protein Orf31_NusA with the insoluble fraction (P) crude extract (CE), flow through (FT) and fractions from washing with different imidazole concentrations to determine purification conditions. The percentage of the target protein was determined to be 40 % in pooled and concentrated fraction.

8.3 Oligonucleotides Used in this Study

Table S 58: List of oligonucleotides used for cloning of the three hydrolases and genetic manipulation of *S. cinnamonensis.*

1102_pl-14thio-fr	atgacatgattacgaattcaccaccaccggctcagaaaccaccaccggctc	ΔmonAIX
1103_pl-14thio-rev	acggccagtgccaagctaaggaggccaagccgttcgacatcggcggcctggtg	
1104_14thio-jun-fr	ttcgcgggcggttcgttcgatctgcgggtgctgcccggcgggcacttctacctc	
1105_14thio-jun-rev	agcacccgcagatcgaacgaaccgcccgcgaacggaaagcagaccagccgcac	
1106_pl-29thio-fr	atgacatgattacgaatttctgctcgatctggaagagctcgactccgggcatgc	ΔmonAX
1107_pl-29thio-rev	acggccagtgccaagctcaggacttctcctcgaacggcgcgaccacc	
1108_29thio-jun-fr	actaccacccccttgcgcaacacttctatctgaacacgcaccagcagggcgtcacg	
1109_29thio-jun-rev	tgcgtgttcagatagaagtgttgcgcaagggggtggtagtaggaggccgagccg	
1110_pl-31lip-fr	atgacatgattacgaattaccaacatgaccaactacagccgccccgagcag	Δorf31
1111_pl-31lip-rev	acggccagtgccaagctcccatcctttattccgcgattcttacgtgatcgaatcccggc	
1112_31lip-jun-fr	aagccgaccgtcctcttcgtgctgctgaacttcccgatcgagctgctgatccacagc	
1113_31lip-jun-rev	agctcgatcgggaagttcagcagcacgaagaggacggtcggcttgtcaccggcgtcac g	
1141_pr14_seq_for	acgtcgtacgaggcgccatcggc	ΔmonAIX sequencing
1142_pr14_seq_rev	atcggagatcgcttcgagtaccgggc	
1143_pr29_seq_for	aaccgggcaccttgaggaacttgcg	ΔmonAX sequencing
1144_pr29_seq_rev	aggccatcacggctggcaggg	
1145_pr31_seq_for	accacgtgtggcagcgggccc	Δorf31 sequencing
1146_pr31_seq_rev	accgtccacccaggtcacggacc	
1195_pr14_seq_long_rev	atcggagatcgcttcgagtaccgggctcatcg	ΔmonAIX screening
1196_pr14-screen-new_long_for	atgttctccgacgaggagcggccgaaggcc	
1154_pr29-screen_for	acctggtcgacccgtcgttctgggcg	ΔmonAX screening
1170_pr29-screen-new_rev	atgatcgtccggtacttgccgccgg	
1197_pr31-screen_long_for	aagcagaccaggcgaacgacggcttccggtcg	Δorf31 screening
1198_pr31_seq_long_rev	accgtccacccaggtcacggacccctcgcg	
1431pro29exp_for	agcggcctggtgccgcgcggcagccatatgtctgccttccccccacccgatatgtcgg	MonAX
1432pro29exp_rev	tctcagtggtggtggtggtggtgctcgagttcaccgagcgttcccccttgctgtcgc	
1464pro14exp_for	agcggcctggtgccgcgcggcagccatatggacaggggcacggcggcgcgggc	MonAIX
1465pro14exp_rev	tctcagtggtggtggtggtggtgctcgagttcagacgcccggccccgccgtcagcgc	
1711_ORF31_pETM21-60_rv	agggcgacatgttcgtgaaggttcctgtggaggtcaccgtgc	Orf31
1712_ORF31_pETM30-60_fw	gaattcggatcctcaccgcgcgtacgggcgcagc	
1670_codA-Bam_for	attattcggatccgctcgaggttgacatcttttgccgattctgg	codA
1671_codA-Bam_rev	aataatcggatccggcatgctcagcgcttgtagtcgatggcc	
111_KR11/12_Y-F_for	aagtggttggccgcaccgaaggcgccctgctggccactgcccc	Null mutations of KR11 and KR12
112_KR11/12_Y-F_rev	agtggccagcagggcgccttcggtgcggccaaccacttcctcgacgcc	

8.4 *In vitro* Activity Assay of Hydrolases

The activity assay was run in a microtiter plate in a volume of 100 µL. For measurement 70 µL of assay buffer supplemented with DTNB (50 mM Tris, 1 mM EDTA, 10 % glycerol, 7 mM DTNB, pH=7.5) were mixed with 10 µL of the substrates in DMSO (5 mM final concentration). In a first attempt activity was tested with five different SNAC-esters (compounds **1-5**). As a next step compounds **6** and **7** were used.

The reaction was started by adding 20 µL of enzyme (MonAIX: 0.36 mg/mL, MonAX: 0.17 mg/mL, Orf31_NusA: 0.40 mg/mL) in assay buffer.
Absorbance at 412 nm was observed for 15 minutes after adding the enzyme. Reaction speed in the linear range at the beginning of the monitoring (2-8 minutes after starting the reaction) were measured in at least triplicates and values were corrected by background hydrolysis of SNAC-esters which was also measured in triplicates.

9 Synthesis

9.1 General Information

9.1.1 Solvents and Reagents

Dry solvents (Et_2O, CH_2Cl_2, THF) were collected from a Solvent-Drying-System from *Mbraun* (SPS-800). In order to dry toluene, freshly distilled toluene was stored for 24h over $CaCl_2$. The pre-dried toluene was distilled, whereas the first 10% of distillate were discarded. Then, toluene was distilled under argon and stored over activated molecular sieve 4 Å. Dry DMF was purchased from *Sigma Aldrich*. Technical grade solvents (PE, CH_2Cl_2, EtOAc, *n*-hexane, acetone) used for flash chromatography or moisture sensitive reactions, were distilled with the rotation evaporator. HPLC-grade solvents were purchased from *Fisher Scientific*. Triethylamine was dried by adding CaH_2 followed by distillation under argon atmosphere. DMSO was dried by storing it over activated molecular sieve 3 Å in a flame-dried Schlenk flask. MeMgBr was purchased from *Sigma Aldrich* as a 3M solution in diethyl ether.

9.1.2 Experimental Setup

Moisture sensitive reactions were performed in flasks, which were flame-dried with a heat gun (630 °C), evacuated and flushed with argon using a Schlenk-system. This procedure was repeated three times. The addition of reagents and solvents was done using syringes and cannulas into septum equipped flasks. Solids were added under an argon-counter stream.

9.1.3 Reaction Control and Purification

Thin layer chromatography (TLC) was performed to monitor the course of the reaction using silica gel coated alumina plates from *Merk* (DC Silicagel 60 F_{254}). For staining, potassium permanganate solution (9 g $KMnO_4$, 60 g K_2CO_3, 15 ml 5% aq. NaOH, 900 ml H_2O) was used. For flash chromatography glass columns packed with silica gel from *Macherey-Nagel* (Particle size 40-63 µm) as stationary phase were used. As mobile phase eluent mixtures were used (petrol ether, ethyl acetate, CH_2Cl_2, MeOH). The exact ratios are listed in the experimental part.

9.2 Characterization Methods

9.2.1 NMR-Spectroscopy

The NMR spectra of the ^{1}H- and ^{13}C-nuclei were measured with spectrometers from *Bruker* type DPX 200 (200 MHz), DPX 250 (250 MHz), DRX-400 (400 MHz). The processing of the spectrums was preformed using *MesterLab MestReNova* 10.0. Deuterated chloroform from *Deutero GmbH* was used as a solvent for NMR samples. Chemical shifts δ are reported in parts per million (ppm) and coupling constants J in Hertz (Hz). The standardization of the spectra was achieved using the chloroform peak from not completely deuterated solvent ($CDCl_3$: δ (^{1}H) = 7.26 and δ (^{13}C) = 77.16). Signal multiplicities were reported using the following abbreviations: s = singlet, d = doublet, t = triplet, q = quartet, quint = quintet, sext = sextet, sept = septet, m = multiplet, dd = doublet of doublet, dt = doublet of triplet, dq = doublet of quartet, bs = broad singlet.

9.2.2 Melting Point Determination

The determination of the melting points was achieved using a melting point meter from *Büchi* (M-565). All measurements were performed under atmospheric pressure.

9.2.3 Specific Rotation $[\alpha]_D^{20}$

The specific rotation was measured using an *Anton Paar* Propol polarimeter. The measurements were conducted using a halogen lamp in a 5 cm cuvette. The used concentrations c for each measurement are listed in the procedures and are stated in g / 100 ml.

9.3 Synopsis ER2^0-Triketide Thioester

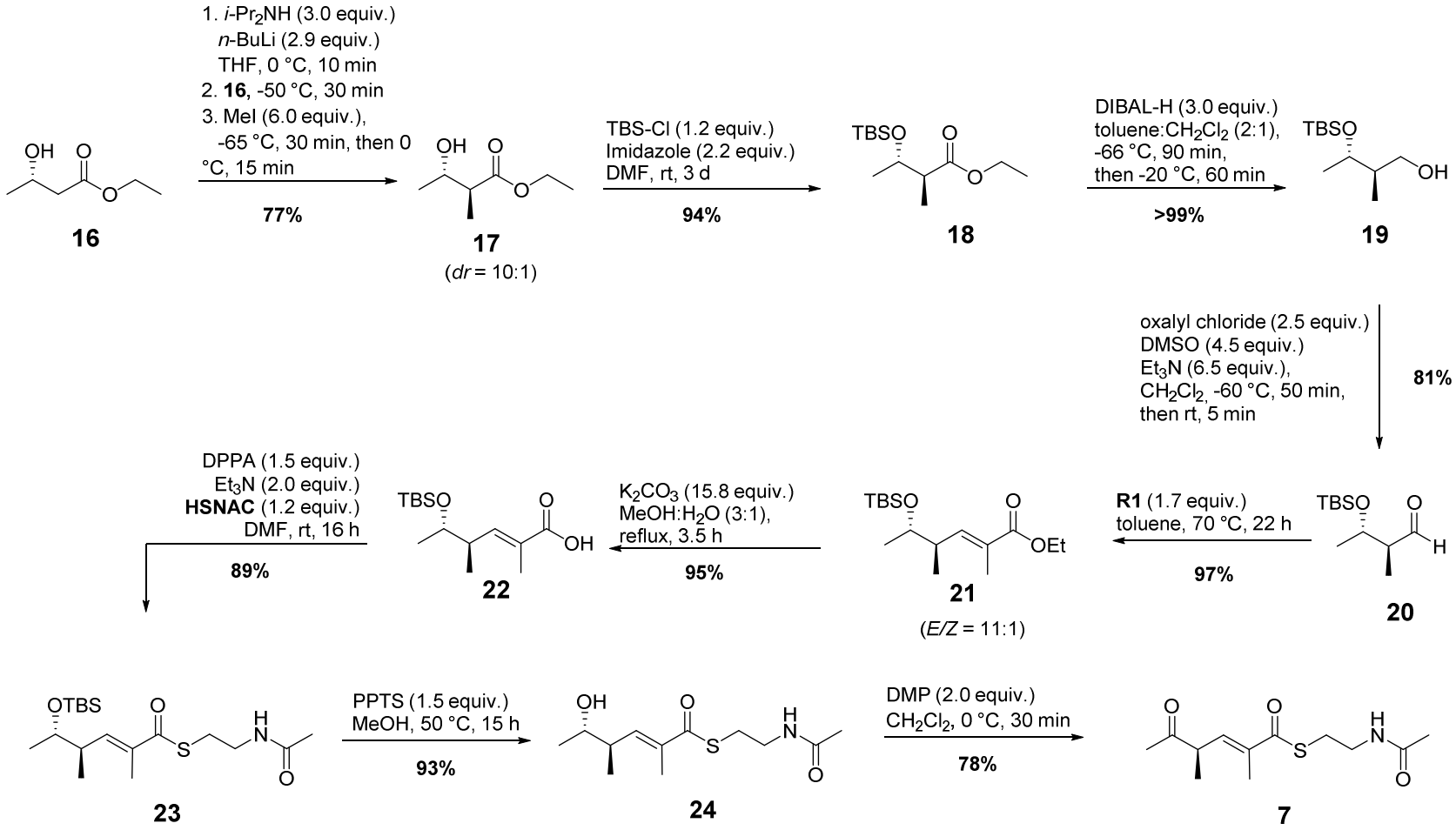

Figure S 53: Synesis synopsis of ER2^0-type triketide.

9.4 Synthetic Procedures for ER2^0-Triketide Thioester

Synthesis of ethyl (2*S*,3*S*)-3-hydroxy-2-methylbutanoate (17)[13]

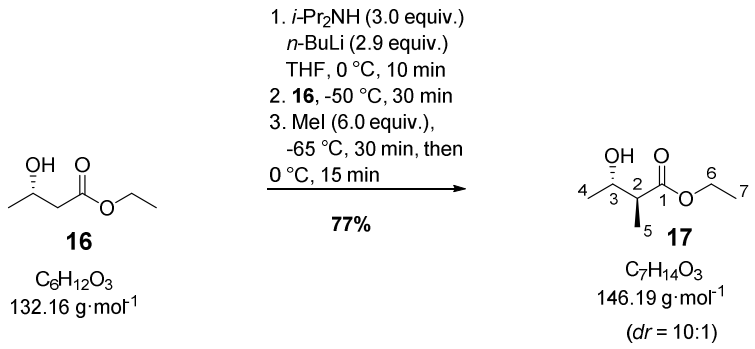

The reaction was performed under argon atmosphere. Freshly distilled diisopropylamine (*i*-Pr_2NH) (31.9 ml, 227 mmol, 3.0 equiv.) was dissolved in dry THF (100 ml) in a flame-dried flask. The solution was cooled to 0 °C and 2.5 M *n*-butyllithium (*n*-BuLi) in hexanes (87.6 ml, 219 mmol, 2.9 equiv.) was added over 30 min. The resulting yellow solution was stirred for another 15 min at 0 °C. Then, the mixture was cooled to -50 °C using a dry ice-acetone bath and ethyl (*S*)-3-hydroxybutanoate **16** (10.0 g, 76 mmol, 1.0 equiv.) dissolved in dry THF (60 ml) was added over 30 min. The solution was stirred for 30 min at -50 °C, before it was cooled to -65 °C. Then, methyl iodide (MeI) (28.4 ml, 454 mmol, 6.0 equiv.) was added over 15 min. The reaction mixture was stirred for 30 min at -65 °C and 15 min at 0 °C. After full conversion of **16** (TLC-control), the reaction mixture was quenched with sat. aq. NH_4Cl (100 ml) and acidified to pH 7 using conc. HCl. Organic and aqueous phase was separated, and the aqueous phase was extracted with diethyl ether (3 x 80 ml). The combined organic phases were washed with brine (150 ml) dried over Na_2SO_4 and concentrated under reduced pressure to give 10.7 g of a yellow liquid. After flash chromatography (PE/EtOAc 9:1 ⟶ 7:3) **17** (8.50 g, 58.1 mmol, 77%) was isolated as a pale-yellow liquid. The diastereomeric ratio was determined using ^{1}H NMR integration of the corresponding signals *dr* = 10:1.

TLC: R_f = 0.67 (PE:EtOAc = 1:1).

Specific rotation: $[\alpha]_D^{20}$ = +31.7° (c = 1.01, CH_2Cl_2).

^{1}H NMR (250 MHz, $CDCl_3$): δ(ppm) = 4.16 (q, ^3J = 7.1 Hz, 2H, C^6-H), 3.87 (quint, ^3J = 6.4 Hz, 1H, C^3-H), 2.58 (s, 1H, O-H), 2.42 (quint, ^3J = 7.2 Hz, 1H, C^2-H), 1.26 (t, ^3J = 7.1 Hz, 3H, C^7-H), 1.20 (d, ^3J = 6.4 Hz, 3H, C^4-H), 1.17 (d, ^3J = 7.3 Hz, 3H, C^5-H).

^{13}C NMR (63 MHz, $CDCl_3$): δ(ppm) = 176.0 (C^1), 69.6 (C^3), 60.7 (C^6), 47.1 (C^2), 20.9 (C^4), 14.3 (C^7), 14.2 (C^5).

Synthesis of ethyl (2S,3S)-3-((tert-butyldimethylsilyl)oxy)-2-methylbutanoate (18)[14]

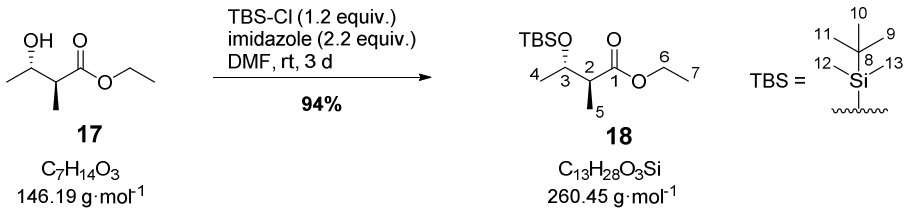

17
$C_7H_{14}O_3$
146.19 g·mol^{-1}

18
$C_{13}H_{28}O_3Si$
260.45 g·mol^{-1}

The reaction was performed under argon atmosphere. Ethyl (2*S*,3*S*)-3-hydroxy-2-methylbutanoate (**17**) (8.40 g, 57.4 mmol, 1.0 equiv.) of was dissolved in dry DMF (85 ml), the solution was cooled to 0 °C and imidazole (8.57 g,1.26 mmol, 2.2 equiv.) was added. After the mixture stirred for 15 min at 0 °C, *tert*-butyldimethylsilyl chloride (TBS-Cl) (10.2 g, 68.0 mmol, 1.2 equiv.) in dry DMF (85 ml) was added over 5 min. Subsequently, the reaction mixture was stirred at rt for 3 d. After full conversion of **17** (TLC-control) the reaction was quenched with water (350 ml) and reaction mixture and the product was extracted with EtOAc (3 x 250 ml). The combined organic phases were washed with 1 M HCl (2 x 100 ml), sat. aq. NH_4Cl (100 ml) and brine (150 ml). Then, the organic phase was dried over $MgSO_4 \cdot H_2O$ and concentrated *in vacuo* to give 16.0 g of a pale-yellow liquid. After flash chromatography (PE/EtOAc 30:1) **18** (14.1 g, 54.2 mmol, 94%) was obtained as a colorless liquid.

TLC: R_f = 0.82 (PE/EtOAc 9:1).

Specific rotation: $[\alpha]_D^{20}$ = +24.6° (c = 0.29, CH_2Cl_2).

^{1}H NMR (400 MHz, $CDCl_3$): δ(ppm) = 4.11 (q, ^3J = 7.1 Hz, 2H, C^6-H), 4.02 (quint, ^3J = 6.2 Hz, 1H, C^3-H), 2.47 (quint, ^3J = 7.1 Hz, 1H, C^2-H), 1.25 (t, ^3J = 7.1 Hz, 3H, C^7-H), 1.12 (d, ^3J = 6.2 Hz, 3H, C^4-H), 1.08 (d, ^3J = 7.1 Hz, 3H, C^5-H), 0.86 (s, 9H, $C^{9/10/11}$-H), 0.05 (s, 3H, C^{12}-H or C^{13}-H), 0.03 (s, 3H, C^{12}-H or C^{13}-H).

^{13}C NMR (101 MHz, $CDCl_3$): δ(ppm) = 175.2 (C^1), 70.3 (C^3), 60.3 (C^6), 48.3 (C^2), 25.9 ($C^{9/10/11}$), 20.7 (C^4), 18.1 (C^8), 14.3 (C^7), 12.8 (C^5), -4.2 ($C^{12/13}$).

Synthesis of (2*R*,3*S*)-3-((*tert*-butyldimethylsilyl)oxy)-2-methyl-butan-1-ol (19)[15]

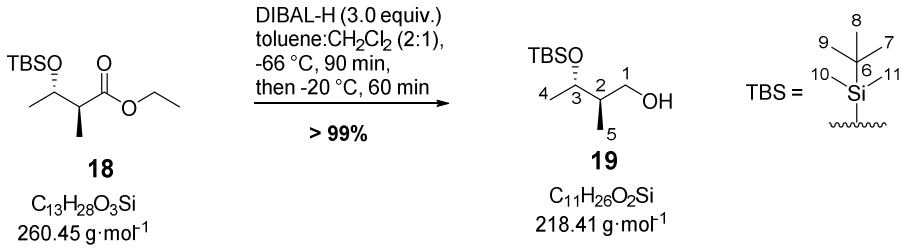

18
$C_{13}H_{28}O_3Si$
260.45 g·mol^{-1}

19
$C_{11}H_{26}O_2Si$
218.41 g·mol^{-1}

The reaction was performed under argon atmosphere. Ethyl (2*S*,3*S*)-3-((*tert*-butyldimethylsilyl)oxy)-2-methylbutanoate (**18**) (10.7 g, 41.1 mmol, 1.0 equiv.) was dissolved in dry toluene (67 ml) and dry CH_2Cl_2 (34 ml) in a flame-dried flask. The solution was cooled to -66 °C with a dry ice/acetone bath and1 M diisobutylaluminium hydride (DIBAL-H) in hexane (123 ml, 123 mmol, 3.0 equiv.) was added over 30 min. The reaction mixture was stirred for 90 min at -66 °C and 60 min at -20 °C. After full conversion of **18** (TLC-control) the reaction was quenched with methanol (42 ml) at -66 °C. After the mixture was stirred for 10 min at -66 °C, then warmed to rt. Then sat. aq. potassium sodium tartrate was added, and the heterogeneous mixture was stirred for 60 min at rt. Then, the phases were separated, and the aqueous phase was extracted with CH_2Cl_2 (2 x 100 ml). The combined organic phases were washed with water (200 ml), brine (200 ml) and dried over Na_2SO_4. After the solvent was removed under reduced pressure **19** (8.94 g, 40.9 mmol, >99%) was isolated as a colourless liquid.

TLC: R_f = 0.22 (PE/EtOAc 19:1).

Specific rotation: $[\alpha]_D^{20}$ = +44.8° (c = 0.20, CH_2Cl_2).

^{1}H NMR (200 MHz, $CDCl_3$): δ(ppm) = 3.85-3.79 (m, 1H, C^1-H^a), 3.77-3.74 (m, 1H, C^3-H), 3.59-3.50 (m, 1H, C^1-H^b), 2.67 (bs, 1H, O-H), 1.70-1.49 (m, 1H, C^2-H), 1.21 (d, ^3J = 6.2 Hz, 3H, C^4-H), 0.96 (d, ^3J = 7.0 Hz, 3H, C^5-H), 0.89 (s, 9H, $C^{7/8/9}$-H), 0.09 (s, 6H, $C^{10/11}$-H).

^{13}C NMR (50 MHz, $CDCl_3$): δ(ppm) = 74.2 (C^3), 66.0 (C^1), 41.8 (C^2), 25.9 ($C^{7/8/9}$), 22.3 (C^4), 18.0 (C^6), 14.8 (C^5), -4.1 (C^{10} or C^{11}), -4.8 (C^{10} or C^{11}).

Synthesis of (2*S*,3*S*)-3-((*tert*-butyldimethylsilyl)oxy)-2-methyl-butanal (20) [15]

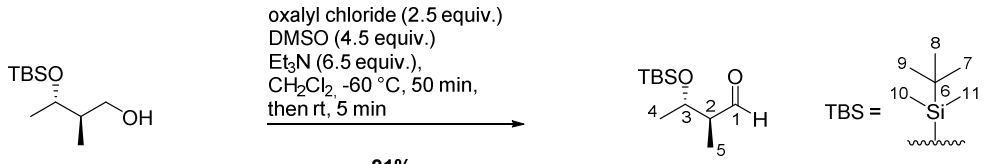

The reaction was performed under argon atmosphere. Oxalyl chloride (0.42 ml, 4.88 mmol, 2.5 equiv.) was dissolved in dry CH_2Cl_2 (9.4 mL) and cooled to -60 °C using a dry ice/acetone bath. Then dry DMSO (0.62 ml, 8.78 mmol, 4.5 equiv.) was added over 5 min and the solution was stirred for 20 min at -60 °C. Subsequently, (2*R*,3*S*)-3-((*tert*-butyldimethylsilyl)oxy)-2-methylbutan-1-ol (SM, **19**) (425 mg, 1.95 mmol, 1.0 equiv.) in dry CH_2Cl_2 (4.7 ml) was added over 10 min and the mixture was stirred for 60 min at -60 °C. Freshly distilled triethylamine (Et_3N) (1.76 ml, 12.7 mmol, 6.5 equiv.) was added over 5 min and the reaction mixture was stirred for 30 min at -60 °C before it was allowed to reach rt. After full conversion of alcohol **19** (TLC-control), the reaction mixture was diluted with CH_2Cl_2 (20 ml) and quenched with water (10 ml) and sat. aq. NH_4Cl. Then, the aqueous phase was extracted with CH_2Cl_2 (3 x 100 ml), the combined organic phases were washed with brine (100 ml) and dried over $MgSO_4$ x H_2O. The solvent was removed under reduced pressure to give 677 mg of yellow needles. Flash chromatography (PE/EtOAc 50:1) yielded **20**(342 mg, 1.58 mmol, 81%) as a yellow oil. The aldehyde **20** was stored in an aluminium foil covered flask at -80 °C under argon atmosphere, because it was observed to be unstable at air, light, and rt (on TLC)

TLC: R_f = 0.57 (PE/EtOAc 19:1).

Specific rotation: $[\alpha]_D^{20}$ = +33.6° (c = 1.27, CH_2Cl_2).

^{1}H NMR (250 MHz, $CDCl_3$): δ(ppm) = 9.75 (d, ^3J = 2.6 Hz, 1H, C^1), 4.03 (quint, ^3J = 6.2 Hz, 1H, C^3-H), 2.44-2.30 (m, 1H, C^2-H), 1.22 (d, ^3J = 6.2 Hz, 3H, C^4-H), 1.07 (d, ^3J = 7.0 Hz, 3H, C^5-H), 0.87 (s, 9H, $C^{7/8/9}$-H), 0.07 (s, 3H, C^{10}-H or C^{11}-H), 0.05 (s, 3H, C^{10}-H or C^{11}-H).

^{13}C NMR (101 MHz, $CDCl_3$): δ(ppm) = 205.3 (C^1), 70.0 (C^3), 53.8 (C^2), 25.9 ($C^{7/8/9}$), 21.9 (C^4), 18.1 (C^6), 10.8 (C^5), -4.1 ($C^{10/11}$).

Synthesis of *N*-acetylcysteamine (HSNAC)[16]

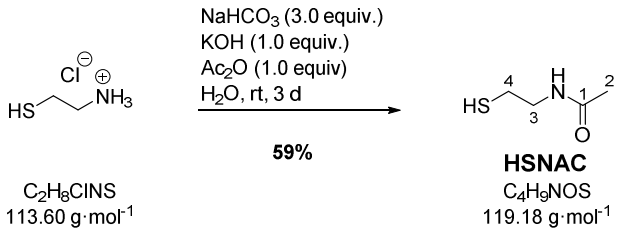

C_2H_8ClNS
113.60 g·mol^{-1}

C_4H_9NOS
119.18 g·mol^{-1}

To a solution of cysteamine hydrochloride (11.4 g, 100 mmol, 1.0 equiv.) in water (250 ml) $NaHCO_3$ (25.2 g, 300 mmol, 3.0 equiv.) and KOH (5.63 g, 100 mmol, 1.0 equiv.) were added. After stirring for 5 min at rt, the solution was cooled to 0 °C using an ice bath and acetic anhydride (Ac_2O) (9.50 ml, 100 mmol, 1.0 equiv.) was added over 5 min, during which gas formation could be observed. Subsequently, the reaction mixture was stirred for 3 d. After full conversion of the startingmaterial (TLC-control), the reaction mixture was acidified to pH 1 with conc. HCl and the aqueous phase was extracted with EtOAc (3 x 150 ml), dried over $MgSO_4$ x H_2O and concentrated under reduced pressure to give **HSNAC** (6.98 g, 58.6 mmol, 59%) as a colorless oil.

TLC: R_f = 0.76 (CH_2Cl_2/MeOH 9:1).

^{1}H NMR (500 MHz, $CDCl_3$): δ(ppm) = 6.02 (bs, 1H, N-H), 3.42 (q, ^3J = 6.2 Hz, 2H, C^3-H), 2.70-2.63 (dt, ^3J = 8.4 Hz, ^3J = 6.4 Hz, 2H, C^4-H), 2.00 (s, 3H, C^2-H), 1.35 (t, ^3J = 8.5 Hz, 1H, S-H).

^{13}C NMR (126 MHz, $CDCl_3$): δ(ppm) = 170.3 (C_1), 42.6 (C_3), 24.8 (C_4), 23.4 (C_2).

Synthesis of *rac*-(1-ethoxy-1-oxopropan-2-yl)triphenyl-phosphonium bromide[17]

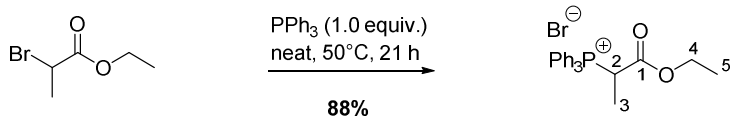

$C_5H_9BrO_2$
181.03 g·mol^{-1}

$C_{23}H_{24}BrO_2P$
443.32 g·mol^{-1}

rac-ethyl 2-bromopropanoate (6.96 g, 38.4 mmol, 1.0 equiv.) and triphenylphosphine (PPh_3) (10.1 g, 38.4 mmol, 1.0 equiv.) were combined in a flask and the suspension was heated to 50 °C. The pale-yellow slurry was stirred at 50 °C for 21 h, after which it became a white-yellow solid. The solid was crushed with a scalpel and pulverized using mortar and pestle. The powder was washed with *n*-hexane (4 x 50 ml) filtered over a sintered glass and air-dried overnight. Product *rac*-(1-ethoxy-1-oxopropan-2-yl)triphenyl-phosphonium bromide (15.0 g, 33.8 mmol, 88%) was obtained as a cream-white solid.

TLC: R_f = 0.52 (CH_2Cl_2/MeOH 9:1).

MP: 139°C.

^{1}H NMR (200 MHz, $CDCl_3$): δ(ppm) = 8.04-7.83 (m, 6H, C^{arom}-H (*meta*)), 7.83-7.57 (m, 9H, C^{arom}-H (*ortho*, *para*)), 6.64 (dq, $^2J^{HP}$ = 14.4 Hz, ^3J = 7.1 Hz, 1H, C^2-H), 4.10-3.84 (m, 2H, C^4-H), 1.65 (dd, $^3J^{HP}$ = 18.5 Hz, ^3J = 7.1 Hz, 3H, C^3-H), 0.97 (t, ^3J = 7.1 Hz, 3H, C^5-H).

^{13}C NMR (50 MHz, $CDCl_3$): δ(ppm) = 168.0 (d, $^2J_{CP}$ = 1.5 Hz, C_1), 135.0 (d, $^4J_{CP}$ = 3.1 Hz, C_{arom} (*para*)), 134.4 (d, $^2J_{CP}$ = 10.0 Hz, C_{arom} (*ortho*)), 130.3 (d, $^3J_{CP}$ = 12.8 Hz, C_{arom} (*meta*)), 117.8 (d, $^1J_{CP}$ = 86.3 Hz, C_{arom} (*ipso*)), 63.0 (s, C_4), 36.8 (d, $^1J_{CP}$ = 50.2 Hz, C_2), 13.7 (s, C_5), 13.1 (d, $^2J_{CP}$ = 2.9 Hz, C_3).

Synthesis of ethyl 2-(triphenyl-λ^5-phosphanylidene)-propanoate (R1)[17]

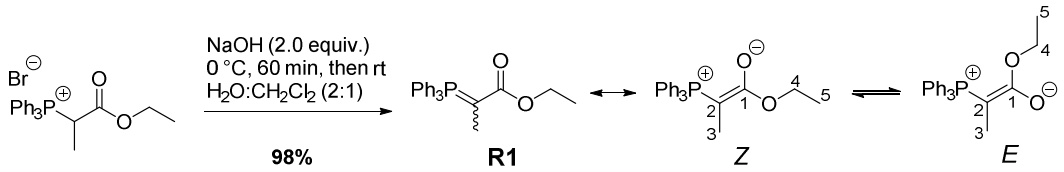

$C_{23}H_{24}BrO_2P$
443.32 g·mol^{-1}

$C_{23}H_{23}O_2P$
362.41 g·mol^{-1}

NaOH (5.25 g, 131 mmol, 2.0 equiv.) was dissolved in water (100 ml) and the solution was cooled to 0 °C using an ice bath. Then, *rac*-(1 ethoxy-1-oxopropan-2-yl)triphenylphospho-nium bromide (*rac*-**27**) (29.1 g, 65.6 mmol, 1.0 equiv.) in CH_2Cl_2 (50 ml) was added over 10 min and the heterogeneous reaction mixture was stirred for 60 min at 0 °C before it was allowed to reach rt over 45 min. Afterwards, the phases were separated and the aqueous phase was extracted with CH_2Cl_2 (3 x 50 ml), the combined organic phases were washed with brine (100 ml) and dried over Na_2SO_4. The solvent was removed under reduced pressure to yield **R1** (23.2 g, 64.1 mmol, 98%) as a neon-yellow solid **R1**. By ^{1}H NMR integration, the diastereomeric ratio was determined to be *E*:*Z* = 1:2.

TLC: R_f = 0.52 (CH_2Cl_2/MeOH 9:1).

MP: 160 °C.

Z-Diastereomer: **^{1}H NMR** (200 MHz, $CDCl_3$): δ(ppm) = 7.69-7.35 (m, 15H, C^{arom}-H), 3.71 (q, 2H, ^3J = 7.1 Hz, C^4-H), 1.61 (d, $^3J^{HP}$ = 13.8 Hz, 3H, C^3-H), 0.45 (t, ^3J = 7.1 Hz, 3H, C^5-H).

E-Diastereomer: **^{1}H NMR** (200 MHz, $CDCl_3$): δ(ppm) = 7.69-7.35 (m, 15H, C^{arom}-H), 4.05 (q, 2H, ^3J = 7.0 Hz, C^4-H), 1.60 (d, $^3J^{HP}$ = 14.4 Hz, 3H, C^3-H), 1.24 (t, ^3J = 7.1 Hz, 3H, C^5-H).

Z-Diastereomer: **^{13}C NMR** (63 MHz, $CDCl_3$): δ(ppm) = 170.8 (s, C_1), 133.7 (d, $^2J_{CP}$ = 9.5 Hz, C_{arom} (*ortho*)), 131.6 (d, $^4J_{CP}$ = 2.8 Hz, C_{arom} (*para*)), 128.5 (d, $^3J_{CP}$ = 12.0 Hz, C_{arom} (*meta*)), 128.4 (d, $^1J_{CP}$ = 90.4 Hz, C_{arom} (*ipso*)), 57.6 (s, C_4), 32.1 (d, $^1J_{CP}$ = 121.8 Hz, C_2), 14.6 (s, C_5), 12.8 (d, $^2J_{CP}$ = 12.8 Hz, C_3).

E-Diastereomer: **^{13}C NMR** (63 MHz, $CDCl_3$): δ(ppm) = 171.0 (s, C^1), 132.2 (d, $^2J^{CP}$ = 9.9 Hz, C^{arom} (*ortho*)), 132.0 (d, $^4J^{CP}$ = 2.8 Hz, C^{arom} (*para*)), 128.6 (d, $^3J^{CP}$ = 12.1 Hz, C^{arom} (*meta*)), 128.4 (d, $^1J^{CP}$ = 90.4 Hz, C^{arom} (*ipso*)), 57.6 (s, C^4), 32.1 (d, $^1J^{CP}$ = 121.8 Hz, C^2), 14.6 (s, C^5), 12.8 (d, $^2J^{CP}$ = 12.8 Hz, C^3).

Synthesis of ethyl (4*R*,5*S*,*E*)-5-((*tert*-butyldimethylsilyl)oxy)-2,4-dimethylhex-2-enoate (21)[18]

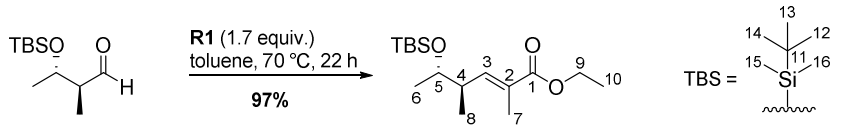

20

$C_{11}H_{24}O_2Si$
216.40 g·mol^{-1}

21
(*E*/*Z* = 11:1)

$C_{16}H_{32}O_3Si$
300.51 g·mol^{-1}

The reaction was performed under argon atmosphere. Prior to the reaction dry toluene (20 ml) was degassed through a flow of argon gas. (2*S*,3*S*)-3-((*tert*-butyldimethylsilyl)oxy)-2-methyl-butanal (**20**) (1.00 g, 4.62 mmol, 1.0 equiv.) and 2-(triphenyl-l5-phosphanylidene)-propanoate (**R1**) (2.85 g, 7.86 mmol, 1.7 equiv.) was added. The reaction mixture was stirred for 22 h at 70 °C. After full conversion of **20** (TLC-control) *n*-hexane (70 ml) was added to the reaction mixture, after which a white solid precipitated in the yellow solution. The suspension was filtered over 3 cm celite and washed with *n*-hexane/EtOAc (4:1; 150 ml). The remaining yellow solution was concentrated under reduced pressure to give 2.81 g of a moist neon-yellow solid. Flash chromatography (PE ⟶ PE/EtOAc 16:1) yielded **21** (1.34 g, 4.46 mmol, 97%) as a pale-yellow oil. By ^{1}H NMR integration, the *E*/*Z* ratio was determined to be *E*:*Z* = 11:1.

TLC: R_f = 0.77 (PE/EtOAc 9:1).

Specific rotation: $[\alpha]_D^{20}$ = +53.3° (c = 0.30, CH_2Cl_2).

^{1}H NMR (250 MHz, $CDCl_3$): δ(ppm) = 6.68 (dd, ^3J = 10.2 Hz, ^4J = 1.4 Hz, 1H, C^3-H), 4.18 (dq, ^3J = 7.1 Hz, 2H, C^9-H$^{a/b}$), 3.78-3.60 (m, 1H, C^5-H), 2.58-2.40 (m, 1H, C^4-H), 1.83 (d, ^4J = 1.4 Hz, 3H, C^7-H), 1.28 (t, ^3J = 7.1 Hz, 3H, C^{10}-H), 1.09 (d, ^3J = 6.2 Hz, 3H, C^6-H), 0.98 (d, ^3J = 6.8 Hz, 3H, C^8-H), 0.87 (s, 9H, $C^{12/13/14}$-H), 0.04 (s, 3H, C^{15}-H or C^{16}-H), 0.03 (s, 3H, C^{15}-H or C^{16}-H).

^{13}C NMR (63 MHz, $CDCl_3$): δ(ppm) = 168.5 (C^1), 145.1 (C^3), 127.6 (C^2), 71.8 (C^5), 60.5 (C^9), 41.2 (C^4), 26.0 ($C^{12/13/14}$), 21.6 (C^6), 18.2 (C^{11}), 16.2 (C^8), 14.4 (C^{10}), 12.7 (C^7), -4.2 (C^{15} or C^{16}), -4.7 (C^{15} or C^{16}).

Synthesis of (4*R*,5*S*,*E*)-5-((*tert*-butyldimethylsilyl)oxy)-2,4-dimethylhex-2-enoic acid (22)[18]

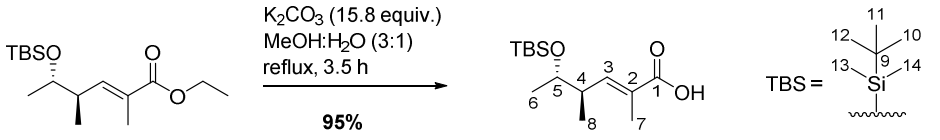

To a solution of ethyl (4*R*,5*S*,*E*)-5-((*tert*-butyl-dimethylsilyl)-oxy)-2,4-dimethylhex-2-enoate (**21**) (3.51 g, 11.7 mmol, 1.00 equiv.) in MeOH (460 ml) was added K_2CO_3 (25.5 g, 185 mmol, 15.8 equiv.) dissolved in water (150 ml). The reaction mixture was stirred and refluxed for 3.5 h. TLC (PE/EtOAc 9:1) showed the full conversion of starting material **21**. After MeOH had been removed *in vacuo*, the remaining aqueous solution was acidified to pH 1 and was immediately extracted with EtOAc (3 x 300 ml). The combined organic phases were dried over Na_2SO_4 and concentrated under reduced pressure to give 3.03 g (11.1 mmol, 95%) of a colourless oil **22**. Acid **22** crystallized in the freezer (-25 °C).

TLC: R_f = 0.76 (CH_2Cl_2/MeOH 9:1).

Specific rotation: $[\alpha]_D^{20}$ = +47.0° (c = 0.41, MeOH).

^{1}H NMR (250 MHz, $CDCl_3$): δ(ppm) = 10.62 (bs, 1H, O-H), 6.84 (dd, ^3J = 10.2 Hz, ^4J = 1.4 Hz, 1H, C^3-H), 3.80-3.61 (m, 1H, C^5-H), 2.60-2.44 (m, 1H, C^4-H), 1.85 (d, ^4J = 1.4 Hz, 3H, C^7-H), 1.10 (d, ^3J = 6.2 Hz, 3H, C^6-H), 0.99 (d, ^3J = 6.8 Hz, 3H, C^8-H), 0.87 (s, 9H, $C^{10/11/12}$-H), 0.04 (s, 3H, C^{13}-H or C^{14}-H), 0.03 (s, 3H, C^{13}-H or C^{14}-H).

^{13}C NMR (63 MHz, $CDCl_3$): δ(ppm) = 173.9 (C^1), 148.0 (C^3), 126.9 (C^2), 71.7 (C^5), 41.5 (C^4), 26.0 ($C^{10/11/12}$), 21.6 (C^6), 18.2 (C^9), 16.1 (C^8), 12.4 (C^7), -4.2 (C^{13} or C^{14}), -4.7 (C^{13} or C^{14}).

Synthesis of *S*-(2-acetamidoethyl) (4*R*,5*S*,*E*)-5-((*tert*-butyl-dimethylsilyl)oxy)-2,4-dimethylhex-2-enethioate (23)[18]

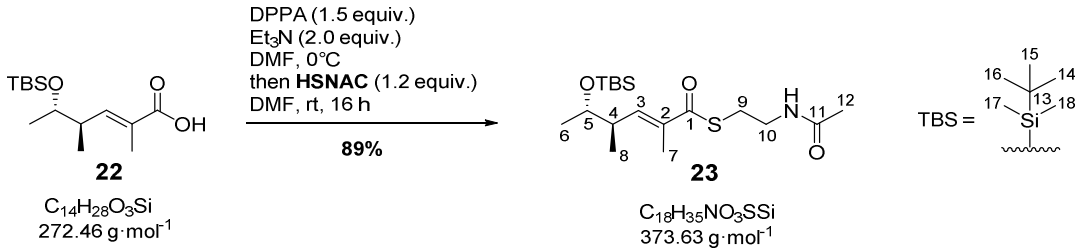

The reaction was performed under argon atmosphere in a flame-dried flask. (4*R*,5*S*,*E*)-5-((*tert*-butyldimethylsilyl)oxy)-2,4-dimethylhex-2-enoic acid (**22**) (3.46 g, 12.7 mmol, 1.0 equiv.) was dissolved in dry DMF (70 ml) and the solution was cooled to 0 °C with an ice bath. Then diphenylphosphoryl azide (DPPA) (4.12 ml, 19.1 mmol, 1.5 equiv.) and triethylamine (Et_3N) (3.52 ml, 25.4 mmol, 2.0 equiv.) were added and the mixture was stirred for 2 h at 0 °C. Afterwards, *N*-acetylcysteamine (**HSNAC**) (1.62 ml, 15.2 mmol, 1.20 equiv.) was added and the mixture was stirred at rt for 17 h. After full conversion of **22** (TLC-control) the reaction was quenched with water (300 ml) was added and the product was extracted with EtOAc (3 x 150 ml). The combined organic phases were washed with water (100 ml), brine (100 ml) and dried over $MgSO_4$. The solvent was removed under reduced pressure yielding 6.10 g of a pale-yellow oil. The crude product was purified using a flash chromatography (PE/EtOAc 1:1) to afford **23** (4.20 g, 11.3 mmol, 89%) as a viscous, colorless oil.

TLC: R_f = 0.27 (PE/EtOAc 3:2).

Specific rotation: $[\alpha]_D^{20}$ = +7.5° (c = 1.18, CH_2Cl_2).

Table S 59: ^1H (250 MHz) and ^{13}C NMR (56 MHz) of **23**.

Position	δH ppm (J in Hz)	δC (ppm)	Position	δH ppm (J in Hz)	δC (ppm)
1	-	194.3	8	1.01 (d, 6.8)	16.4
2	-	135.6	9	3.06 (t, 6.4)	28.4
3	6.73 (dd, 9, 1.2)	144.8	10	3.45 (q, 6.0)	40.1
4	2.61-2.44 (m)	41.4	11	-	170.7
5	3.81-3.63 (m)	71.5	12	1.97 (s)	23.2
6	1.09 (d, 6.2)	21.9	13	-	18.1
N-H	6.06 (bs)	-	14-15	(0.88, s)	25.9
7	1.87 (d, 1.3)	12.8	17-18	(0.05, s and/or 0.03, s)	4.2 or 4.7

Synthesis of *S*-(2-acetamidoethyl) (4*R*,5*S*,*E*)-5-hydroxy-2,4-dimethylhex-2-enethioate (24)[18]

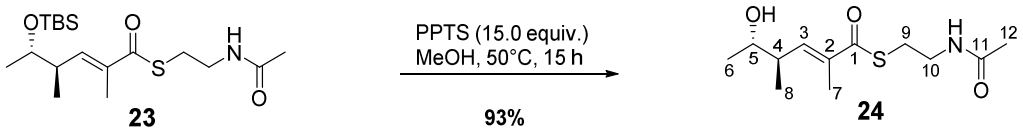

$C_{18}H_{35}NO_3SSi$
373.63 g·mol^{-1}

$C_{12}H_{21}NO_3S$
259.36 g·mol^{-1}

To a solution of *S*-(2-acetamidoethyl) (4*R*,5*S*,*E*)-5-((*tert*-butyl-dimethylsilyl)oxy)-2,4-dimethylhex-2-enethioate (**23**) (2.50 g, 6.69 mmol, 1.0 equiv.) in MeOH (90 ml) pyridinium *p*-toluenesulfonate (PPTS) (25.1 g, 100 mmol, 15.0 equiv.) was added. The reaction mixture was stirred for 15 h at 50 °C. After full conversion of **23** (TLC-control) water (50 ml) was added to the reaction mixture and MeOH was removed *in vacuo*. The aqueous solution was extracted with EtOAc (7 x 150 ml). The combined organic phases were washed with brine (150 ml), dried over $MgSO_4$ and concentrated under reduced pressure to give 1.95 g of a colorless oil. The crude product was purified by flash chromatography (EtOAc) to give **24** (1.62 g, 6.25 mmol, 93%) of a very viscous, colourless oil.

TLC: R_f = 0.64 (CH_2Cl_2/MeOH 9:1).

Specific rotation: $[\alpha]_D^{20}$ = +9.9° (c = 1.06, CH_2Cl_2).

Table S 60: ^{1}H (200 MHz) and ^{13}C NMR (63 MHz) of **24**.

Position	δH ppm (J in Hz)	δC (ppm)	Position	δH ppm (J in Hz)	δC (ppm)
1	-	194.0	7	1.91 (d, 1.4)	12.9
2	-	136.6	8	1.05 (d, 6.8)	16.3
3	6.69 (dd, 9.9, 1.4)	143.6	9	3.13-3.01 (m)	28.4
4	2.66-2.45 (m)	41.1	10	3.45 (q, 6.1)	40.2
5	3.74 (quint, 6.2)	71.3	11	-	171.6
6	1.20 (d, 6.3)	21.2	12	2.00 (s, 3H)	22.8
NH	6.34 (bs)	-			

Synthesis of *S*-(2-Acetamidoethyl)(4*R*,*E*)-5-oxo-2,4-dimethylhex-2-enthioat (7)

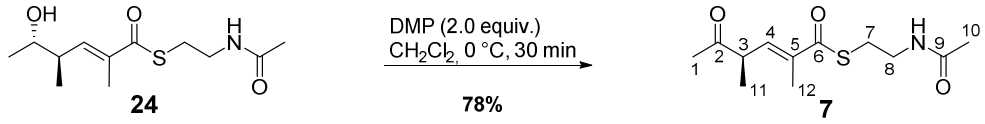

24

$C_{12}H_{21}NO_3S$
259.36 g·mol^{-1}

7

$C_{12}H_{19}NO_3S$
257.35 g·mol^{-1}

Under an argon atmosphere **24** (56 mg, 215 µmol, 1.0 equiv.) was dissolved in dry CH_2Cl_2 (40 ml), cooled to 0 °C and Dess-Martin periodinane (DMP) (182 mg, 430 µmol, 2.0 equiv.) were added. The mixture was stirred for 30 min at 0 °C. After full conversion of **24** (TLC-control) water (40 ml) was added and the phases were separated. The organic phase was washed with sat. aq. $NaHCO_3$ (40 ml) and dried over Na_2SO_4 and the solvent was removed under reduced pressure at 30 °C and purification via flash chromatography (CH_2Cl_2:MeOH = 100:0 → 97.5:2.5) yielded the product *S*-(2-Acetamidoethyl)(4*R*,*E*)-5-oxo-2,4-dimethylhex-2-enthioat (**7**) (43 mg, 78%) as a colorless oil.

TLC: R*f* = 0.66 (CH_2Cl_2:MeOH = 9.4:0.6).

Table S 61: ^{1}H (250 MHz) and ^{13}C NMR (101 MHz) of

Position	δH ppm (J in Hz)	δC (ppm)	Position	δH ppm (J in Hz)	δC (ppm)
1	2.10 (s)	21.0	7	3.01 (t, 6.3)	39.3
2	-	207.2	8	3.36 (q, 6.1)	28.5
3	3.41-3.56 (m	47.1	9	-	170.3
4	6.58 (dq, 9.6, 1.3)	138.2	10	1.91 (s)	23.0
5	-	137.1	11	1.19 (d, 6.8)	15.9
6	-	193.4	12	1.88 (d, 1.3)	12.7
NH	6.37 (bs)	-	-	-	-

Table S 62: Mass spectrometric data of compound **1**.

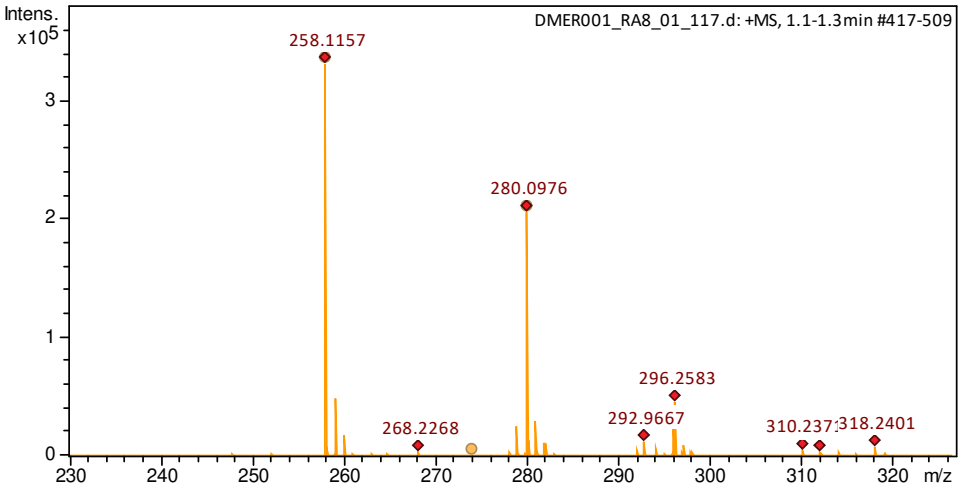

Sum Formula	ion formula	found m/z	calc´d m/z	err [ppm]	mSigma
$C_{12}H_{20}NO_3S$	[M+H]	258.1157	258.1158	0.5	3
$C_{12}H_{19}NNaO_3S$	[M+Na]	280.0976	280.0978	0.6	3
$C_{12}H_{19}KNO_3S$	[M+K]	296.0715	296.0717	0.8	10

9.5 Synopsis Wildtype Triketide Thioester

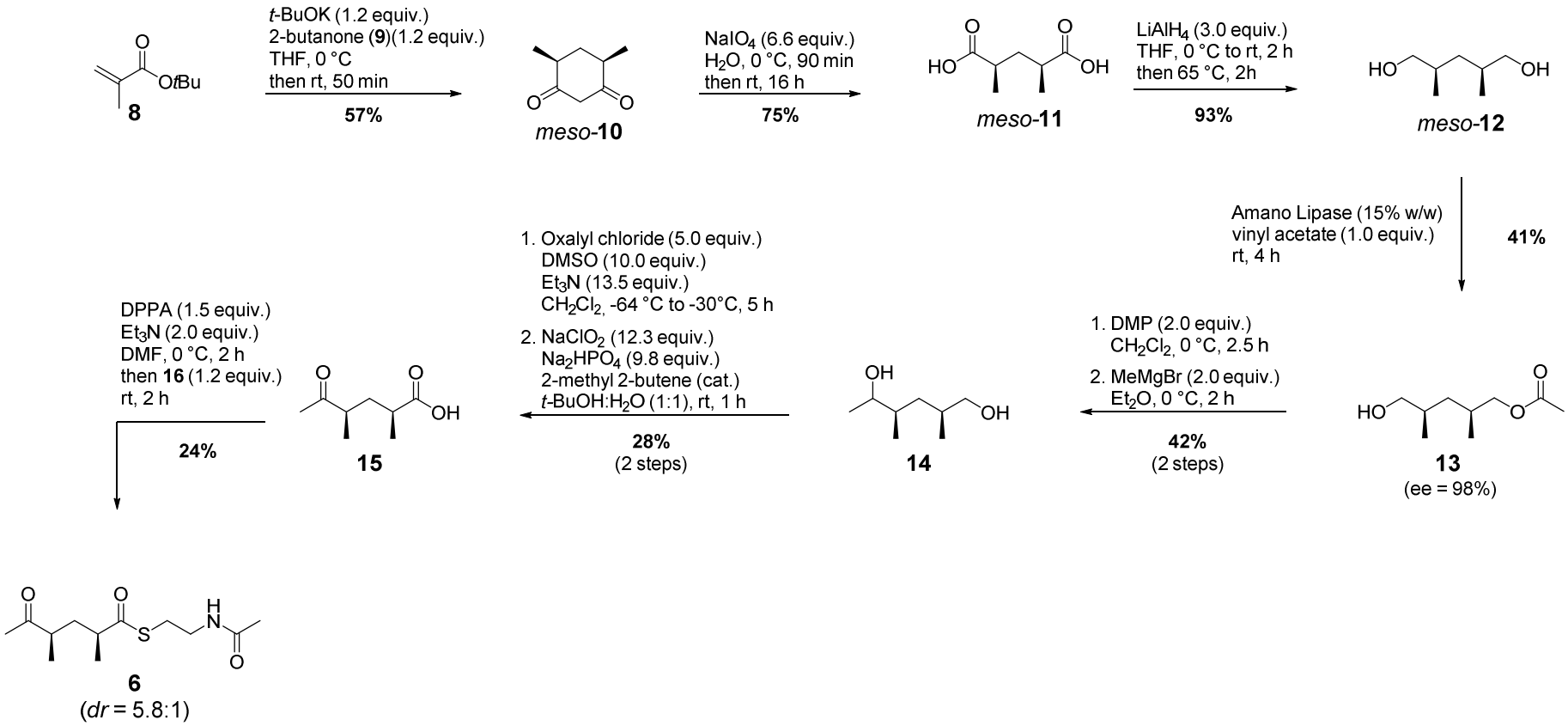

Figure S 54: Synopsis.

9.6 Synthesis Wildtype Triketide Thioester

Synthesis of *meso*-4,6-dimethylcyclohexane-1,3-dione (*meso*-10)[19]

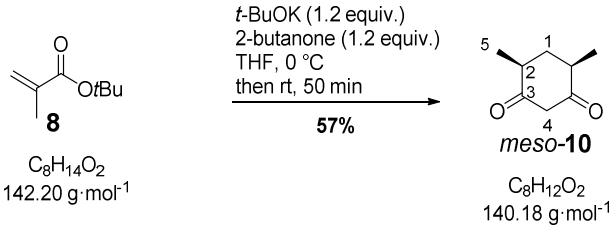

The reaction was performed under argon atmosphere. 2-Butanone (**9**) (12.0 g, 166 mmol, 1.2 equiv.) and *tert*-butyl methacrylate (**8**) (19.7 g, 139 mmol, 1.0 equiv.) were dissolved in dry THF (120 ml) in a flame-dried flask. The resulting solution was cooled to 0 °C and potassium *tert*-butoxide (*t*-BuOK) (18.6 g, 166 mmol, 1.2 equiv.) was added. The upcoming thick, cream-colored suspension was the stirred at rt for 50 min. After full conversion of **8** (TLC-control) sat. aq. NH_4Cl (100 ml) was added and the product was extracted with CH_2Cl_2 (9 x 130 ml), EtOAc (9 x 130 ml) and Et_2O (6 x 150 ml). The combined organic phases were dried over $MgSO_4$ x H_2O and concentrated under reduced pressure to give 16.0 g of a white solid. The crude product was purified by flash chromatography (PE/EtOAc 6:1 ⟶ 3:2) to give *meso*-**10** (11.0 g, 78.6 mmol, 57%) as a white solid.

TLC: R_f = 0.48 (PE/EtOAc 1:1).

MP: 115°C.

^{1}H NMR (200 MHz, $CDCl_3$): δ(ppm) = 3.53-3.24 (m, 2H, C^1-H), 2.78-2.55 (m, 2H, C^3 H), 2.12 (dt, ^2J = 13.8 Hz, ^3J = 5.6 Hz, 1H, C^4-H^a), 1.27-1.04 (m, 1H, C^4-H^b), 1.11 (d, ^3J = 6.5 Hz, 6H, C^5-H).

^{13}C NMR (50 MHz, $CDCl_3$): δ(ppm) = 204.7 (C^2), 58.3 (C^1), 44.8 (C^3), 35.9 (C^4), 13.9 (C^5).

Synthesis of *meso*-2,4-dimethylpentanedioic acid (*meso*-11)[20]

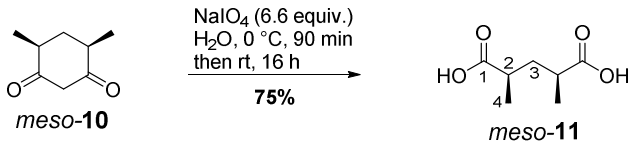

meso-**10**

$C_8H_{12}O_2$
140.18 g·mol^{-1}

meso-**11**

$C_7H_{12}O_4$
160.17 g·mol^{-1}

meso-4,6-dimethylcyclohexane-1,3-dione (*meso*-**10**) (7.54 g, 53.8 mmol, 1.0 equiv.) was suspended in water (750 ml). The mixture was cooled to 0 °C and $NaIO_4$ (75.7 g, 354 mmol, 6.6 equiv.) was added portion-wise. The resulting suspension was stirred for 90 min at 0 °C and at rt for for 16 h. After full conversion of *meso*-**10** (TLC-control), the reaction mixture was quenched with sat. aq. Na_2SO_3 (500 ml) and Na_2SO_3 were added. The aqueous solution (pH 6) was acidified to pH 3 using approximately conc. HCl (400 ml). The aqueous phase was extracted with Et_2O (5 x 600 ml) and the combined organic phases were washed with water (200 ml) and dried over $MgSO_4$ x H_2O. After solvent removal *in vacuo*, 7.13 g of a white solid was obtained. The crude product was recrystallized from toluene yielding *meso*-**11** (6.47 g, 40.4 mmol, 75%) as a cream-white solid.

TLC: R_f = 0.33 (CH_2Cl_2/MeOH 9:1).

MP: 126°C.

^{1}H NMR (200 MHz, $CDCl_3$): δ(ppm) = 11.28 (bs, 2H, O-H), 2.54 (dqd, ^3J = 10.4, 7.0, 3.4 Hz, 2H, C^2-H), 2.11 (dt, ^2J = 13.9 Hz, ^3J = 11.1 Hz, 1H, C^3 H^a), 1.49 (dt, ^2J = 13.9 Hz, ^3J = 3.4 Hz, 1H, C^3-H^b), 1.20 (d, ^3J = 7.0 Hz, 6H, C^4-H).

^{13}C NMR (50 MHz, $CDCl_3$): δ(ppm) = 183.3 (C^1), 39.4 (C^2), 38.4 (C^3), 18.6 (C^4).

Synthesis of *meso*-2,4-dimethylpentane-1,5-diol (*meso*-12)[21]

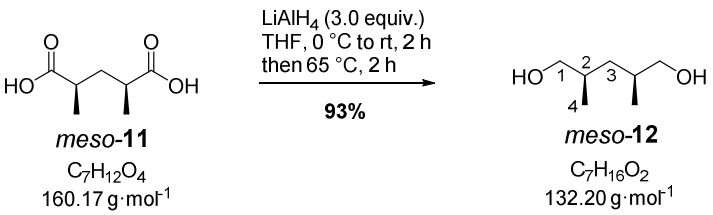

The reaction was performed under a continuous argon flow. $LiAlH_4$ (4.39 g, 116 mmol, 3.0 equiv.) was suspended in dry THF (120 ml) in a flame-dried flask. The grey suspension was cooled to 0 °C and *meso*-2,4 dimethylpentanedioic acid (*meso*-**11**) (6.17 g, 38.5 mmol, 1.0 equiv.) was added dissolved in dry THF (16 ml) over 25 min, during which gas formation (H_2) could be observed. The reaction mixture was stirred at rt for 1 h. Then, the mixture was heated to 65°C and was stirred for 2 h. After full conversion of *meso*-**11** the reaction mixture was cooled 0 °C and the excess $LiAlH_4$ was quenched very slowly with H_2O (9 ml), 15% NaOH (9 ml) and H_2O (20 ml), during which strong gas development was observed (process of quenching under a continuous argon flow). The precipitated aluminium salts were separated by filtration and washed with Et_2O (3 x 15 ml; 1 x 50 ml). The filtrate was concentrated under reduced pressure and the resulting residue was dissolved in water (50 ml). The aqueous phase was extracted with Et_2O (9 x 60 ml) and the combined organic phases were washed with brine (70 ml) and dried over $MgSO_4$ x H_2O. After concentration under reduced pressure *meso*-**12(**4.71 g, 35.6 mmol, 93%) was isolated as a colourless oil. Diol *meso*-**12** crystallized in the freezer (- 25 °C).

TLC: R_f = 0.50 (CH_2Cl_2/MeOH 9:1).

^{1}H NMR (200 MHz, $CDCl_3$): δ(ppm) = 3.53-3.32 (m, 4H, C^1-H), 2.99 (s, 2H, O-H), 1.82-1.60 (m, 2H, C^2-H), 1.54 (q, ^3J = 6.6 Hz, 1H, C^3-H^a), 0.92-0.76 (m, 1H, C^3-H^b), 0.91 (d, ^3J = 6.5 Hz, 6H, C^4 H).

^{13}C NMR (50 MHz, $CDCl_3$): δ(ppm) = 67.6 (C^1), 37.0 (C^3), 33.1 (C^2), 17.8 (C^4).

Synthesis of (2*S*,4*R*)-5-hydroxy-2,4-dimethylpentyl acetate (13)[22]

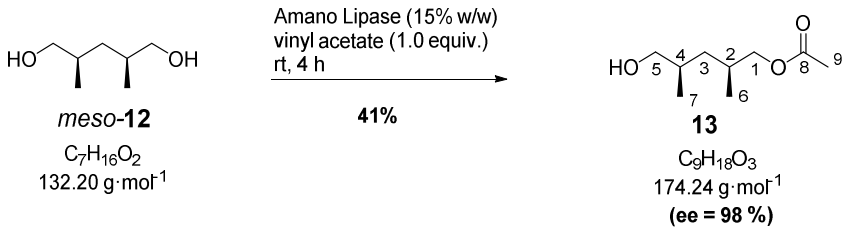

meso-**12**
$C_7H_{16}O_2$
132.20 g·mol^{-1}

13
$C_9H_{18}O_3$
174.24 g·mol^{-1}
(ee = 98 %)

The reaction was performed under argon atmosphere. To a solution of meso-2,4-dimethylpentane-1,5-diol (*meso*-**12**) (4.42 g, 33.4 mmol, 1.0 equiv.) of in vinyl acetate (3.09 ml, 33.4 mmol, 1.0 equiv.), Amano Lipase from *Pseudomonas fluorescens* (668 mg, 15% w/w) was added in a flame-dried flask. The reaction mixture was stirred at rt for 4 h. Then water (60 ml) was added and the product was extracted with Et_2O (4 x 40 ml). The combined organic phases were dried over $MgSO_4$ x H_2O and concentrated in vacuo to give 5.22 g of a milky, pale yellow oil. After flash chromatography (PE/EtOAc 7:3) 13 (2.35 g, 13.5 mmol, 41%) was isolated as a pale-yellow liquid.

TLC: Rf = 0.29 (PE/EtOAc 7:3).

Specific rotation: $[\alpha]_D^{20}$ = +3.9° (c = 1.41, CH_2Cl_2).

^{1}H NMR (200 MHz, $CDCl_3$): δ(ppm) = 3.94 (dd, $^2\mathcal{J}$ = 10.8 Hz, $^3\mathcal{J}$ = 5.4 Hz, 1H, C^1-H^a), 3.81 (dd, $^2\mathcal{J}$ = 10.8 Hz, $^3\mathcal{J}$ = 6.7 Hz, 1H, C^1-H^b), 3.47 (dd, $^2\mathcal{J}$ = 10.5 Hz, $^3\mathcal{J}$ = 5.4 Hz, 1H, C^5-H^a), 3.37 (dd, 2J = 10.5 Hz, $^3\mathcal{J}$ = 6.3 Hz, 1H, C^5-H^b), 2.03 (s, 3H, C^9-H), 2.02 (bs, 1H, O-H), 1.97-1.77 (m, 1H, C^2-H), 1.81-1.60 (m, 1H, C^4-H), 1.41 (dt, $^2\mathcal{J}$ = 13.7 Hz, $^3\mathcal{J}$ = 6.8 Hz, 1H, C^3-H^a), 1.05-0.87 (m, 1H, C^3-H^b), 0.93 (d, $^3\mathcal{J}$ = 6.7 Hz, 3H, C^6 H), 0.92 (d, $^3\mathcal{J}$ = 6.7 Hz, 3H, C^7 H).

^{13}C NMR (50 MHz, $CDCl_3$): δ(ppm) = 171.5 (C^8), 69.3 (C^1), 68.1 (C^5), 37.4 (C^3), 33.1 (C^4), 30.1 (C^2), 21.1 (C^9), 18.0 (C^6), 17.4 (C^7).

The enantiomeric excess of (**13**) (**ee** = 98.2%) was determined by HPLC. Therefore, the 4-nitro-benzoate derivative (**25**) and (rac-**25**) (*vide infra*) were synthesized and analyzed via HPLC-UV. For this purpose, a small amount of racemic monoacetate ((±)-**13**) was prepared.

Synthesis of (2*S*,4*R*)-2,4-dimethylhexane-1,5-diol (14) [23]

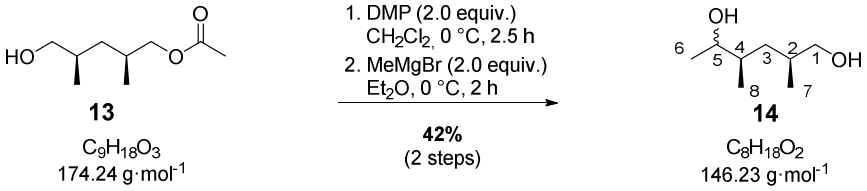

Under argon atmosphere and in a flame-dried flask (2S,4R)-5-hydroxy-2,4-dimethylpentyl acetate (**13**) (904 mg, 5.19 mmol, 1.0 equiv.) was dissolved in dry CH_2Cl_2 (150 ml) and cooled to 0 °C. Then Dess–Martin periodinane (DMP) (4.40 g, 10.4 mmol, 2.0 equiv.) was added. The reaction mixture was stirred at 0 °C for 2.5 h and at rt for 5 min. After full conversion of **13** (TLC-control), the heterogeneous mixture was washed with water (150 ml) and sat. aq. $NaHCO_3$ (2 x 125 ml) and was dried over $MgSO_4$ x H_2O. Concentration under reduced pressure gave 2.69 g of a moist white solid. The crude product was filtered through a silica plug (approximately 5 cm in height), using PE/EtOAc (7:3) as the eluent. The corresponding aldehyde (736 mg) was isolated as a pale-yellow liquid, which was observed to be unstable at air, light, and rt (on TLC). Therefore, the aldehyde was directly used for the subsequent reaction. The crude aldehyde intermediate was dissolved in a flame-dried flask under an argon atmosphere in dry Et_2O (10 ml) and cooled to 0 °C. Then, 3 M methylmagnesium bromide (MeMgBr) in Et_2O (2.85 ml, 8.55 mmol, 2.0 equiv.) was added over 30 min. The reaction mixture was stirred at 0 °C for 2 h, during which a hard, brown solid formed, which prevented a good mixing. After full conversion of aldehyde intermediate, the reaction was quenched with water (100 ml) and the aqueous phase was extracted with Et_2O (12 x 50 ml) and the combined organic phases were dried over $MgSO_4$ x H_2O and concentrated under reduced pressure to give 500 mg of an orange-yellow oil. Flash chromatography (EtOAc/PE 1:1 ⟶ 7:3) afforded **14** (318 mg, 2.17 mmol, 42% over 2 steps) as a 1:1 mixture of syn/anti diastereomers (determined by ^{1}H NMR integration).

TLC: R_f = 0.15 (EtOAc/PE 1:1).

Specific rotation: $[\alpha]_D^{20}$ = +3.6° (c = 0.44, CH_2Cl_2).

^{1}H NMR (400 MHz, $CDCl_3$): δ(ppm) = 3.76 (qd, ^3J = 6.4, 3.2 Hz, 1H, C^5-H (*syn* or *anti*)), 3.58 (quint, ^3J = 6.2 Hz, 1H, C^5-H (*anti* or *syn*)), 3.50-3.39 (m, 2H, C^1-$H^{a/b}$), 2.44 (s, 2H, O-H), 1.75-1.64 (m, 1H, C^2-H), 1.64-1.52 (m, 2H, C^4-H and C^3-H^a), 1.12 (d, ^3J = 6.4 Hz, 3H, C^6-H), 0.94 (d, ^3J = 6.7 Hz, 3H, C^7 H (*syn* or *anti*)), 0.91 (d, ^3J = 6.7 Hz, 3H, C^7 H (*anti* or *syn*)), 0.91-0.84 (m, 1H, C^3-H^b), 0.86 (d, ^3J = 6.6 Hz, 3H, C^8 H).

^{13}C NMR (101 MHz, $CDCl_3$): δ(ppm) = 72.2 (C^5 (*syn* or *anti*)), 70.1 (C^5 (*anti* or *syn*)), 67.7 (C^1 (*syn* or *anti*)), 67.2 (C^1 (*anti* or *syn*)), 37.9 (C^4 (*syn* or *anti*)), 37.1 (C^4 (*anti* or *syn*)), 36.8 (C^3 (*syn* or *anti*)), 36.0 (C^3 (*anti* or *syn*)), 33.5 (C^2 (*syn* or *anti*)), 33.1 (C^2 (*anti* or *syn*)), 19.8 (C^6 (*syn* or *anti*)), 19.7 (C^6 (*anti* or *syn*)), 18.3 (C^7 (*syn* or *anti*)), 18.0 (C^7 (*anti* or *syn*)), 15.9 (C^8 (*syn* or *anti*)), 15.1 (C^8 (*anti* or *syn*)).

Synthesis of (2*S*,4*R*)-2,4-dimethyl-5-oxohexanoic acid (15)[24]

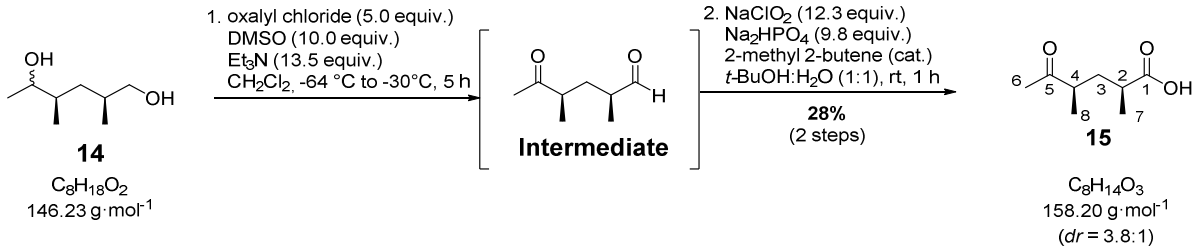

Under argon atmosphere in a flame-dried flask oxalyl chloride (247 µl, 2.87 mmol, 5.0 equiv.) was dissolved in dry CH_2Cl_2 (15 ml) and cooled to -64 °C using a dry ice/acetone bath. Then dry DMSO (408 µl, 5.74 mmol, 10.0 equiv.) was added over 5 min and the solution was stirred for at 64 °C for 1 h. Then, a solution of (2*S*,4*R*)-2,4-dimethylhexane-1,5-diol (**14**) (84.0 mg, 0.574 mmol, 1.0 equiv.) in dry CH_2Cl_2 (3 ml) was added and the mixture was stirred at -64°C for 2 h. Afterwards, freshly distilled triethylamine (Et_3N) (1.08 ml, 7.76 mmol, 13.5 equiv.) was added and the reaction mixture was stirred at -64°C for 1 h and at -30 °C for 1 h. After full conversion of diol **14** (TLC-control) PE/toluene 3:1 (30 ml) was added and a white solid precipitated. The solid was separated by filtration using celite and washed with PE/toluene 3:1 (30 ml). After the solvents were removed *in vacuo*, the **intermediate** (204 mg) was obtained as a pale-yellow oil. Because keto-aldehyde **intermediate** was assumed to be unstable at air, light, and rt, the crude product was directly used for the subsequent reaction.

The crude keto-aldehyde **intermediate** was dissolved in *tert*-butanol (12 ml) and 25 drops of 2-methyl-2-butene. Then, $NaClO_2$ (639 mg, 7.06 mmol, 12.3 equiv.) and Na_2HPO_4 (1.00 g, 5.63 mmol, 9.80equiv.) dissolved in water (12 ml) were added over 10 min. The reaction mixture was stirred for 60 min at rt. After full conversion of the keto-aldehyde **intermediate** (TLC-control) the reaction mixture was supplemented with water (25 ml), brine (50 ml), sat. aq. $Na_2S_2O_3$ (50 ml) and the aqueous phase (pH 7) was washed with Et_2O (50 ml) (product remains in the aqueous phase). Then, the aqueous phase was acidified to pH 3 using conc. HCl, and it was extracted with Et_2O (2 x 80 ml). The combined organic phases were dried over $MgSO_4$ and concentrated *in vacuo* to give 39 mg of a pale yellow solid. After flash chromatography (CH_2Cl_2/MeOH 19:1) **15** (25 mg, 0.16 mmol, 28%) was isolated as a yellow oil. Due to epimerization, product **15** was obtained as a mixture of diastereomers. By ^{1}H NMR integration, the diastereomeric ratio was determined to be *dr* = 3.8:1.

TLC: R_f = 0.40 (CH_2Cl_2/MeOH 9:1).

^{1}H NMR (250 MHz, $CDCl_3$): δ(ppm) = 2.71-2.39 (m, 2H, C^2-H and C^4-H), 2.18-2.04 (m, 1H, C^3-H^a), 2.16 (s, 3H, C^6-H), 1.44-1.31 (m, 1H, C^3-H^b), 1.21 (d, ^3J = 7.0 Hz, 3H, C^7-H), 1.13 (d, ^3J = 7.0 Hz, 3H, C^8 H).

^{13}C NMR (50 MHz, $CDCl_3$): δ(ppm) = 212.1 (C^5), 181.7 (C^1), 45.1 (C^4), 37.3 (C^2), 36.2 (C^3), 28.1 (C^6), 17.7 (C^7), 16.4 (C^8).

Synthesis of *S*-(2-acetamidoethyl) (2*S*,4*R*)-2,4-dimethyl-5-oxo-hexanethioate (6)[25]

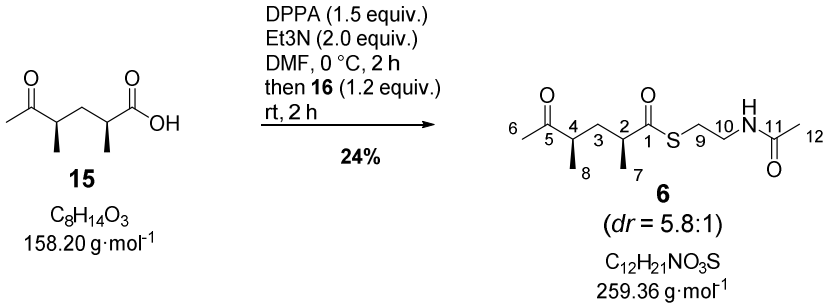

The reaction was performed under argon atmosphere in a flame-dried flask. (2*S*,4*R*)-2,4-dimethyl-5-oxohexanoic acid (**15**, *dr* = 3.8:1) (25 mg, 0.16 mmol, 1.0 equiv.) was dissolved in dry DMF (1 ml). The solution was cooled to 0 °C and diphenylphosphoryl azide (DPPA) (51 µl, 0.24 mmol, 1.5 equiv.) and triethylamine (Et_3N) (44 µl, 0.32 mmol, 2.0 equiv.) were added and stirred for 0 °C for 2 h. Subsequently, *N*-acetylcysteamine (**HSNAC**) (20 µl, 0.19 mmol, 1.2 equiv.) was added stirred and the reaction mixture was stirred at rt for 3 h. After full conversion of the acid **15** (TLC-control) sat. aq. NH_4Cl (20 ml) was added and the aqueous phase was extracted with EtOAc (13 x 30 ml). The combined organic phases were dried over $MgSO_4$ and concentrated under reduced pressure to give 91 mg of a viscous orange oil. The crude product was purified using flash chromatography (CH_2Cl_2/MeOH 99:1 ⟶ 32:1) yielding **6** (10 mg, 0.039 mmol, 24%) as a viscous, colourless oil. Product **6** was obtained as a mixture of diastereomers. By ^{1}H NMR integration, the diastereomeric ratio was determined to be *dr* = 5.8:1.

TLC: R_f = 0.54 (CH_2Cl_2/MeOH 9:1).

Specific rotation: $[\alpha]_D^{20}$ = +7.4° (c = 0.37, CH_2Cl_2).

Table S 63: ^{1}H ($CDCl_3$, 400 MHz) and ^{13}C NMR ($CDCl_3$, 101 MHz) of **2**

Position	δH ppm (J in Hz)	δC (ppm)	Position	δH ppm (J in Hz)	δC (ppm)
1	-	203.8	7	1.18 (d, 6.9)	18.7
2	2.69 (dqd, 8.9, 7.0, 5.6)	46.8	8	1.11 (d, 7.0)	16.9
3	2.19-2.10 (m) and 1.36 (ddd, 14.0, 7.0, 5.6)	36.7	9	3.02 (t, 6.4)	28.6
4	2.54 (sext, 7.0)	45.2	10	3.50-3.36 (m)	39.5
5	-	211.8	11	-	170.4
6	2.14 (s)	28.0	12	1.97 (s)	23.3
NH	6.02 (bs)	-	-	-	-

Table S 64: Mass spectrometric data of compound **2**.

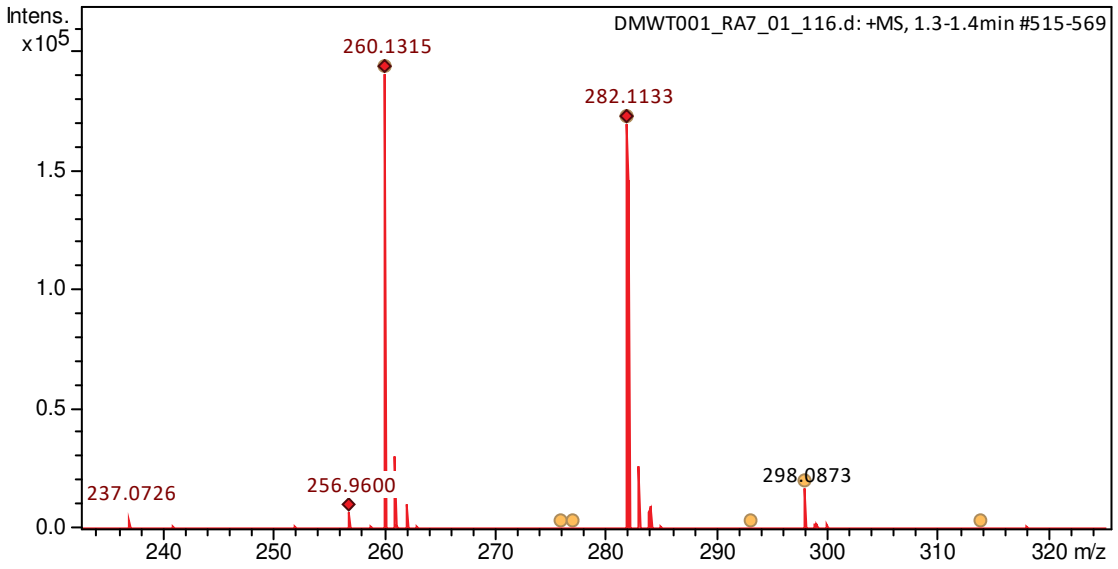

Sum Formula	ion formula	found m/z	Calc m/z	error [ppm]	mSigma
$C_{12}H_{22}NO_3S$	[M+H]	260.1315	260.1315	0.13	7.3
$C_{12}H_{21}NNaO_3S$	[M+Na]	282.1133	282.1134	0.53	5.5
$C_{12}H_{21}KNO_3S$	[M+K]	298.0873	298.0874	0.3	9.1

(2*R*,4*S*)-5-acetoxy-2,4-dimethylpentyl 4-nitrobenzoate (25)

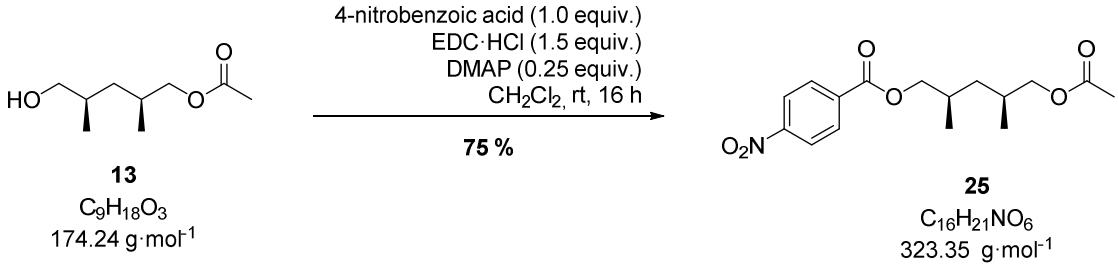

13
$C_9H_{18}O_3$
174.24 g·mol^{-1}

25
$C_{16}H_{21}NO_6$
323.35 g·mol^{-1}

Compound **13** (100 mg, 0.57 mmol, 1.0 equiv.) and 4-nitrobenzoic acid (143 mg, 0.86 mmol, 1.5 equiv.) were dissolved in CH_2Cl_2 (5 mL). Subsequently, EDC·HCl (164 mg, 0.86 mmol, 1.5 equiv.) and DMAP (17 mg, 0.14 mmol, 0.25 equiv.) were added and the mixture was stirred at rt until complete conversion of the starting material was observed (TLC-Control after 16 h). The reaction was quenched by adding sat. aq. $NaHCO_3$ (5 mL) and the organic phase was separated and immediately washed with sat. aq. $NaHCO_3$ (5 mL), sat. aq. NH_4Cl (2 x 5 mL) and brine (5 mL) and dried over Na_2SO_4. The crude product was purified using flash chromatography (petrol ether/EtOAc 7:3 isocratic) yielding **25** (138 mg, 0.43 mmol, 75%) as a viscous, colorless oil.

TLC: R_f = 0.76 (petrol ether/EtOAc 7:3).

Specific rotation: $[\alpha]_D^{20}$ = -1.16°(c = 1.2, $CHCl_3$).

^{1}H NMR (400 MHz, $CDCl_3$): δ(ppm) = 8.30 (d, J = 8.7 Hz, 2H), 8.20 (d, J = 8.8 Hz, 2H), 4.26 (dd, J = 10.8, 5.4 Hz, 1H), 4.15 (dd, J = 10.8, 6.6 Hz, 1H), 3.97 (dd, J = 10.8, 5.6 Hz, 1H), 3.88 (dd, J = 10.8, 6.5 Hz, 1H), 2.14 – 2.05 (m, 1H), 2.03 (s, 3H), 2.00 – 1.91 (m, 1H), 1.53 (dt, J = 13.8, 6.9 Hz, 1H), 1.14 (dt, J = 14.4, 7.4 Hz, 1H), 1.07 (d, J = 6.7 Hz, 3H), 1.00 (d, J = 6.7 Hz, 3H).

^{13}C NMR (50 MHz, $CDCl_3$): δ(ppm) = 171.3, 164.8, 150.7, 135.9, 130.8, 123.7, 70.6, 69.1, 37.7, 30.3, 30.2, 21.1, 17.9, 17.8.

HRMS (LCMS-ESI):

Sum Formula	ion formula	found m/z	calc'd m/z	error [ppm]	mSigma
$C_{16}H_{22}NO_6$	$[M+H]^+$	324.1442	324.1442	-0.1	2
$C_{16}H_{21}NNaO_6$	$[M+Na]^+$	346.1261	346,1261	0.1	3.3

(2*R*,4*S*)-5-acetoxy-2,4-dimethylpentyl 4-nitrobenzoate ((±)-13)

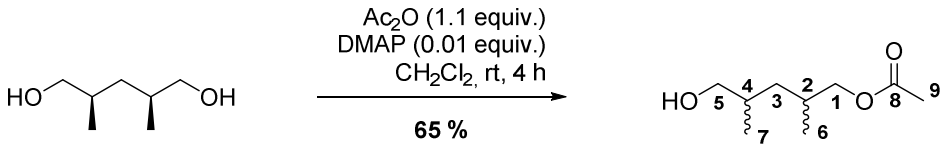

meso-**12**
$C_7H_{16}O_2$
132.20 g·mol^{-1}

(±)-13
$C_9H_{18}O_3$
174.24 g·mol^{-1}

Compound *meso*-**12** (18 mg, 136 µmol, 1.0 equiv.) and Ac_2O (14.5 µL , 150 µmol, 1.1 equiv.) were dissolved in CH_2Cl_2 (5 mL). Subsequently, DMAP (0.5 mg, 4.3 µmol, 0.01 equiv.) was added and the mixture was stirred at rt until complete conversion of the starting material was observed (TLC-Control after 16 h). The reaction was quenched by adding sat. aq. $NaHCO_3$ (1 mL) and the organic phase was separated and immediately washed with sat. aq. $NaHCO_3$ (1 mL), sat. aq. NH_4Cl (2 x 1 mL) and brine (1 mL) and dried over Na_2SO_4. The crude product was purified using flash chromatography (petrol ether/EtOAc 95:5→ 70:30) yielding **(±)-13** (15 mg, 88.4 µmol, 65%) as a viscous, colorless oil.
The observed data was consistent in all regards (except for optical rotation) with that reported for compound **13**.

5-acetoxy-2,4-dimethylpentyl 4-nitrobenzoate ((±)-25)

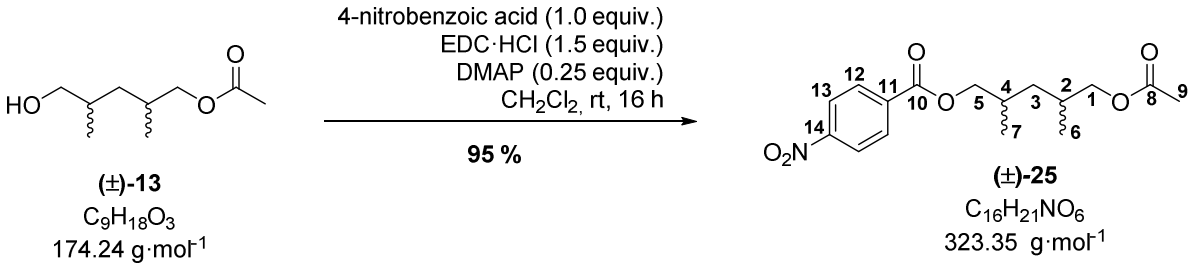

Compound **13** (3 mg, 17 µmol, 1.0 equiv.) and 4-nitrobenzoic acid (4.3 mg, 26 µmol, 1.5 equiv.) were dissolved in CH_2Cl_2 (5 mL). Subsequently, EDC·HCl (5 mg, 26 µmol, 1.5 equiv.) and DMAP (0.5 mg, 4.3 µmol, 0.25 equiv.) were added and the mixture was stirred at rt until complete conversion of the starting material was observed (TLC-Control after 16 h). The reaction was quenched by adding sat. aq. $NaHCO_3$ (5 mL) and the organic phase was separated and immediately washed with sat. aq. $NaHCO_3$ (5 mL), sat. aq. NH_4Cl (2 x 5 mL) and brine (5 mL) and dried over Na_2SO_4. The crude product was purified using flash chromatography (petrol ether/EtOAc 7:3 isocratic) yielding **rac-25** (8 mg, 24.7 µmol, 95%) as a viscous, colorless oil.

The observed data was consistent in all regards (except for optical rotation) with that reported for compound **25**.

Determination of enantiomeric excess of compound 25 (13)

HPLC device: Dionex Ultimate 3000 HPLC System (consisting of a pump, autosampler, column oven and UV detector)

Column: Chiralpak AGP Analytic 5#m, 100 mm x 4 mm

Sample: Compounds were dissolved in mobile phase buffer system (10 mm NH_4Ac-buffer (pH 5.7):2-PrOH = 95:5)

Method:

Mobile phase: 10 mM NH_4Ac-buffer (pH 5.7):2-PrOH = 95:5 isocratic.

UV-Absorption: 270 nm.

Total Runtime: 10 min.

Retentiontime:

25 major enantiomer = 3.2 min; Area = 79.21

25 minor enantiomer = 5.7 min; Area = 0.73

ee = $\frac{79.21-0.73}{79.21+0.73}$ = 98.2 %.

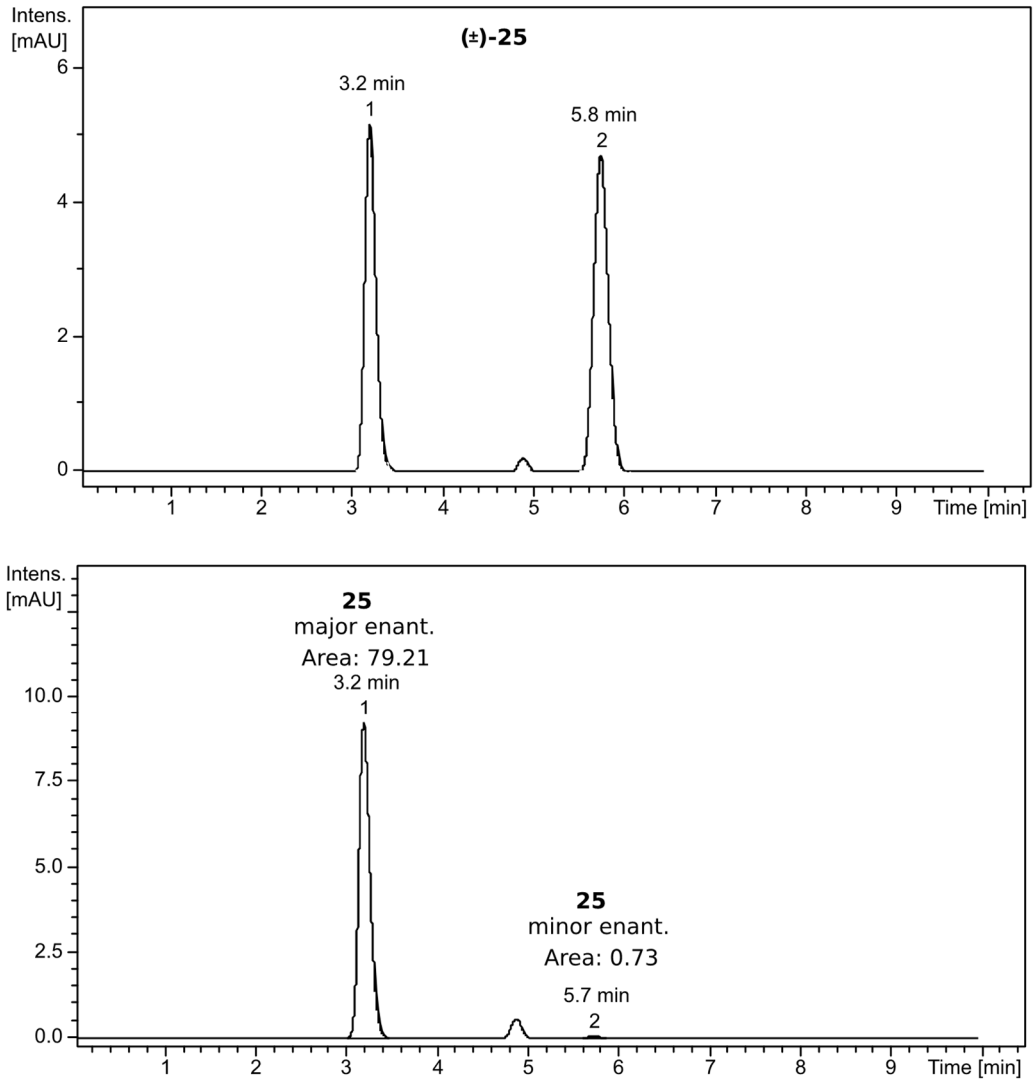

Figure S 55: UV chromatograms of rac-25 (top) and 25 (bottom).

9.7 VCD Spectrum of Compound 13 to Verify Absolute Configuration

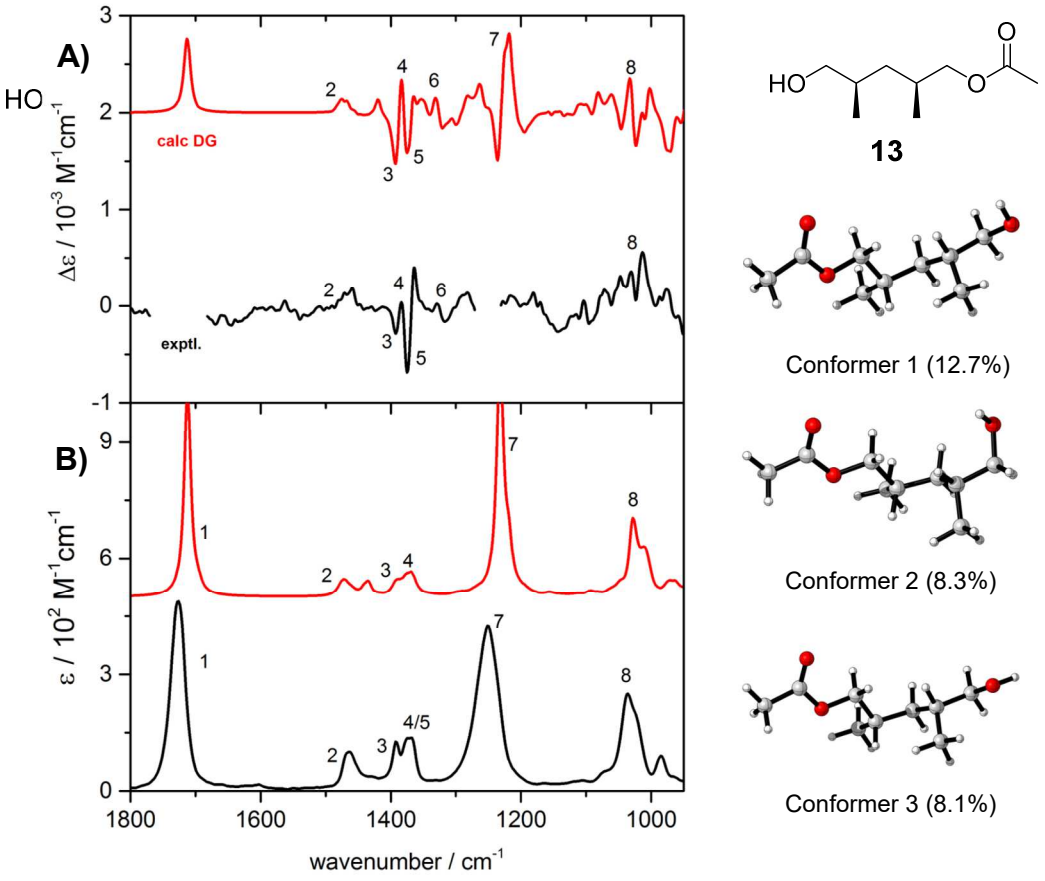

Figure S 56: Verification of absolute configuration of key intermediate **13** by comparison of the measured VCD (vibrational circular dichroism) spectrum (black line in **A**) and IR (infrared) spectrum (black line in **B**) with the respective calculated spectra (red lines). Measurement was conducted with a *Bruker* Vertex 70 IR spectrometer coupled with a *Bruker* PMA50 VCD spectrometer (run in a 0.1 mm thick BaF_2 cell, solvent: $CDCl_3$, c = 50 mg/ml). The VCD spectrum shows the average value over 34080 scans (the two missing parts originate from a too high sample concentration). Calculation was performed using *Wavefunction* Spartan software. All possible conformers of compound **13** were generated via a force field optimization (functional: B3LYP, basis set: 6-311+G(2d,p). Solvation effects were modelled using the polarizable continuum model (PCM). Band assignment: 1709 cm^{-1} (C=O stretch, 1), 1476 cm^{-1} (C-H deformation, 2), 1390 cm^{-1} (C-H wagging, 3), 1386 cm^{-1} (C-H wagging, 4), 1359 cm^{-1} (C-H wagging, 5), 1355 cm^{-1} (C-H asymmetric stretch, 6), 1233 cm^{-1} (C-H asymmetric stretch, 7), 1045 cm^{-1} (C-H rocking, 8). The 3D structures of the three most populated conformers of compound **13** at room temperature are shown on the right with the percentage of population in brackets. Measurements and calculations were performed by the Merten group.

9.8 NMR-Spectra of the Synthesis Part (Following Pages)

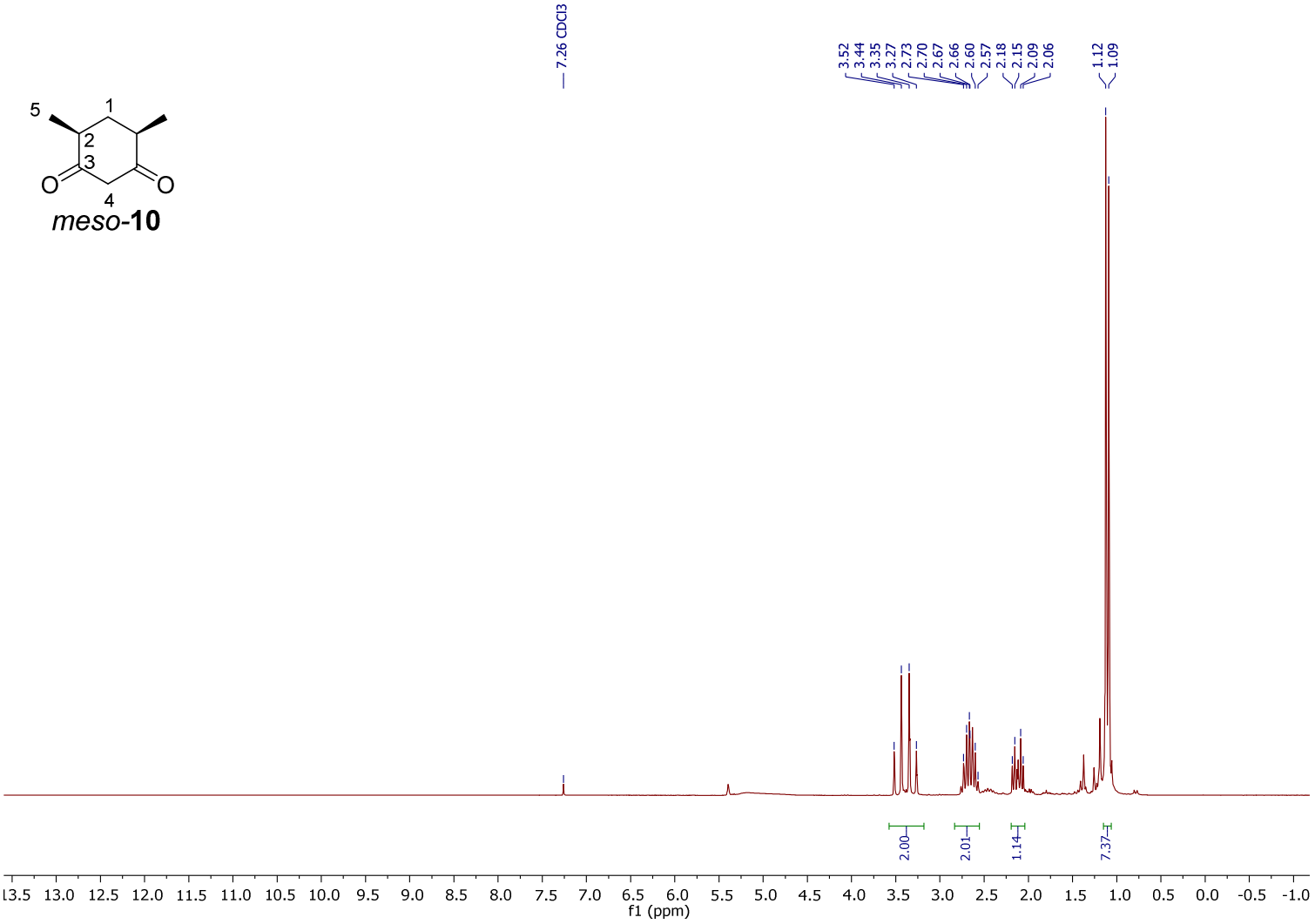

Figure S 57: ^{1}H NMR of Cpd *meso*-**10**.

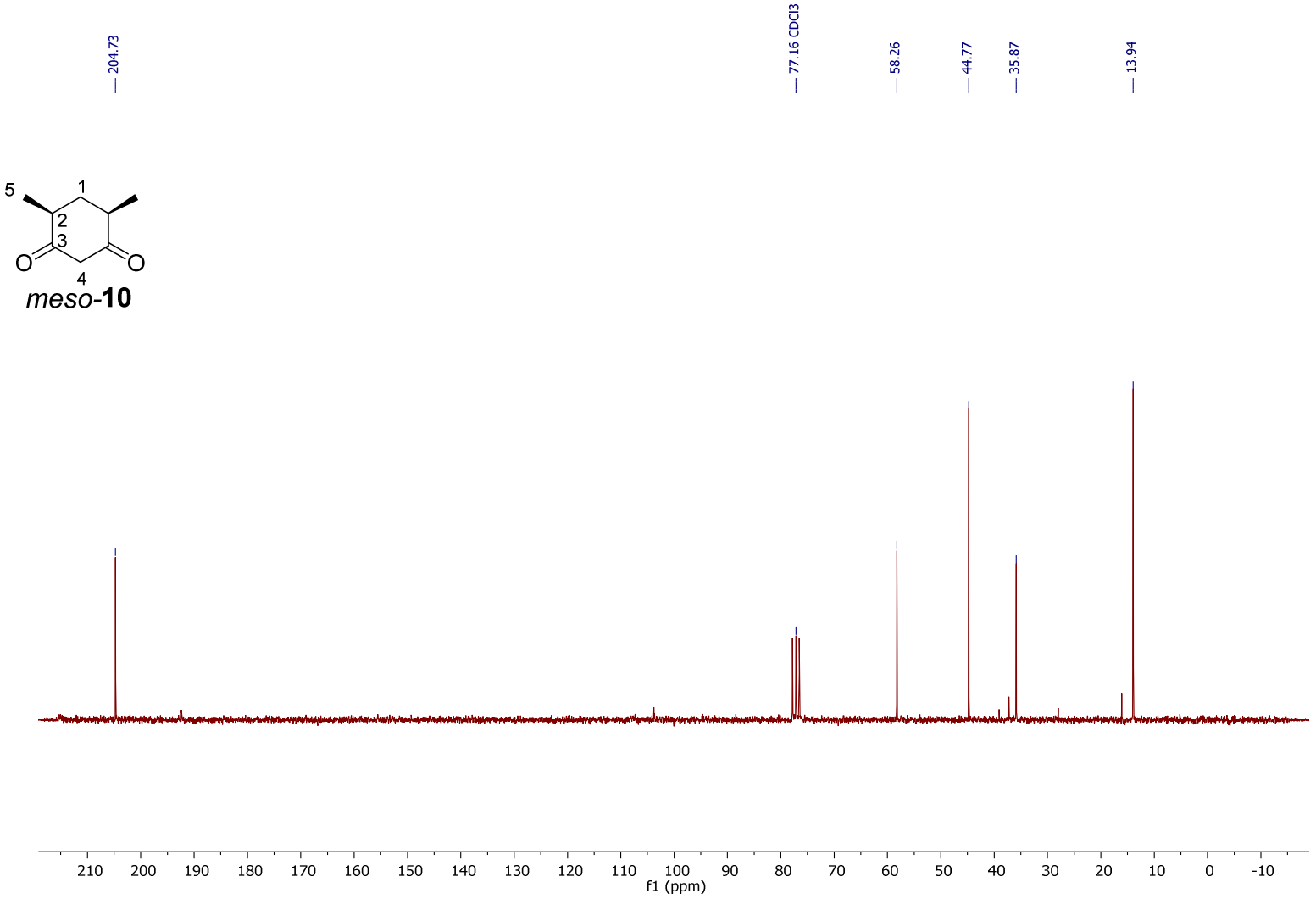

Figure S 58: ^{13}C NMR of *meso*-**10**.

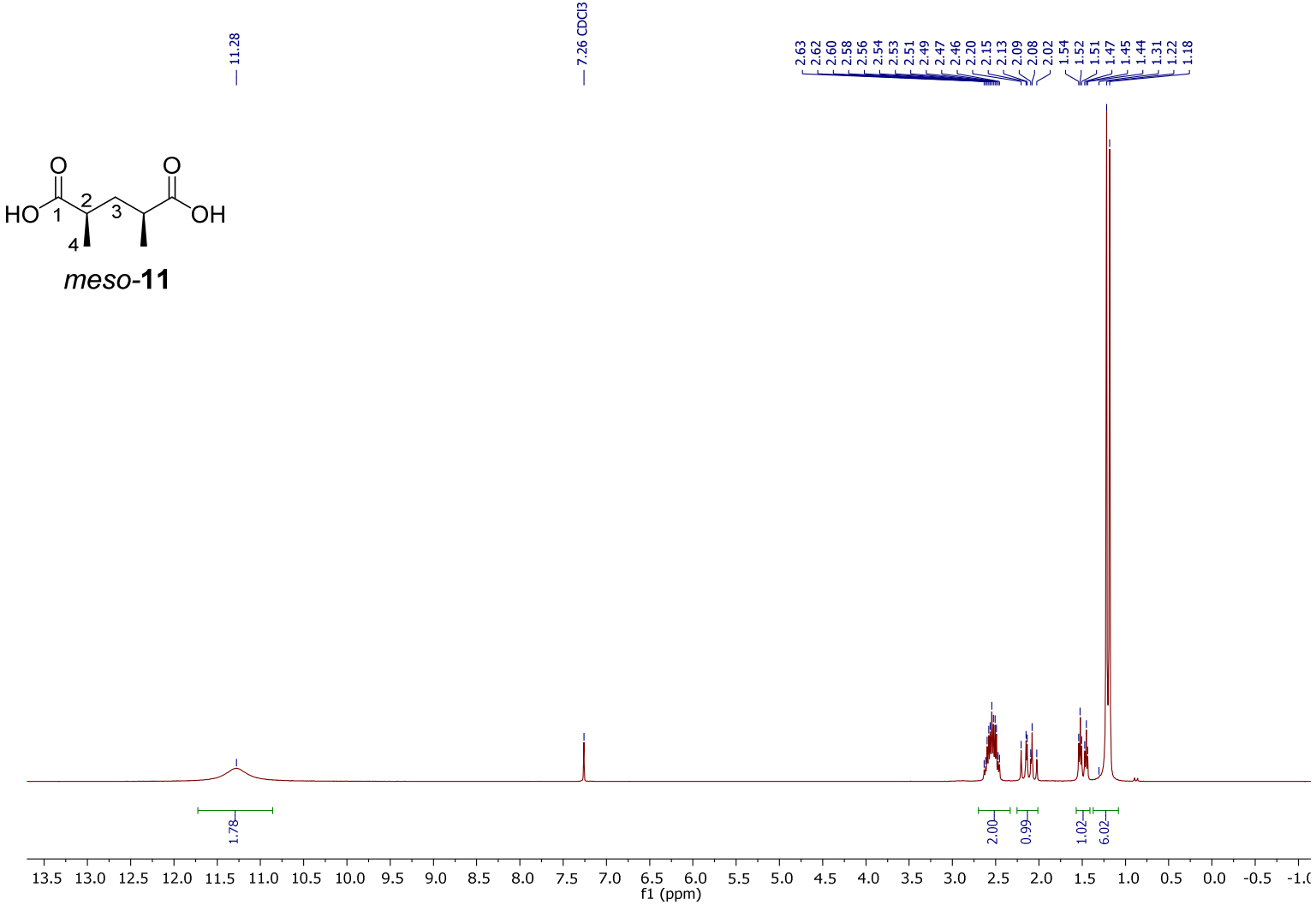

Figure S 59: ^{1}H NMR of Cpd *meso*-**11**

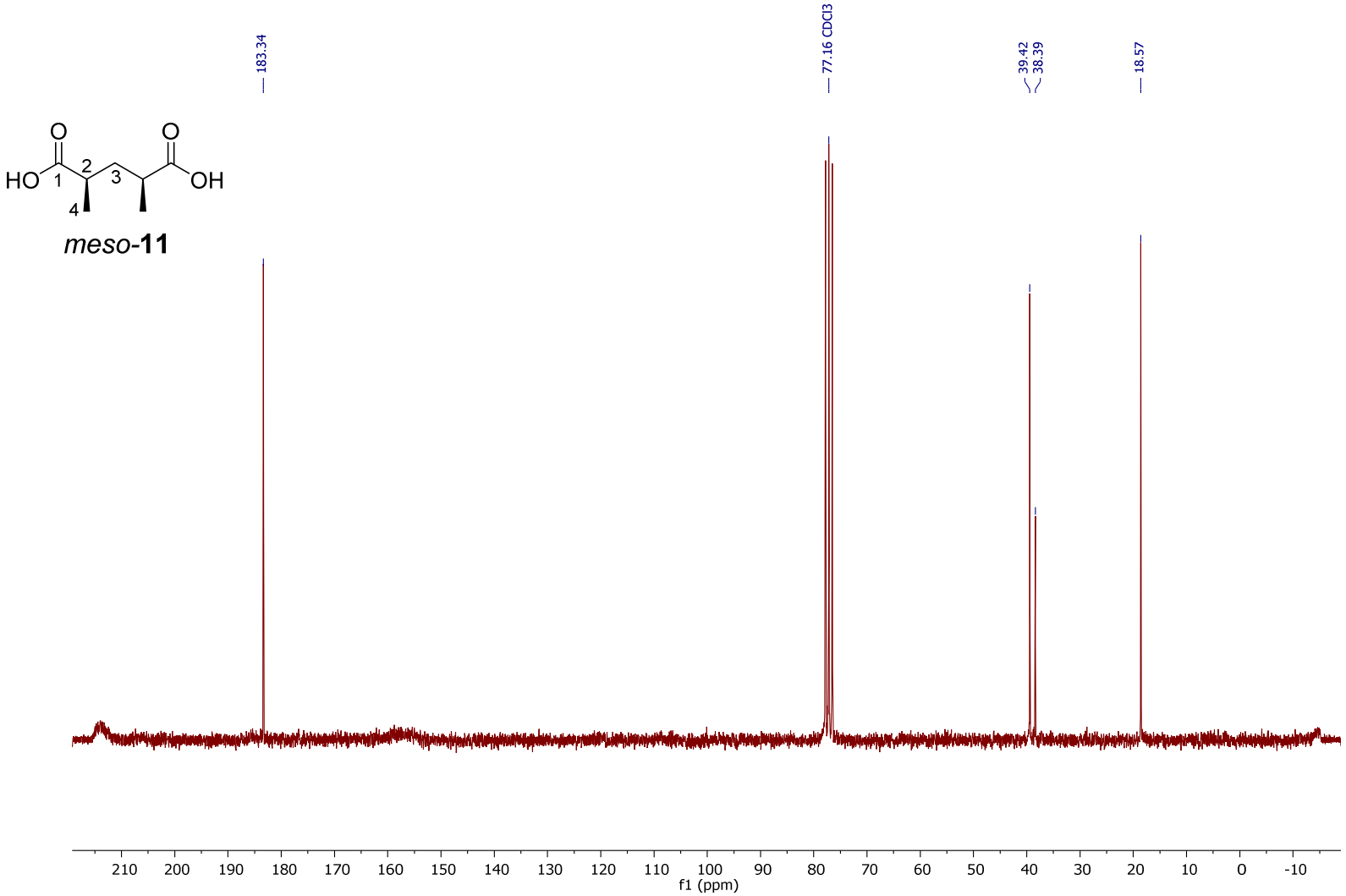

Figure S 60: ^{13}C NMR of Cpd *meso*-**11**.

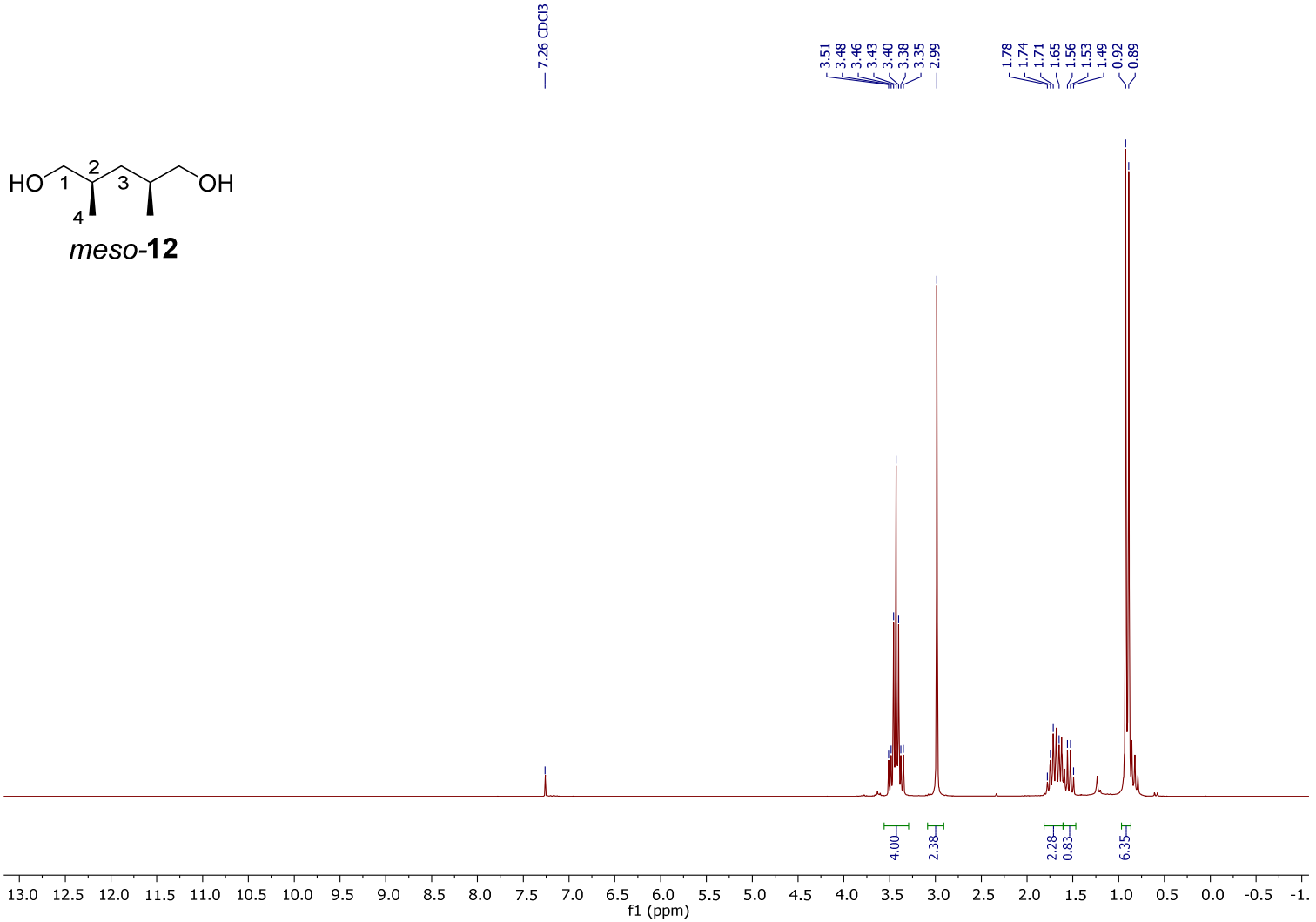

Figure S 61: ^{1}H NMR of Cpd *meso*-**12**.

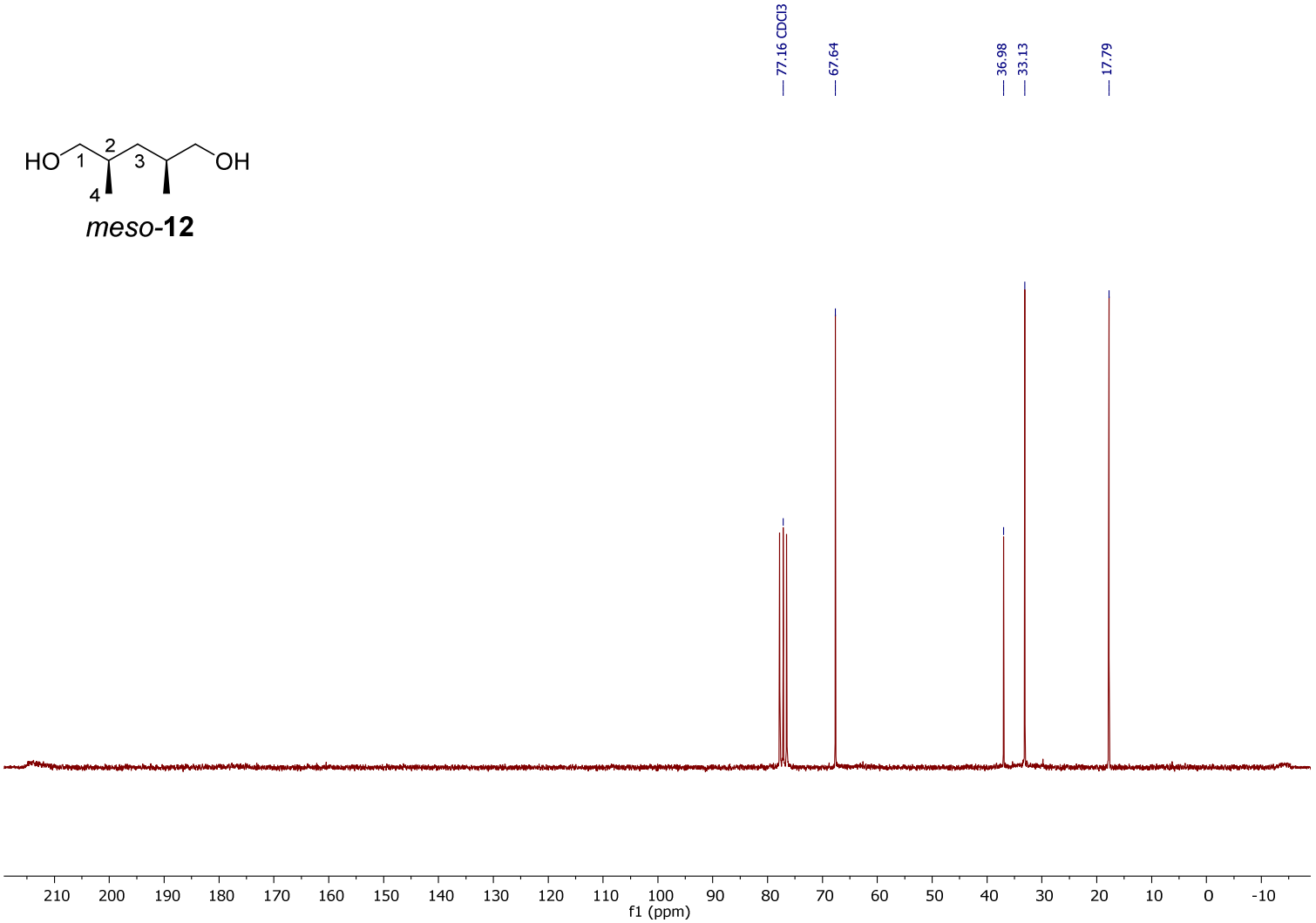

Figure S 62: ^{13}C NMR of Cpd *meso*-**12**.

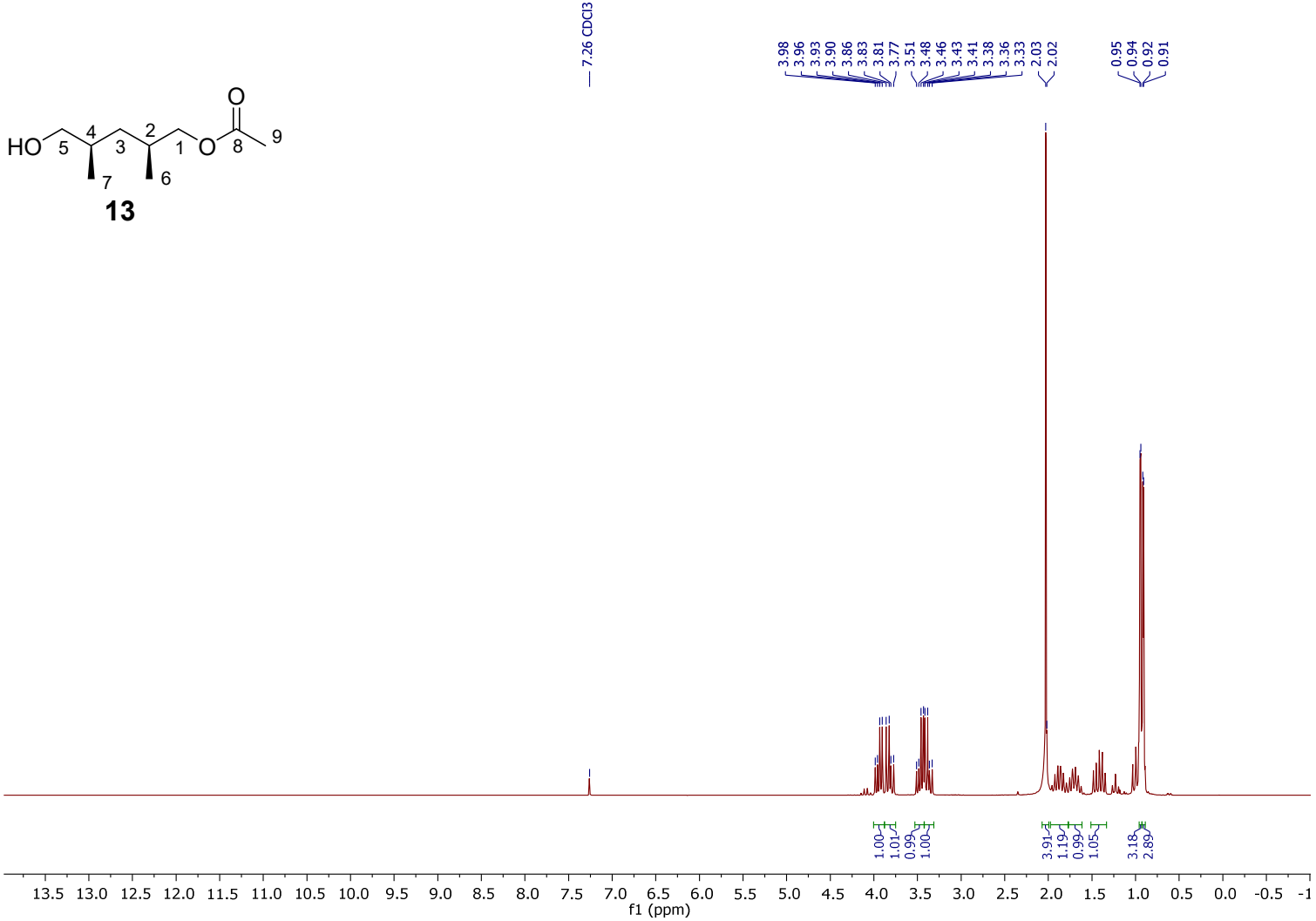

Figure S 63: ^{1}H NMR of Cpd **13**.

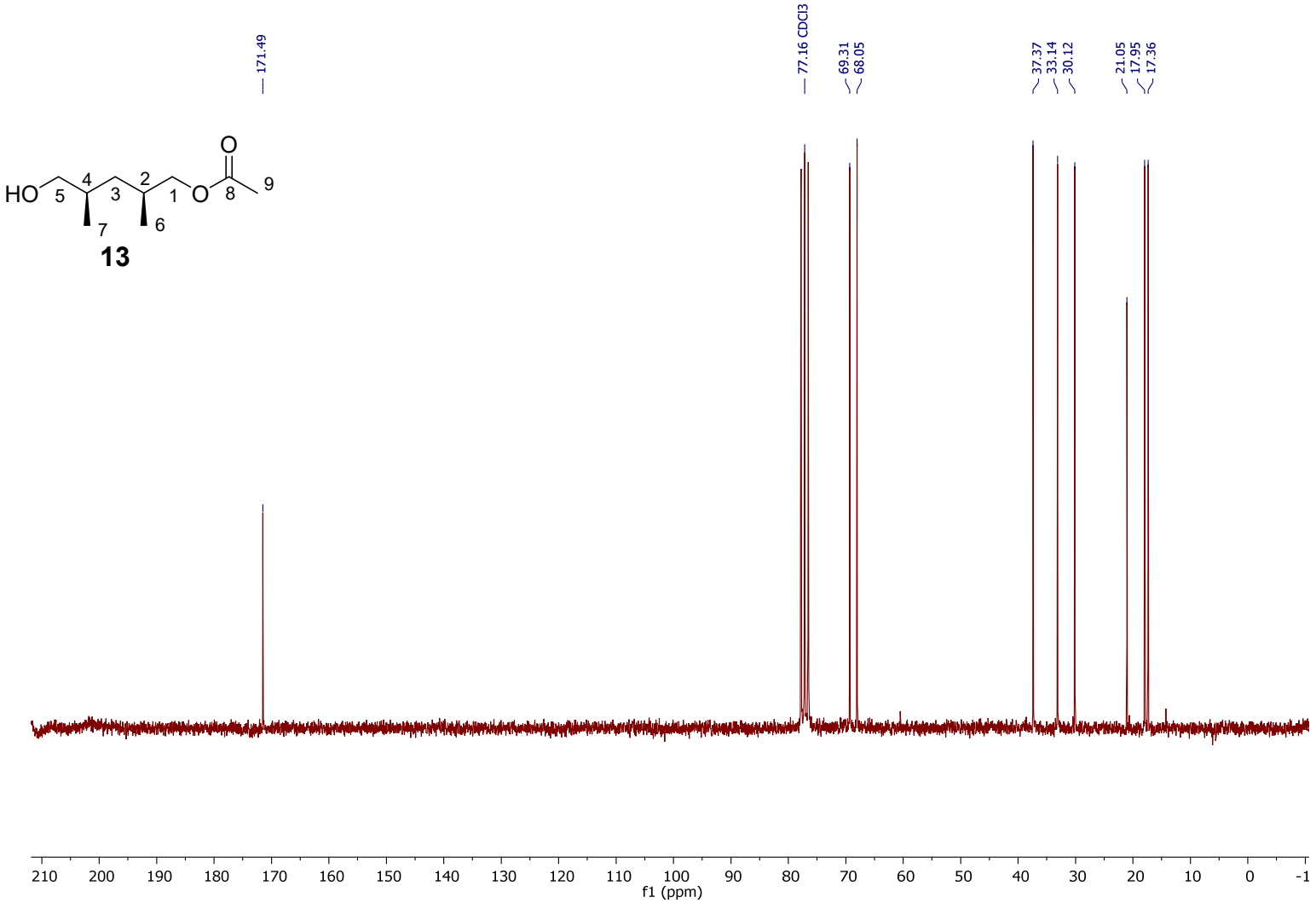

Figure S 64: ^{13}C NMR of Cpd **13**.

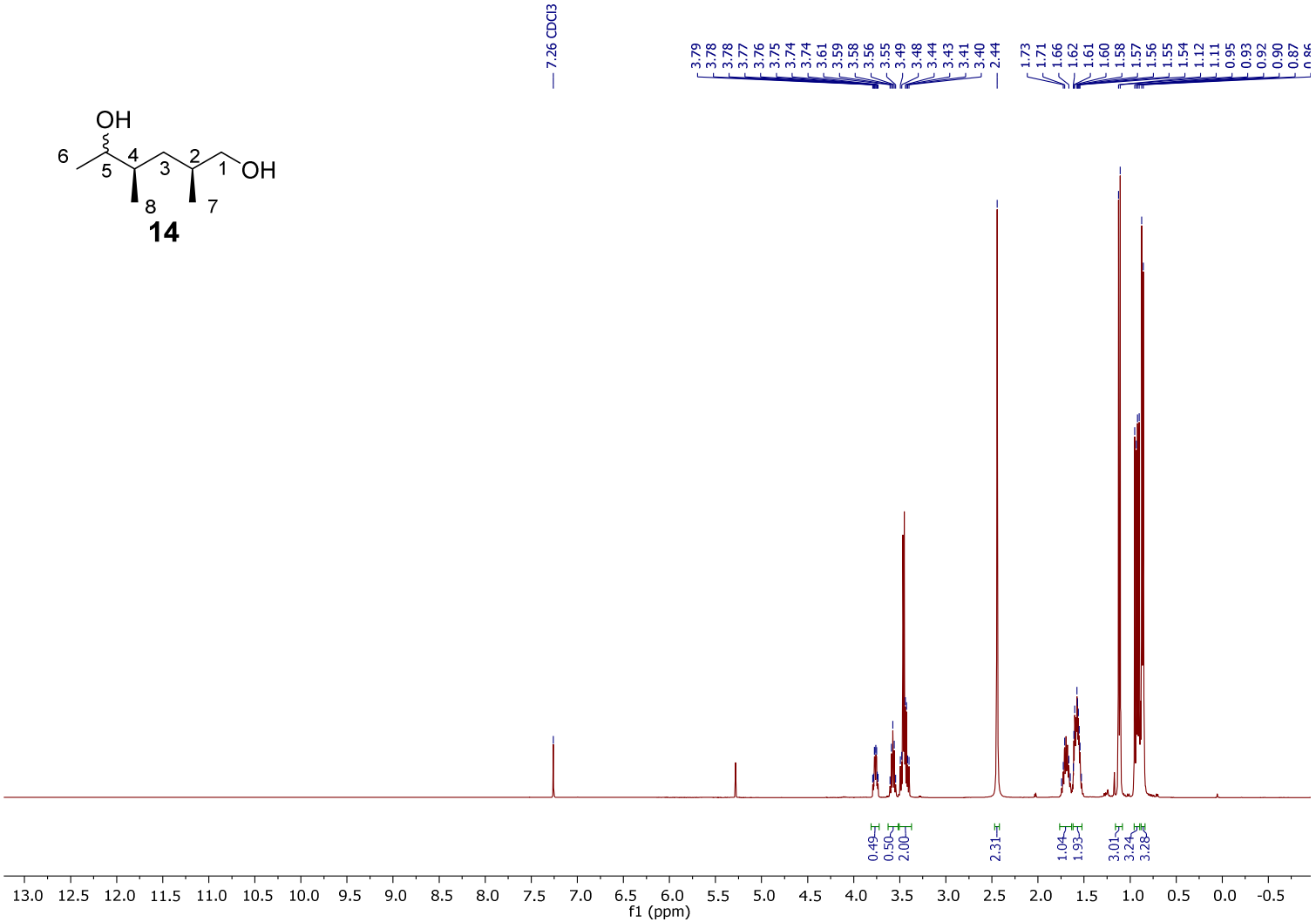

Figure S 65: ^{1}H NMR of Cpd **14**.

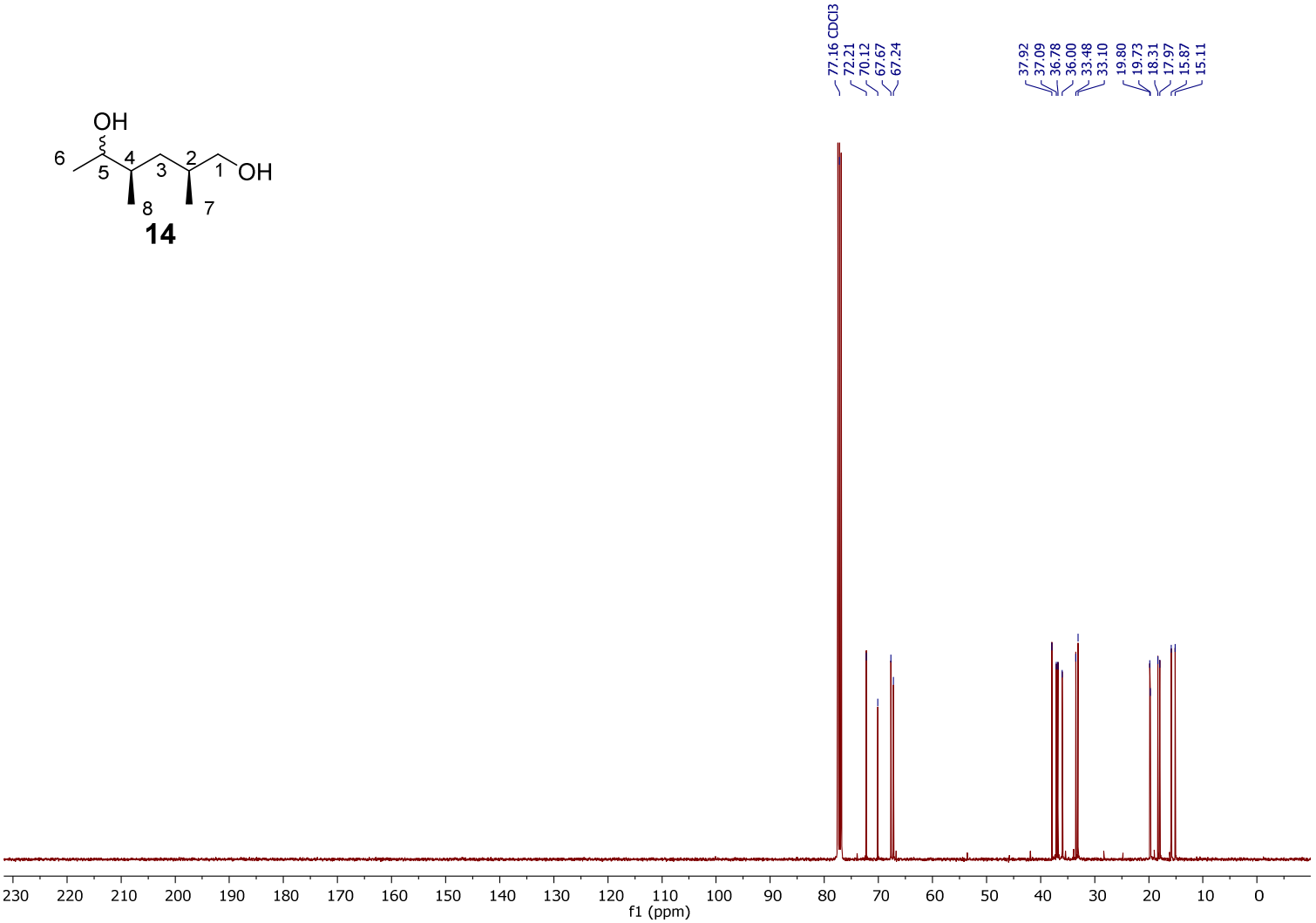

Figure S 66: ^{13}C NMR of Cpd **14**.

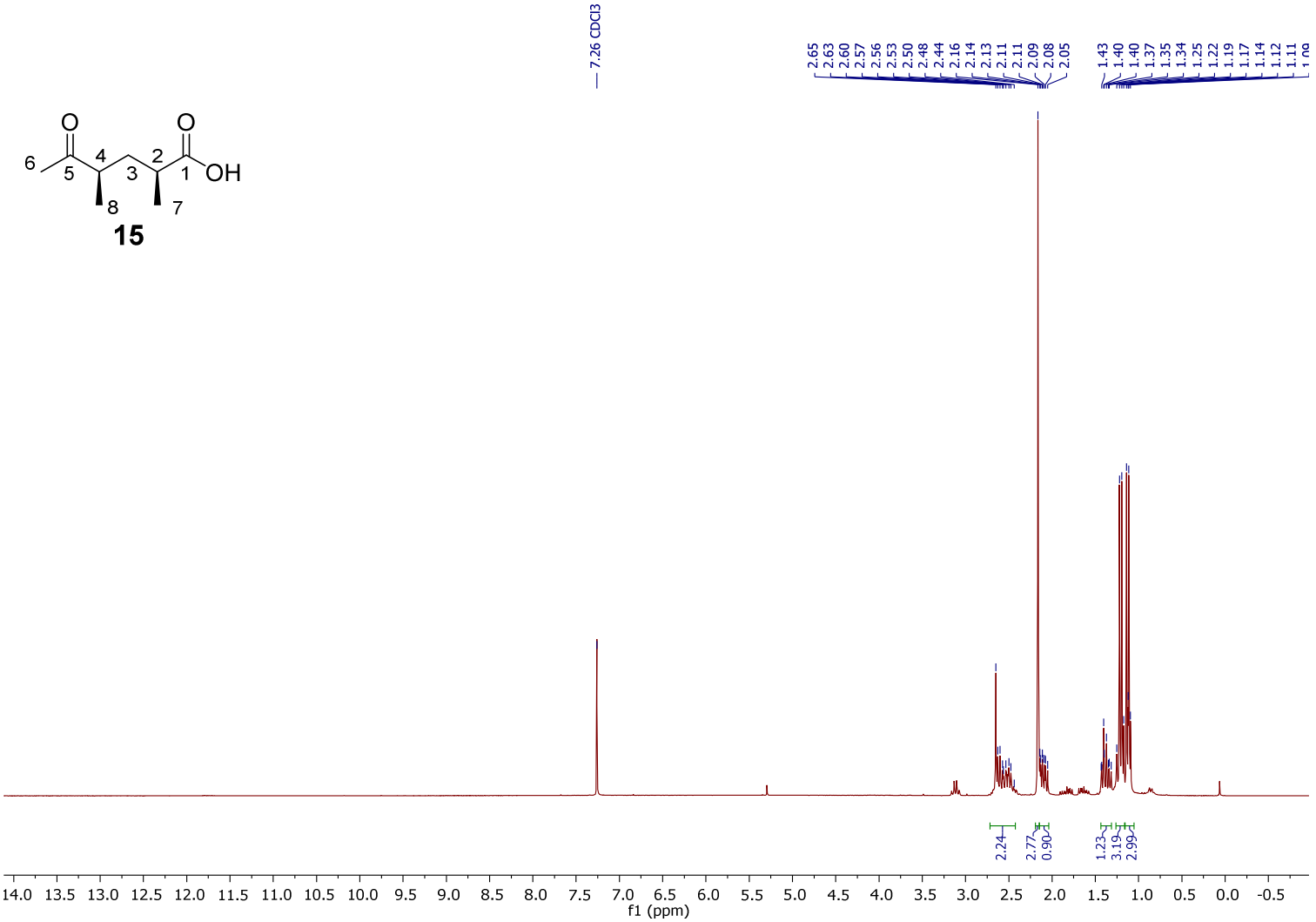

15

Figure S 67: [1]H NMR of Cpd **15**.

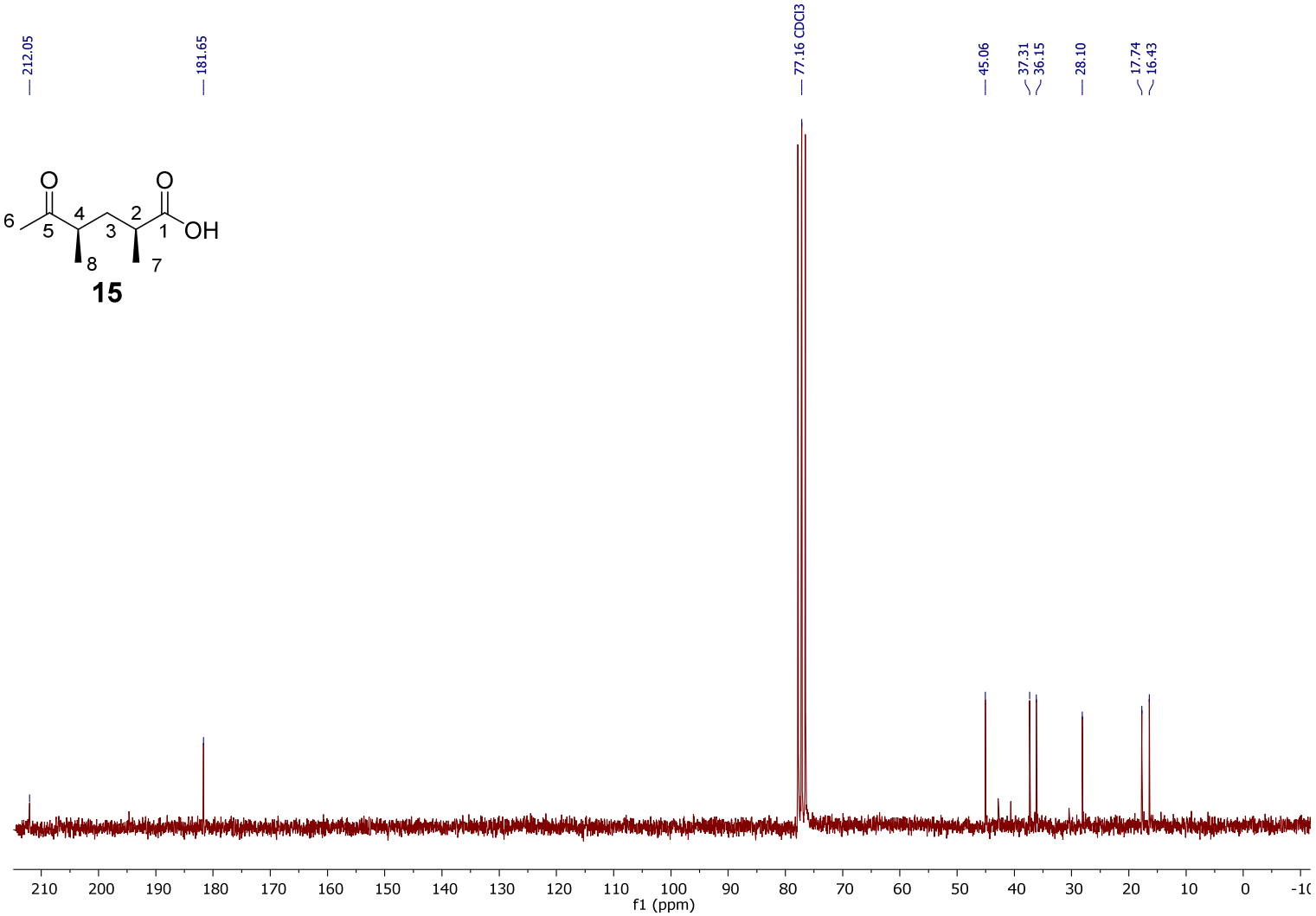

Figure S 68: ^{13}C NMR of Cpd **15**.

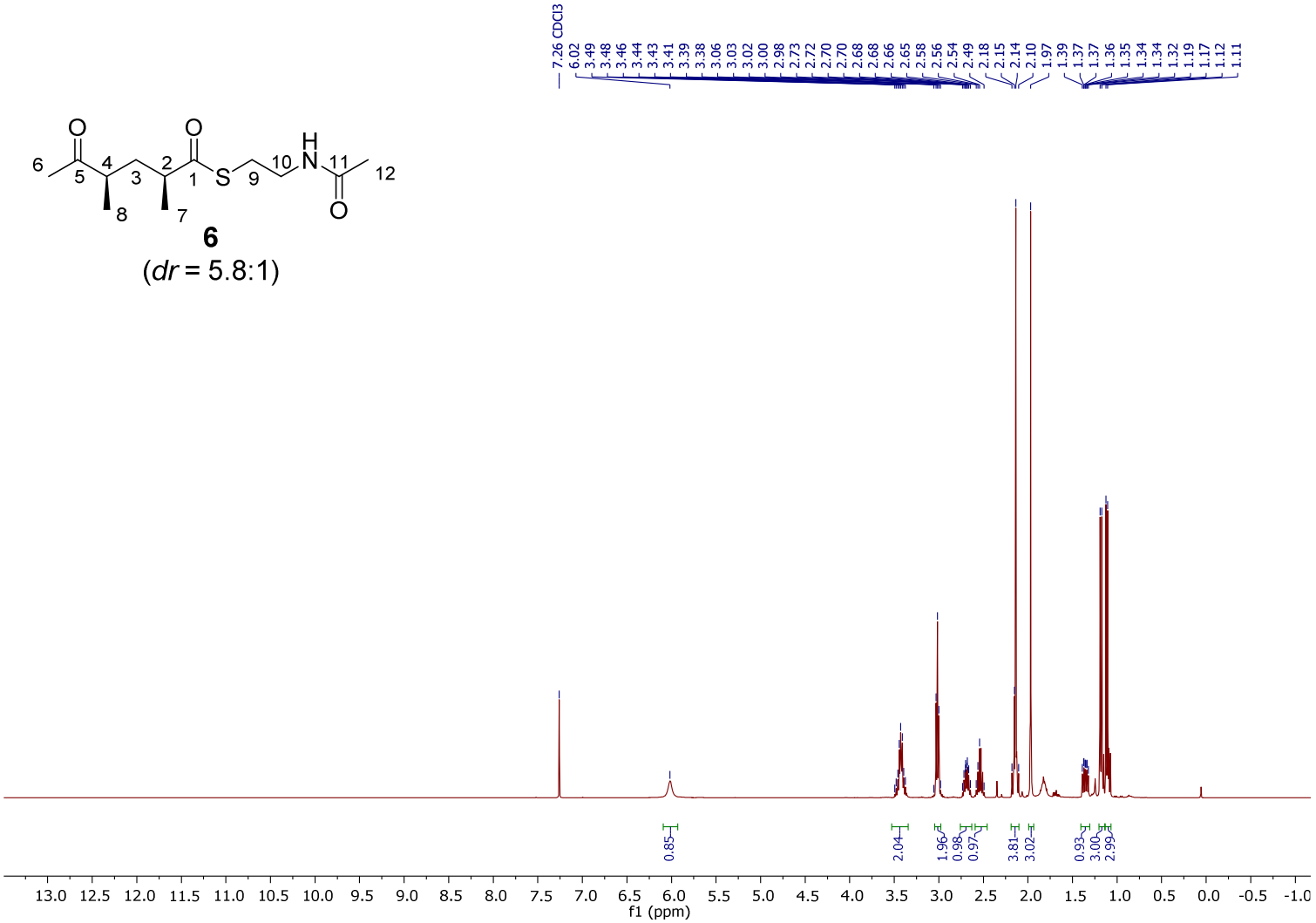

6

(*dr* = 5.8:1)

Figure S 69: ^{1}H NMR of Cpd **6**.

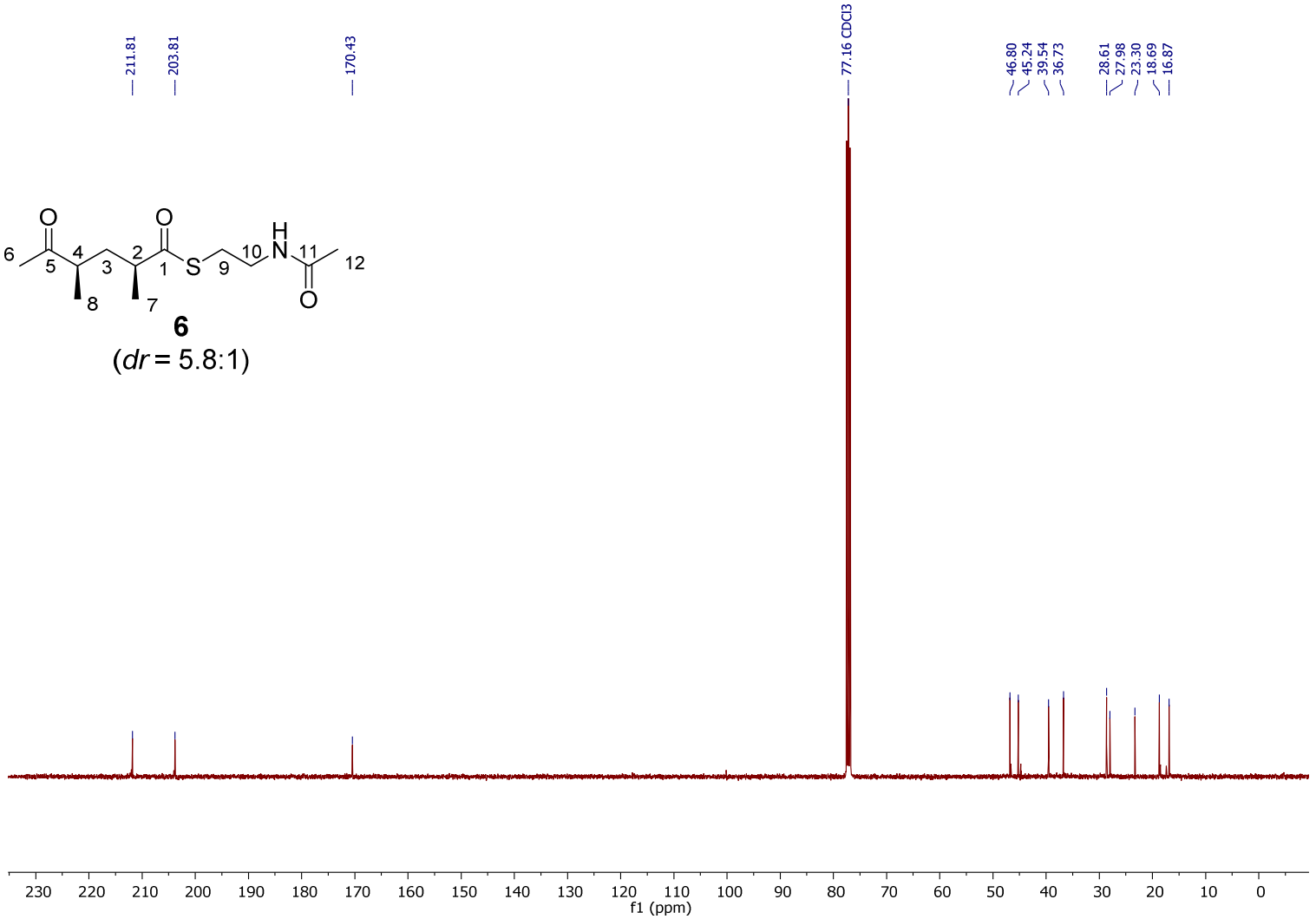

Figure S 70: ^{13}C NMR of Cpd **6**.

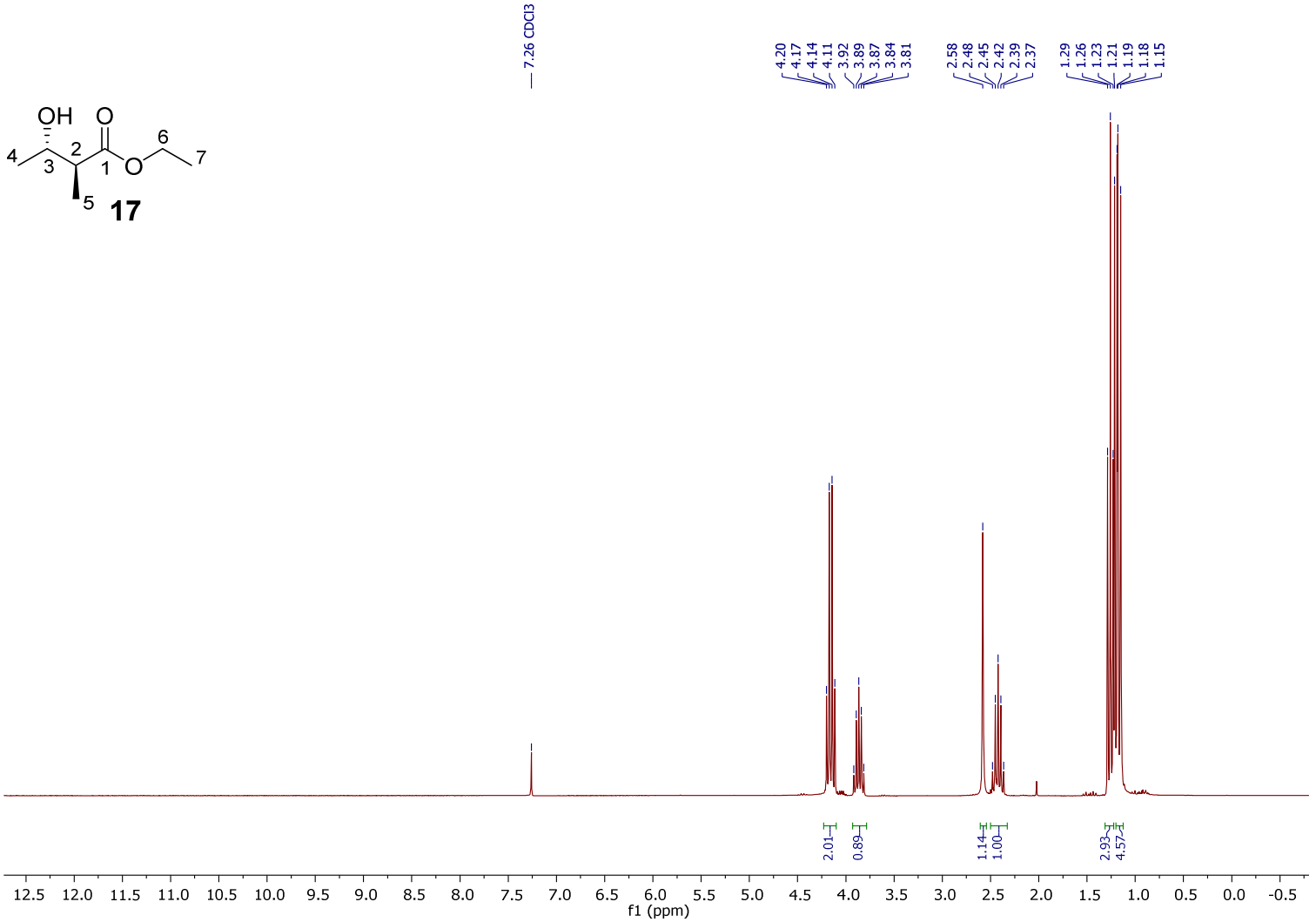

Figure S 71: ^{1}H NMR of Cpd **17**.

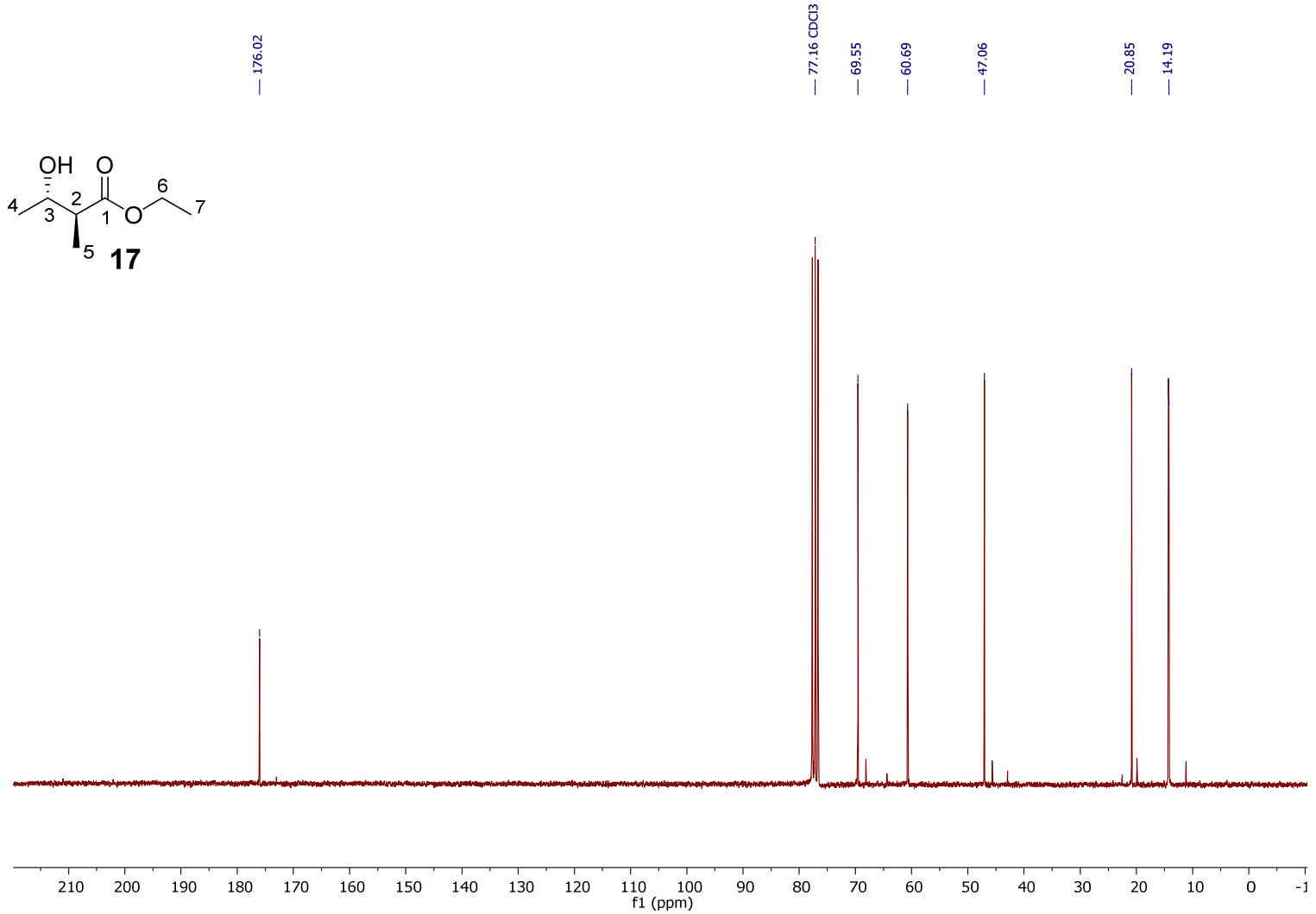

Figure S 72: ^{13}C NMR of Cpd **17**.

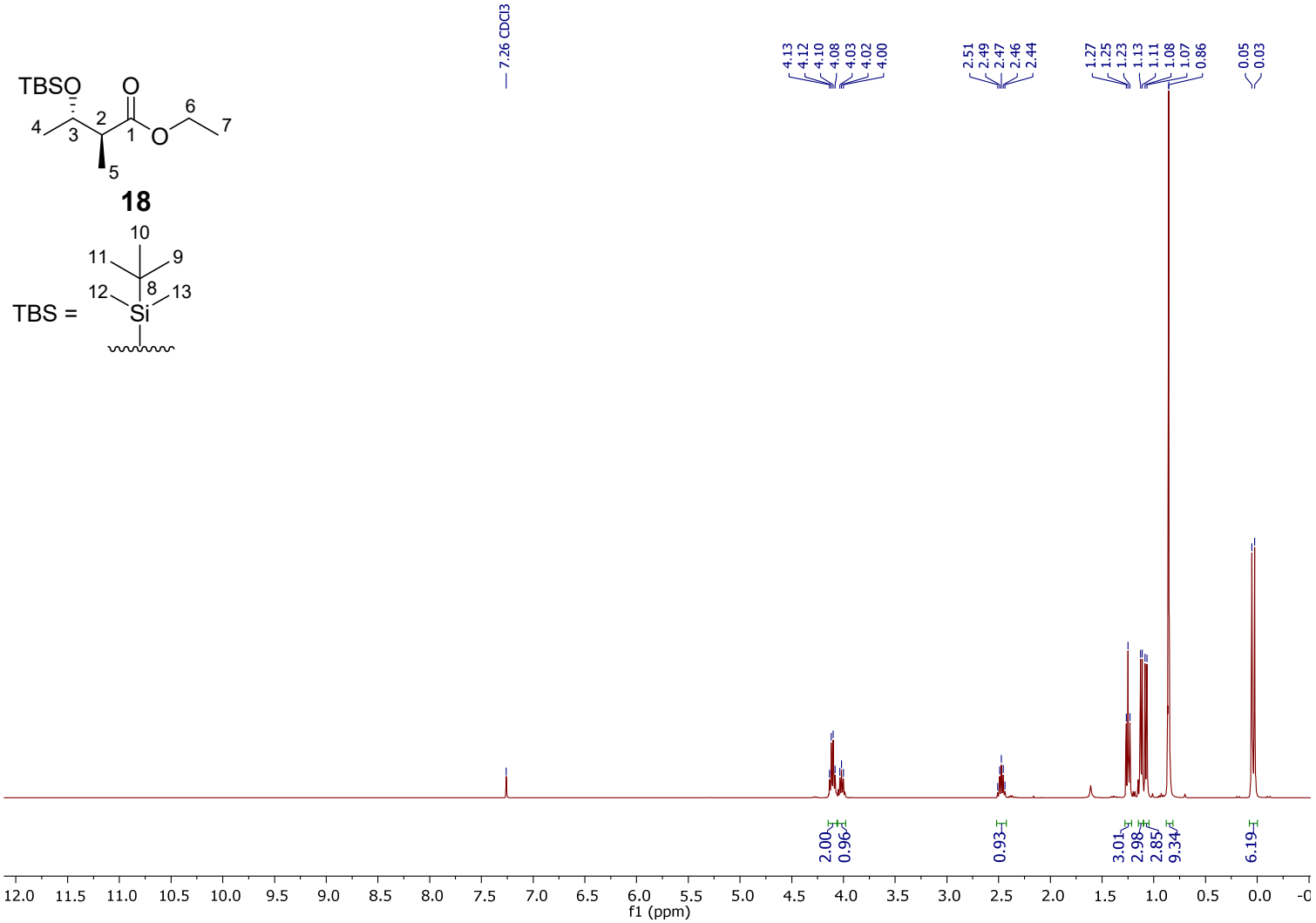

Figure S 73: ^{1}H NMR of Cpd **18**.

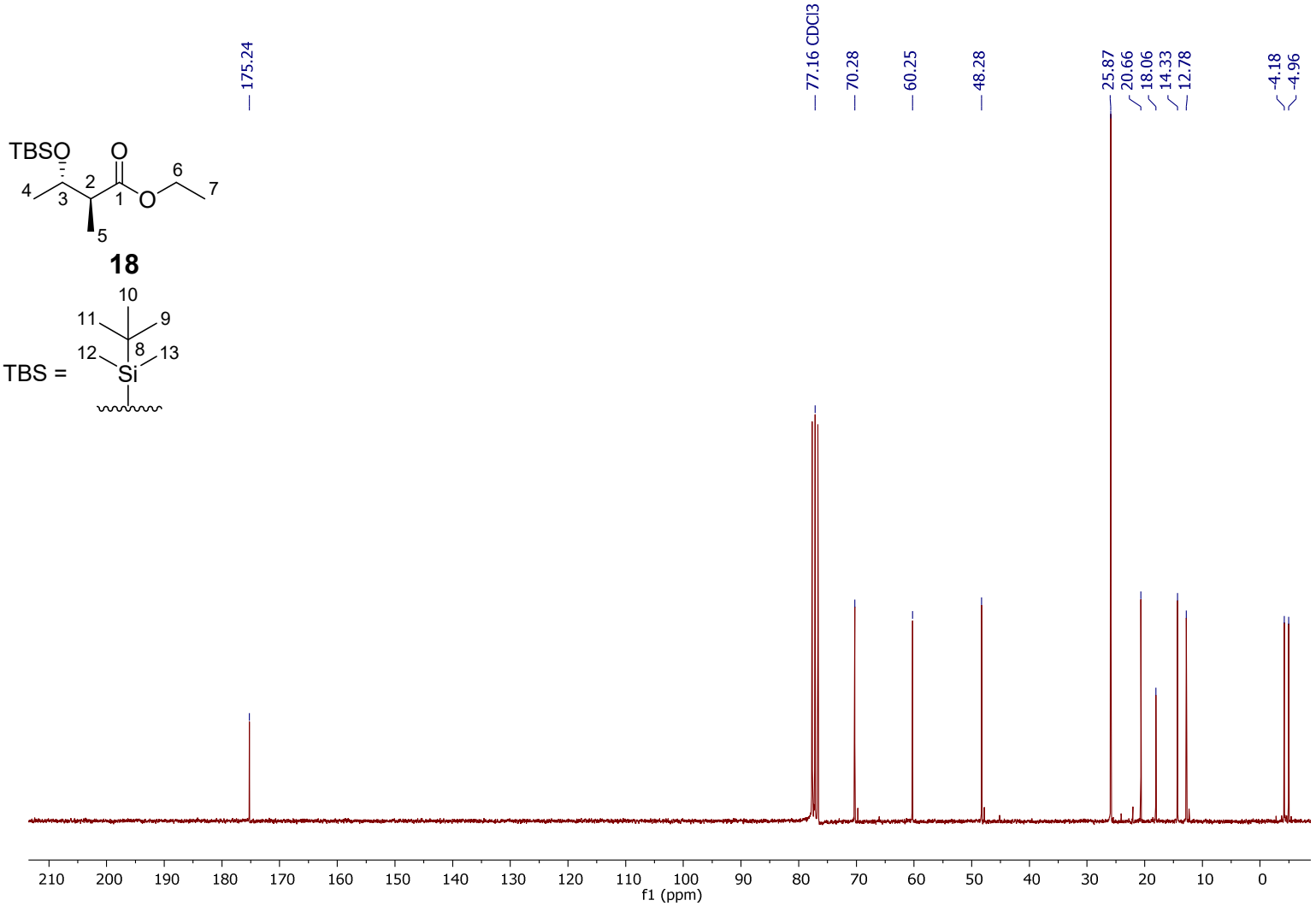

Figure S 74: ^{13}C NMR of Cpd **18**.

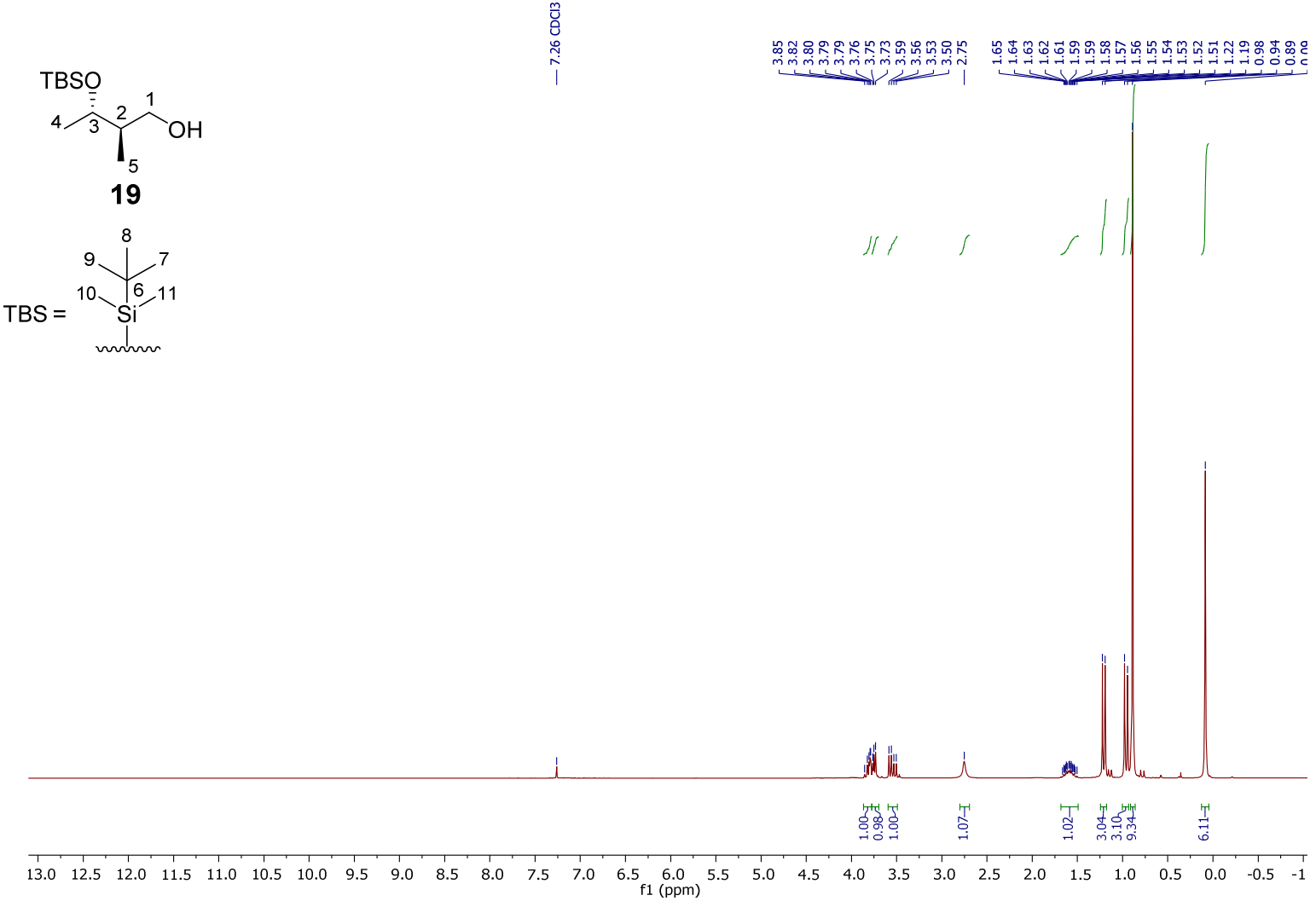

Figure S 75: ^{1}H NMR of Cpd **19**.

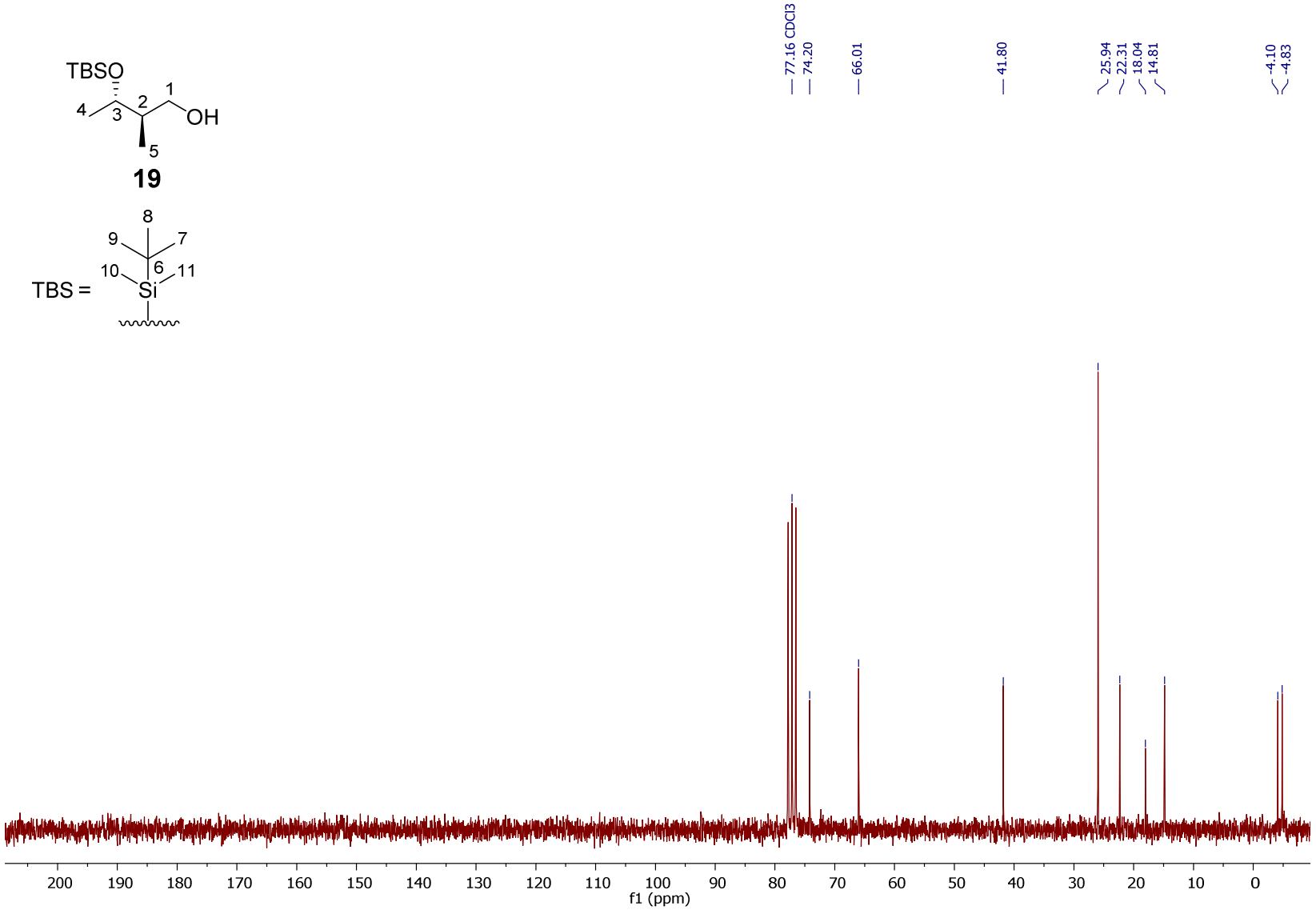

Figure S 76: ^{13}C NMR of Cpd **19**.

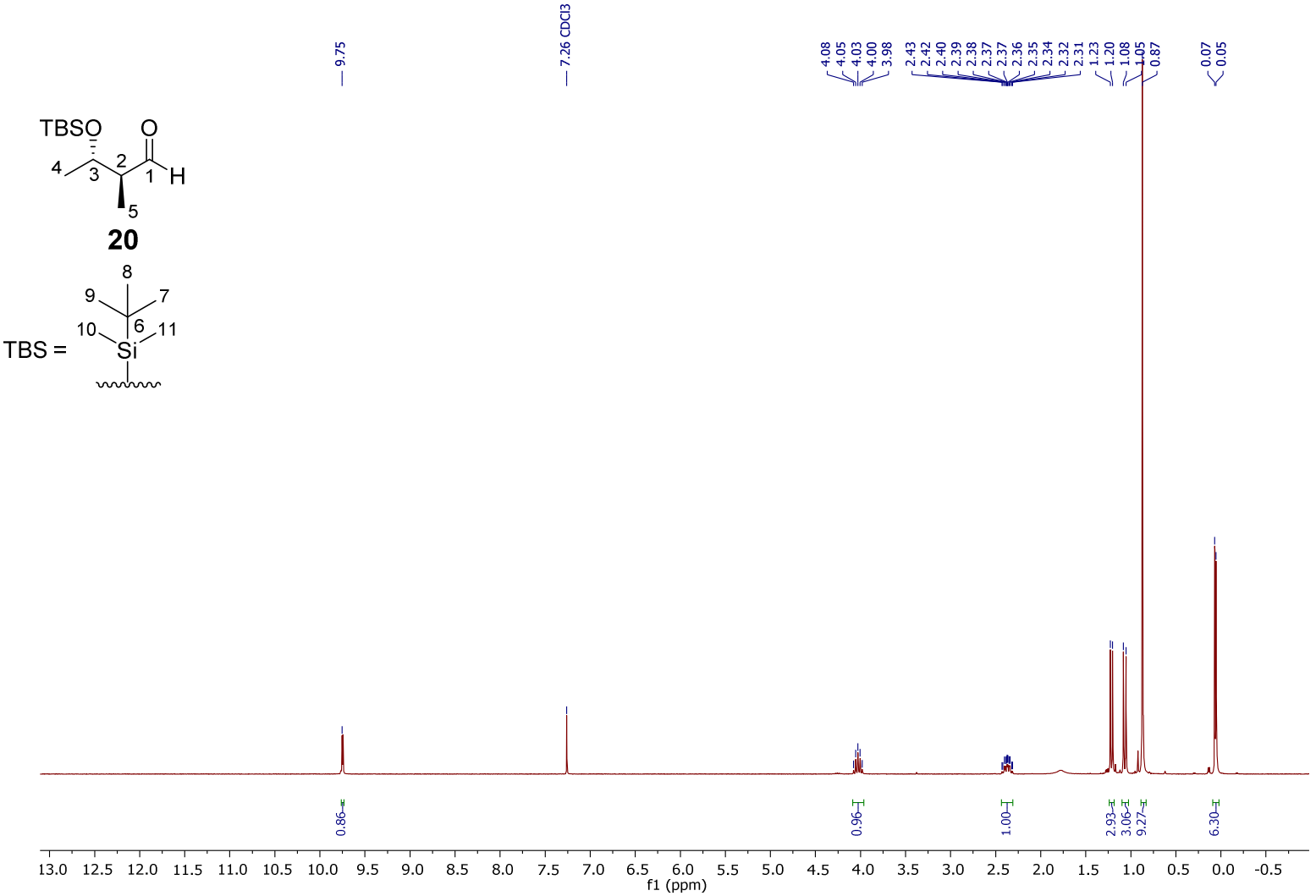

Figure S 77: ^{1}H NMR of Cpd **20**.

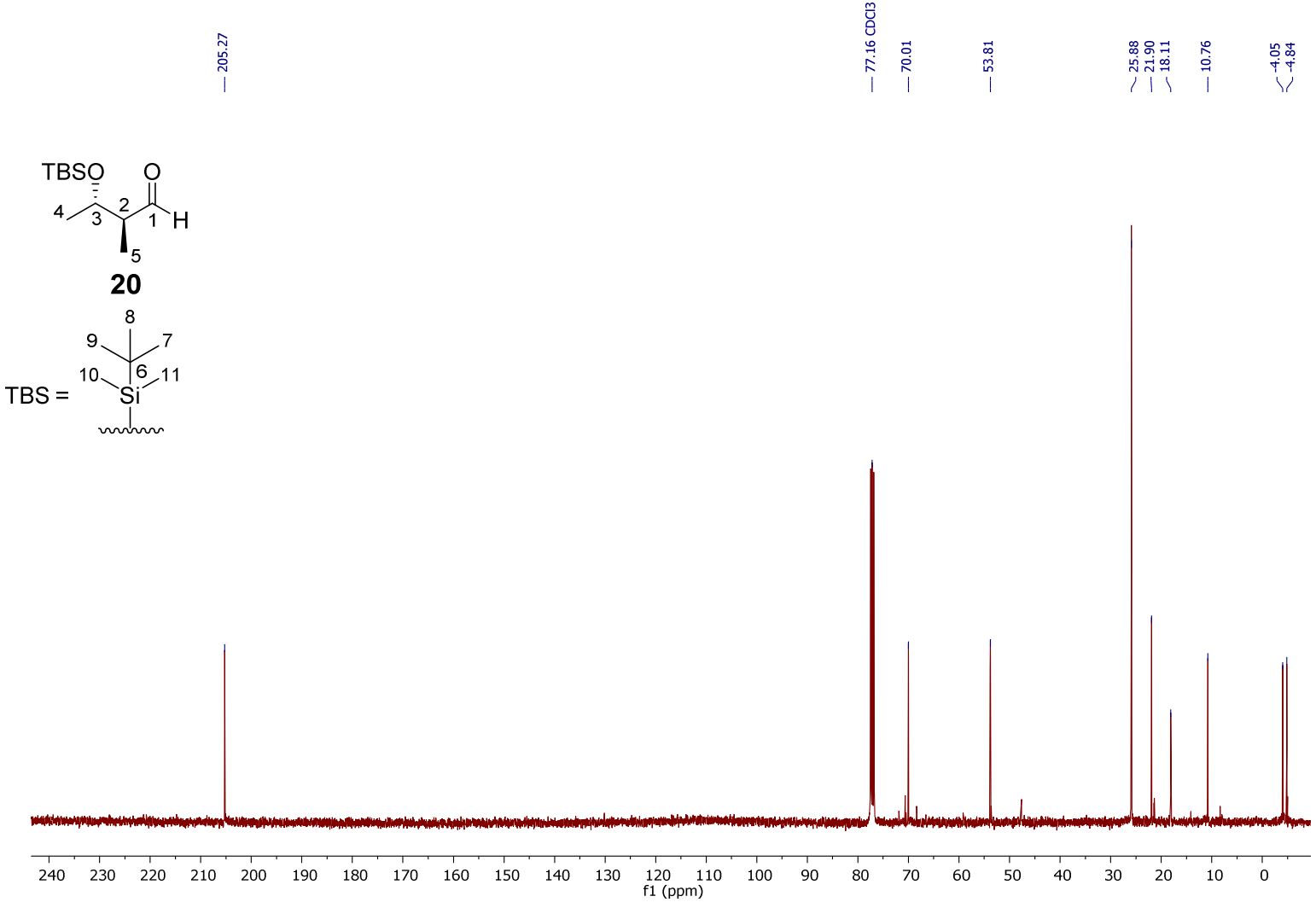

Figure S 78: ^{13}C NMR of Cpd **20**.

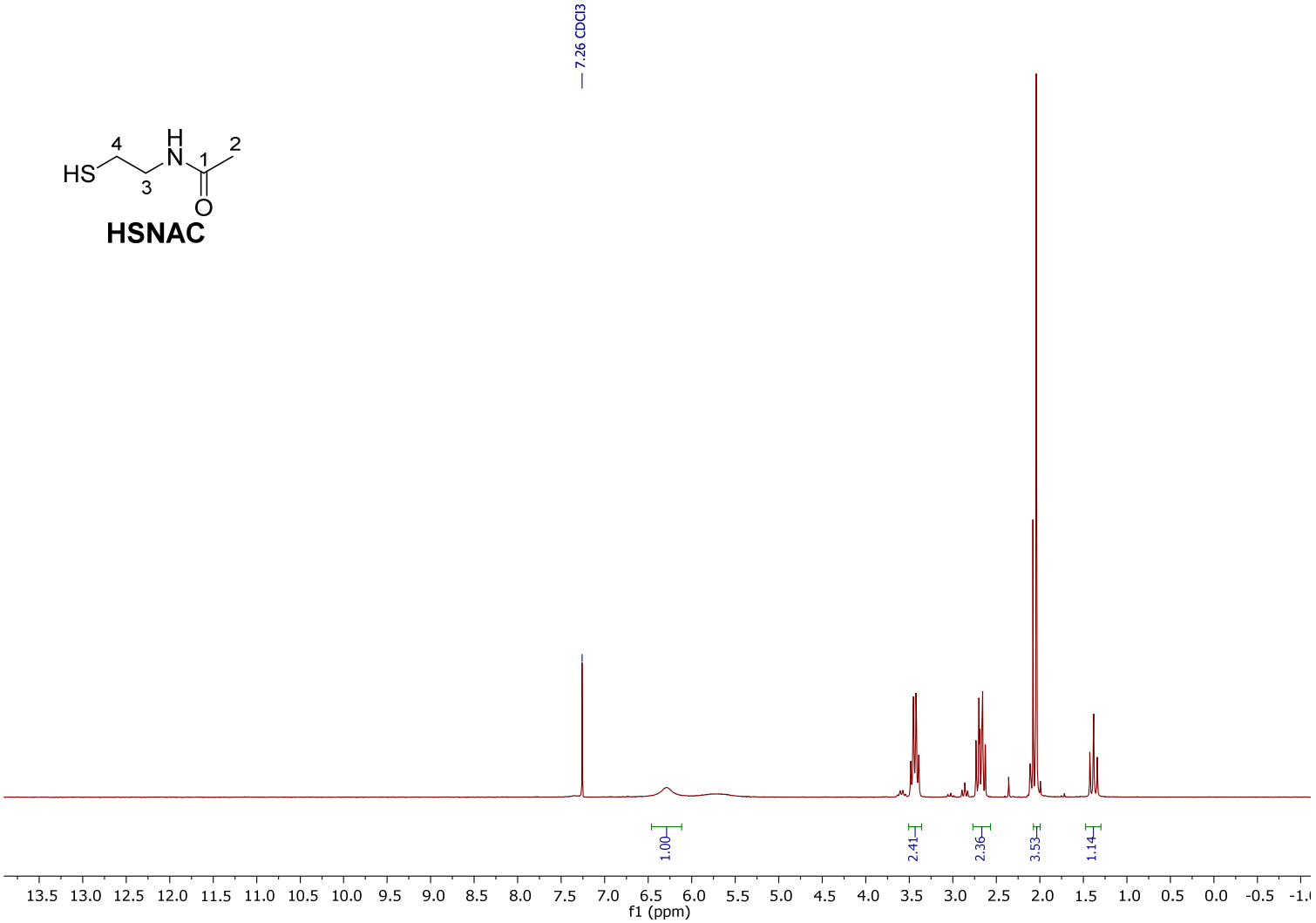

Figure S 79: ^{1}H NMR of **HSNAC**.

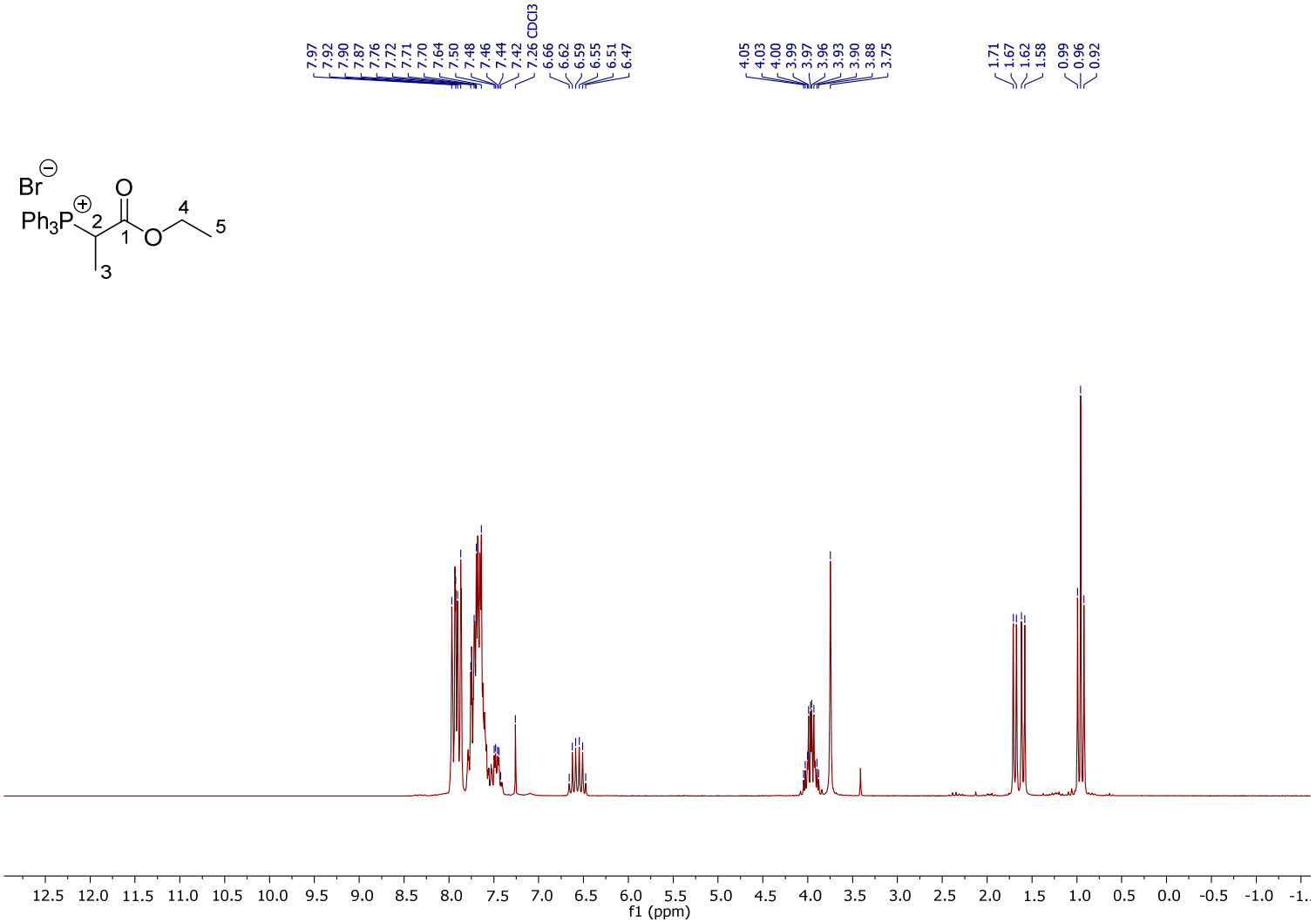

Figure S 80: ^{1}H NMR of ***rac*-(1-ethoxy-1-oxopropan-2-yl)triphenyl-phosphonium bromide**

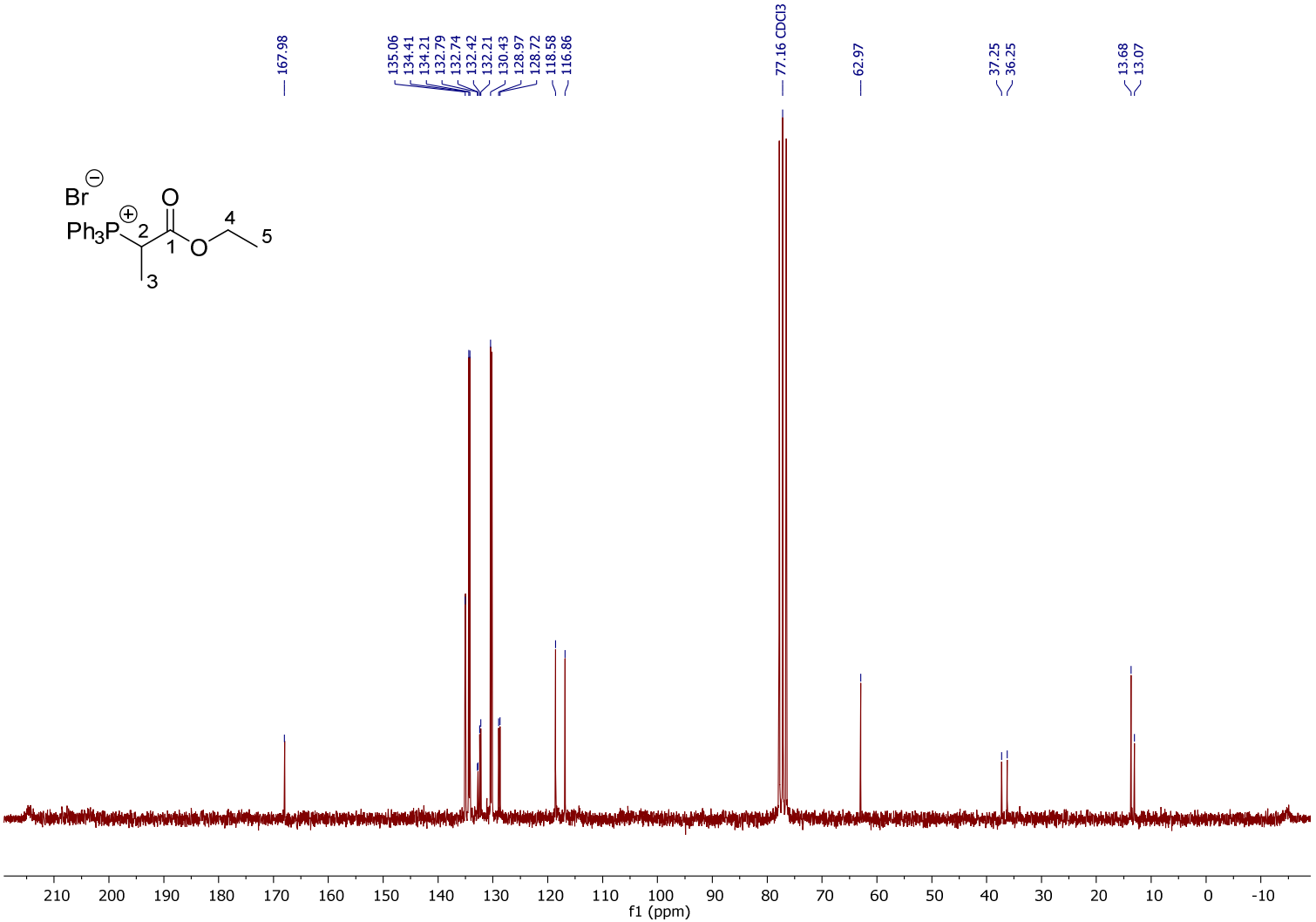

Figure S 81: ^{13}C NMR of Cpd ***rac*-(1-ethoxy-1-oxopropan-2-yl)triphenyl-phosphonium bromide.**

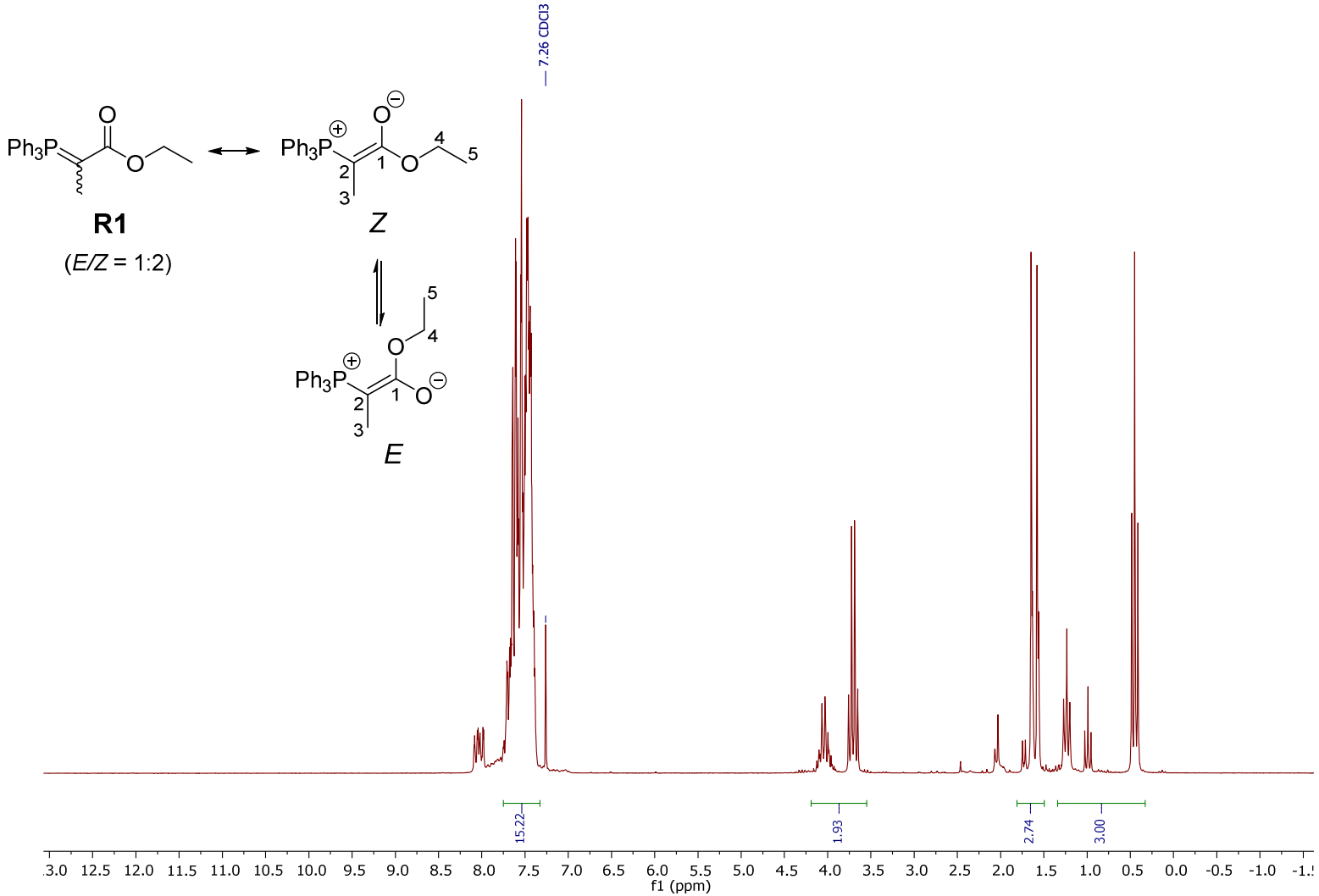

Figure S 82: ^{1}H NMR of **ethyl 2-(triphenyl-λ^{5}-phosphanylidene)-propanoate (R1).**

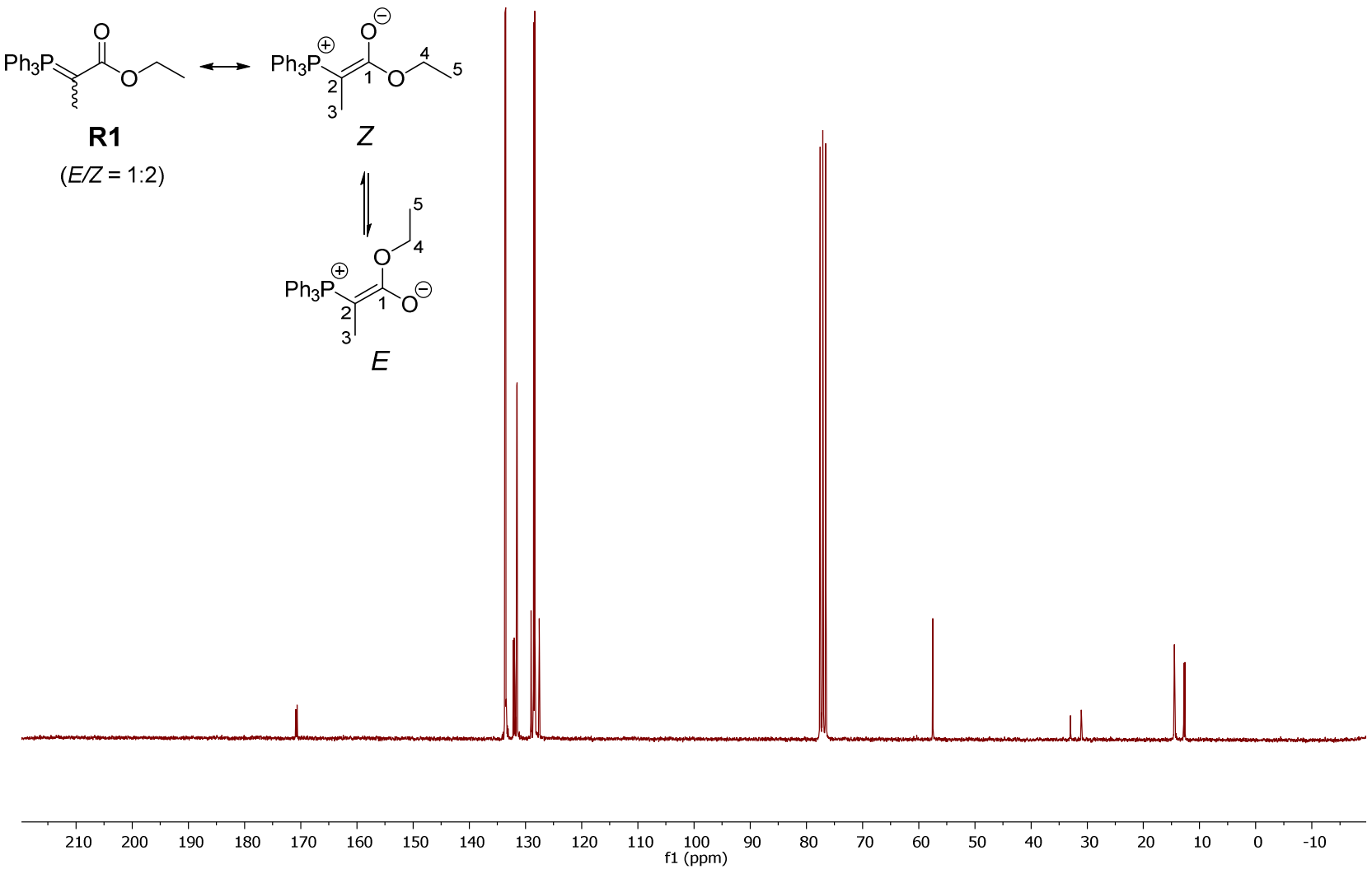

Figure S 83: ^{13}C NMR of **ethyl 2-(triphenyl-λ^5-phosphanylidene)-propanoate (R1).**

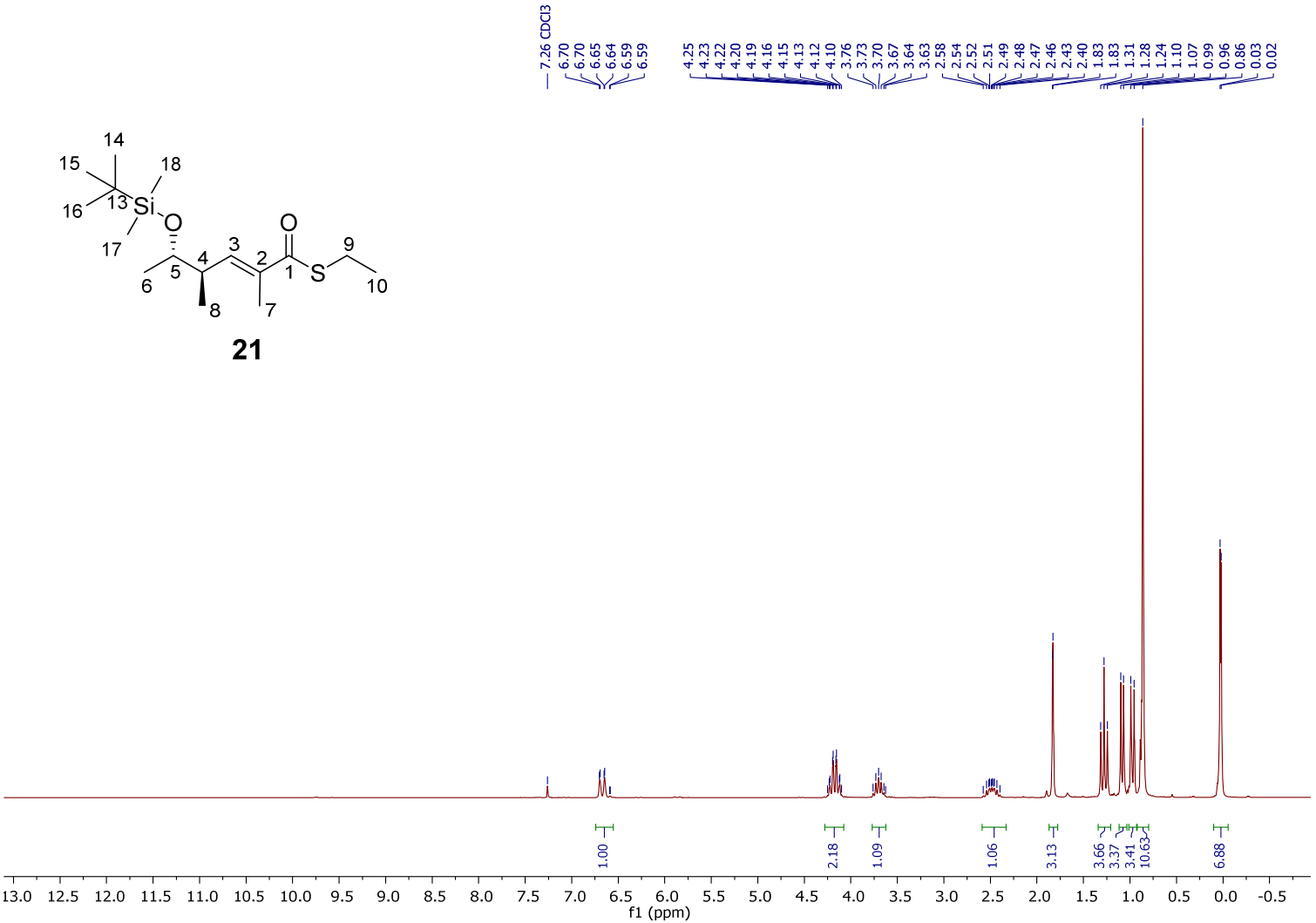

Figure S 84: ^{1}H NMR of Cpd **21**.

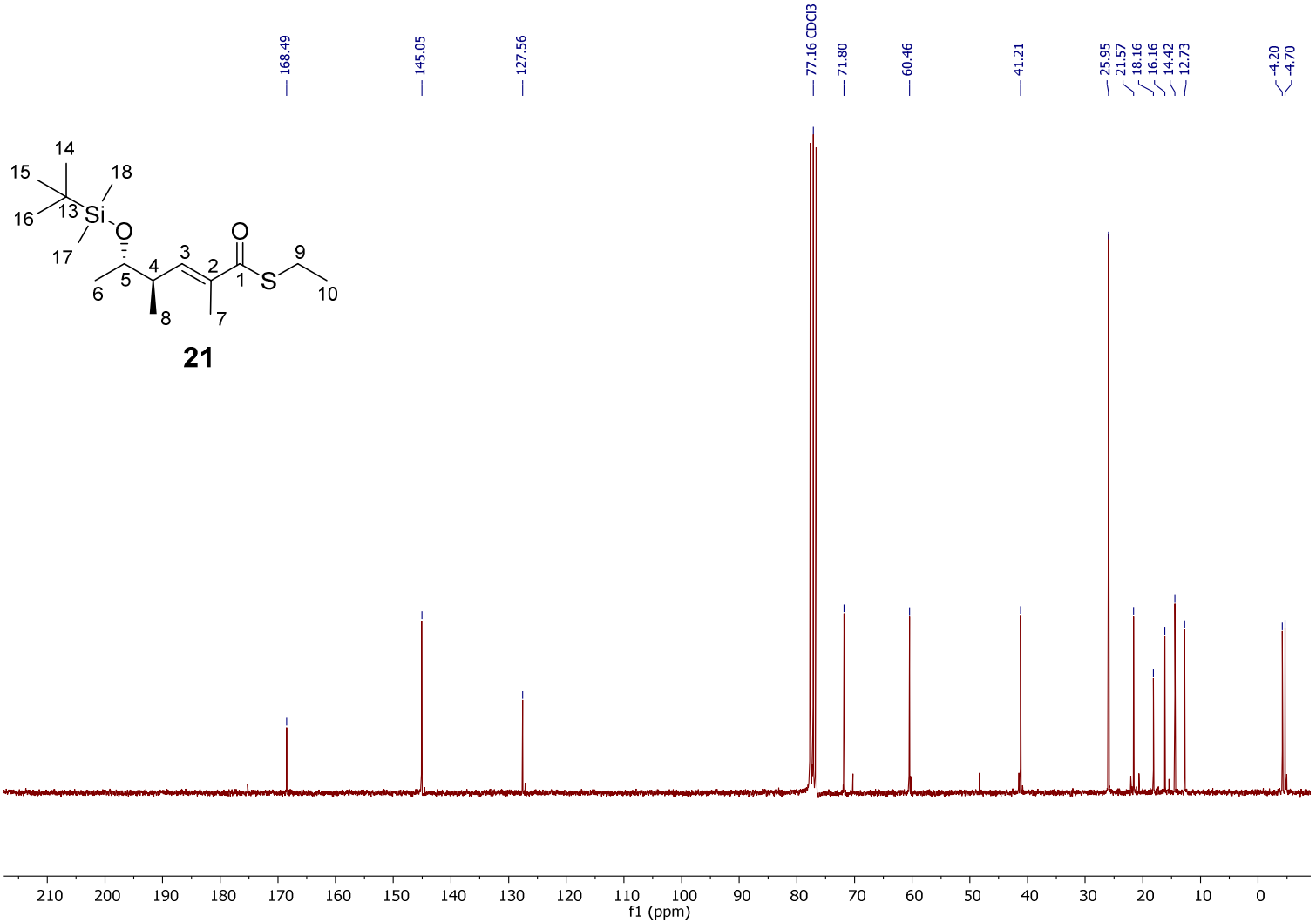

Figure S 85: ^{13}C NMR of Cpd **21**.

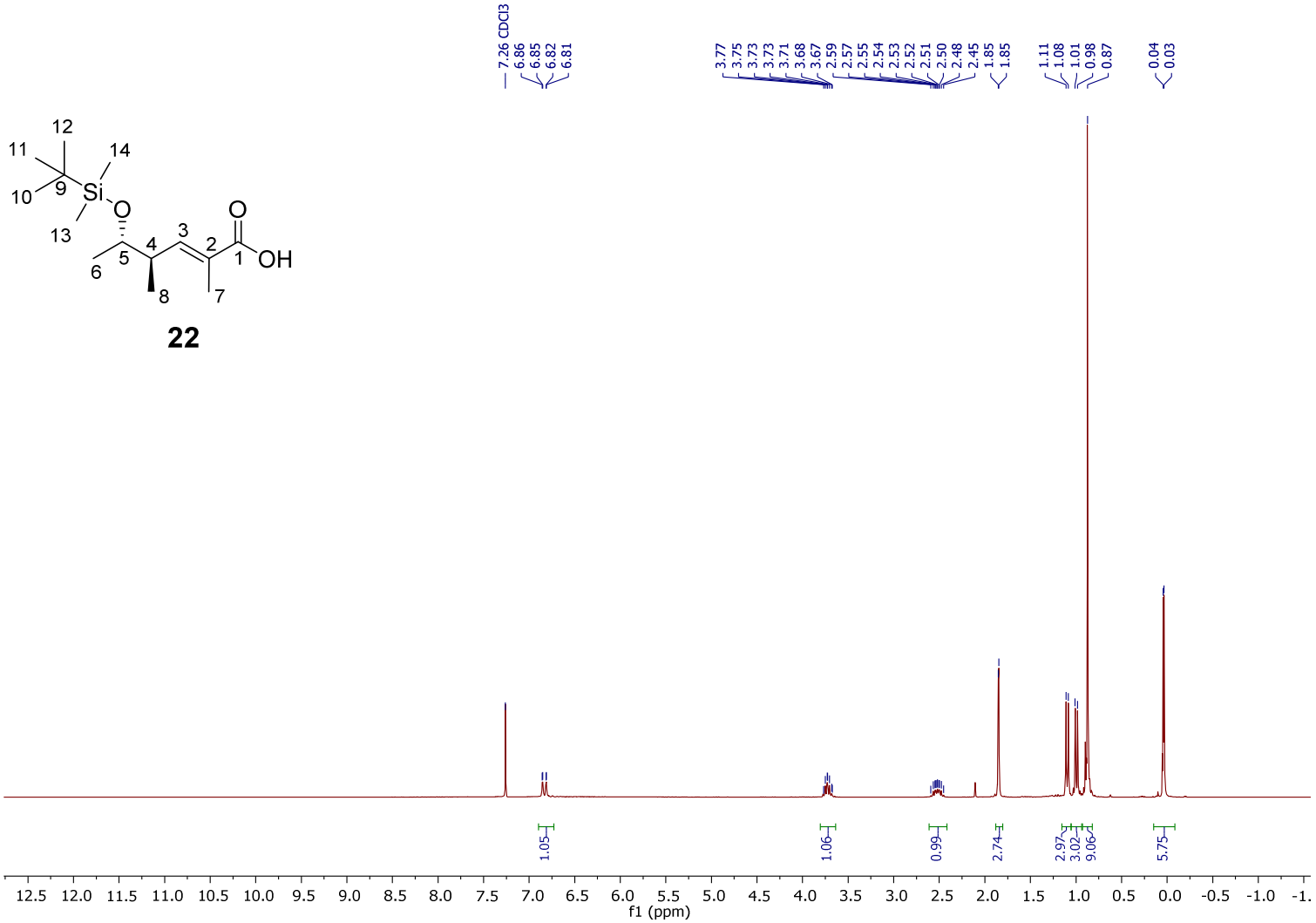

22

Figure S 86: ^{1}H NMR of Cpd **22**.

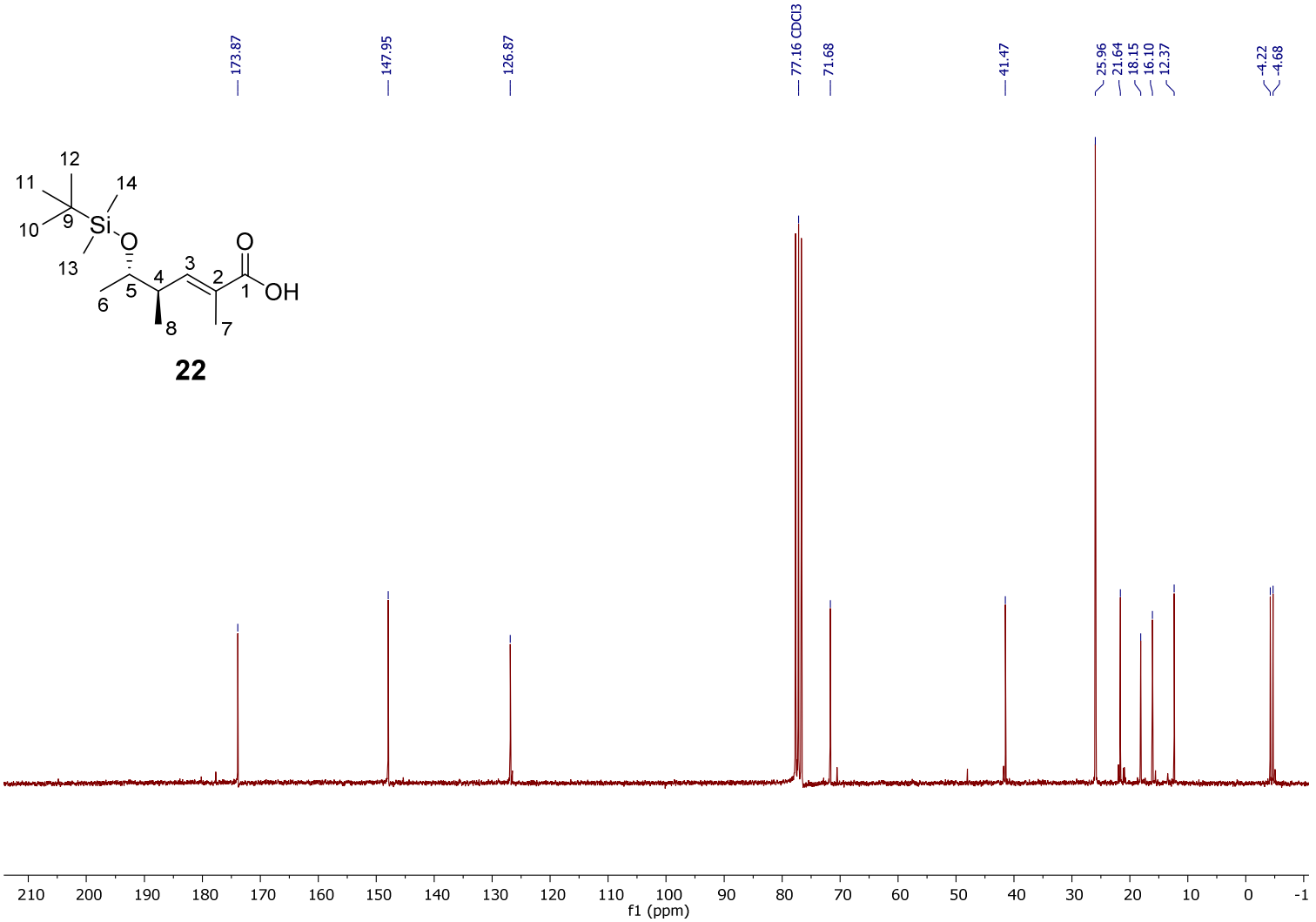

Figure S 87: ^{13}C NMR of Cpd **22**.

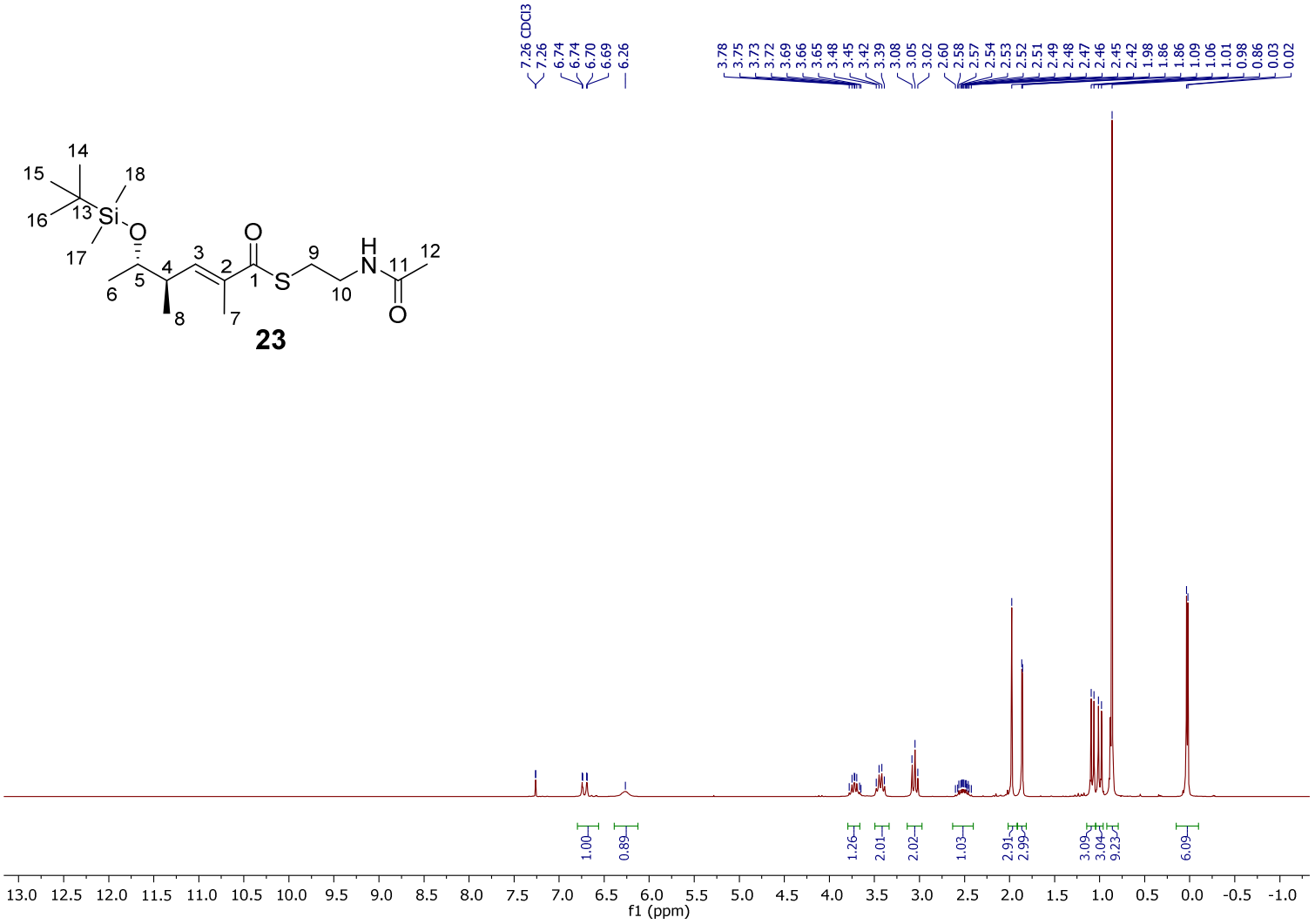

23

Figure S 88: ^{1}H NMR of Cpd **23**.

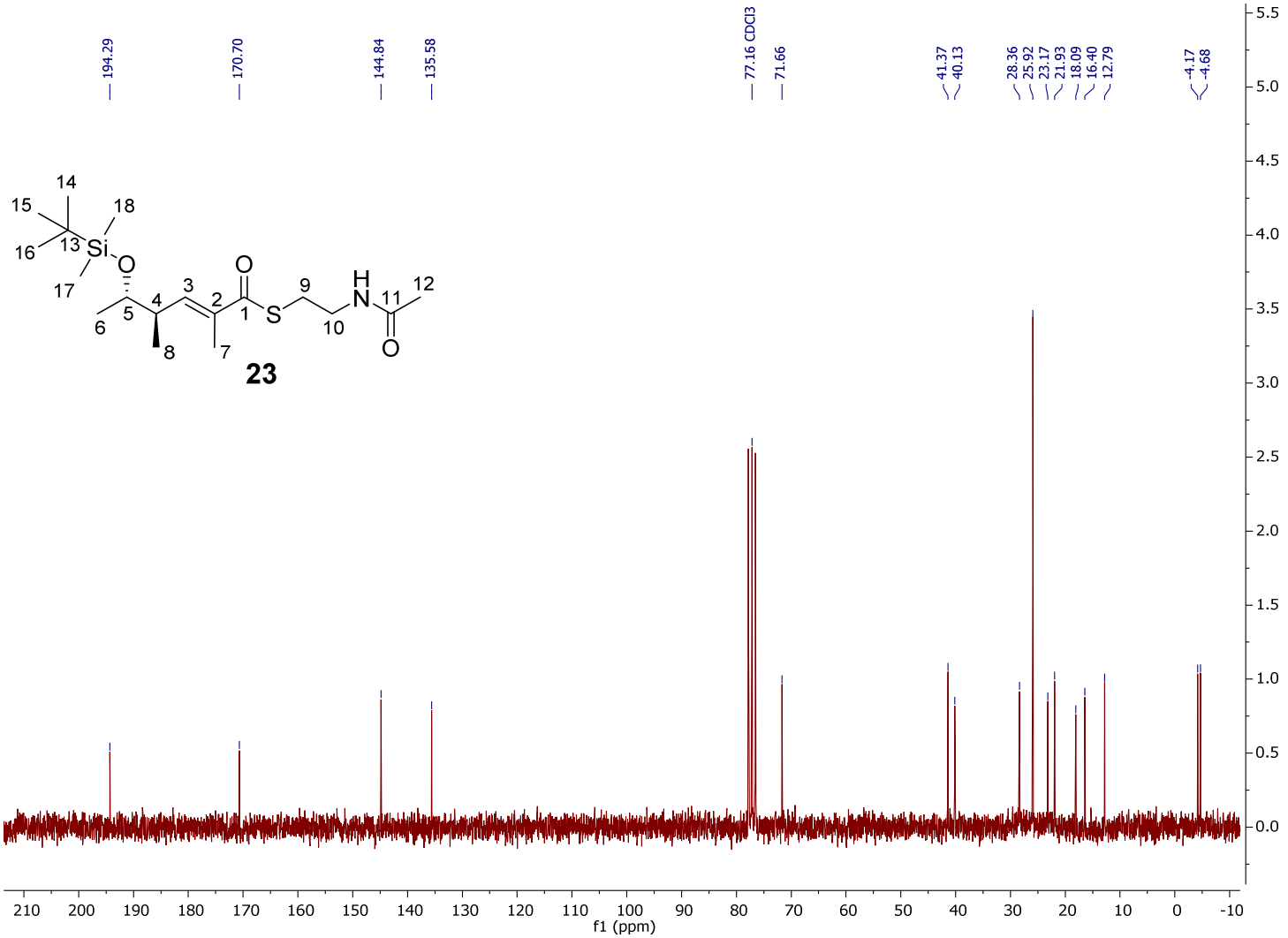

Figure S 89: ^{13}C NMR of Cpd **23**.

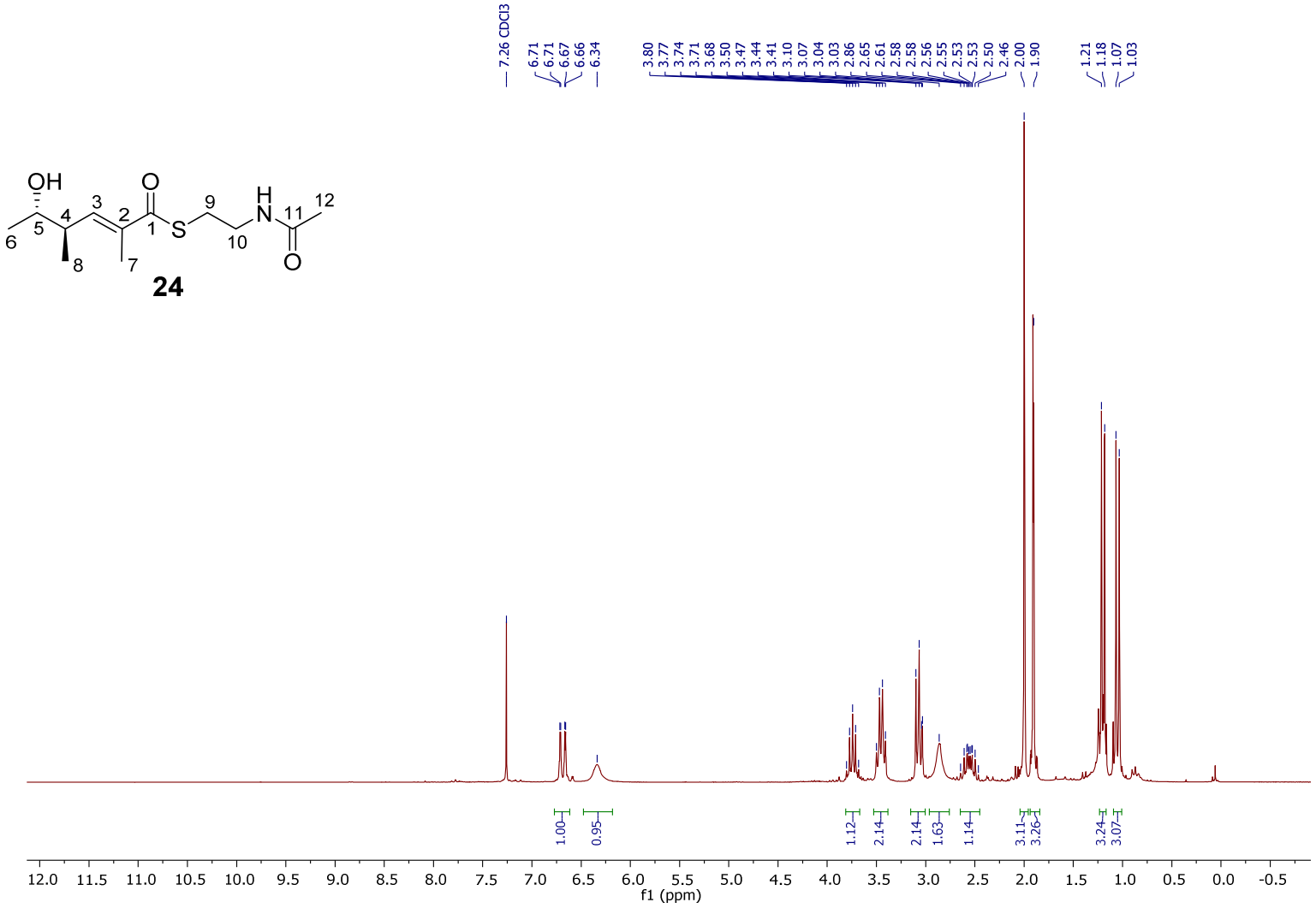

Figure S 90: ^{1}H NMR of Cpd **24**.

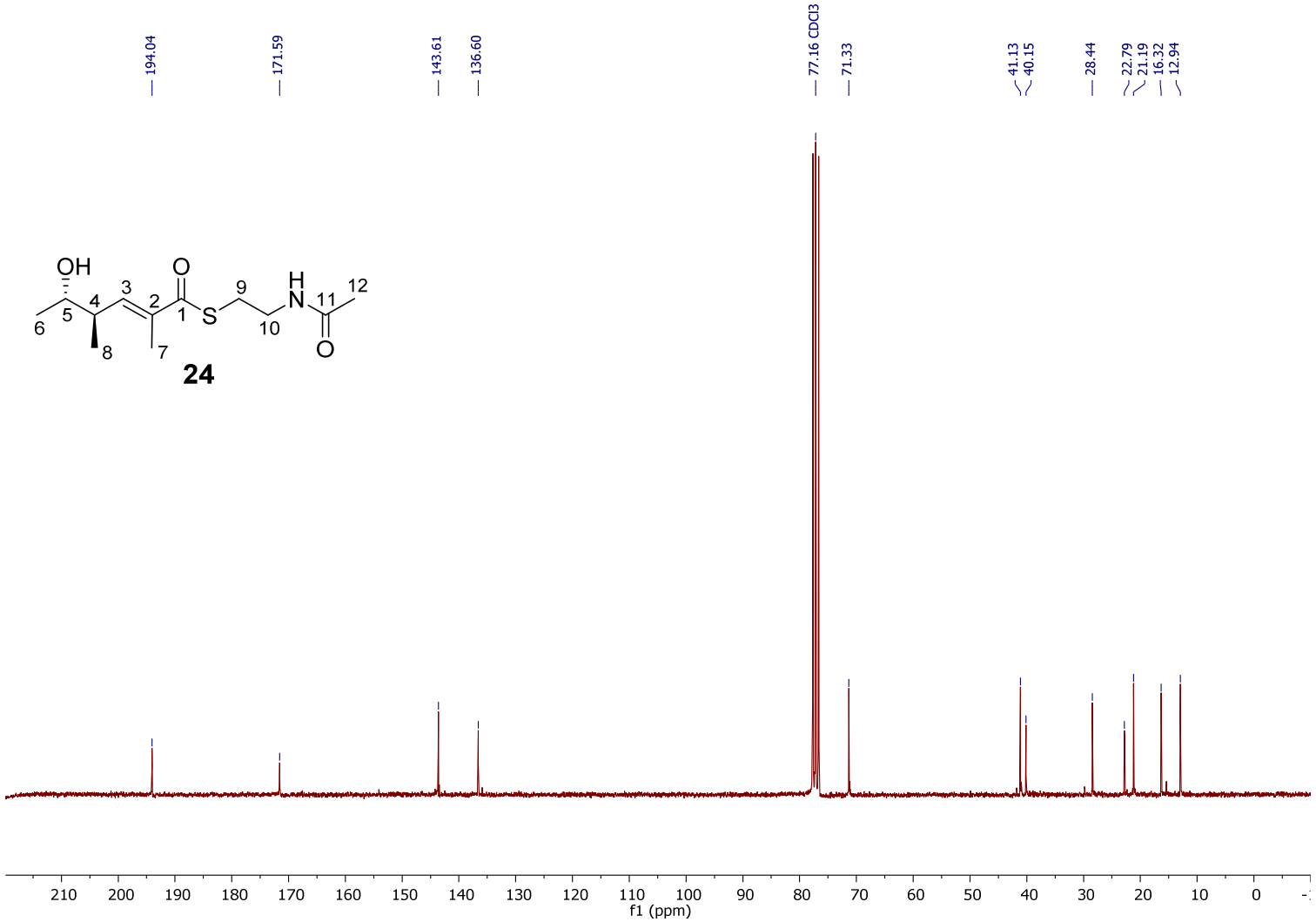

Figure S 91: ^{13}C NMR of Cpd **24**.

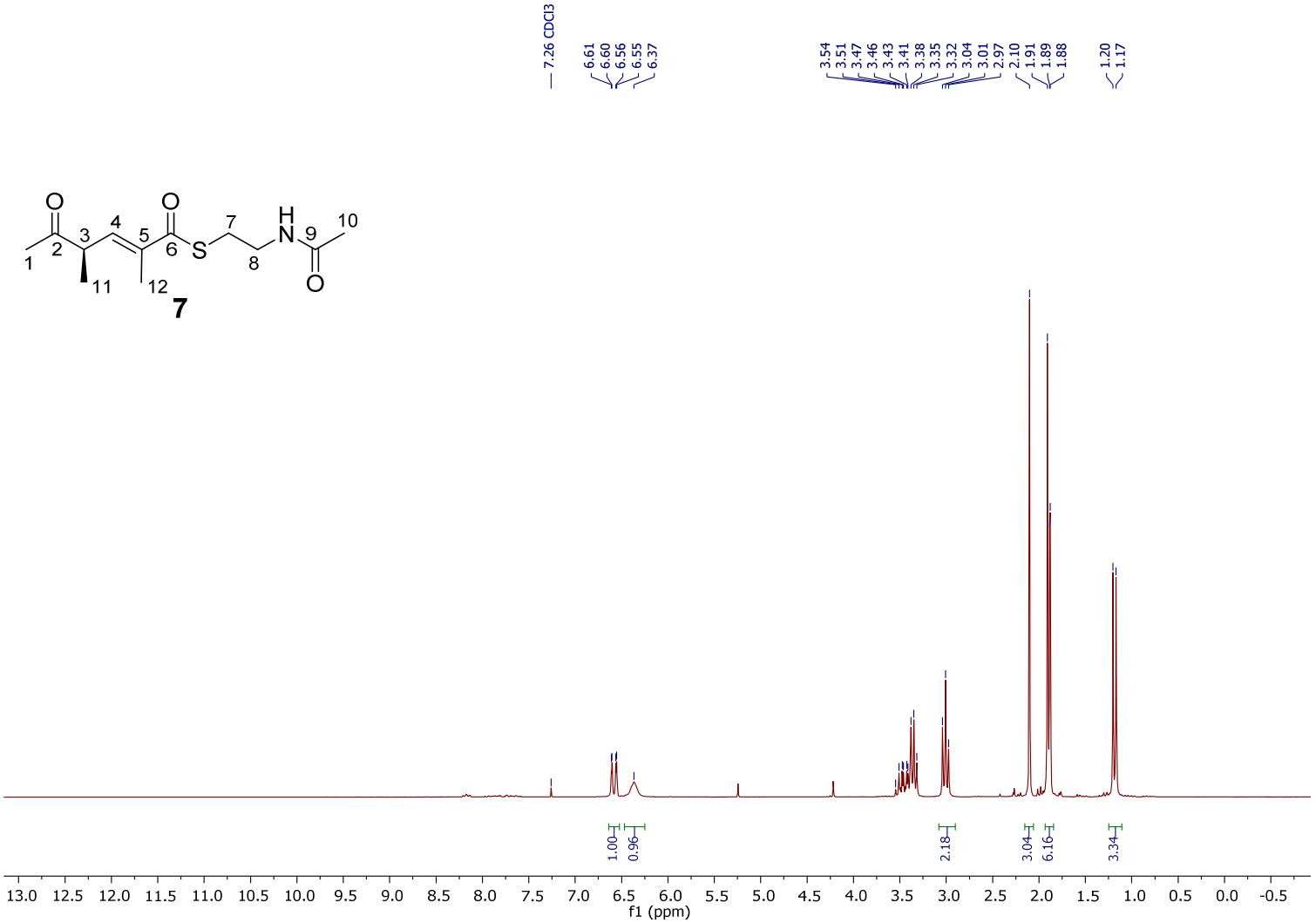

7

Figure S 92: ^{1}H NMR of Cpd **7**.

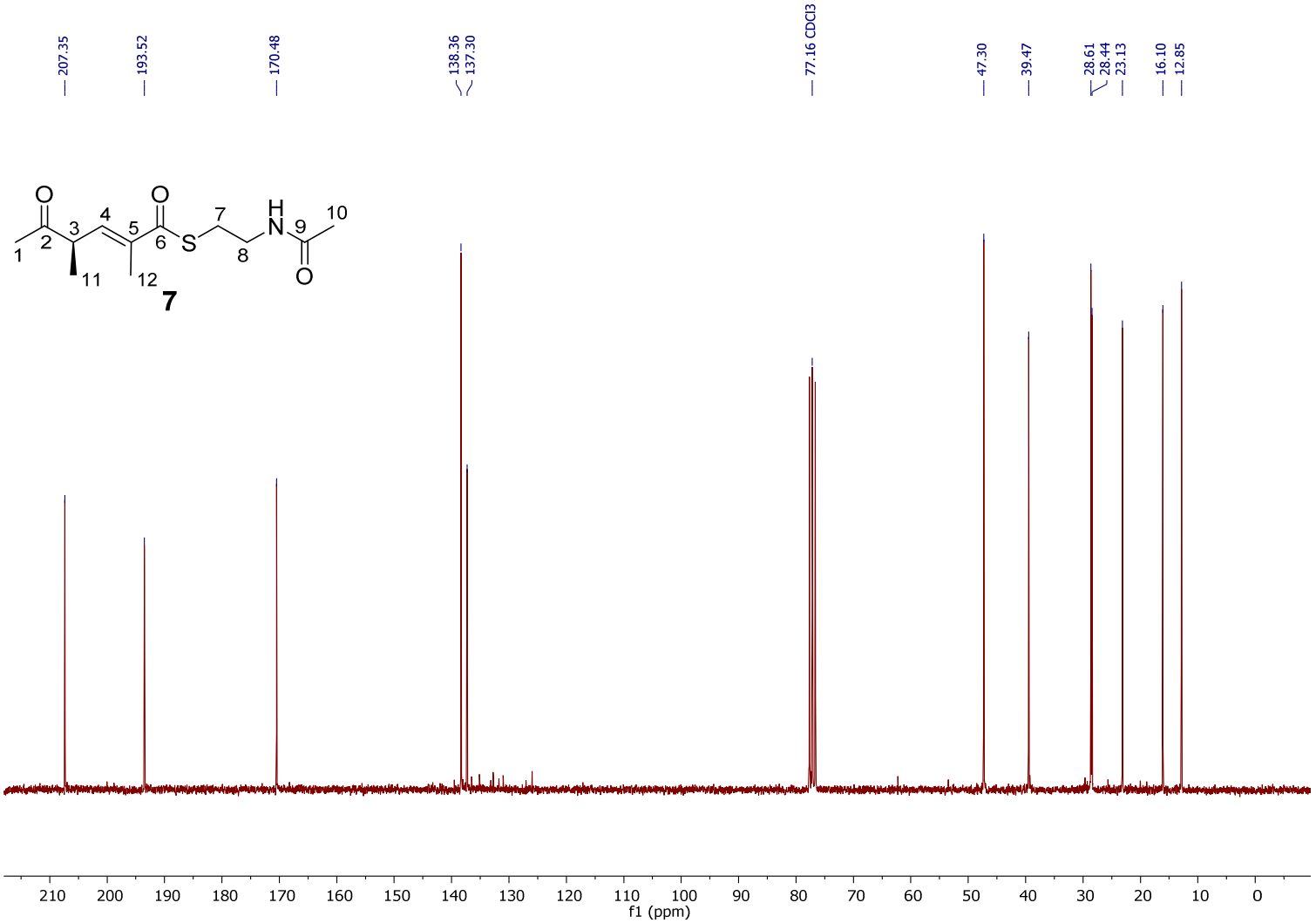

Figure S 93: ^{13}C NMR of Cpd **7**.

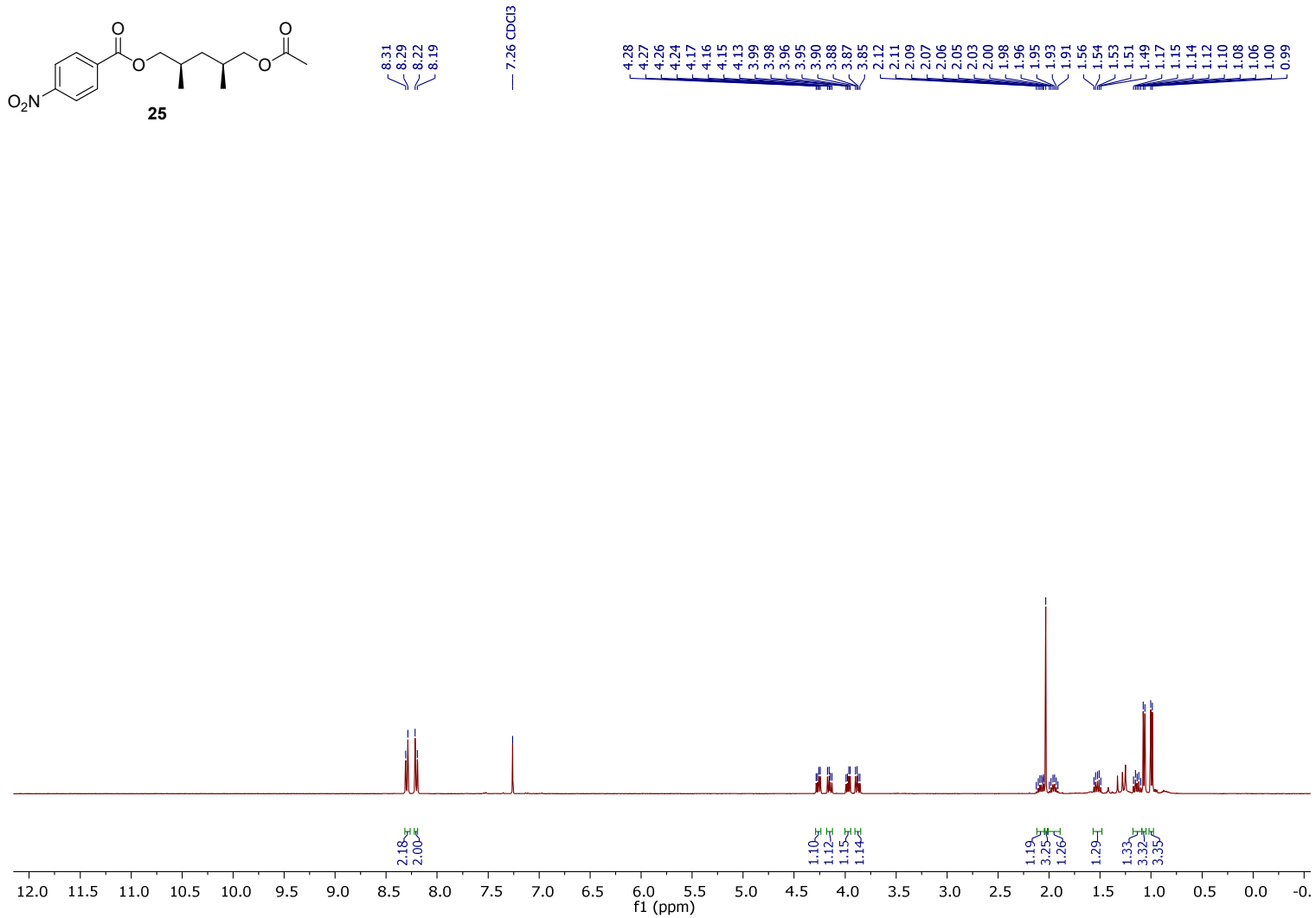

Figure S 94: ^{1}H NMR of Cpd **25**

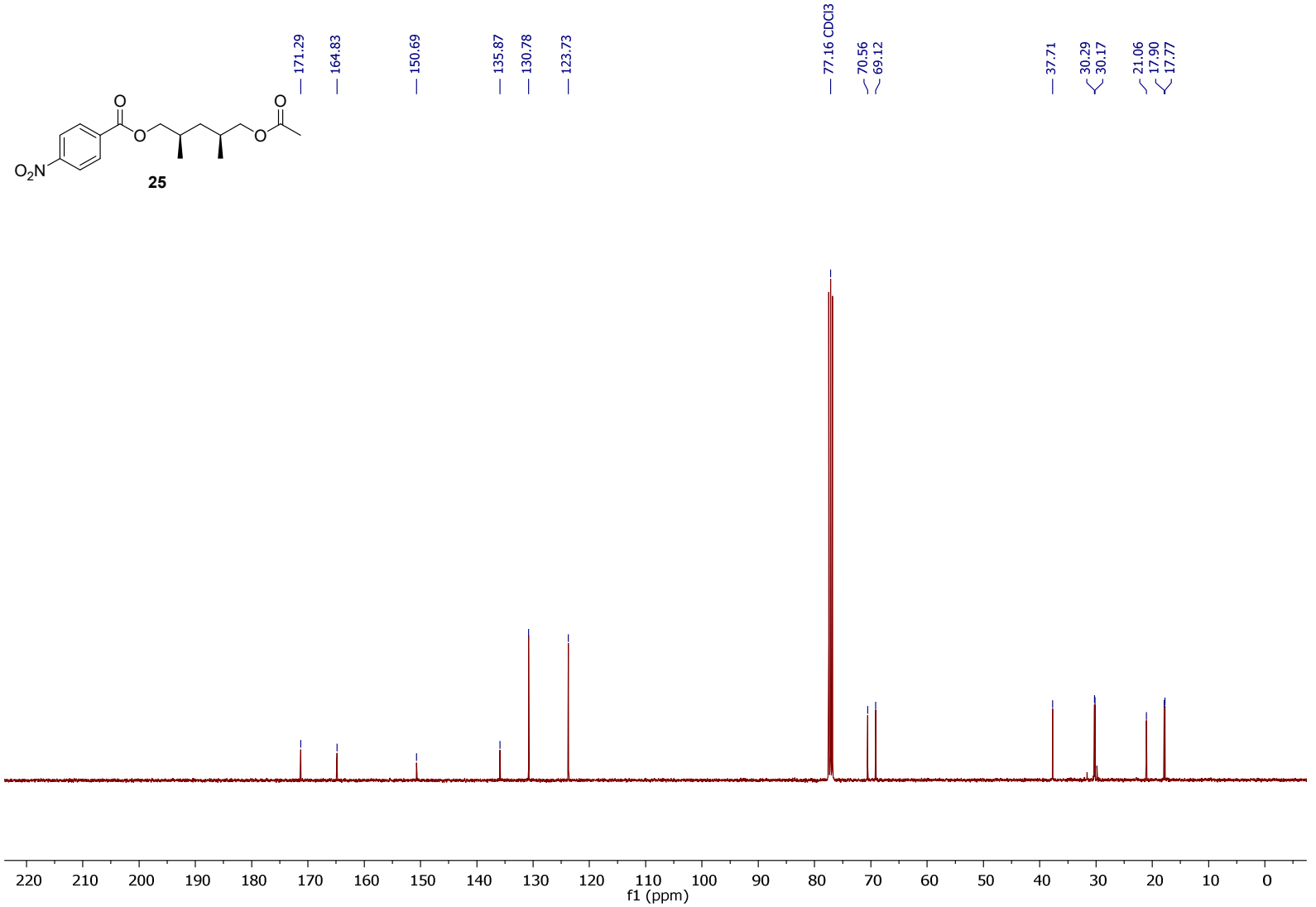

Figure S 95: ^{13}C NMR of Cpd **25**.

10 References

1. Ojanperä, S., A. Pelander, M. Pelzing, I. Krebs, E. Vuori, and I. Ojanperä, Isotopic pattern and accurate mass determination in urine drug screening by liquid chromatography/time-of-flight mass spectrometry. *Rapid Communications in Mass Spectrometry*, **2006**. 20: 1161-1167
2. Rockwood, A.L., S.L. Van Orden, and R.D. Smith, Rapid Calculation of Isotope Distributions. *Analytical Chemistry*, **1995**. 67: 2699-2704
3. Tenhosaari, A., Computer-assisted composition analysis of unknown compounds by simultaneous analysis of the intensity ratios of isotope patterns of the molecular ion and daughter ions in low-resolution mass spectra. *Organic Mass Spectrometry*, **1988**. 23: 236-239
4. Gallimore, A.R., The biosynthesis of polyketide-derived polycyclic ethers. *Natural Product Reports*, **2009**. 26: 266--280
5. Leadlay, P.F., J. Staunton, M. Oliynyk, C. Bisang, J. Cortés, E. Frost, Z.A. Hughes-Thomas, M.A. Jones, S.G. Kendrew, J.B. Lester, P.F. Long, H.A. McArthur, E.L. McCormick, Z. Oliynyk, C.B. Stark, and C.J. Wilkinson, Engineering of complex polyketide biosynthesis--insights from sequencing of the monensin biosynthetic gene cluster. *Journal of Industrial Microbiology and Biotechnology*, **2001**. 27: 360--367
6. Bhatt, A., C.B.W. Stark, B.M. Harvey, A.R. Gallimore, Y.A. Demydchuk, J.B. Spencer, J. Staunton, and P.F. Leadlay, Accumulation of an E,E,E-triene by the monensin-producing polyketide synthase when oxidative cyclization is blocked. *Angewandte Chemie-International Edition*, **2005**. 44: 7075-7078
7. Minami, A., H. Oguri, K. Watanabe, and H. Oikawa, Biosynthetic machinery of ionophore polyether lasalocid: enzymatic construction of polyether skeleton. *Current Opinion in Chemical Biology*, **2013**. 17: 555--561
8. Migita, A., M. Watanabe, Y. Hirose, K. Watanabe, T. Tokiwano, H. Kinashi, and H. Oikawa, Identification of a Gene Cluster of Polyether Antibiotic Lasalocid from Streptomyces lasaliensis. *Biosci. Biotechnol., Biochem.*, **2009**. 73: 169--176
9. Yurkovich, M.E., P.A. Tyrakis, H. Hong, Y. Sun, M. Samborskyy, K. Kamiya, and P.F. Leadlay, A Late-Stage Intermediate in Salinomycin Biosynthesis Is Revealed by Specific Mutation in the Biosynthetic Gene Cluster. *ChemBioChem*, **2012**. 13: 66--71
10. Sun, Y., X. Zhou, H. Dong, G. Tu, M. Wang, B. Wang, and Z. Deng, A Complete Gene Cluster from Streptomyces nanchangensis NS3226 Encoding Biosynthesis of the Polyether Ionophore Nanchangmycin. *Chemistry & Biology*, **2003**. 10: 431--441
11. Demydchuk, Y., Y. Sun, H. Hong, J. Staunton, J.B. Spencer, and P.F. Leadlay, Analysis of the tetronomycin gene cluster: insights into the biosynthesis of a polyether tetronate antibiotic. *ChemBioChem*, **2008**. 9: 1136--1145
12. Zhang, L., T. Hashimoto, B. Qin, J. Hashimoto, I. Kozone, T. Kawahara, M. Okada, T. Awakawa, T. Ito, Y. Asakawa, M. Ueki, S. Takahashi, H. Osada, T. Wakimoto, H. Ikeda, K. Shin-ya, and I. Abe, Characterization of Giant Modular PKSs Provides Insight into Genetic Mechanism for Structural Diversification of Aminopolyol Polyketides. *Angewandte Chemie International Edition*, **2017**. 56: 1740-1745
13. Gallenkamp, D. and A. Fürstner, Stereoselective Synthesis of E,Z-Configured 1,3-Dienes by Ring-Closing Metathesis. Application to the Total Synthesis of Lactimidomycin. *Journal of the American Chemical Society*, **2011**. 133: 9232-9235
14. Barrish, J.C., H.L. Lee, T. Mitt, G. Pizzolato, E.G. Baggiolini, and M.R. Uskokovic, Total synthesis of pseudomonic acid C. *The Journal of Organic Chemistry*, **1988**. 53: 4282-4295
15. Jacolot, M., M. Jean, N. Levoin, and P. van de Weghe, The Prins Reaction Using Ketones: Rationalization and Application toward the Synthesis of the Portentol Skeleton. *Organic Letters*, **2012**. 14: 58-61
16. Galkin, K.I., E.A. Krivodaeva, L.V. Romashov, S.S. Zalesskiy, V.V. Kachala, J.V. Burykina, and V.P. Ananikov, Critical Influence of 5-Hydroxymethylfurfural Aging and Decomposition on

the Utility of Biomass Conversion in Organic Synthesis. *Angewandte Chemie-International Edition*, **2016**. 55: 8338-8342
17. Petr, K. and K. Martin, Enantioselective Allylation of (2E,4E)-2,4-Dimethylhexadienal: Synthesis of (5R,6S)-(+)-Pteroenone. *Chemistry – A European Journal*, **2015**. 21: 7408-7412
18. Kinoshita, K., P.G. Williard, C. Khosla, and D.E. Cane, Precursor-directed biosynthesis of 16-membered macrolides by the erythromycin polyketide synthase. *Journal of the American Chemical Society*, **2001**. 123: 2495-2502
19. Ishikawa, T., R. Kadoya, M. Arai, H. Takahashi, Y. Kaisi, T. Mizuta, K. Yoshikai, and S. Saito, Revisiting [3 + 3] Route to 1,3-Cyclohexanedione Frameworks: Hidden Aspect of Thermodynamically Controlled Enolates. *The Journal of Organic Chemistry*, **2001**. 66: 8000-8009
20. Wolfrom, M.L. and J.M. Bobbitt, Periodate Oxidation of Cyclic 1,3-Diketones. *Journal of the American Chemical Society*, **1956**. 78: 2489-2493
21. Fotiadou, A.D. and A.L. Zografos, Accessing the Structural Diversity of Pyridone Alkaloids: Concise Total Synthesis of Rac-Citridone A. *Organic Letters*, **2011**. 13: 4592-4595
22. Yadav, J.S., D.N. Chary, N.N. Yadav, S. Sengupta, and B.V.S. Reddy, Divergent Enantioselective Total Synthesis of Siphonarienal, Siphonarienone, and Pectinatone. *Helvetica Chimica Acta*, **2013**. 96: 1968-1977
23. Gray, K.C., D.S. Palacios, I. Dailey, M.M. Endo, B.E. Uno, B.C. Wilcock, and M.D. Burke, Amphotericin primarily kills yeast by simply binding ergosterol. *Proceedings of the National Academy of Sciences of the United States of America*, **2012**. 109: 2234-2239
24. Guo, X., T.G. Liu, C.R. Valenzano, Z.X. Deng, and D.E. Cane, Mechanism and Stereospecificity of a Fully Saturating Polyketide Synthase Module: Nanchangmycin Synthase Module 2 and Its Dehydratase Domain. *Journal of the American Chemical Society*, **2010**. 132: 14694-14696
25. Block, M.H. and D.E. Cane, Synthesis of Proposed Chain-Elongation Intermediates of the Monensin Biosynthetic-Pathway. *Journal of Organic Chemistry*, **1988**. 53: 4923-4928